3. Ambient Air Quality

This chapter is intended to provide background and documentation of the ambient concentrations used in estimating the direct atmospheric deposition of nitrogen, phosphorus, and particles to Lake Tahoe. A description of the LTADS deposition methodologies and the deposition estimates themselves are presented in Chapters 4 (dry) and 5 (wet). The level of detail and analysis presented in each section varies depending on the use of that data in constructing the deposition estimates. Some material presented initially in previous LTADS documents might only be summarized or referenced herein but the complete material is included as an appendix.

Six general types of air quality data were used to support the development of the LTADS deposition estimates. They were:

1) Historical and current regulatory air quality gas and aerosol data: intermittent 24-hour integrated TSP, PM10, PM2.5 aerosol mass and chemistry, and hourly gaseous pollutant data collected by the States of California and Nevada,
2) Historical and current visibility monitoring data: 24-hour integrated PM10 and PM2.5 filter samples collected by the federal IMPROVE Network and TRPA (following IMPROVE protocols),
3) 24^{+}-hour integrated aerosol filter samples collected during LTADS using portable "Mini-volume" samplers (MVS) around the basin and on buoys anchored on the Lake,
4) Two-week integrated aerosol and gas chemical speciation samples collected during LTADS with Two-Week Samplers (TWS) deployed at selected monitoring sites,
5) Hourly TSP, PM10, and PM2.5 mass concentrations collected during LTADS by Beta Attenuation Monitors (BAMs), and
6) Minute to hourly, size-resolved ambient particle counts (in six size ranges) collected in specialized short-term "dust" experiments during LTADS.

A description of the TWS and MVS sampling networks for LTADS is provided in **Table 3-1**. **Figure 3-1** shows the locations of air quality and aloft meteorological monitoring sites used as part of LTADS. The locations of the surface meteorological sites are shown in Figure 2-2.

Table 3-1. Lake Tahoe Atmospheric Deposition Study (LTADS) Two-Week-Sampler (TWS) and Mini-Volume Sampler (MVS) Networks.

Site Name (*)	Setting	Description	Sampling Network	PM Size Cuts	Sample Duration
Lake Forest (8)	Tahoe City North Lake Shore	20 meters S from Hwy 28	TWS	TSP, PM10, PM2.5	2 Weeks
Coast Guard Pier (14)	Tahoe City North Lake Shore	Pier 300 meters SSE from LF	MVS	TSP	1 Week
Thunderbird (11)	East Lake Shore - Distant from Hwy 28	Elephant House 10 meters E	TWS	TSP, PM10, PM2.5	2 Weeks
Zephyr Cove (14)	Zephyr Cove Marina, East Lake Shore	Pier 200 meters W from Hwy 50	MVS	TSP	1 Week
Timber Cove (14)	South Lake Tahoe, South Lake Shore	Pier 200 meters N from SOLA	MVS	TSP	48 Hours
SLT - SOLA (5)	South Lake Tahoe, South Lake Shore	30 meters N from Hwy 50	TWS	TSP, PM10, PM2.5	2 Weeks
SLT - Sandy Way (4)	South Lake Tahoe, South Lake Inland	40 meters S from Hwy 50	TWS	TSP, PM10, PM2.5	2 Weeks
Bliss State Park (6)	West Lake Shore Inland Mountain	20 meters W from Hwy 89	MVS	TSP	1 Week
Wallis Res - Tower (7)	West Lake Shore	20 meters E from Hwy 89	MVS	TSP	1 Week
Wallis Res - Pier (17)	West Lake Shore	Pier 50 meters E from Tower	MVS	TSP	1 Week
Buoy TB1 East (14)	Mid Lake North East	-	MVS	TSP	24 Hours
Buoy TB4 West (14)	Mid Lake North West	-	MVS	TSP	24 Hours
Big Hill (1)	Outside the Basin Near Loon Lake	25 miles SW of DL Bliss	TWS	TSP, PM10, PM2.5	2 Weeks

* (#) indicates number of site as depicted on map in Figure 3-1.

Figure 3-1. Map of LTADS study sites and activities at each site - November 2002 to March 2004.

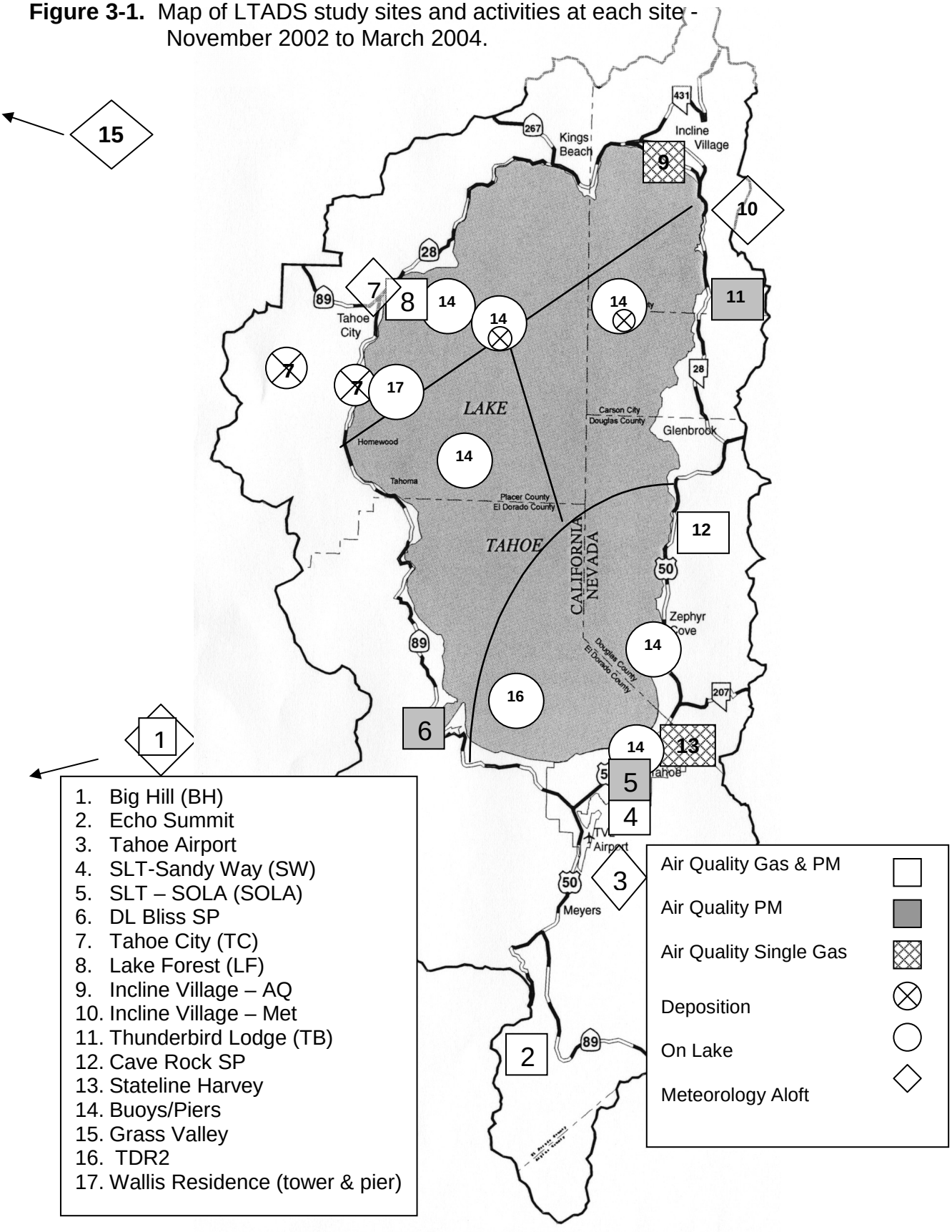

3.1 Data Quality

The monitoring programs in place before the initiation of LTADS have standard, established quality assurance protocols. The quality assurance for these two programs can be examined at websites identified in the following paragraphs.

The federal Environmental Protection Agency's Aerometric Information Retrieval System (AIRS) quality assurance programs have set guidelines for historical and current regulatory air quality gas and aerosol data. These guidelines apply to such data collected at Tahoe and are discussed in full detail at the following world wide web location: http://www.epa.gov/oar/oaqps/qa/.

Quality Assurance activities for the federal IMPROVE network and the associated TRPA sampling programs, applicable to samples collected at Tahoe, can be found in section 2.8 of "Semi-Annual Data Summary Report for Chemical Speciation of PM2.5 Filter Samples Project, July 8 to December 31, 2003, RTI." This report completed on August 26, 2004 can be found at the following world wide web location: http://www.epa.gov/ttn/amtic/files/ambient/pm25/spec/datsumspec.pdf.

The focus of this chapter is quality assurance of the remaining four general types of air quality sampling programs used to develop the LTADS deposition estimates. This section is also intended to provide sufficient analytical detail to give other researchers and interested scientists a fuller understanding of the strengths and weaknesses of the LTADS database. Please refer to the CARB LTADS website (http://www.arb.ca.gov/research/ltads/ltads.htm) or the TRPA TIIMS website (http://www.tiims.org/) for guidance on accessing the data collected during LTADS.

3.1.1 TWS and MVS Data

LTADS established a network of Two Week Samplers (TWS) whose performance during the Children's Health Study (CHS) showed ruggedness, reliability, and the ability to accommodate a nearly complete suite of chemical species measurements (Fitz, et al., 1996). This system was operated at a flow rate of 1.3 liter per minute (lpm). TWS included gaseous denuders for ammonia and nitric acid and filter collections for mass, ions, elements, and organic species for three size cuts of total suspended particulate matter (TSP), PM below 10 micrometers in aerodynamic diameter (PM10), and PM below 2.5 micrometers in aerodynamic diameter (PM2.5).

The TWS filter system likely converted peroxy and alk-oxy acetyl nitrates (PAN type species), which are also recognized as organic nitrates, into nitrate either through the Teflon filter itself or through the back-up filter. LTADS nitrates concentrations should therefore be treated as an upper limit of true nitrate concentrations at Tahoe.

The TWS denuder system has also been tested and found reliable for nitric acid (Fitz, et al., 1996). However, nitrous acid (HONO) is recognized to be an artifact included in this measurement approach. As such, LTADS nitric acid concentration data should be treated as an upper limit of true nitric acid concentrations at Tahoe. The ammonia TWS denuder system followed the standard methodologies developed for ammonia

extraction from annular denuder. The same measurement technique, used onboard the airplane for measurements aloft, experienced problems with high blank values (Carroll et al., 2004 and Zhang et al., 2002). Although field blank values for NH_3 were comparable to the minimum measurements at Thunderbird Lodge, the cleanest TWS site during LTADS, most of the NH_3 measurements by TWS were well above the field blank amounts.

The Mini-Volume Sampler (MVS) network used the standard Air Metrics Mini-Volume Sampler, which operates at 5.0 lpm. These were generally equipped with the same type of Teflon filters as for the TWS network. Unlike the TWS filter network that was equipped with a back-up filter to sequester volatilized nitric acid and nitrates, the MVS network had no back-up filters.

3.1.2 DRI TWS and MVS Data Validation

TSP, PM10, and PM2.5 samples were gravimetrically analyzed for total mass concentration and detailed chemical speciation profiles. A total of 129 sets of TWS samples, including TSP, PM10, and PM2.5, 36 sets for buoy Mini-Vol TSP samples, and 129 sets for non-buoy Mini-Vol TSP samples were collected in LTADS. Replicate analysis was performed on 10% of the ambient samples.

Field blanks were collected to subtract the background contribution from the sampling environment and field operation. TWS field blanks were only collected at SOLA. MVS field blanks were collected at the Wallis Tower and Zephyr Cove. The limited, variable, and site-specific field blanks increase the uncertainty of ambient sample concentrations.

The chemical data were evaluated for internal consistency by examining the physical consistency and balance of reconstructed mass, based on chemical species versus measured mass. In general, the samples collected met the criteria of internal physical consistency. A few TWS samples were suspected to be outliers; however, no field flag was noted for these samples (with the exception of one laboratory flag).

The annual average mass concentrations and chemical species were the highest in TSP and the lowest in PM2.5 at the same site; however such physical consistency was not necessarily observed for TWS samples in every sampling period. Such sampling artifacts can result from a number of factors: 1) the TWS design and low sampling flow rate of 1.3 liters per minute, which can contribute to an undersampling of TSP, 2) the frequently low mass concentration of ambient particulate matter in the Tahoe Basin, 3) the random bounce and penetration of particles larger than the 50% cutpoint of the sampling inlet, and 4) the potential sampling artifacts of semi-volatile species associated with the long sampling duration (2-weeks).

Scatter plots of duration showed that Mini-Vol samples were poorly correlated spatially and temporally; therefore, temporal and spatial variations were only examined for TWS samples. The highest annual average TSP (21.9 $\mu g/m^3$) and PM10 (18.8 $\mu g/m^3$) mass concentrations were observed at the SOLA site and the highest annual average PM2.5 mass concentration (9.0 $\mu g/m^3$) was observed at the SW site. The lowest TSP, PM10, and PM2.5 mass concentration were 6.2, 6.0, and 3.6 $\mu g/m^3$, respectively, and were

observed at the TB site. Similar annual averages of organic carbon (OC), elemental carbon (EC), ammonium, and sulfate in TSP, PM10, and PM2.5 were observed. PM10 mass comprised 80-90% of TSP mass and was approximately twice that of PM2.5 mass. The most abundant chemical species were OC (16.5%-29.8%), silicon (10.8%-16.0%), and aluminum (3.9%-4.7%) for TSP; OC (16.2%-27.8%), silicon (10.0%-21.1%), and aluminum (3.5%-6.6%) for PM10; and OC (42.1%-52.0%), EC (4.9%-16.4%), and ammonium (3.1%-5.8%) for PM2.5.

The lowest TWS TSP, PM10, and PM2.5 mass concentrations were observed from March to April 2003 at all five sites. TWS TSP, PM10, and PM2.5 mass concentrations observed at the BH, TB, and LF sites from May to October 2003 were twice as high as those observed from November 2002 to February 2003; however, TWS TSP, PM10, and PM2.5 mass concentrations were comparable during these two periods at the SOLA and SW sites. The elevated TWS TSP, PM10, and PM2.5 mass concentrations at the SOLA and SW sites from November 2002 to February 2003 were due to elevated OC and EC concentrations, which were likely the result of increased traffic volume for winter activities. Wood smoke also contributed to elevated PM2.5 mass concentrations during winter.

3.1.3 Sample Preparation, Shipment, Receiving, and Analysis

3.1.3.1 Sample Preparation

3.1.3.1.1 Configurations of TWS and Mini-Volume Samplers in the LTADS

Filter-based measurements of atmospheric pollutants were obtained using two types of samplers: Two Week Samplers (TWS) and AirMetrics Mini-Vol samplers. The TWS were operated for two-week durations and collected integrated samples representing total suspended particulate (TSP), PM10 and PM2.5 (particles with aerodynamic diameters less than 10 and 2.5 µm, respectively), and nitric acid and ammonia via denuder measurements. The TWS were operated at a nominal flow rate of 1.3 lpm from 11/20/02 to 01/06/04 at five sites (four sites in the Tahoe Basin and one site upwind of the Basin).

The Mini-Vol samplers without PM2.5 or PM10 inlets (i.e., TSP samples) were deployed on lake buoys, piers, and at some land-based sites. All of the buoy samples and a few of the pier samples were collected for the duration of the sampler battery (typically 24-30 hours). The duration of the non-buoy samples that operated on AC power varied due to sampler malfunctions; typically, the sampling filters were replaced on a weekly schedule. The Mini-Vol samplers were operated at a nominal flow rate of 5.0 lpm from 09/26/02 to 04/26/04.

Each TWS had eight channels: three channels contained Teflon-membrane filters to measure TSP, PM10 and PM2.5 mass and elements; three channels contained quartz filters to measure TSP, PM10, and PM2.5 ions and carbon; and two channels were used to collect ammonia and nitric acid denuder samples. Mini-Vol samplers were run in pair, where one sampler contained a Teflon-membrane filter and the other contained a quartz-fiber filter. All sampling media collected by the TWS and Mini-Vol samplers

were prepared and chemically analyzed by the Desert Research Institute's Environmental Analysis Facility.

3.1.3.1.2 Sampling Media

Teflon-membrane filters were equilibrated for weighing after passing acceptance testing by X-ray flourescence (XRF). Initial weights were performed after the filters equilibrated for a minimum of four weeks. A minimum of two filters per lot (approximately 100 filters per lot) received from the manufacturer were analyzed for chemical species to verify that pre-established specifications had been met. The lot was rejected if the verification filters did not pass this acceptance test. Each filter was individually examined over a light table prior to use for discoloration, pinholes, creases, or other defects. In addition to laboratory blanks, 5 to 10% of all filters were designated as field blanks per standard operating procedures.

Quartz-fiber filters absorb organic gases from ambient air and organic artifacts from the manufacturing process. By pre-firing the quartz-fiber filters, these absorbed gases and artifacts are reduced to constant, insignificant, levels. The filters were pre-fired in preparation for thermal/optical reflectance carbon (TOR) analysis, which is a thermal desorption process subjecting the filters to temperatures between 25 to 800^{o} C; therefore, the filters were pre-fired at 900^{o} C to remove all possible TOR analysis interferences. Sets of filters with levels that exceeded 1.5 µg/cm^{2} for organic carbon (OC) and 0.5 µg/cm^{2} for elemental carbon (EC) were re-fired or rejected. Pre-fired filters were sealed and stored in a freezer prior to preparation for field sampling.

Cellulose fiber filters were impregnated with a solution of sodium chloride (5% NaCl, 5% glycerol and 90% distilled de-ionized water [DDW]) and used for the collection of volatilized nitrate. These filters were prepared in batches and subjected to acceptance testing prior to use in accordance with DRI SOP #2-104.3. Filter packs for the TWS were prepared in accordance with the CARB standard operating procedures (SOP) for TWS. Glass denuders were coated and handled according to the CARB SOP for TWS. Filter packs for the Mini Vol samplers were prepared in accordance with DRI's SOP # 2-110.4.

3.1.3.1.3 Sample Shipping and Receiving

The TWS filter packs were packaged and shipped to two locations for deployment. Filter packs for the Lake Forest (LF) and Big Hill (BH) sites were shipped to the CARB in Sacramento, CA; filter packs for the South Lake Tahoe (SL), Thunderbird (TB), and Sandy Way (SW) sites were shipped to the Tahoe Regional Planning Agency (TRPA) in South Lake Tahoe, CA. Each sampling set of eight filter packs was sealed in large, re-closable freezer bags (with the site marked on the outside of each bag and the associated field data sheet enclosed).

Mini-Vol sampler filter packs were packaged and shipped to two locations for deployment at the request of the operator. Due to sampler variation, two types of holders were deployed. The filters for use at the North Shore (NS) site were loaded into blue cassettes and shipped to the Tahoe Research Group, Tahoe City, CA. The filters

for use at the South Shore (SS) site were loaded into nucleopore holders and shipped to the TRPA, South Lake Tahoe, CA. Mini-Vol sampler filter packs were sealed in reclosable bags with a field data sheet for each set of filters (paired Teflon-membrane and quartz-fiber filter packs).

All filter packs were placed in coolers refrigerated with blue ice for shipment. The coolers were then shipped by second-day service for arrival by Tuesday of the designated sample change-out week. Entries of the shipment and the sample ID of the filter packs were made in the DRI/EAF shipping logbook.

3.1.3.2 Analysis Methods

3.1.3.2.1 Gravimetric Analysis

Unexposed and exposed Teflon-membrane filters were equilibrated at a temperature of 21.5 ± 1.5^{o} C and a relative humidity of 35 ± 5% for a minimum of 24 hours prior to weighing (Chow et al., 2005). Weighing was performed on a Mettler MT-5 electro microbalance with ±0.001 mg sensitivity. The charge on each filter was neutralized by exposure to a polonium-210 source for 30 seconds before the filter was placed on the balance pan. The balance was calibrated with a 200 mg Class S weight and the tare was set prior to weighing each batch of filters. After every 10 filters were weighed, the calibration and tare were re-checked. If the results of these performance tests deviated from specifications by more than ±5 µg, the balance was re-calibrated.

All initial filter weights were checked by an independent technician. Samples were re-weighed if these check-weights did not agree with the original weights within ±0.010 mg. At least 30% of the exposed filter weights were checked by an independent technician. Samples were re-weighed if these check-weights did not agree with the original weights within ±0.015 mg. Pre- and post-weights, check weights, and re-weights (if required) were recorded on data sheets and directly entered into a data base via an RS232 connection. All weights were entered by filter number into the DRI aerosol data base.

3.1.3.2.2 Elements by XRF

After gravimetric analysis, a Kevex model 700 energy dispersive X-ray fluorescence analyzer (EDXRF) (Watson, et al, 1999) was used to quantify sodium (Na), magnesium (Mg), aluminum (Al), silicon (Si), phosphorus (P), sulfur (S), chlorine (Cl), potassium (K), calcium (Ca), titanium (Ti), vanadium (V), chromium (Cr), manganese (Mn), iron (Fe), cobalt (Co), nickel (Ni), copper (Cu), zinc (Zn), gallium (Ga), arsenic (As), selenium (Se), bromine (Br), rubidium (Rb), strontium (Sr), yttrium (Y), zirconium (Zr), molybdenum (Mo), palladium (Pd), silver (Ag), cadmium (Cd), indium (In), tin (Sn), antimony (Sb), barium (Ba), gold (Au), mercury (Hg), thallium (Tl), lead (Pb), lanthanum (La), and uranium (U) on Teflon-membrane samples. Calibration was performed using thin film standards from Micromatter Inc. A multi-element thin film standard was analyzed with each run to monitor for calibration drift and was used as the indicator for routine calibrations.

3.1.3.2.3 Organic and Elemental Carbon

The thermal/optical reflectance (TOR) method measures total carbon (TC), organic carbon (OC) and elemental carbon (EC). The TOR method is based on the principle that different types of carbon-containing particles are converted to gases under designated temperature and oxidation conditions. These specific carbon fractions also help to distinguish between seven carbon fractions reported by TOR, following the Interagency Monitoring of Protected Visual Environments (IMPROVE) protocol (Chow, et al, 1993):

- The carbon evolved in a helium (He) atmosphere at temperatures between ambient (~25^{o} C) and 120^{o} C (OC1)
- The carbon evolved in a He atmosphere at temperatures between 120^{o} C and 250^{o} C (OC2)
- The carbon evolved in a He atmosphere at temperatures between 250^{o} C and 450^{o} C (OC3)
- The carbon evolved in a He atmosphere between 450^{o} C and 550^{o} C (OC4)
- The carbon evolved in an oxidizing atmosphere at 550^{o} C (EC1)
- The carbon evolved in an oxidizing atmosphere between 550^{o} C and 700^{o} C (EC2)
- The carbon evolved in an oxidizing atmosphere between 700^{o} C and 800^{o} C (EC3)

The thermal/optical reflectance carbon analyzer consists of a thermal system and an optical system. The thermal system consists of a quartz tube placed inside a coiled heater. Current through the heater is controlled to attain and maintain pre-set temperatures for given time periods. A portion of a quartz-fiber filter is placed in the heating zone and heated to designated temperatures under non-oxidizing and oxidizing atmospheres. The optical system consists of a He-Ne laser, a fiber optic transmitter and receiver, and a photocell. The filter deposit faces a quartz light tube so that the intensity of the reflected laser beam can be monitored throughout the analysis.

As the temperature is increased from ambient (~25^{o} C) to 550^{o} C in a non-oxidizing He atmosphere, OC compounds are volatilized from the filter while EC is not oxidized. When oxygen (O_2) is added to the He at temperatures greater than 550^{o} C, the EC burns and enters the sample stream. The evolved gases pass through an oxidizing bed of heated manganese dioxide, where they are oxidized to carbon dioxide (CO_2), and then across a heated nickel catalyst that reduces the CO_2 to methane (CH_4). The CH_4 is then quantified with a flame ionization detector (FID).

The reflected laser light is continuously monitored throughout the analysis cycle. The negative change in reflectance is proportional to the degree of pyrolytic conversion from OC to EC that occurs during OC analysis. After O_2 is introduced, the reflectance increases rapidly as the light-absorbing carbon is burned off of the filter. The carbon measured after the reflectance attains the value it had at the beginning of the analysis cycle is classified as EC. This adjustment for pyrolysis can be as high as 25% of OC or EC and therefore cannot be ignored.

The instrument was calibrated by analyzing samples of known amounts of CH_4, CO_2 and potassium hydrogen phthalate (KHP). The FID response was compared to a reference level of CH_4 injected at the end of each sample analysis. Performance tests of the instrument's calibration were conducted at the beginning and end of each day's operation. Intervening samples were re-analyzed when calibration changes greater than ±10% are found.

Known amounts of American Chemical Society (ACS) certified reagent grade crystal sucrose and KHP were committed to TOR as a verification of the OC fractions. Fifteen different standards were used for each calibration; however, widely accepted primary standards for EC and OC are still lacking. Results of the TOR analysis of each filter were entered into the DRI data base.

3.1.3.2.4 Inorganic Ion Analyses

Water-soluble chloride, nitrate, sulfate, ammonium, sodium, magnesium, calcium, and potassium were obtained by extracting the quartz-fiber particle filter in 15 ml of DDW. The extraction vials were capped and sonicated for 60 minutes, shaken for 60 minutes, then aged overnight to assure complete extraction of the deposited material in the solvent. The ultrasonic bath water was monitored to prevent temperature increases from the dissipation of ultrasonic energy in the water. After extraction, these solutions were stored under refrigeration prior to analysis.

3.1.3.2.5 Ion Chromatographic Analysis for Chloride, Nitrate, and Sulfate

Water-soluble chloride (Cl^-), nitrate (NO_3^-), and sulfate ($SO_4^=$) were measured with the Dionex 2020i (Sunnyvale, CA) ion chromatograph (IC) (Chow and Watson, 1999). The IC uses an ion-exchange column to separate the sample ions in time for individual quantification by a conductivity detector. Prior to detection, the column effluent enters a suppressor column where the chemical composition of the component is altered and results in a matrix of low conductivity. The ions are identified by their elution/retention times, and are quantified by the conductivity peak area. Approximately 2.0 ml of the filter extract are injected into the IC. The resulting peaks are integrated and the peak integrals are converted to concentrations using calibration curves derived from solution standards. The Dionex system for the analysis of Cl^-, NO_3^-, and $SO_4^=$ contains a guard column (AG4a column, Cat. No. #37042), an anion separator column (AS4a column, Cat. No. #37041) with a strong basic anion exchange resin, and an anion micro-membrane suppressor column (250 ´ 6 mm ID) with a strong acid ion exchange resin. The anion eluent consists of sodium carbonate (Na_2CO_3) and sodium bicarbonate ($NaHCO_3$) prepared in DDW. The DDW is verified to have a conductivity of less than 1.8 ´ 10-5 ohm/cm prior to preparation of the eluent. For quantitative determinations, the IC is operated at a flow rate of 2.0 ml per minute.

The primary standard solution containing NaCl, $NaNO_3$, and $(Na)_2SO_4$ were prepared with reagent-grade salts dried in an oven for one hour at 105^o C and then brought to room temperature in a desicator. The anhydrous salts were weighed to the nearest 0.10 mg on a routinely calibrated analytical balance under controlled temperature (~20

^{O}C) and relative humidity (±30%). The salts were then diluted in precise volumes of DDW. Calibration standards were prepared at least once per month by diluting the primary standard solution to concentrations covering the range expected in the filter extracts. The standards were then stored in a refrigerator. Calibration concentrations of 0.1, 0.2, 0.5, 1.0, and 2.0 mg/ml were prepared or each of the analysis species.

Calibration curves were performed weekly. Chemical compounds were identified by matching the retention time of each peak in the unknown sample with the retention times of peaks in the chromatograms of the standards. A DDW blank was analyzed after every 20 samples and a calibration standard was analyzed after every 10 samples. These quality control checks verified the baseline and the calibration, respectively. Environmental Research Associates (ERA, Arvada, CO) standards were used daily as an independent quality assurance (QA) check. These standards (ERA Wastewater Nutrient and ERA Mineral WW) are traceable to the National Institute of Standards and Technology (NIST) simulated rainwater standards. If the values obtained for these standards did not coincide within a pre-specified uncertainty level (typically three standard deviations of the baseline level, or ±5%), the samples analyzed between that standard and the previous calibration standards were re-analyzed.

After analysis, the printout for each sample in the batch was reviewed for the following: 1) proper operational settings, 2) correct peak shapes and integration windows, 3) peak overlaps, 4) correct background subtraction, and 5) quality control sample comparisons. When values for replicates differed by more than ±10% or values for standards differed by more than ±5%, samples before and after these quality control checks were designated for re-analysis in a subsequent batch. Individual samples with unusual peak shapes, background subtractions, or deviations from standard operating parameters were also designated for re-analysis.

Water soluble nitrate and nitric acid concentrations were obtained from the cellulose backup filter and the nitric acid denuder, respectively, using the same IC analysis procedure. IC analysis procedures are detailed in DRI SOP # 2-203.5.

3.1.3.2.6 Ammonium Analysis

An Astoria 2 Automated Colorimetry (AC) system (Astoria–Pacific, Clackamas, OR) was used to measure ammonium concentrations by the indolphenol method. Each sample was mixed with reagents and subjected to appropriate reaction periods before submission to the colorimeter. Beer's Law relates the liquid's absorbency to the amount of the ion in the sample. A photomultiplier tube measured this absorbency through an interference filter specific to ammonium. Two ml of extract in a sample vial were placed in a computer-controlled auto-sampler. Calibration curves were produced with each daily batch of samples.

Ammonia concentrations from the citric acid denuders were determined using the same analysis method.

3.1.3.2.7 Atomic Absorption Analysis for Soluble Metals

Soluble sodium, magnesium, potassium and calcium were measured using a Varian Spectra AA-880 atomic absorption spectrophotometer. In atomic absorption spectrophotometry, the sample is aspirated into a flame and atomized. A light beam from a hollow cathode lamp is directed through the flame into a monochromator, and then onto a photoelectric detector that measures the amount of light absorbed by the atomized element in the flame. The cathode of a hollow cathode lamp contains the pure metal which results in a line source emission spectrum. Since each element has its own characteristic absorption wavelength, the source lamp composed of that element is used. The amount of energy of the characteristic wavelength absorbed in the flame is proportional to the concentration of the element in the sample. Calibration curves were produced with each daily batch of samples.

3.1.3.2.8 Nitric Acid & Ammonia – TWS Limits of Detection and Uncertainties

For various reasons, the first seven samples at Big Hill and 13 samples at other sites failed to properly collect any material for analysis. Additionally, two nitric acid and three ammonia cassettes failed leak checks; the concentrations are reported with the proper warnings attached. Nitric acid and ammonia concentrations were above uncertainty levels 99% and 96% of the time, respectively:

Tarnay et al. (2001) reported minimum detection limits of approximately 0.30 ug/m^3 for nitric acid and ammonia for a field study in the Tahoe Basin. Adjusting for different flow rates and sampling duration (Tarnay et al. (2001) sampled at 10 lpm for 12 hours while LTADS TWS sampled at 1.3 lpm for two weeks), an equivalent detection limit (using same laboratory equipment and procedures) for the LTADS TWS measurements is about 0.08 ug/m^3. This detection value is comparable to the minimum nitric acid concentration of 0.08 ug/m^3 but twice the minimum ammonia concentration reported during LTADS with the TWS sampler.

3.1.4 Database Management and Data Validation

Numerous air quality studies have been conducted over the past decade, but the data are not often available or applicable to analysis and modeling because the databases lack documentation with regard to sampling and analysis methods, quality control/quality assurance procedures, accuracy specifications, precision calculations, and data validity. Lioy et al. (1980), Chow and Watson (1989), Watson and Chow (1992), and Chow and Watson (1994a) summarized the requirements, limitations, and current availability of ambient and source databases in the United States. The data sets for LTADS intend to meet these requirements. The data files for this study have the following attributes:

- They contain the ambient observables needed to assess source and receptor relationships.
- They are available in a well-documented, computerized form accessible by personal computers and over the Internet.
- Measurement methods, locations, and schedules are documented.

- Precision and accuracy estimates are reported.
- Validation flags are assigned.

This section introduces the features, data structures, and contents of the LTADS data archive. **Figure 3-2** illustrates the approach followed to obtain the final data files. These data are available on floppy diskettes in Microsoft Excel format for convenient distribution to data users. The file extension identifies the file type according to the following definitions:

- TXT = ASCII text file
- DOC = Microsoft Word document
- XLS = Microsoft Excel spreadsheet

The assembled aerosol database for filter pack measurements taken during LTADS is fully described in the Microsoft Excel file (see **Table 3-2**), which documents variable names, descriptions, and measurement units.

Figure 3-2. Flow diagram of the database management system.

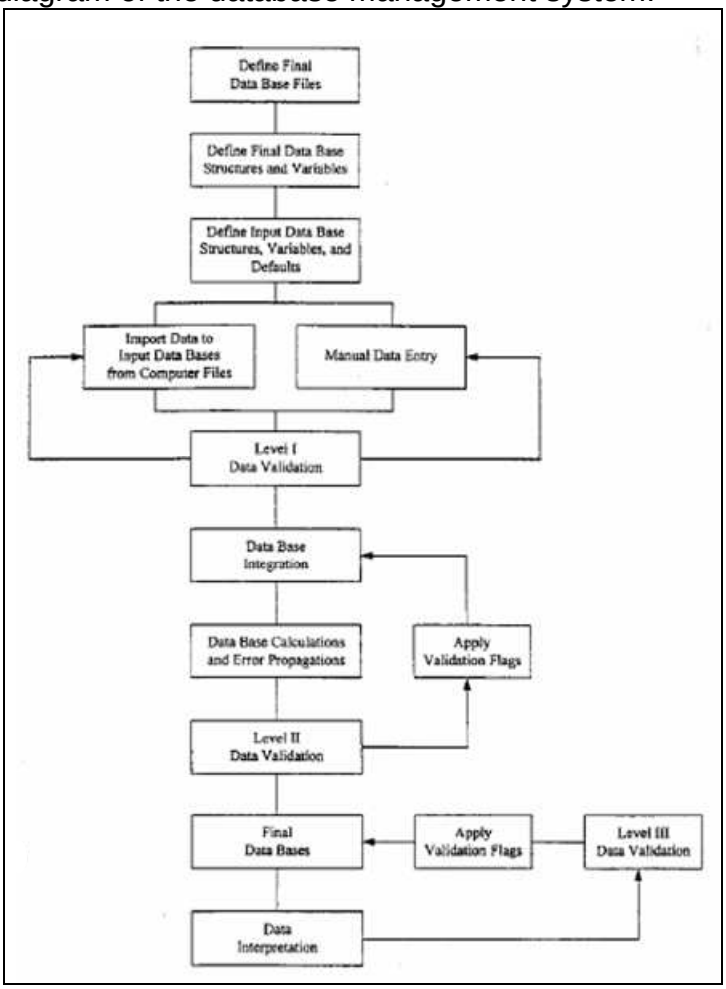

Table 3-2. Variable names, descriptions, and measurement units in the assembled aerosol database for filter pack measurements taken during the study.

Field Code Description Measurement Unit

SITE - Sampling site
DATE - Sampling date
SIZE - Sample particle size cut, µm
DATEI - Sample start date
DATEF - Sample end date
TID - Teflon filter pack ID
QID - Quartz filter pack ID
TFFLG - Teflon filter pack field flag
QFFLG - Quartz filter pack field flag
MSGF - Gravimetry analysis flag
NHCF - Ammonia analysis flag
HNIF - Volatilized nitrate analysis flag
ANIF - Anion analysis flag
N4CF - Ammonium analysis flag
KPAF - Soluble potassium analysis flag
OETF - Carbon analysis flag
ELXF - XRF analysis flag
TVOC - Teflon filter volume, m^3
TVOU - Teflon filter volume uncertainty, m^3
QVOC - Quartz filter volume, m^3
QVOU - Quartz filter volume uncertainty, m^3
MSGC - Mass concentration, $\mu g/m^3$
MSGU - Mass concentration uncertainty, $\mu g/m^3$
NHCC - Ammonia (NH_3) concentration, $\mu g/m^3$
NHCU - Ammonia (NH_3) concentration uncertainty, $\mu g/m^3$
HNIC - Volatilized nitrate concentration, $\mu g/m^3$
HNIU - Volatilized nitrate concentration uncertainty, $\mu g/m^3$
CLIC - Chloride concentration, $\mu g/m^3$
CLIU - Chloride concentration uncertainty, $\mu g/m^3$
N3IC - Nitrate concentration, $\mu g/m^3$
N3IU - Nitrate concentration uncertainty, $\mu g/m^3$
S4IC - Sulfate concentration, $\mu g/m^3$
S4IU - Sulfate concentration uncertainty, $\mu g/m^3$
N4CC - Ammonium concentration, $\mu g/m^3$
N4CU - Ammonium concentration uncertainty, $\mu g/m^3$
KPAC - Soluble Potassium concentration, $\mu g/m^3$
KPAU - Soluble Potassium concentration uncertainty, $\mu g/m^3$
O1TC - Organic Carbon fraction one concentration, $\mu g/m^3$
O1TU - OC fraction one concentration uncertainty, $\mu g/m^3$
O2TC - Organic Carbon fraction two concentration, $\mu g/m^3$
O2TU - OC fraction two concentration uncertainty, $\mu g/m^3$
O3TC - Organic Carbon fraction three concentration, $\mu g/m^3$

Table 3-2 (continued)

O3TU - OC fraction three concentration uncertainty, µg/m^3
O4TC - Organic Carbon fraction four concentration, µg/m^3
O4TU - OC fraction four concentration uncertainty, µg/m^3
OPTC - Pyrolyzed Organic carbon concentration, µg/m^3
OPTU - Pyrolyzed OC concentration uncertainty, µg/m^3
OCTC - Organic Carbon concentration, µg/m^3
OCTU - Organic Carbon concentration uncertainty, µg/m^3
E1TC - Elemental Carbon fraction one concentration, µg/m^3
E1TU - EC fraction one concentration uncertainty, µg/m^3
E2TC - Elemental Carbon fraction two concentration, µg/m^3
E2TU - EC fraction two concentration uncertainty, µg/m^3
E3TC - Elemental Carbon fraction three concentration, µg/m^3
E3TU - EC fraction three concentration uncertainty, µg/m^3
ECTC - Elemental Carbon concentration, µg/m^3
ECTU - Elemental Carbon concentration uncertainty, µg/m^3
TCTC - Total Carbon concentration, µg/m^3
TCTU - Total Carbon concentration uncertainty, µg/m^3
NAXC - Sodium concentration, µg/m^3
NAXU - Sodium concentration uncertainty, µg/m^3
MGXC - Magnesium concentration, µg/m^3
MGXU - Magnesium concentration uncertainty, µg/m^3
ALXC - Aluminum concentration, µg/m^3
ALXU - Aluminum concentration uncertainty, µg/m^3
SIXC - Silicon concentration, µg/m^3
SIXU - Silicon concentration uncertainty, µg/m^3
PHXC - Phosphorous concentration, µg/m^3
PHXU - Phosphorous concentration uncertainty, µg/m^3
SUXC - Sulfur concentration, µg/m^3
SUXU - Sulfur concentration uncertainty, µg/m^3
CLXC - Chlorine concentration, µg/m^3
CLXU - Chlorine concentration uncertainty, µg/m^3
KPXC - Potassium concentration, µg/m^3
KPXU - Potassium concentration uncertainty, µg/m^3
CAXC - Calcium concentration, µg/m^3
CAXU - Calcium concentration uncertainty, µg/m^3
TIXC - Titanium concentration, µg/m^3
TIXU - Titanium concentration uncertainty, µg/m^3
VAXC - Vanadium concentration, µg/m^3
VAXU - Vanadium concentration uncertainty, µg/m^3
CRXC - Chromium concentration, µg/m^3
CRXU - Chromium concentration uncertainty, µg/m^3
MNXC - Manganese concentration, µg/m^3
MNXU - Manganese concentration uncertainty, µg/m^3
FEXC - Iron concentration, µg/m^3

Table 3-2 (continued)

FEXU - Iron concentration uncertainty, µg/m^3
COXC - Cobalt concentration, µg/m^3
COXU - Cobalt concentration uncertainty, µg/m^3
NIXC - Nickel concentration, µg/m^3
NIXU - Nickel concentration uncertainty, µg/m^3
CUXC - Copper concentration, µg/m^3
CUXU - Copper concentration uncertainty, µg/m^3
ZNXC - Zinc concentration, µg/m^3
ZNXU - Zinc concentration uncertainty, µg/m^3
GAXC - Gallium concentration, µg/m^3
GAXU - Gallium concentration uncertainty, µg/m^3
ASXC - Arsenic concentration, µg/m^3
ASXU - Arsenic concentration uncertainty, µg/m^3
SEXC - Selenium concentration, µg/m^3
SEXU - Selenium concentration uncertainty, µg/m^3
BRXC - Bromine concentration, µg/m^3
BRXU - Bromine concentration uncertainty, µg/m^3
RBXC - Rubidium concentration, µg/m^3
RBXU - Rubidium concentration uncertainty, µg/m^3
SRXC - Strontium concentration, µg/m^3
SRXU - Strontium concentration uncertainty, µg/m^3
YTXC - Yttrium concentration, µg/m^3
YTXU - Yttrium concentration uncertainty, µg/m^3
ZRXC - Zirconium concentration, µg/m^3
ZRXU - Zirconium concentration uncertainty, µg/m^3
MOXC - Molybdenum concentration, µg/m^3
MOXU - Molybdenum concentration uncertainty, µg/m^3
PDXC - Palladium concentration, µg/m^3
PDXU - Palladium concentration uncertainty, µg/m^3
AGXC - Silver concentration, µg/m^3
AGXU - Silver concentration uncertainty, µg/m^3
CDXC - Cadmium concentration, µg/m^3
CDXU - Cadmium concentration uncertainty, µg/m^3
INXC - Indium concentration, µg/m^3
INXU - Indium concentration uncertainty, µg/m^3
SNXC - Tin concentration, µg/m^3
SNXU - Tin concentration uncertainty, µg/m^3
SBXC - Antimony concentration, µg/m^3
SBXU - Antimony concentration uncertainty, µg/m^3
BAXC - Barium concentration, µg/m^3
BAXU - Barium concentration uncertainty, µg/m^3
LAXC - Lanthanum concentration, µg/m^3
LAXU - Lanthanum concentration uncertainty, µg/m^3
AUXC - Gold concentration, µg/m^3

Table 3-2 (continued)

AUXU - Gold concentration uncertainty, µg/m^3
HGXC - Mercury concentration, µg/m^3
HGXU - Mercury concentration uncertainty, µg/m^3
TLXC - Thallium concentration, µg/m^3
TLXU - Thallium concentration uncertainty, µg/m^3
PBXC - Lead concentration, µg/m^3
PBXU - Lead concentration uncertainty, µg/m^3
URXC - Uranium concentration, µg/m^3
URXU - Uranium concentration uncertainty, µg/m^3
COMMENT - Sampling and/or analysis comments

3.1.5 Database Structures and Features

The raw LTADS data were processed with Microsoft FoxPro 2.6 for Windows (Microsoft Corp., 1994), a commercially available relational database management system. FoxPro can accommodate 256 fields of up to 4,000 characters per record and up to one billion records per file. This system can be implemented on most IBM PC-compatible desktop computers. The database files (*.DBF) can also be read directly into a variety of popular statistical, plotting, database, and spreadsheet programs without requiring any specific conversion software. After processing, the final LTADS data were converted from FoxPro to Microsoft Excel format for reporting purposes.

In FoxPro, one of five field types (character, date, numerical, logical, or memo) was assigned to each observable. Sampling sites and particle size fractions were defined as "character" fields, sampling dates were defined as "date" fields, and measured data were defined as "numeric" fields, "logical" fields were used to represent a "yes" or "no" value applied to a variable, and "memo" fields accommodated large blocks of text and were used to document the data validation results.

Data contained in different database files can be linked by indexing on and relating to common attributes in each file. Generally, sampling site, sampling hour, sampling period, particle size, and sampling substrate IDs were the common fields used to relate the data between files.

To assemble the final data files, information was merged from many data files derived from field monitoring and laboratory analyses by relating information on the common fields cited above.

3.1.6 Measurement and Analytical Specifications

Every measurement consists of: 1) a value; 2) a precision; 3) an accuracy; and 4) a validity (Hidy, 1985; Watson et al., 1989, 1995). The measurement methods described in this chapter were used to obtain the value. Performance testing via regular submission of standards, blank analysis, and replicate analysis were used to estimate precision. The submission and evaluation of independent standards through quality audits were used to estimate accuracy. Validity applied to both the measurement

method and to each measurement taken with that method. The validity of each measurement was indicated by appropriate flagging within the database and the validity of the methods used in this study has been evaluated.

3.1.7 Definitions of Measurement Attributes

The precision, accuracy, and validity of the LTADS aerosol measurements are defined as follows (Chow et al., 1993):

- A **measurement** is an observation at a specific time and place that possesses: 1) value – the center of the measurement interval; 2) precision – the width of the measurement interval; 3) accuracy – the difference between measured and reference values; and 4) validity – the compliance with assumptions made in the measurement method.
- A **measurement method** is the combination of equipment, reagents, and procedures that provides the value of a measurement. The full description of the measurement method requires substantial documentation. For example, two methods may use the same sampling systems and the same analysis systems; however, they are not identical if one method performs acceptance testing on the filter media and the other does not. Seemingly minor differences between methods can result in major differences in measurement values.
- **Measurement method validity** is the identification of measurement method assumptions, the quantification of the effects of deviations from those assumptions, the evaluation that deviations are within reasonable tolerances for the specific application, and the creation of procedures to quantify and minimize those deviations during a specific application.
- **Sample validation** is accomplished by procedures that identify deviations from measurement assumptions and the assignment of flags to individual measurements to indicate for potential deviations from assumptions.
- The **comparability and equivalence of sampling and analysis methods** are established by the comparison of values and precisions for the same measurement obtained by different measurement methods. Inter-laboratory and intra-laboratory comparisons are usually made to establish this comparability. Simultaneous measurements of the same observable are considered equivalent when more than 90% of the values differ by no more than the sum of two one-sigma precision intervals for each measurement.
- **Completeness** measures how many environmental measurements with specified values, precisions, accuracies, and validities were obtained out of the total number attainable. It measures the practicability of applying the selected measurement processes throughout the measurement period. Databases which have excellent precision, accuracy, and validity may be of little use if they have so many missing values that data interpretation is impossible. A database with numerous data points, such as the one used in this study, requires detailed documentation of precision, accuracy, and validity of the measurements. This and following sections address the procedures followed to define these quantities and present the results of those procedures.

3.1.8 Definitions of Measurement Precision

Measurement precisions were propagated from precisions of the volumetric measurements, the chemical composition measurements, and the field blank variability using the methods of Bevington (1969) and Watson et al. (1995).

Dynamic field blanks were periodically placed in each sampling system without air being drawn through them to estimate the magnitude of passive deposition for the period of time during which the filter packs remained in a sampler. Field blanks for the TWS were collected only at the SOLA site. Field blanks for the MVS were collected at two sites - Wallis Tower and Zephyr Cove. No statistically significant differences in field blank concentrations were found for any species after removal of outliers (i.e., concentration exceeding three times the standard deviations of the field blanks). The average field blank concentrations (with outliers removed) were calculated for each species on each substrate (e.g., Teflon-membrane, quartz-fiber).

3.1.9 Analytical Specifications

Blank precisions (σBi) are defined as the higher value of the standard deviation of the blank measurements (STDBi) or the square root of the averaged squared uncertainties of the blank concentrations (SIGBi). If the average blank for a species was less than its precision, the blank was set to zero. The precisions (σMi) for XRF analysis were determined from counting statistics unique to each sample; therefore, the σMi is a function of the energy-specific peak area, the background, and the area under the baseline.

3.1.10 Quality Assurance

Quality control (QC) and quality auditing establish the precision, accuracy, and validity of measured values. Quality assurance (QA) integrates QC, quality auditing, measurement method validation, and sample validation into the measurement process. The results of quality assurance are data values with specified precisions, accuracies, and validities.

For TWS, field blanks were only acquired at SOLA; and only field blanks were acquired for Mini-Vol TSP samplers at Wallis Residence Platform and Zephyr Cove, as shown in **Table 3-3**. Replicate analyses were performed for ~10% of all ambient samples.

Quality audits of sample flow rates were conducted at the beginning, middle, and end of the study period, and these audits determined that flow rates were within ±10% of specifications. Data were submitted to three levels of data validation (Chow et al., 1994b; Watson et al., 2001). Detailed data validation processes are documented in the following subsections.

Table 3-3. Field blanks collected in LTADS (reported as concentration for typical air sample volume).

SITE	Start Date	End Date	Size	Period	Mass Concentration (ug)	Uncertainty of [mass] (ug)
Two Week Samplers						
SOLA	2002/12/4	2002/12/18	TSP	2	12.00	4.92
SOLA	2002/12/4	2002/12/18	PM10	2	9.00	4.92
SOLA	2002/12/4	2002/12/18	PM2.5	2	1.00	4.92
SOLA	2003/5/21	2003/6/4	TSP	14	30.00	7.40
SOLA	2003/5/21	2003/6/4	PM10	14	5.00	7.40
SOLA	2003/5/21	2003/6/4	PM2.5	14	5.00	7.40
SOLA	2003/7/16	2003/7/30	TSP	18	8.00	7.98
SOLA	2003/7/16	2003/7/30	PM10	18	1.00	7.98
SOLA	2003/7/16	2003/7/30	PM2.5	18	13.00	7.98
Mini-Vol Samplers						
Wallis Tower	2003/7/25	2003/8/1	TSP		15.00	7.24
Wallis Tower	2003/8/1	2003/8/8	TSP		6.00	7.24
Zephyr Cove	2003/7/8	2003/7/15	TSP		4.00	7.24

* Field blank samples set 2 and set 14 are used for the background subtraction for two week samplers from 12/4/2002 to 6/4/2003

** Field blank sample set 18 is used for the background subtraction for two week samplers from period 6/18/2003 to 1/6/2004

*** Average of Mini-vol sampler field blanks is used for the background subtraction for all mini-vol samples.

3.1.11 Data Validation

Ambient measurements can be sequentially subjected to four levels of data validation:

- Level 0 sample validation: designates data as they come off the instrument. This process ascertains that the field or laboratory instrument is functioning properly.
- Level I sample validation: 1) flags samples where significant deviation from measurement assumptions have occurred, 2) verifies computer file entries against data sheets, 3) eliminates values for measurements that are known to be invalid because of instrument malfunctions, 4) replaces data from a backup data acquisition system in the event of failure of the primary system, and 5) adjusts values for quantifiable calibration or interference biases.
- Level II sample validation applies consistency tests to the assembled data based on known physical relationships between variables.
- Level III sample validation is part of the data interpretation process. The first assumption upon finding a measurement that is inconsistent with physical expectations is that the unusual value is due to a measurement error. If, upon

tracing the path of the measurement, nothing unusual is found, then it may be assumed the value was the result of a valid environmental cause. Unusual values are identified during the data interpretation process as: 1) extreme values, 2) values which would otherwise normally track the values of other variables in a time series, and 3) values for observables which would normally follow a qualitatively predictable spatial or temporal pattern.

Air quality data acquired during LTADS were submitted to three data validation levels: 0, I, and II. Level I validation flags and comments are included with each data record in the database. Level II validation tests and results are described in the following subsections. Level II tests evaluate the chemical data for internal consistency. In this study, Level II data validations were made for: 1) physical consistency and 2) balance of reconstructed mass based on chemical species versus measured mass. Correlations and linear regression statistics were computed and scatter plots prepared to examine the data.

3.1.12 Physical Consistency

The compositions of chemical species concentrations measured by different chemical analysis methods were examined. Physical consistency was tested for: 1) sum of chemical species vs. measured mass, 2) $SO_4^=$ versus total sulfur (S), 3) ammonium balance, 4) anion/cation balance, and 5) K^+ versus total potassium (K).

3.1.12.1 Sum of chemical species vs. measured mass

Chemical species, including elements, ions, and cations analyzed by XRF, IC, and AA, respectively, and OC and EC, were summed and compared to mass measured by gravimetric analysis. Oxygen was not considered in the form of metal oxides and organic carbon; therefore, it was expected that the slope and ratio of the sum of chemical species to measured mass would be less than 1. The correlation (r^2) and intercept vary by site and sampling period and are dependent on chemical compositions in particulates; therefore, they are not used for data QA/QC. **Figure 3-3(a-c)** shows that the slopes between the sum of chemical species and measured mass at all five sites for TWS TSP, PM10, and PM2.5 were 0.40, 0.54, and 0.65, respectively. The average ratios between the sum of chemical species and measured mass for TWS TSP, PM10, and PM2.5 were 0.65, 0.68, and 0.84, respectively. The slopes in the scatter plots of sum of species to measured mass (**Figures 3-3d,e**) are 0.40 and 0.45, for TSP collected by Mini-vol sampler on lake shore (non-buoy Mini-vol samplers) and TSP collected by Mini-vol sampler on buoys (buoy Mini-vol sampler), respectively. The average ratio between the sum of chemical species and measured mass are generally less than one, except that for the buoy TSP Mini-vol samplers. The sampling duration for buoy TSP Mini-vol sampler is generally less than 24 hours with low TSP mass concentrations. In addition, the samples were left on the buoy till the scheduled collection date may results in high uncertainty of the sample quality. These slopes and ratios met the expected criteria. A lab flag was noted on 12/04/02 for the measured mass (fiber or fuzz observed on filter) at the Lake Forest site, which may explain the high measured mass but low sum of chemical species.

3.1.12.2 Sulfate ($SO_4^=$) versus total sulfur (S)

Sulfate was measured by IC analysis on quartz-fiber filters and S was measured by XRF analysis on Teflon-membrane filters. The mass ratio of $SO_4^=$:S should equal 3:1 if all S is present as $SO_4^=$. **Figure 3-4**(a-c) shows scatter plots of $SO_4^=$ versus S concentrations at five sites for TSP, PM10, and PM2.5. The average $SO_4^=$:S ratios for TSP, PM10, and PM2.5 were 2.1 ± 0.93, 2.3 ± 1.1, and 2.3 ± 1.0, respectively, which were lower than the 3:1 ratio. This suggests that a significant amount of S in particulate matter (PM) consists of non-soluble S compounds. The regression statistics gave slopes of 1.883 with an intercept of.0.033 µg/m^3 for TSP, 1.618 with an intercept of 0.117 µg/m^3 for PM10, and 1.651 with an intercept of 0.099 µg/m^3 for PM2.5. The correlation (r^2) between $SO_4^=$ and S increased from 0.60 to 0.76 as particle size range decreased from TSP to PM2.5, which agrees with the expectation that most of the S in PM2.5 is in the form of $SO_4^=$ and therefore better correlated. For the buoy TSP Mini-vol samplers, the average $SO_4^=$:S ratio in **Figure 3-4d** is 3.05 ± 2.41.and the slope is 2.17 with intercept of 0.04 µg/m^3 and high r^2 of 0.82; the average ratio is 2.83 ± 8.44 and the slope is 1.26 with intercept of 0.15 µg/m^3 and high r^2 of 0.41, for non-buoy TSP Mini-vol samplers (**Figure 3-4e**). The high standard deviation of the average $SO_4^=$:S ratio for the non-buoy TSP Mini-Vol samplers is probably due to the various sampling durations and locations. Nevertheless, the slopes of $SO_4^=$:S and average $SO_4^=$:S ratio are less than 3:1, which suggests that a significant amount of sulfur in PM consists of non-soluble sulfur compounds.

Figure 3-3. Comparisons of Sum of Chemical Species and Measured Mass at Five Sites for (a) TSP, b) PM10, and c) PM2.5, d) Buoy Mini-Vol TSP, and e) Non-buoy Mini-Vol TSP.

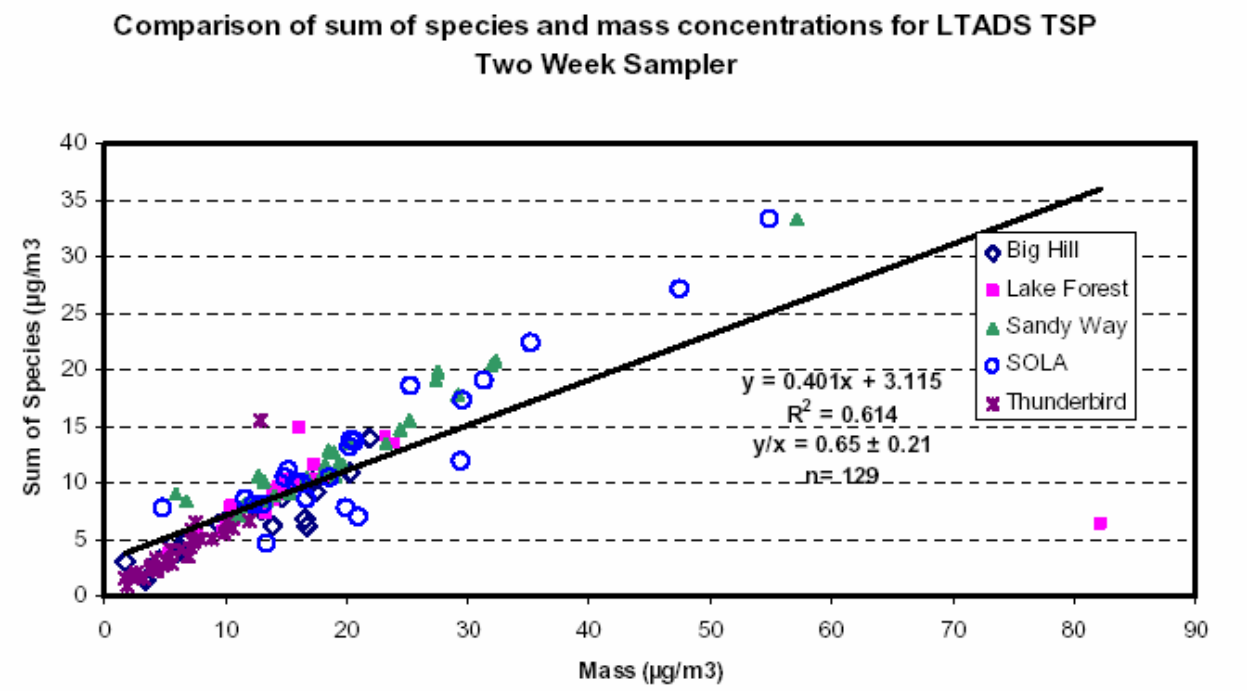

(a)

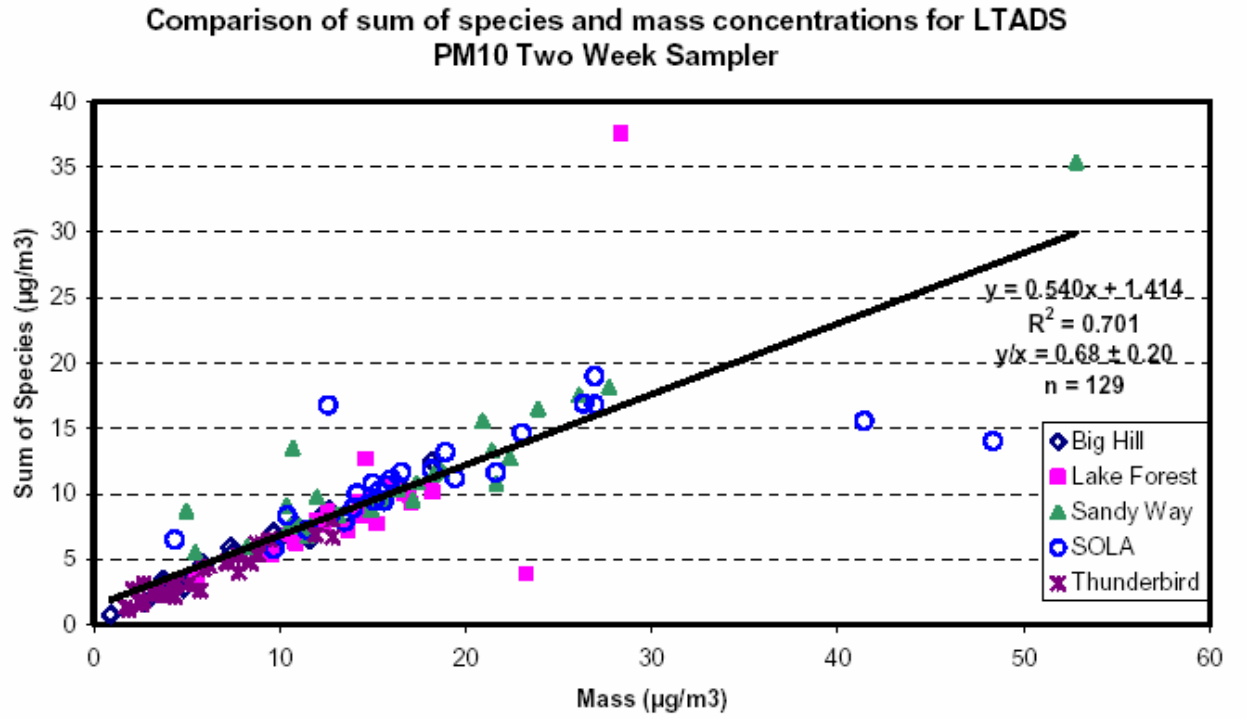

(b)

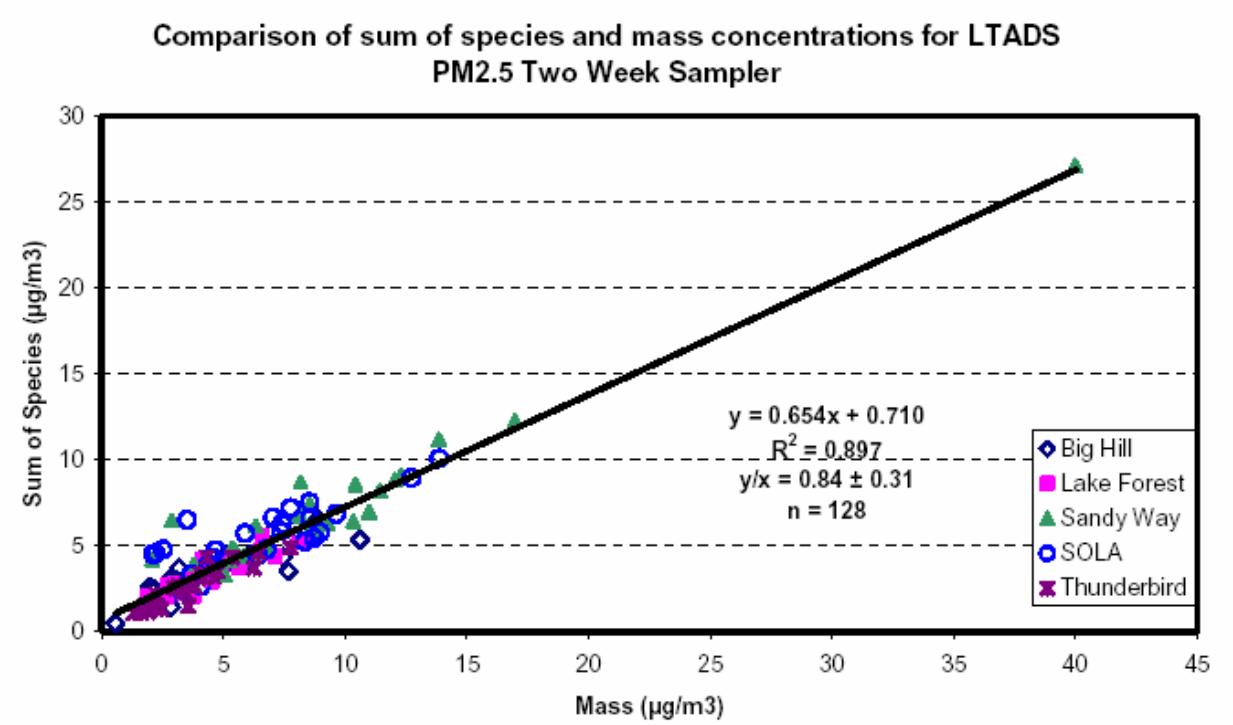
Comparison of sum of species and mass concentrations for LTADS
PM2.5 Two Week Sampler
Sum of Species (µg/m3)
Mass (µg/m3)
y = 0.654x + 0.710
R2 = 0.897
y/x = 0.84 ± 0.31
n = 128
Big Hill
Lake Forest
Sandy Way
SOLA
Thunderbird

(c)

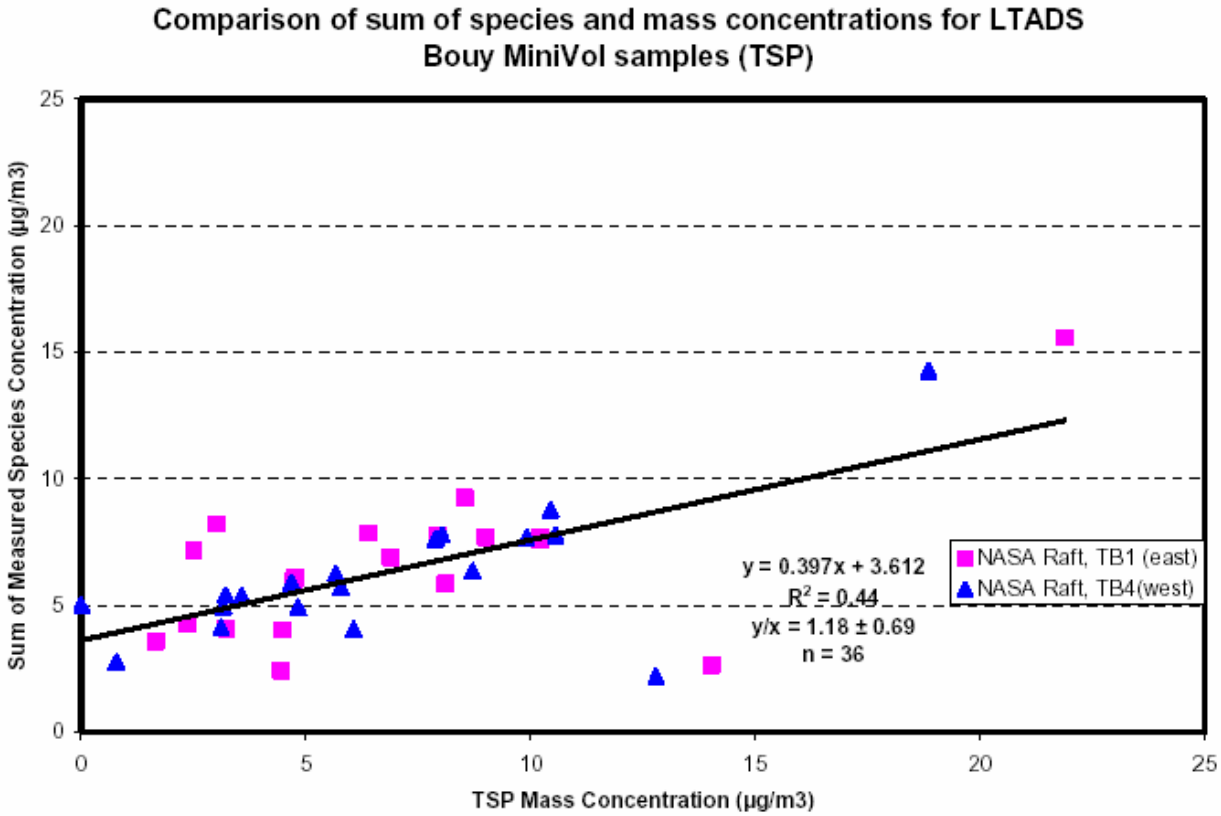
Comparison of sum of species and mass concentrations for LTADS
Bouy MiniVol samples (TSP)
Sum of Measured Species Concentration (µg/m3)
TSP Mass Concentration (µg/m3)
y = 0.397x + 3.612
R2 = 0.44
y/x = 1.18 ± 0.69
n = 36
NASA Raft, TB1 (east)
NASA Raft, TB4(west)

(d)

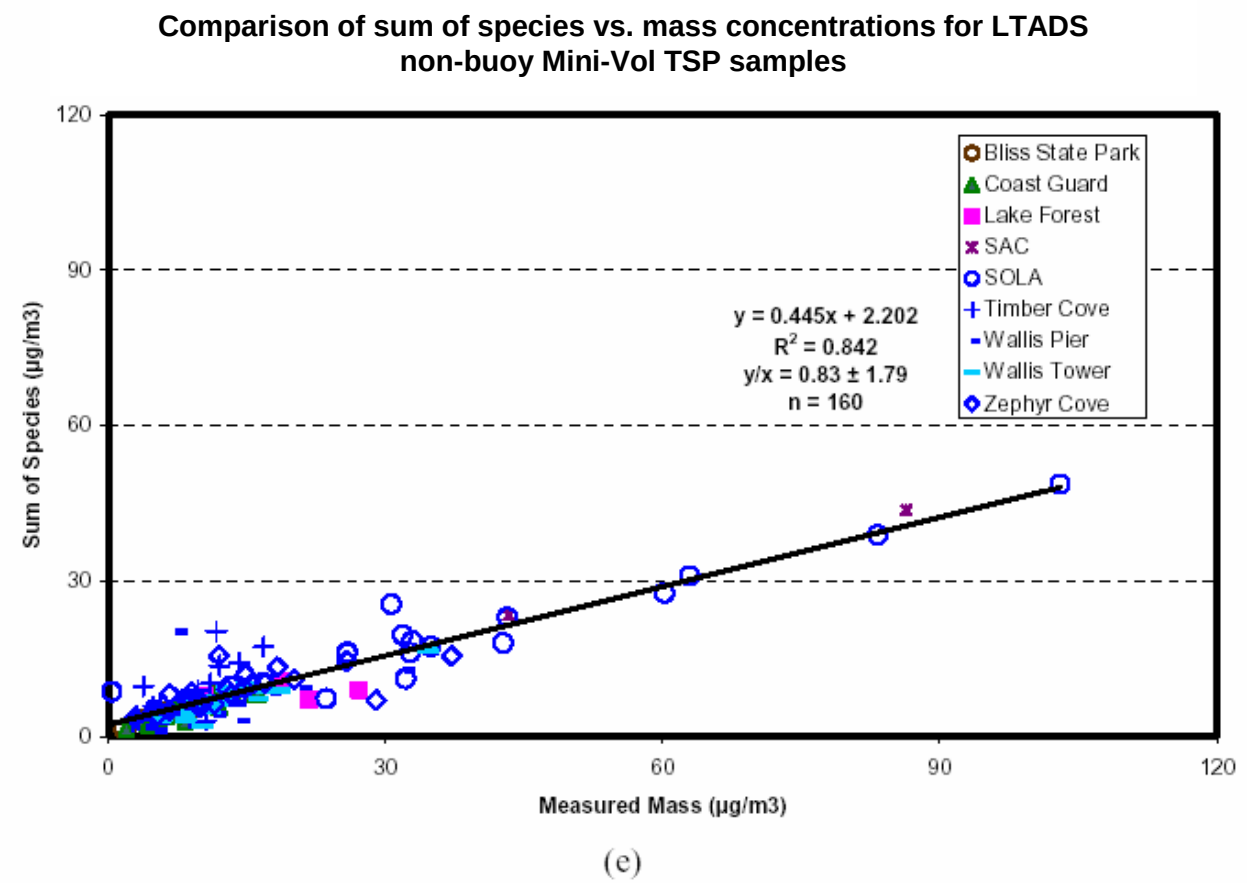
Comparison of sum of species vs. mass concentrations for LTADS non-buoy Mini-Vol TSP samples
Sum of Species (µg/m3)
Measured Mass (µg/m3)
0
30
60
90
120
y = 0.445x + 2.202
R2 = 0.842
y/x = 0.83 ± 1.79
n = 160
Bliss State Park
Coast Guard
Lake Forest
SAC
SOLA
Timber Cove
Wallis Pier
Wallis Tower
Zephyr Cove

(e)

Figure 3-4. Scatter Plot of Sulfate Versus Sulfur Concentrations at the Five Sites for a) TSP, b) PM10, and, c) PM2.5, d) Buoy Mini-Vol TSP, and e) Non-buoy Mini-Vol TSP.

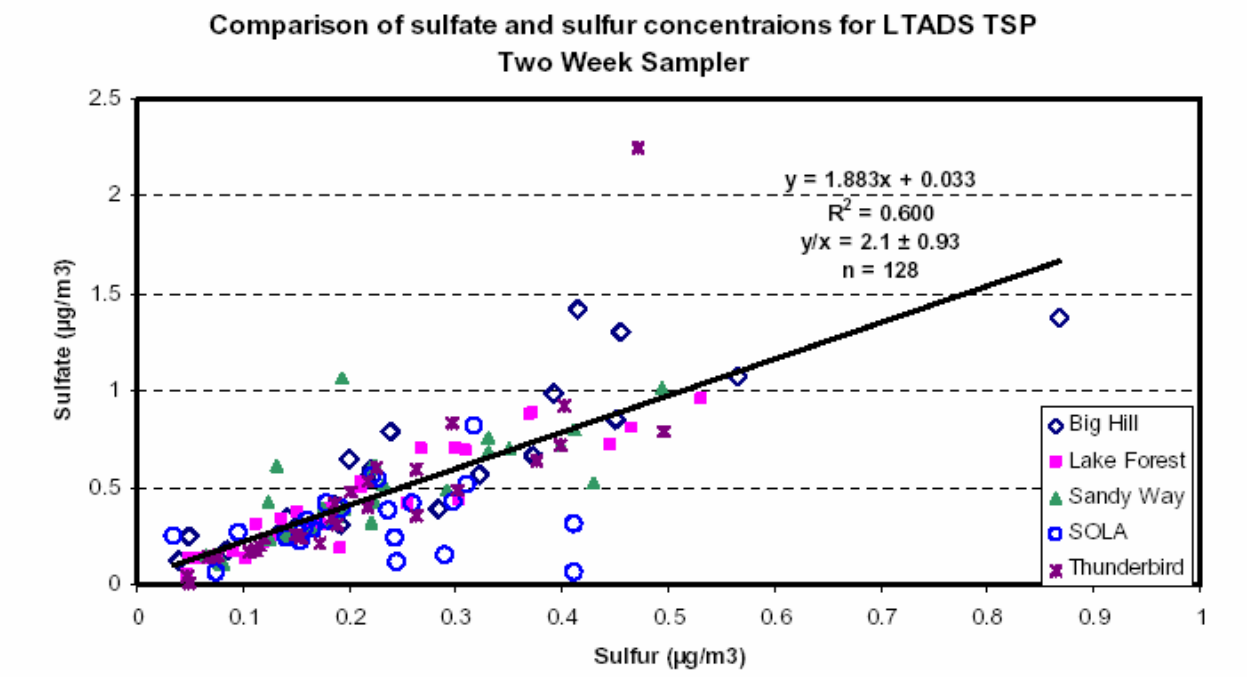

(a)

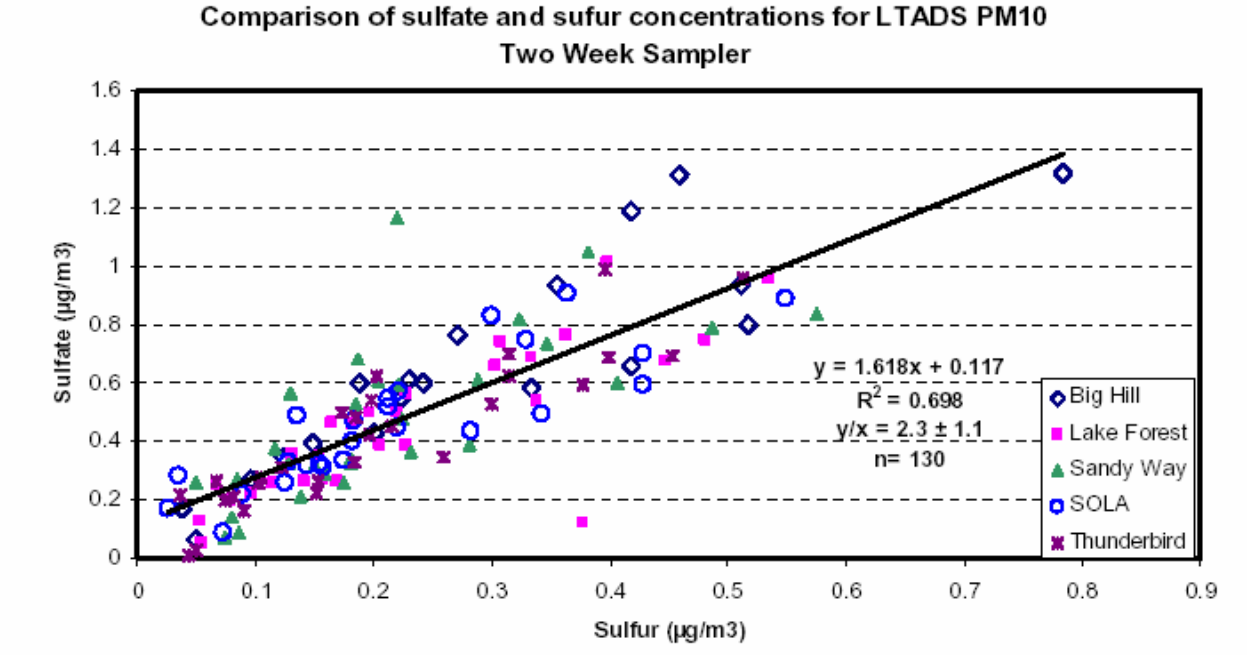

(b)

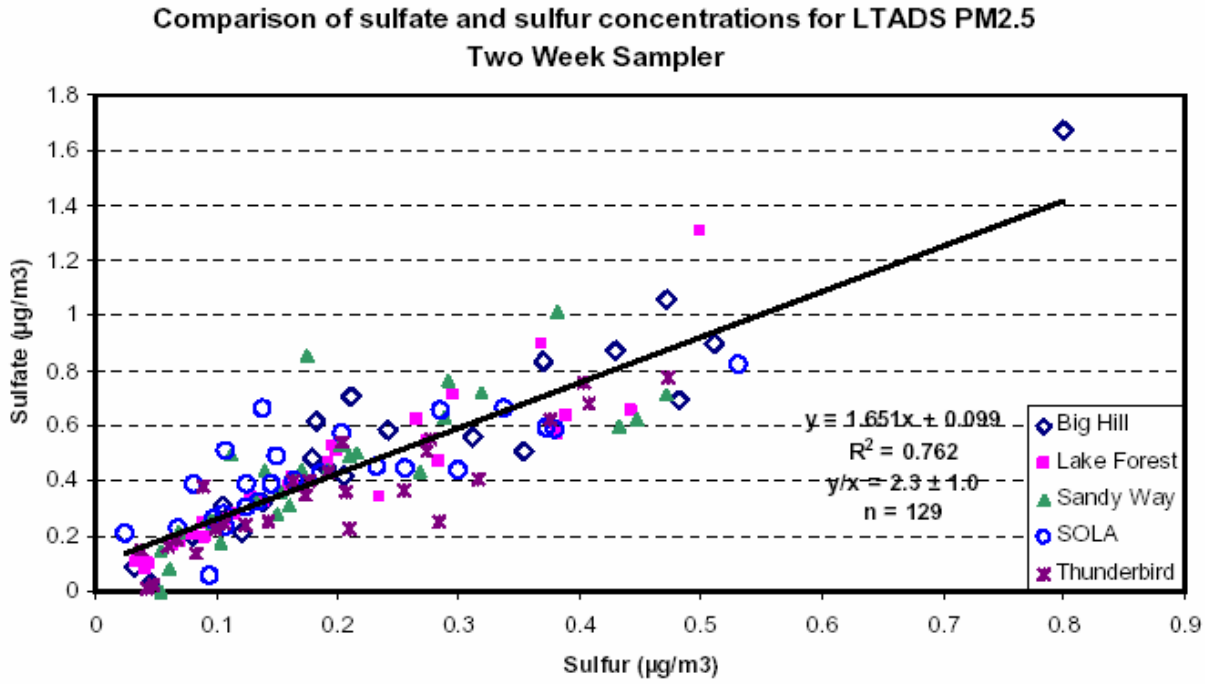
Comparison of sulfate and sulfur concentrations for LTADS PM2.5
Two Week Sampler
Sulfate (µg/m3)
Sulfur (µg/m3)
y = 1.651x + 0.099
R2 = 0.762
y/x = 2.3 ± 1.0
n = 129
Big Hill
Lake Forest
Sandy Way
SOLA
Thunderbird

(c)

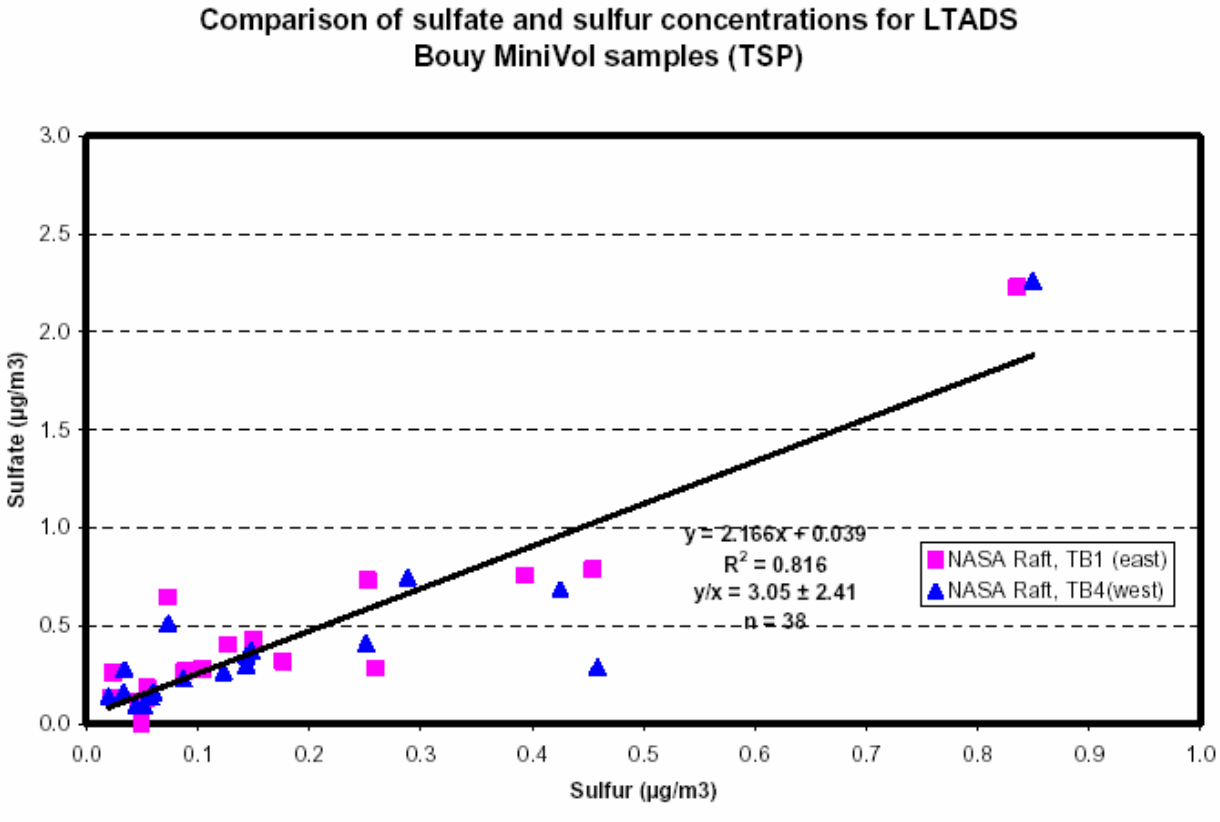
Comparison of sulfate and sulfur concentrations for LTADS
Bouy MiniVol samples (TSP)
Sulfate (µg/m3)
Sulfur (µg/m3)
y = 2.166x + 0.039
R2 = 0.816
y/x = 3.05 ± 2.41
n = 38
NASA Raft, TB1 (east)
NASA Raft, TB4(west)

(d)

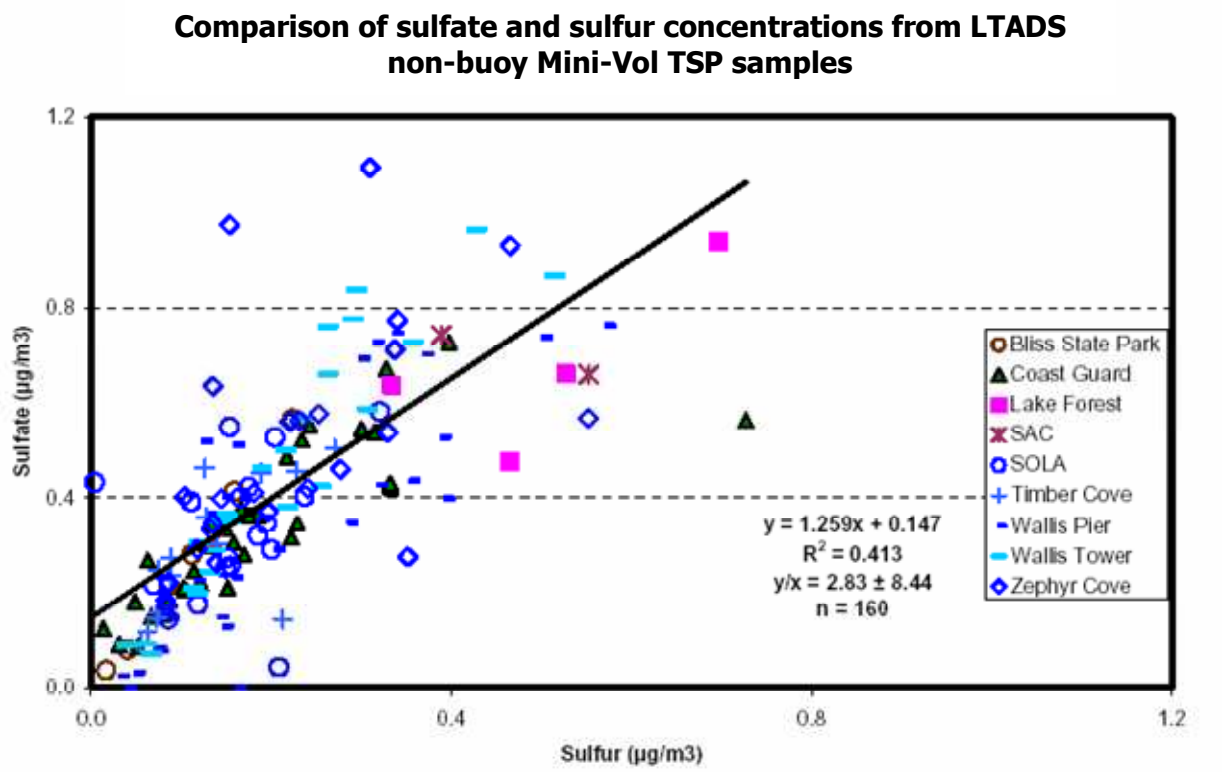

(e)

3.1.12.3 *Ammonium balance*

Ammonium in particles occurs most commonly as ammonium nitrate (NH_4NO_3), ammonium sulfate [$(NH_4)_2SO_4$], ammonium bisulfate [$(NH_3)HSO_4$], and ammonium chloride (NH_4Cl). Measured ammonium can be compared to calculated ammonium, which is the sum of ammonium assumed to be associated with nitrate and sulfate ($0.29 \times NO_3^- + 0.192 \times HSO_4^-$) or nitrate and bisulfate ($0.29 \times NO_3^- + 0.3 \times SO_4^=$). NH_4Cl was not used for ammonium balance because Lake Tahoe is generally not influenced by sea salt. The slopes between sulfate based ammonium and measured ammonium are shown in **Figure 3-5** (a-c) and were 0.92, 0.85, and 0.71 for TWS TSP, PM10, and PM2.5, respectively. These slopes were higher than the bisulfate based ammonium slopes of 0.57, 0.49, and 0.40 for TWS TSP, PM10, and PM2.5, respectively. The regression slopes between sulfate and bisulfate based ammonium and measured ammonium (**Figure 3-5d**) are 0.89 and 0.44 for buoy Mini-Vol TSP samples with poor correlation (<0.35). The slopes for non-buoy Mini-Vol TSP samples (**Figure 3-5e**) are close to unity with moderate correlation. This agrees with atmospheric chemistry, where ammonium sulfate is more stable than ammonium bisulfate. The slopes of measured ammonium and sulfate based ammonium were less than unity, which suggests potential excess ammonia in the atmosphere was absorbed onto the quartz-fiber filter. The decreasing slopes between calculated ammonium and measured ammonium as particle size fraction decreases from TSP to PM2.5 can be attributed to the sampling artifacts of volatilized ammonium nitrate, which becomes ammonia and nitric acid gas. The

disassociated ammonia is absorbed onto the quartz-fiber filter media. Such sampling artifacts are more pronounced at low ammonium nitrate particulate concentrations (Chang et al., 2000a; Pathak et al., 2004).

Figure 3-5. Scatter Plot of Calculated and Measured Ammonium Concentrations for: a) TSP, b) PM10, and, c) PM2.5, d) Buoy Mini-Vol TSP, and e) Non-Buoy Mini-Vol TSP.

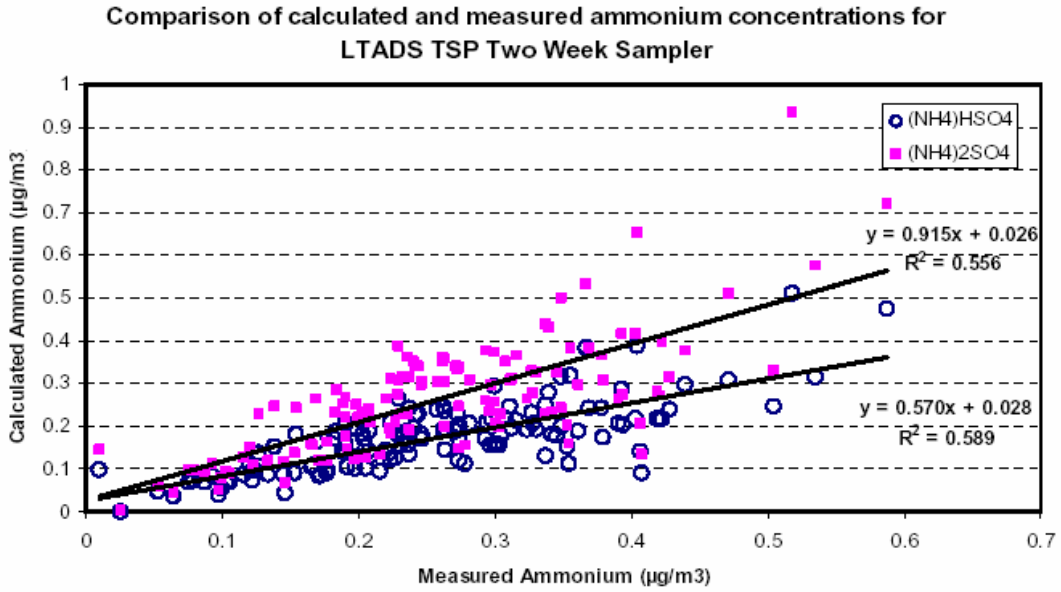

(a)

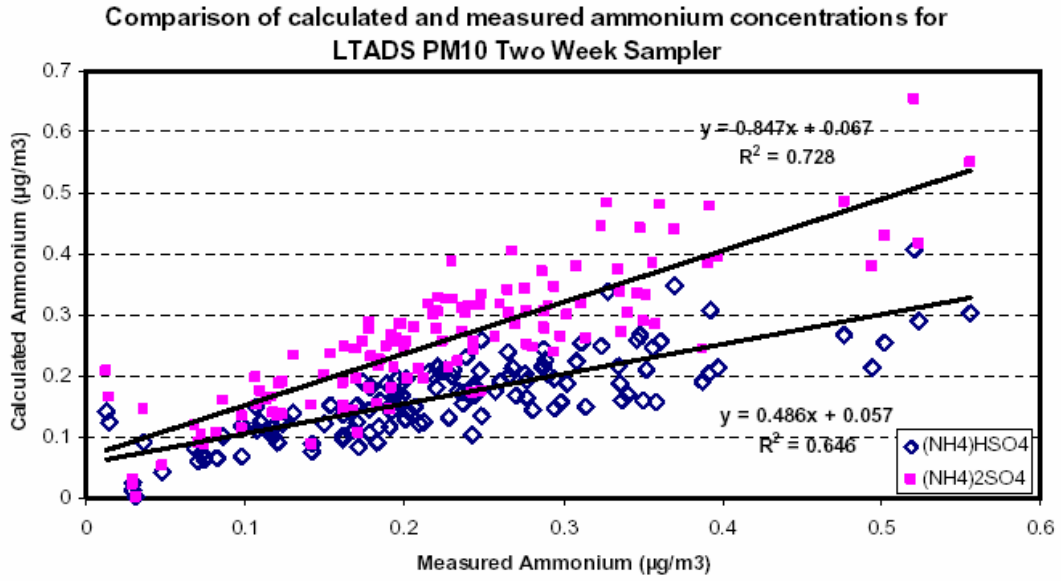

(b)

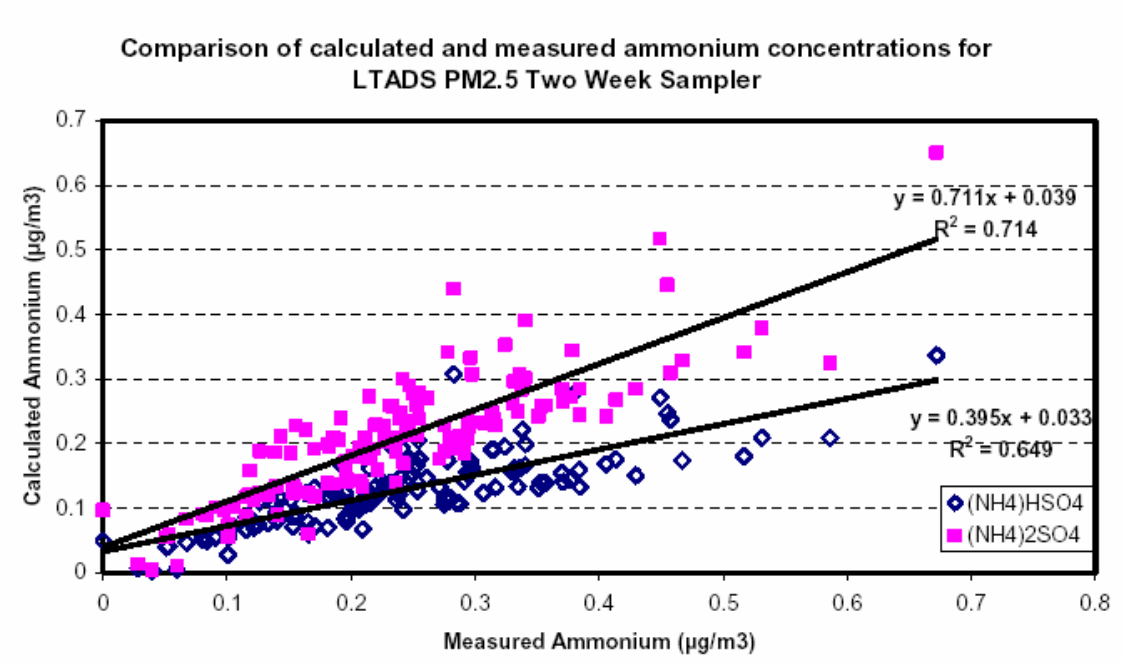
Comparison of calculated and measured ammonium concentrations for LTADS PM2.5 Two Week Sampler
Calculated Ammonium (µg/m3)
Measured Ammonium (µg/m3)
y = 0.711x + 0.039
R2 = 0.714
y = 0.395x + 0.033
R2 = 0.649
(NH4)HSO4
(NH4)2SO4
0
0.1
0.2
0.3
0.4
0.5
0.6
0.7
0.8

(c)

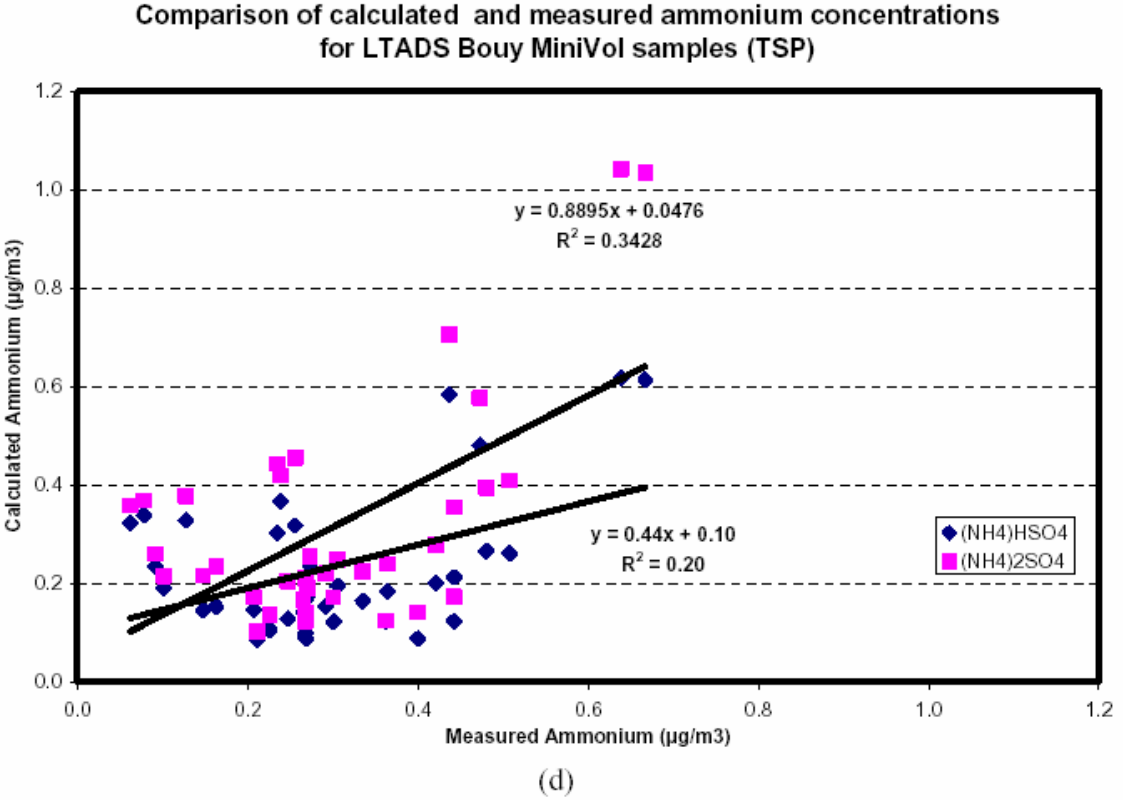
Comparison of calculated and measured ammonium concentrations for LTADS Bouy MiniVol samples (TSP)
Calculated Ammonium (µg/m3)
Measured Ammonium (µg/m3)
y = 0.8895x + 0.0476
R2 = 0.3428
y = 0.44x + 0.10
R2 = 0.20
(NH4)HSO4
(NH4)2SO4
0.0
0.2
0.4
0.6
0.8
1.0
1.2

(d)

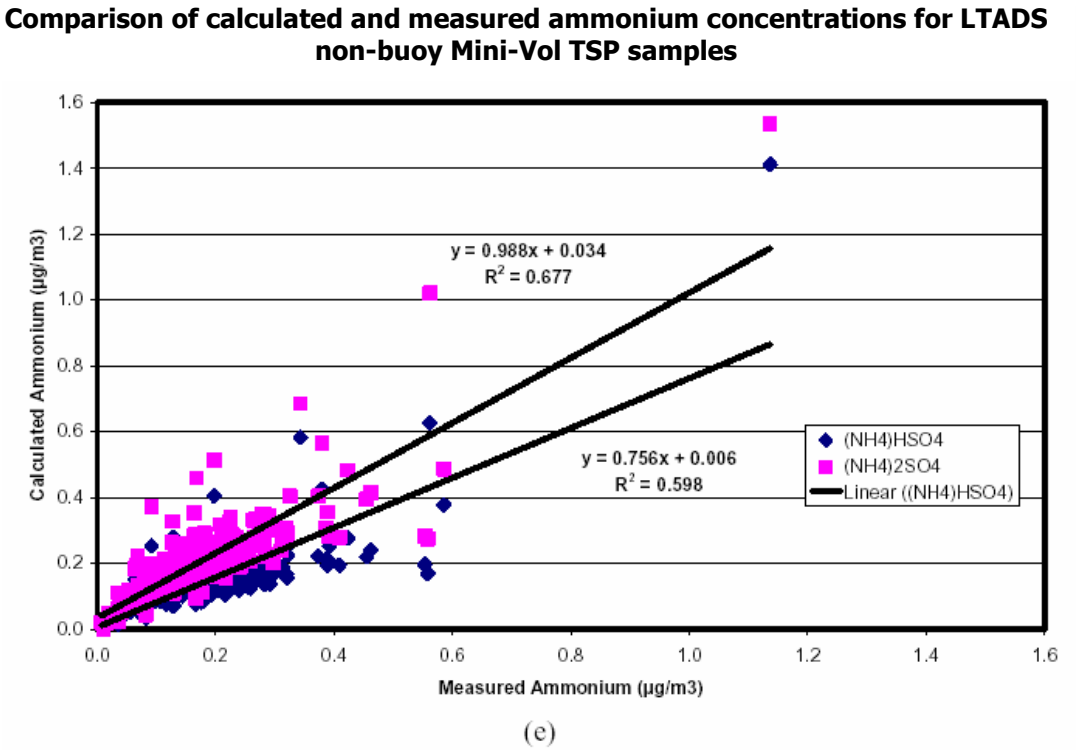

(e)

3.1.12.4 Anion and cation balance

The balance of anions and cations was calculated by comparing the sum of Cl^-, NO_3^-, and $SO_4^=$ to the sum of NH_4^+, K^+, and Na^+ in microequivalence/m^3. Microequivalence/m^3 of each species is calculated as the product of mass concentration (Cm) (in µg/m^3) divided by the atomic weight of the chemical species multiplied by the species' charge. Therefore, microequivalence/m^3 for anion = Cm,Cl^-/35.453 + Cm,NO_3^- /62 + Cm, $SO_4^=$/96x2 microequivalence/m^3 for cations = Cm,$NH4^+$/18 + Cm,K^+/39.1 + Cm,Na^+/23. **Figure 3-6 (a-c)** shows plots of anion and cation balance in microequivalence/m^3 for TWS TSP, PM10, and PM2.5. The slopes are within the range of 0.65-0.68 for all particle sizes, and have moderate correlation (r^2=0.65-0.70). The ratios between anions and cations for TWS TSP, PM10, and PM2.5 were 0.92±0.98, 0.94±0.27, and 0.84±0.23, respectively. The slopes between anions and cations are 1.07 (r^2=0.61) and 1.08 (r^2=0.82), and average ratios are 1.1±0.41, 0.98±0.0.25, for buoy and non-buoy Mini-Vol TSP samples, respectively. The slightly difference between the average ratio of anion and cations versus slopes for TWS samples were because the slopes are more sensitive to high and low concentrations in the data. However, each pair of anion and cation data was weighed equally in ratio. The average PM2.5 anion and cation ratio was 11.6 measured at the TB site on 05/07/03, which is suspected to be an outlier.

Figure 3-6. Scatter Plot of Anion and Cation Balance in Microequivalence/m^3 for: a) TSP, b) PM10, and, c) PM2.5, d) Buoy Mini-Vol TSP, and e) Non-buoy Mini-Vol TSP.

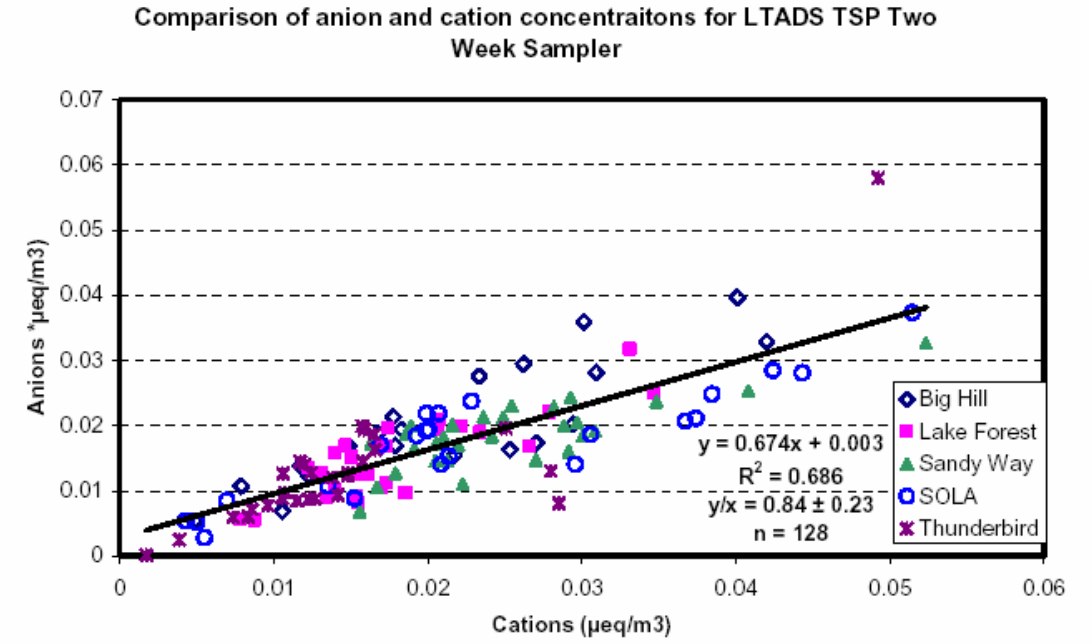

(a)

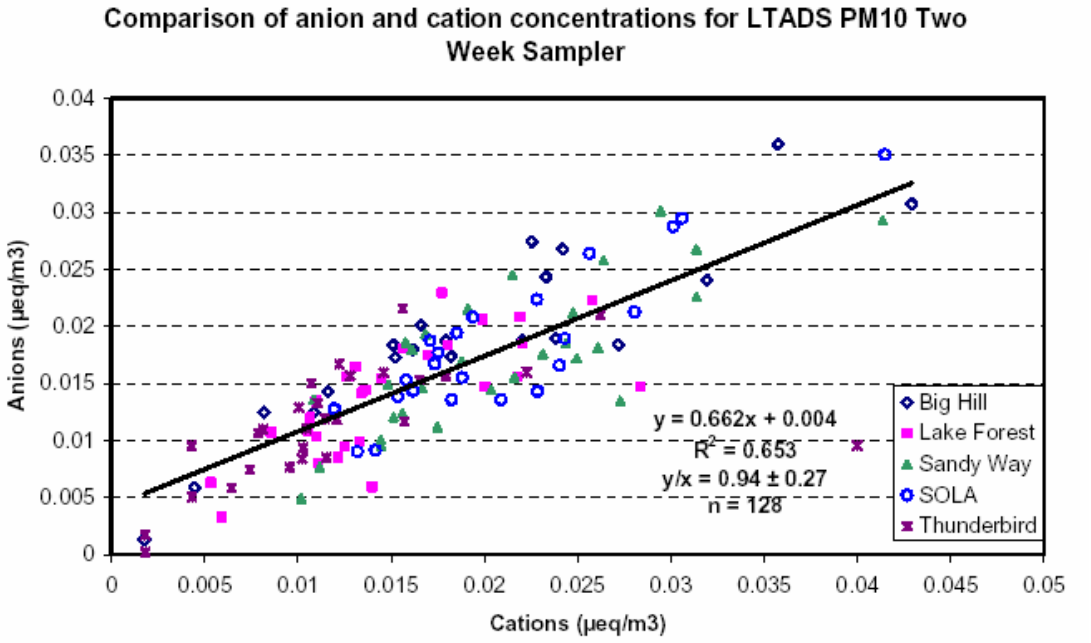

(b)

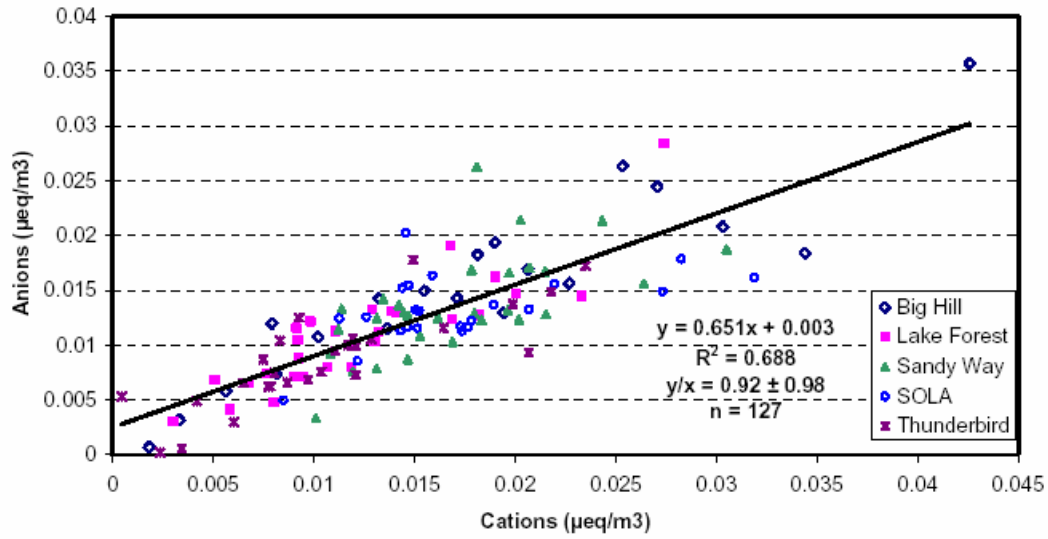
Comparison of anion and cation concentrations for LTADS PM2.5
Two Week Sampler
Anions (µeq/m3)
Cations (µeq/m3)
0.04
0.035
0.03
0.025
0.02
0.015
0.01
0.005
0
0
0.005
0.01
0.015
0.02
0.025
0.03
0.035
0.04
0.045
y = 0.651x + 0.003
R2 = 0.688
y/x = 0.92 ± 0.98
n = 127
Big Hill
Lake Forest
Sandy Way
SOLA
Thunderbird

(c)

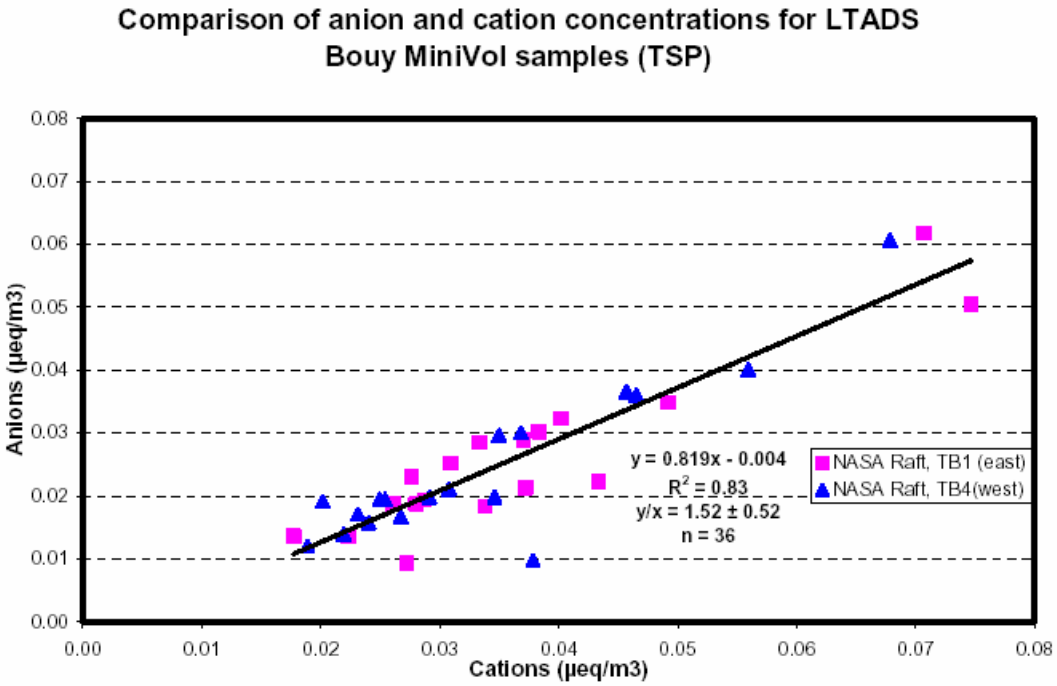
Comparison of anion and cation concentrations for LTADS
Bouy MiniVol samples (TSP)
Anions (µeq/m3)
Cations (µeq/m3)
0.08
0.07
0.06
0.05
0.04
0.03
0.02
0.01
0.00
0.00
0.01
0.02
0.03
0.04
0.05
0.06
0.07
0.08
y = 0.819x - 0.004
R2 = 0.83
y/x = 1.52 ± 0.52
n = 36
NASA Raft, TB1 (east)
NASA Raft, TB4(west)

(d)

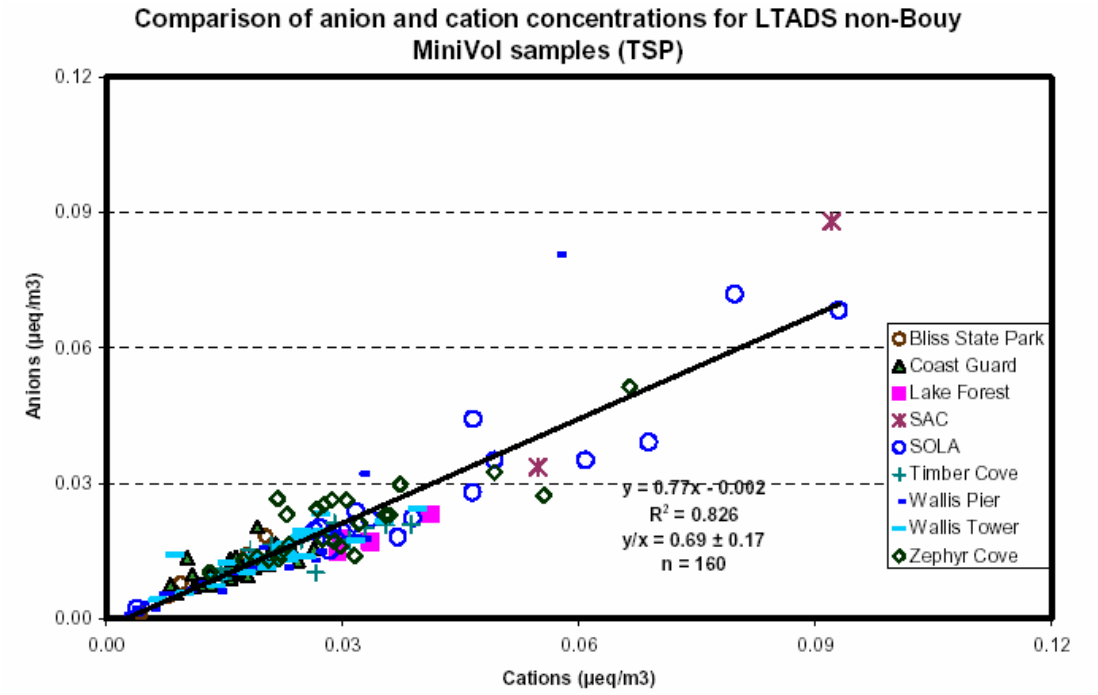

(e)

3.1.12.5 Water-soluble potassium (K^+) versus potassium (K)

K^+ was measured by atomic adsorption spectrophotometry (AAS) analysis on quartz-fiber filter and K was measured by XRF on Teflon-membrane filters. **Figure 3-7 (a-c)** shows scatter plots of K^+ versus K concentrations for TWS TSP, PM10, and PM2.5; and **Figure 3-7 (d, e)** show those for buoy and non-buoy Mini-Vol TSP samples. Very weak correlations between K^+ and K were observed in TWS TSP and PM10, buoy Mini-Vol TSP, and non-buoy Mini-Vol TSP. A high K concentration (1.544 µg/m^3) in PM10 and much lower K^+ concentrations (0.061 µg/m^3 and 0.043 µg/m^3 in TSP and PM2.5, respectively) were observed on 11/15/03. It is suspected that the sample was contaminated. The regression statistics show moderate correlations (r^2 = 0.62) between K^+ and K measured in PM2.5. This suggests the major sources of K^+ in PM2.5 in the Lake Tahoe area are wood smoke from residential cooking and heating processes or from biomass burning.

Figure 3-7. Scatter plot of water-soluble potassium versus potassium concentrations for: a) TSP, b) PM10, c) PM2.5, d) Buoy Mini-Vol TSP, and e) Non-buoy Mini-Vol TSP.

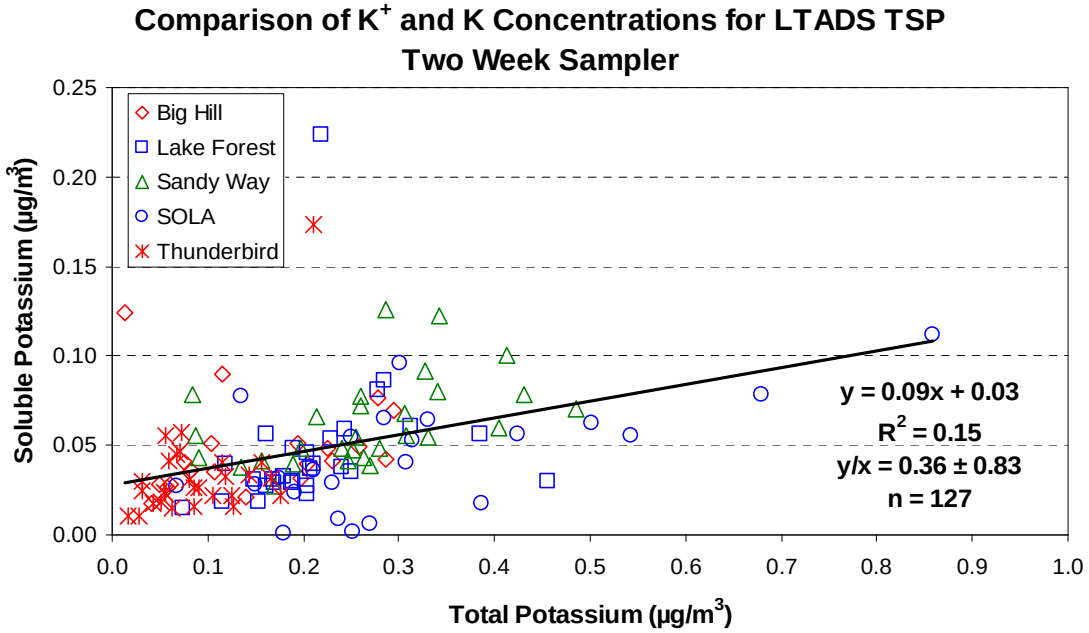

(a)

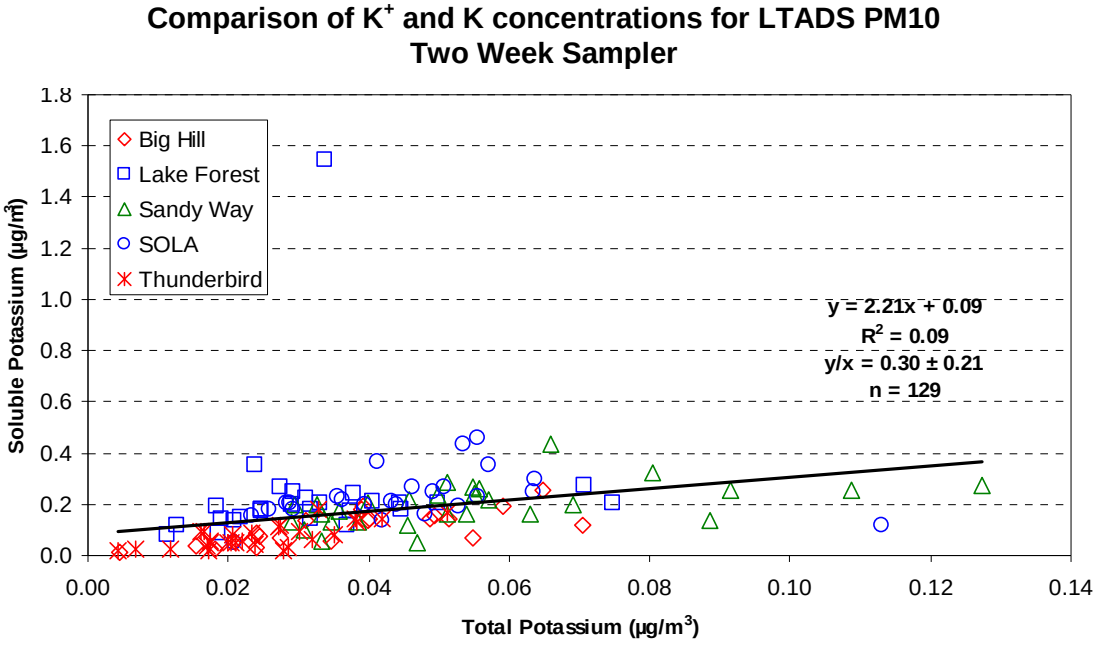

(b)

Comparison of K^+ and K concentrations for LTADS PM2.5 Two-Week-Sampler

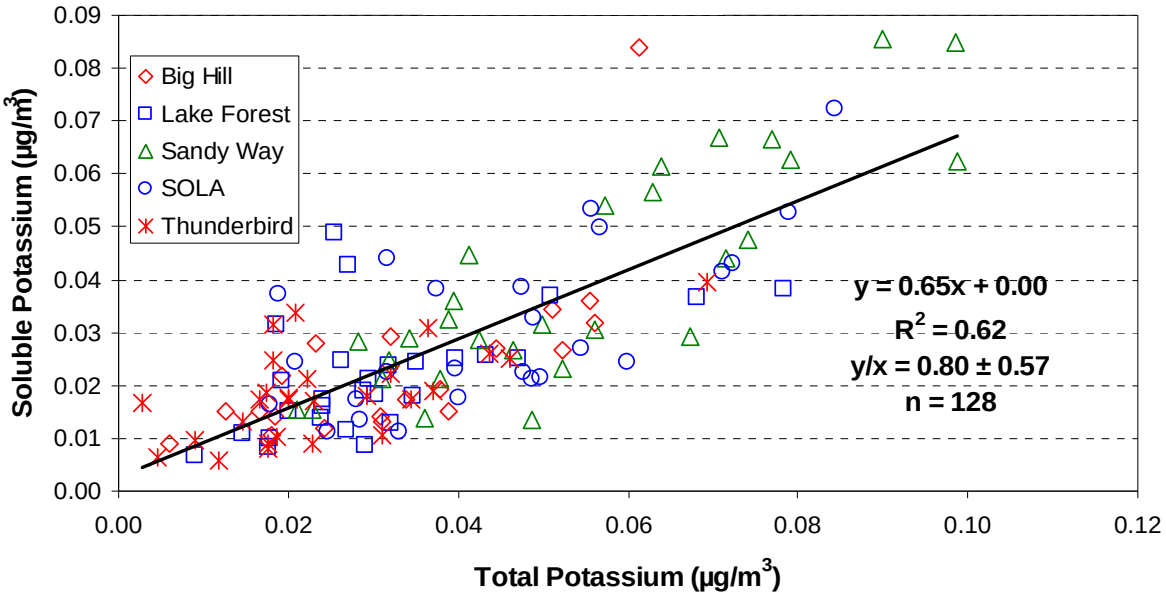

(c)

Comparison of K^+ and K concentrations for LTADS buoy Mini-Vol TSP samples

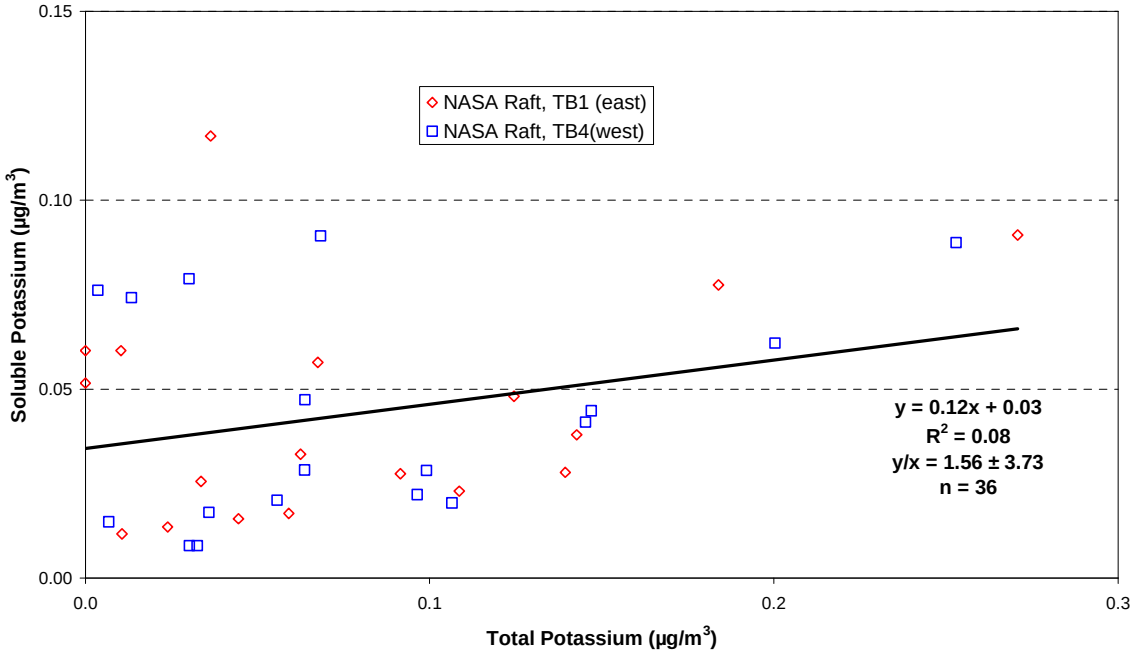

(d)

Comparison of K^+ and K concentrations for LTADS non-buoy Mini-Vol TSP samples

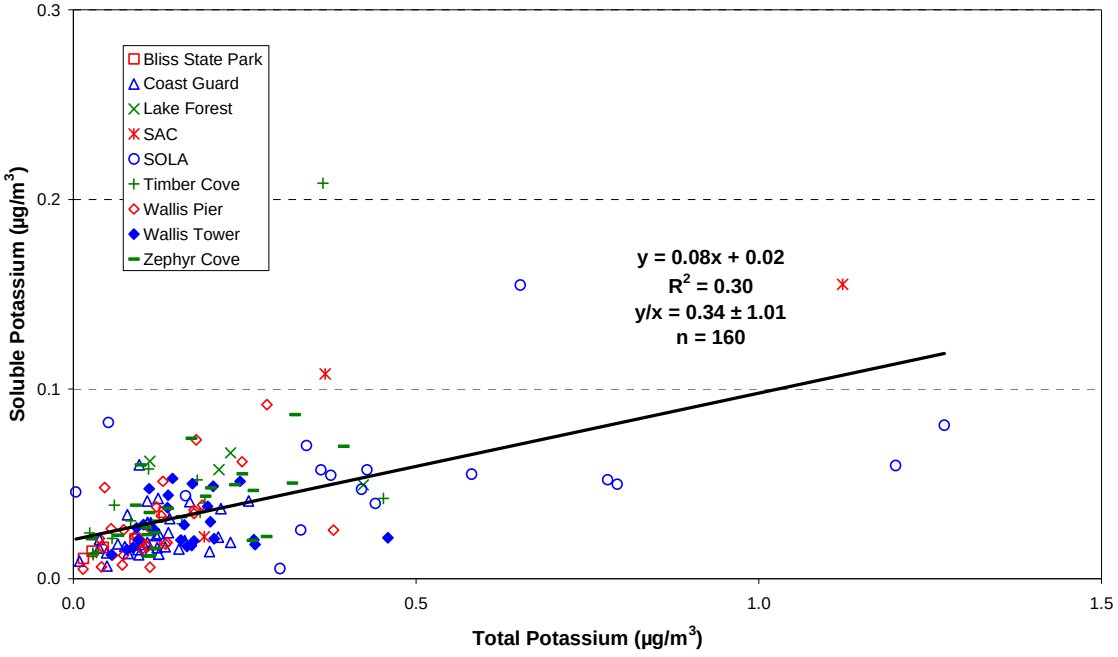

(e)

3.1.13 BAM, TWS, MVS, and FRM Equivalency Demonstrations

Several different instruments and sampling/monitoring technologies for measuring particulate matter were used during LTADS. Because some of these instruments have seldom been used in such a clean, high-altitude, and cold location as Lake Tahoe before, the concentration measurements from different collocated instruments were compared to confirm the assumed equivalency of the measurement methods.

In **Figure 3-8**, hourly TSP data from the Beta Attenuation Monitor (BAM) at SOLA were averaged over the comparable sampling periods of TSP with a collocated mini-volume sampler (MVS). Discounting the two periods when the MVS malfunctioned (data indicated with red circles), the TSP concentrations as measured with the BAM and MVS compared very well (m=1.06, b=0.7 ug/m^3, and r^2=0.97).

TSP concentrations when an MVS was collocated with the TWS at SOLA are plotted in **Figure 3-9**. Only four contemporaneous samples are available but the data indicate a consistent bias toward lower TSP concentrations with the TWS (~5-7 ug/m^3 lower). This low TSP bias with the TWS is very likely due to its design (low flow rate, large precipitation shield, and, to a lesser extent, its inverted sampler inlet (drawing air up to the filter face rather than down to the filter)).

PM data were collected in PM2.5 and PM10 sizes with both a BAM (continuous hourly measurement) and a Federal Reference Method (24-hour filter sample) at the SLT –

Sandy Way site. The BAM data were temporally matched with the FRM samples during 2003. The 24-hour averaged BAM measurements for PM2.5 and PM10 are compared with the FRM measurements in **Figure 3-10**. The relationship between the methods is excellent for PM2.5 (m=0.997; b=0.59 ug/m^3; r^2=0.81) and good for PM10 (m=0.892; b=2.84 ug/m^3; r^2=0.87). It appears that some type of offset that occurred during six sampling periods might be biasing the PM10 regression line toward a higher intercept and a lower slope than normally would exist between the two measurement methods at low concentrations. In general, the BAM measurements corresponded well with the standard (official) FRM measurements. Matched 2-week average PM concentrations by TWS and BAM are shown by site and measurement size in **Figure 3-11**. In almost all cases, the measurement methods are comparable for PM2.5 and PM10 with differences less than 5 ug/m^3. On average, the [PM2.5] was 0.5 ug/m^3 higher and the [PM10] was 1.0 ug/m^3 lower with the TWS than with the BAM measurement; these differences are approximately 10% of the means. The [TSP]s by the two methods exhibited more scatter, particularly at the more polluted locations. On average, the [TSP] was 4.1 ug/m^3 higher by BAM than by TWS; this difference is about 20% of the BAM mean.

Figure 3-8. TSP Concentrations: Mini-Volume Sampler vs. BAM at South Lake Tahoe – SOLA.

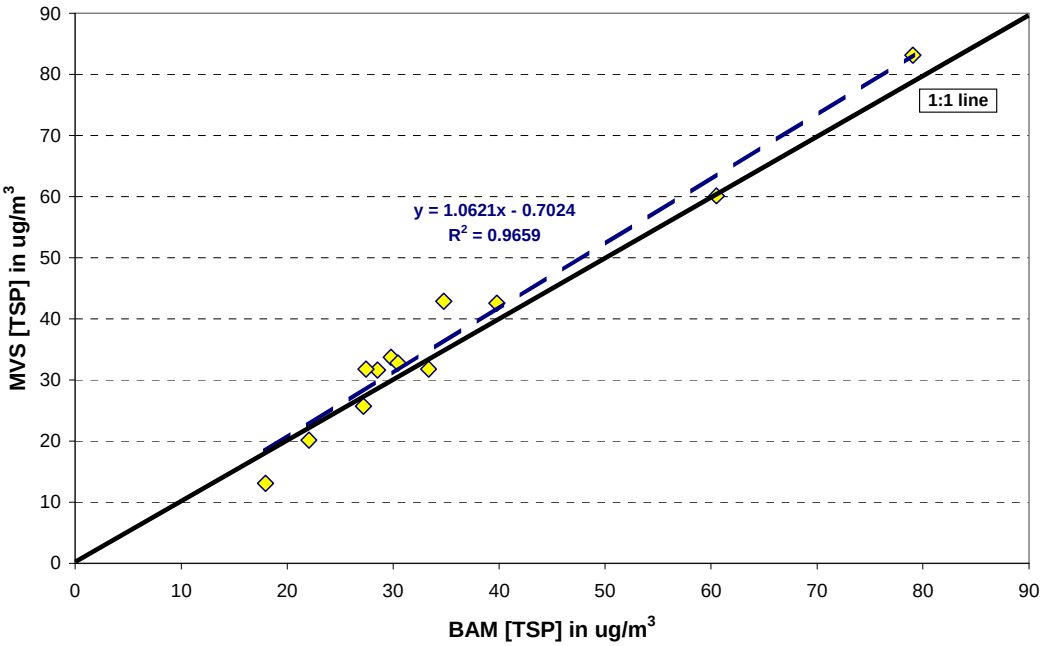

Figure 3-9. TSP Concentrations: Mini-Volume Sampler vs. Two-Week-Sampler at South Lake Tahoe – SOLA.

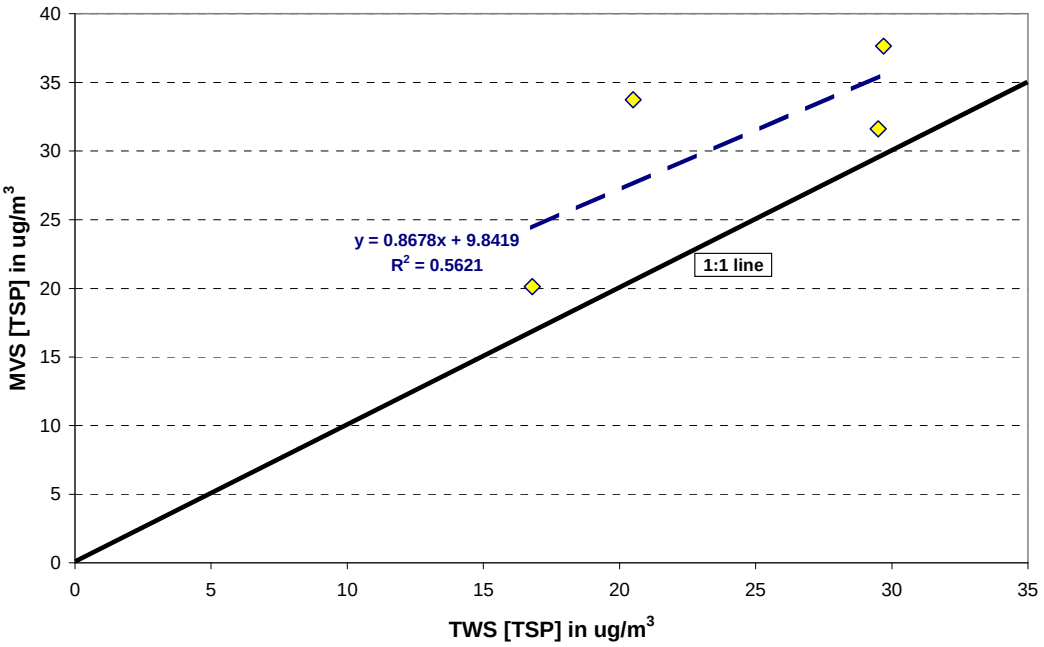

Figure 3-10. BAM PM versus Federal Reference Method PM at SLT-Sandy Way Site in 2003.

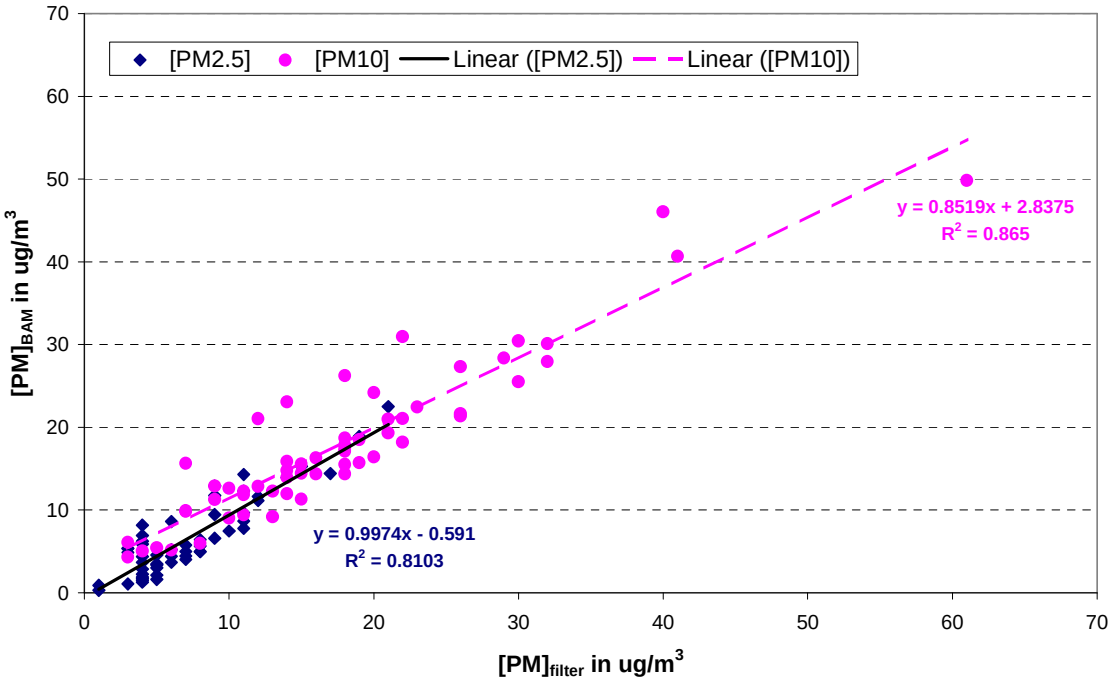

Figure 3-11. Matched 2-week average particulate matter concentrations by collocated TWS and BAM. (Note: all outliers > 10 µg/m^3 from the 1:1 relationship, and the lone case when the [TWS] was > 5 µg/m^3 above the 1:1 relationship, were associated with the two SLT sites.)

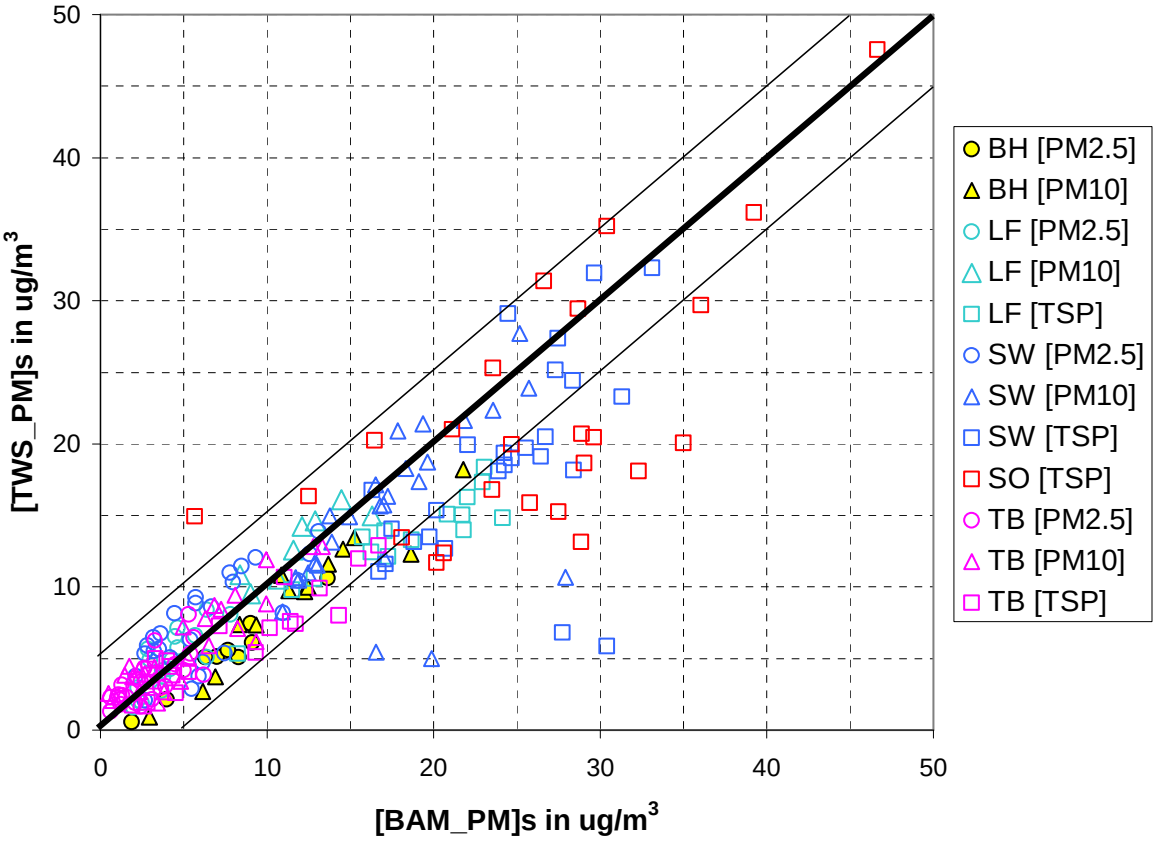

3.1.14 Comparison of Optical Particle Counts to Mass Measurements

The principal instrumentation used in the dust experiments was a set of Climet CI-500 optical particle counters. These counters draw a stream of air through an optical chamber where, one-at-a-time, particles in the air stream pass through the beam of a solid-state laser. Light scattered by a particle is sensed photoelectrically, with the strength of the scattering converted into particle size based on scattering cross-section, and the number of particles in each size "bin" is recorded over a standard sampling period (typically one to a few minutes). There is a maximum count rate, beyond which multiple particles are sensed together (causing miss-sizing), but concentrations observed in the Tahoe region never exceeded the count-rate capability of the instruments.

These instruments are calibrated at the factory, and cannot be adjusted by the user. Validation of calibration was determined by side-by-side testing of multiple instruments, and comparison of estimated aerosol mass with BAM data. Examples are shown in **Figure 3-12a-g**.

Figure 3-12. Cross-Comparison of Optical Particle Counter Instruments by Size Bin.

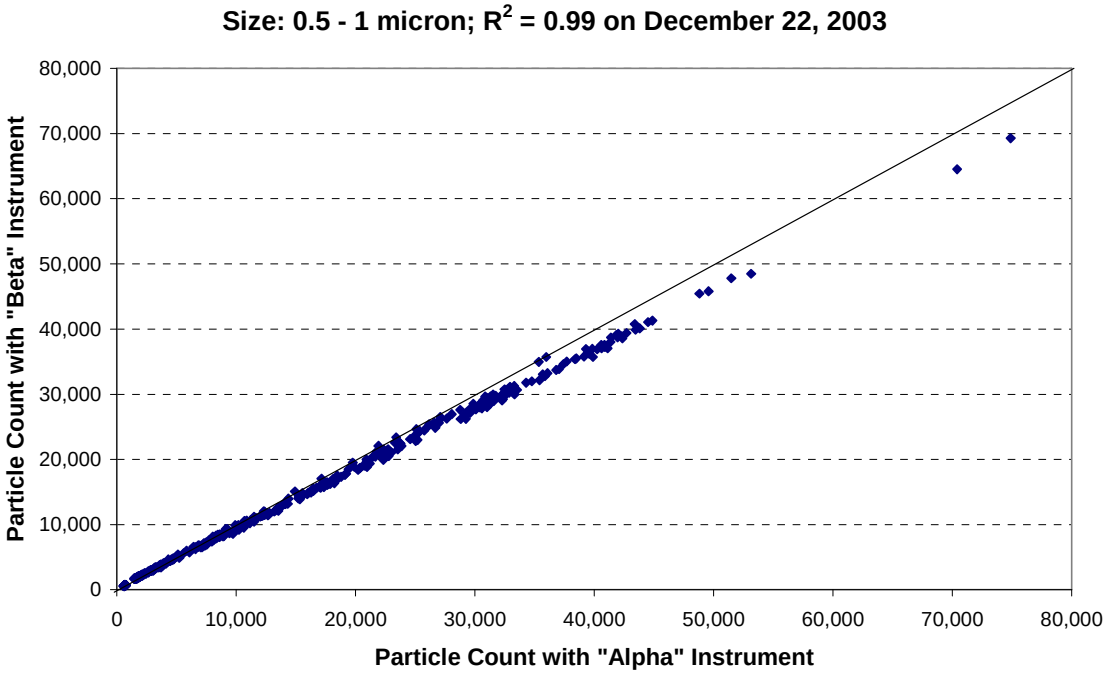

a)

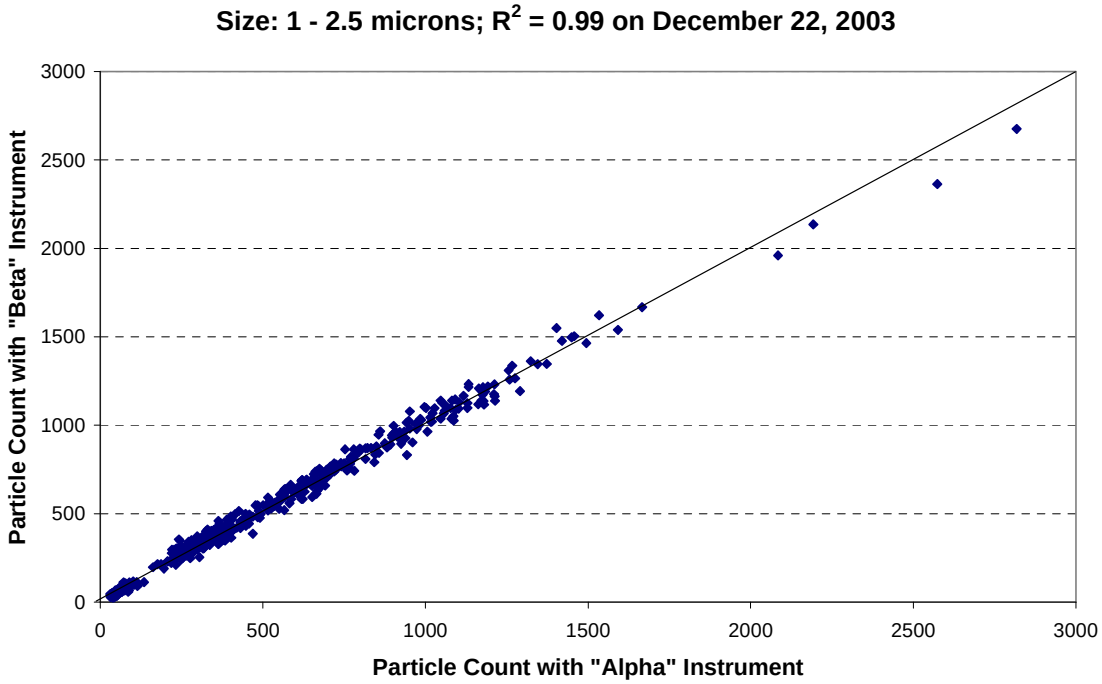

b)

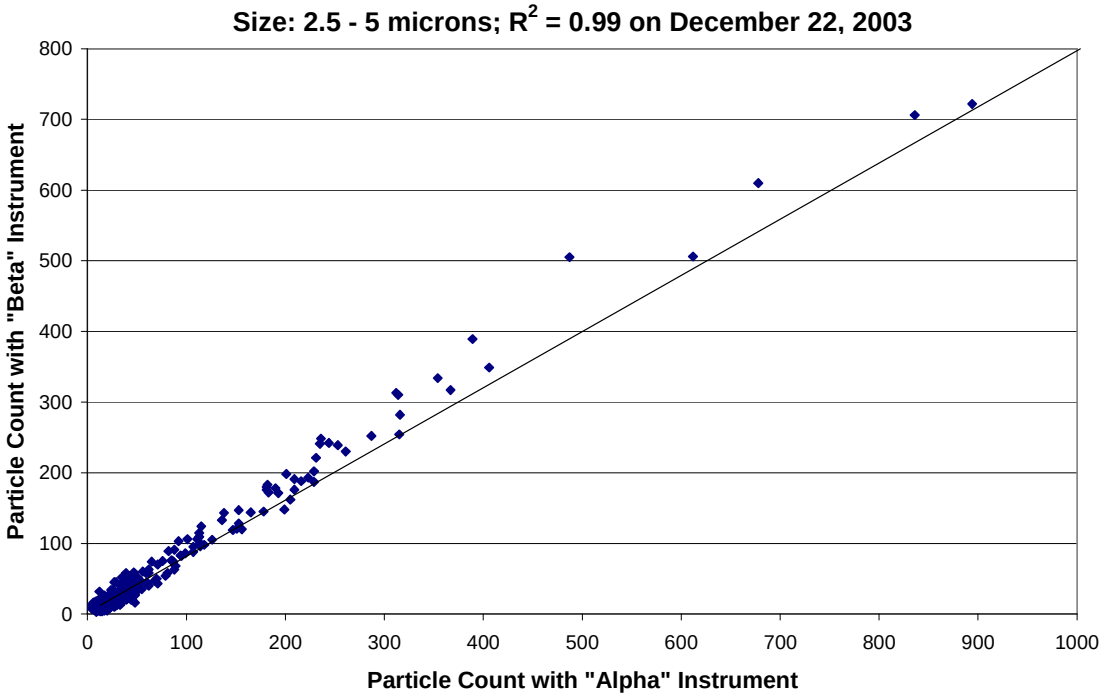
Size: 2.5 - 5 microns; R2 = 0.99 on December 22, 2003
Particle Count with "Beta" Instrument
Particle Count with "Alpha" Instrument
0
100
200
300
400
500
600
700
800
900
1000

c)

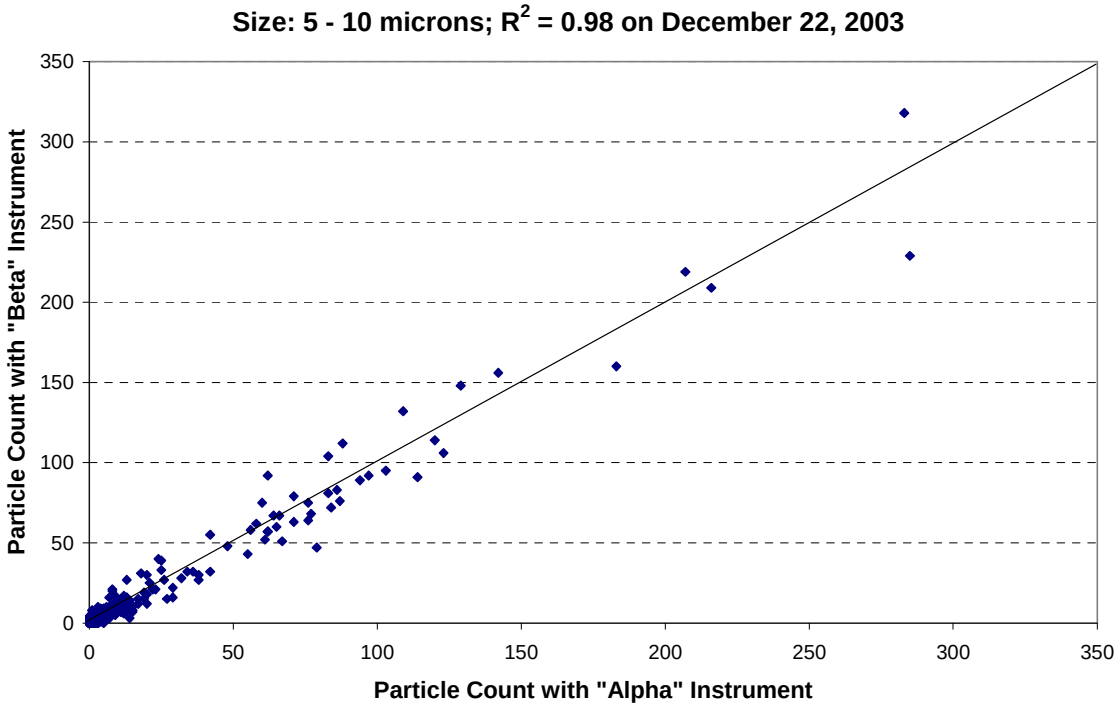
Size: 5 - 10 microns; R2 = 0.98 on December 22, 2003
Particle Count with "Beta" Instrument
Particle Count with "Alpha" Instrument
0
50
100
150
200
250
300
350

d)

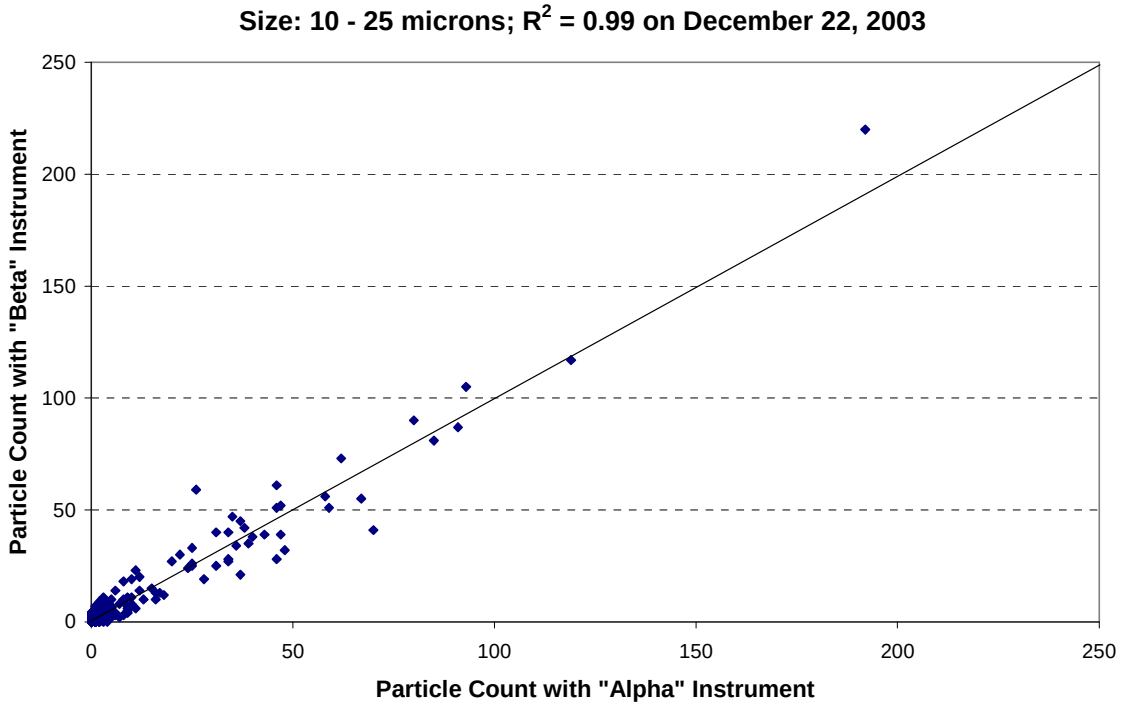
Size: 10 - 25 microns; R2 = 0.99 on December 22, 2003
Particle Count with "Beta" Instrument
Particle Count with "Alpha" Instrument
0
50
100
150
200
250

e)

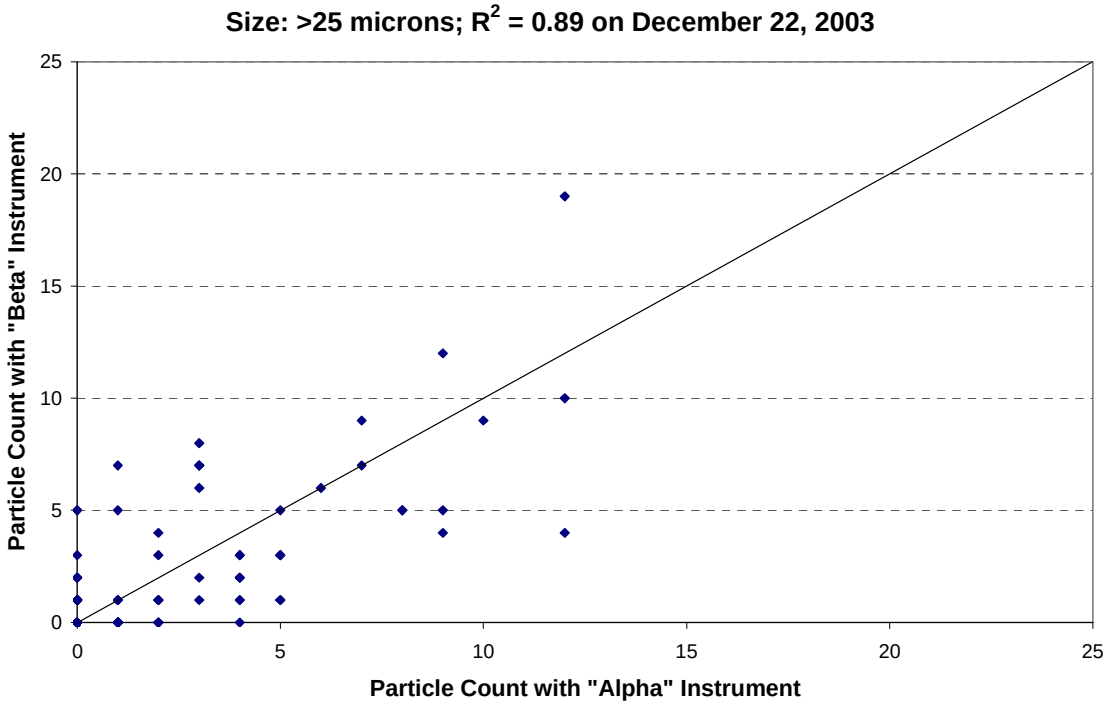
Size: >25 microns; R2 = 0.89 on December 22, 2003
Particle Count with "Beta" Instrument
Particle Count with "Alpha" Instrument
0
5
10
15
20
25

f)

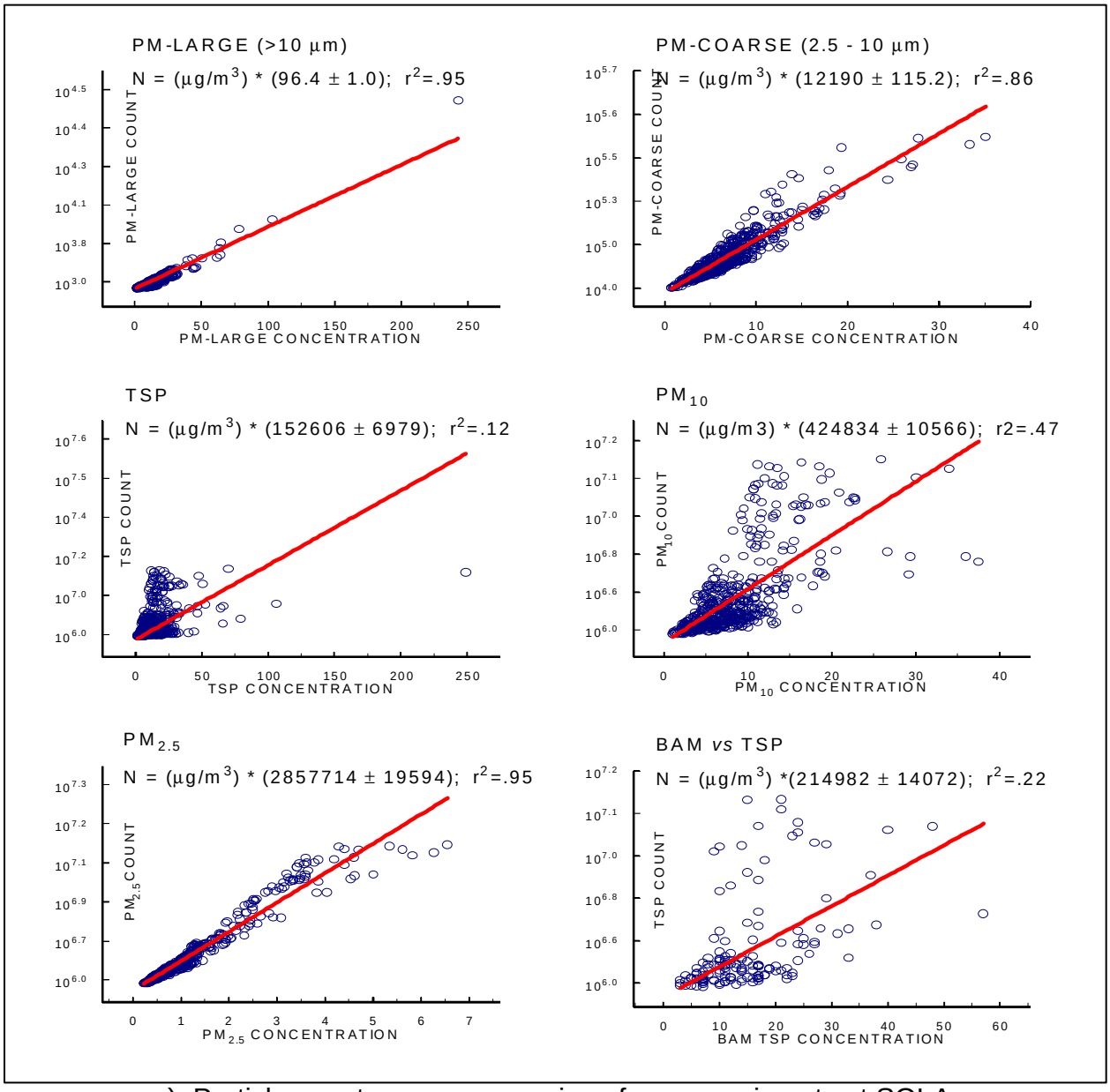

g) Particle count - mass regressions from experiments at SOLA.

3.2 Ambient Concentrations

Various data summaries of the LTADS measurements are presented and discussed in this section.

3.2.1 Particulate Matter

3.2.1.1 Variations in the Sampling Durations of Particulate Measurements

In general, good contemporaneous TWS sampling occurred at BH, LF, TB, SW, and SOLA sites due to a formal sampling schedule. A modification was made to the initial shipping schedule to ensure that refrigerated sampling filters were always available for deployment on the scheduled days. Winter storms and power outages caused most of the deviations from the planned 2-week sampling periods early in the field study. The most severe problem was wind damage that delayed the initiation of sampling at the BH site about three months, until late February 2003.

The sampling schedule with the Mini-Vol samplers was less formal and varied due to differences in power availability, limited access due to weather conditions, sampler malfunctions, etc. The number of Mini-Vol samples and sample duration statistics are summarized by sampling location in **Table 3-4**. The average sampling duration and the number of samples collected were similar for the five primary MVS sites: Coast Guard Pier, Wallis Pier, Zephyr Cove Pier, Wallis Tower, and SOLA. The typical sampling duration was about 170 hours (1 week) and more than 20 samples were collected at these five sites. Sampler malfunctions and occasional two-week samples created a wide range of sampling durations. Fewer than 10 MVS samples were collected at Lake Forest, Bliss State Park, Timber Cove Pier (battery power only), and Sacramento (part of the dry deposition methods comparison study). Of particular interest and effort was the collection of MVS samples on two buoys. These samplers operated on battery power only and sampling durations were typically about 30 hours. The variable sampling durations and pattern of contemporaneous measurements with the MVS network limit spatial and temporal analyses to case studies. However, the TSP mass and major specie measurements are plotted by sample start_date later in this chapter to provide an indication of seasonal and spatial patterns.

Table 3-4. Number of samples and sample duration statistics for Mini-Vol samplers.

Site Name	Number of Samples Collected	Average Sampling Duration (hours)	Minimum Sampling Duration (hours)	Maximum Sampling Duration (hours)
Coast Guard Pier	45	174.9	0.0	338.5
Wallis Pier	41	141.7	0.0	341.9
Zephyr Cove Pier	39	152.0	0.0	394.0
Wallis Tower	32	157.6	0.0	368.0
SOLA	21	233.8	0.0	368.0
Timber Cove Pier	14	43.2	11.5	60.3
Lake Forest	8	182.6	117.1	298.6
Bliss State Park	7	141.5	0.0	283.5
Sacramento	6	115.5	0.0	240.3
TB4 (west) buoy	21	29.3	14.8	48.2
TB1 (east buoy)	21	30.0	24.0	47.1

3.2.1.2 Annual Summary of TWS Aerosol Mass and Chemical Concentrations

Table 3-5 (a-c) presents the annual averages for TWS TSP, PM10, and PM2.5 mass and chemical fractions concentrations from November 2002 to December 2003 at the BH, TB, LF, SW, and SOLA sites. The highest annual average TSP mass concentration was found at the SOLA site (21.9 µg/m^3), followed by the SW (20.1 µg/m^3), LF (14.5 µg/m^3), BH (11.4 µg/m^3), and TB (6.2 µg/m^3) sites. The most abundant chemical species (>1%) in TSP were OC (16.5-29.8%), silicon (10.8-16.0%), aluminum (3.9-4.7%), EC (2.5- 6.2%), calcium (1.7-2.4%), iron (2.1-2.7%), potassium (1.3-1.4%), nitrate (1.2-3.5%), ammonium (1.2-3.3%), and sulfur (1.1-3.4%).

The annual average PM10 mass concentration was highest at the SOLA site (18.8 µg/m^3), followed by the SW (16.8 µg/m^3), LF (14.0 µg/m^3), BH (8.8 µg/m^3), and TB (6.0 µg/m^3) sites. The most abundant chemical species in PM10 were OC (16.2-27.8%), silicon (10.0- 21.1%), aluminum (3.5-6.6%), EC (3.0-7.0%), iron (1.8-3.3%), calcium (1.6-2.9%), nitrate (1.3-3.6%), ammonium (1.3-3.2%), potassium (1.2-1.7%), and sulfur (1.2%-3.5%). The highest annual average PM2.5 mass concentration was found at the SW site (9.0 µg/m^3), followed by the SOLA (6.5 µg/m^3), BH (5.0 µg/m^3), LF (4.3 µg/m^3), and TB (3.6 µg/m^3) sites. The most abundant chemical species in PM2.5 were OC (42-51%), EC (4.9- 16.4%), ammonium (3.1-5.8%), sulfur (2.2-5.7%), nitrate (1.6-3.4%), and silicon (1.3- 2.6%).

The lowest annual average PM10 and PM2.5 mass concentrations were observed at the TB site and the highest PM10 and PM2.5 mass concentrations were observed at the SOLA and SW sites. Mass concentrations of TSP, PM10 and PM2.5 at the BH site were higher than those at the TB site. Similar trends were found for OC, EC, nitrate, ammonium, and sulfate concentrations in PM10 and PM2.5. PM10 and PM2.5 OC and EC concentrations at the SW and SOLA sites were two to three times greater than

those at the LF and TB sites, which could be explained by the influence of increased vehicle emissions at the SOLA and SW sites.

These results agree with the assumed characteristics of the sites identified for the LTADS: the TB site represents a local background site and the SOLA and SW sites represent heavy urban sites. PM2.5 mass and chemical concentrations were lower at the TB site than those at the BH site, which suggests that PM losses due to deposition and settling during transportation from the BH site to the Lake Tahoe region. Silicon and aluminum concentrations at these sites were high in PM10 but low in PM2.5, which suggests a significant contribution of re-suspended dust to coarse particles. The re-suspended dust contribution could be the result of vehicle traffic and wind.

3.2.1.3 Temporal and Spatial Variations in TWS Aerosol Mass and Composition

The temporal and spatial variations of the TWS mass and chemical compositions are presented in this section. When data are summarized by particle size, the following definitions are applied: PM_fine = PM2.5; PM_coarse = PM10 minus PM2.5; PM_large = TSP minus PM10.

An abbreviated summary of the TWS measurements is presented by TWS sampling period in **Figures 3-13 through 3-15**. TWS sampling periods 1-3 include data collected near the end of 2002; all the other TWS sampling periods include data collected during 2003. These figures show the contributions of particle size (PM_fine, PM_coarse, and PM_large) to total mass, nitrate, and ammonium at each site. Samples collected when events occurred that could impact the analytical results are identified as "**uncertain**". These sampling events include sampling durations different than planned, flow rate abnormalities, filter damage, etc. The events themselves do not necessarily invalidate the results but do indicate that non-standard sampling conditions occurred; data analysts should review the data for appropriate usage in specific applications. PM_coarse and PM_large data are derived from the PM2.5, PM10, and TSP measurements. Negative concentrations for PM_coarse or PM_large indicate that one or both of the source measurements may be invalid or, in the case of small negative values, that the difference in concentrations is less than the accuracy of the measurements. In general, PM_large contributed the least to the TSP mass. The rural sites (Big Hill and Thunderbird Lodge) tended to have PM_fine as a significant component of the TSP while the more urban sites (SW, SOLA, and Lake Forest) tended to have the greatest contribution to TSP in the PM_coarse size fraction. As might be expected, most of the ammonium, and much of the nitrate, was in the PM_fine fraction.

Figures 3-16, 3-17, and 3-18 show the variation of the relative contribution of each major component to TSP, PM10, and PM2.5, respectively, at each site. The dates in these figures indicate the start of TWS sampling. The BH site was selected to evaluate the transportation of atmospheric pollutants from areas outside the Lake Tahoe region. The TWS TSP mass concentrations measured at the BH site from 05/21/03 to 10/22/03 ranged from 10-22 $\mu g/m^3$, which were more than twice the TSP mass concentrations (1.8-6.7 $\mu g/m^3$) measured at this site from 02/26/03 to 04/23/03 and 12/03/03 to

Table 3-5a. Annual average TSP mass and chemical fractions for Two-Week Samplers

	Big Hill		Thunderbird		Lake Forest		Sandy Way		SOLA	
	Average Concentration (ug/m3)	% Mass	Average Concentration (ug/m3)	% Mass	Average Concentration (ug/m3)	% Mass	Average Concentration (ug/m3)	% Mass	Average Concentration (ug/m3)	% Mass
Number in Average	19		28		28		29		25	
Mass	11.355	100.000	6.206	100.000	16.466	100.000	20.118	100.000	21.895	100.000
Volatalized Nitrate	0.833	7.340	0.429	6.907	0.345	2.093	0.671	3.335	0.446	2.037
Chloride	0.009	0.079	0.026	0.415	0.090	0.549	0.089	0.444	0.167	0.761
Nitrite	0.000	0.000	0.000	0.000	0.000	0.000	0.000	0.000	0.000	0.000
Nitrate	0.394	3.470	0.171	2.753	0.205	1.246	0.382	1.899	0.373	1.705
Phosphate	0.000	0.000	0.000	0.000	0.000	0.000	0.000	0.000	0.000	0.000
Sulfate	0.655	5.768	0.452	7.285	0.435	2.643	0.470	2.335	0.331	1.512
Ammonium	0.305	2.689	0.206	3.314	0.214	1.302	0.318	1.579	0.258	1.178
Soluble Sodium	0.075	0.663	0.056	0.905	0.111	0.671	0.137	0.683	0.187	0.856
Soluble Magnesium	0.012	0.107	0.010	0.161	0.012	0.074	0.015	0.072	0.012	0.057
Soluble Potassium	0.047	0.417	0.034	0.549	0.046	0.282	0.063	0.311	0.045	0.204
Soluble Calcium	0.109	0.958	0.080	1.296	0.117	0.708	0.144	0.717	0.165	0.752
O1TC	0.106	0.934	0.063	1.010	0.097	0.586	0.420	2.087	0.280	1.277
O2TC	0.304	2.677	0.213	3.432	0.321	1.951	0.920	4.572	0.661	3.021
O3TC	1.170	10.304	0.846	13.628	1.437	8.728	3.269	16.247	2.468	11.274
O4TC	0.487	4.289	0.350	5.644	0.588	3.572	1.157	5.749	0.869	3.967
OPTC	0.241	2.125	0.185	2.987	0.277	1.682	0.240	1.194	0.205	0.935
OCTC	2.308	20.329	1.657	26.701	2.720	16.518	6.005	29.849	4.483	20.473
E1TC	0.342	3.012	0.265	4.268	0.481	2.919	1.129	5.610	0.986	4.503
E2TC	0.171	1.505	0.156	2.521	0.270	1.642	0.340	1.690	0.321	1.464
E3TC	0.016	0.138	0.009	0.150	0.018	0.108	0.028	0.138	0.016	0.074
ECTC	0.287	2.531	0.245	3.953	0.492	2.988	1.256	6.243	1.118	5.106
TCTC	2.596	22.860	1.902	30.654	3.212	19.506	7.261	36.093	5.601	25.580
Sodium	0.029	0.258	0.019	0.303	0.053	0.323	0.042	0.211	0.050	0.227
Magnesium	0.012	0.106	0.017	0.270	0.024	0.144	0.011	0.054	0.016	0.071
Aluminum	0.529	4.658	0.255	4.102	0.839	5.096	0.779	3.873	1.006	4.595
Silicon	1.230	10.830	0.767	12.356	2.643	16.049	2.556	12.703	3.472	15.859
Phosphorus	0.000	0.001	0.000	0.005	0.001	0.008	0.001	0.003	0.001	0.003
Sulfur	0.291	2.561	0.211	3.403	0.215	1.305	0.222	1.103	0.236	1.079
Chlorine	0.004	0.037	0.006	0.099	0.084	0.512	0.119	0.591	0.203	0.928
Potassium	0.151	1.328	0.089	1.432	0.212	1.289	0.263	1.307	0.307	1.403
Calcium	0.180	1.586	0.121	1.943	0.388	2.359	0.334	1.661	0.460	2.101
Titanium	0.024	0.210	0.011	0.181	0.047	0.288	0.043	0.214	0.050	0.227
Vanadium	0.001	0.005	0.000	0.007	0.001	0.006	0.001	0.006	0.001	0.004
Chromium	0.001	0.005	0.000	0.004	0.001	0.004	0.001	0.004	0.001	0.004
Manganese	0.008	0.067	0.003	0.050	0.009	0.053	0.009	0.044	0.011	0.049
Iron	0.263	2.315	0.130	2.100	0.446	2.708	0.458	2.276	0.596	2.724
Cobalt	0.002	0.017	0.001	0.015	0.004	0.023	0.004	0.018	0.005	0.022
Nickel	0.000	0.003	0.000	0.003	0.000	0.002	0.000	0.002	0.000	0.002
Cupper	0.009	0.077	0.002	0.028	0.003	0.019	0.007	0.033	0.006	0.027
Zinc	0.008	0.067	0.004	0.063	0.008	0.046	0.017	0.083	0.019	0.085
Gallium	0.000	0.001	0.000	0.002	0.000	0.000	0.000	0.000	0.000	0.000
Arsenic	0.000	0.001	0.000	0.002	0.000	0.001	0.000	0.002	0.000	0.001
Selenium	0.000	0.001	0.000	0.001	0.000	0.000	0.000	0.000	0.000	0.000
Bromine	0.001	0.013	0.001	0.021	0.001	0.009	0.002	0.008	0.002	0.008
Rubidium	0.001	0.006	0.000	0.005	0.001	0.004	0.001	0.005	0.001	0.005
Strontium	0.001	0.010	0.001	0.015	0.006	0.039	0.004	0.021	0.006	0.028
Yttrium	0.000	0.003	0.000	0.005	0.000	0.002	0.000	0.002	0.000	0.002
Zirconium	0.000	0.004	0.000	0.004	0.002	0.010	0.001	0.006	0.002	0.007
Molybdenum	0.000	0.003	0.000	0.002	0.000	0.002	0.000	0.001	0.000	0.001
Palladium	0.000	0.002	0.000	0.003	0.000	0.001	0.000	0.001	0.000	0.001
Silver	0.000	0.002	0.000	0.003	0.000	0.002	0.000	0.001	0.000	0.002
Cadmium	0.000	0.001	0.000	0.003	0.000	0.002	0.000	0.002	0.000	0.001
Indium	0.001	0.007	0.000	0.006	0.000	0.002	0.001	0.003	0.001	0.003
Tin	0.001	0.013	0.001	0.023	0.001	0.009	0.001	0.007	0.002	0.007
Antimony	0.001	0.011	0.001	0.019	0.001	0.007	0.001	0.006	0.001	0.005
Barium	0.005	0.046	0.006	0.097	0.013	0.080	0.013	0.063	0.021	0.095
Lanthanum	0.008	0.071	0.007	0.118	0.006	0.038	0.005	0.023	0.006	0.028
Gold	0.000	0.001	0.000	0.002	0.000	0.001	0.000	0.001	0.000	0.001
Mercury	0.000	0.001	0.000	0.002	0.000	0.001	0.000	0.000	0.000	0.001
Thallium	0.000	0.001	0.000	0.001	0.000	0.001	0.000	0.000	0.000	0.001
Lead	0.001	0.010	0.001	0.015	0.001	0.008	0.002	0.008	0.001	0.006
Uranium	0.000	0.001	0.000	0.003	0.000	0.001	0.000	0.001	0.000	0.001

Table 3-5b. Annual average PM10 mass and chemical fractions for Two Week

	Big Hill		Thunderbird		Lake Forest		Sandy Way		SOLA	
	Average Concentration (ug/m3)	% Mass	Average Concentration (ug/m3)	% Mass	Average Concentration (ug/m3)	% Mass	Average Concentration (ug/m3)	% Mass	Average Concentration (ug/m3)	% Mass
Number in Average	19		28		28		29		25	
Mass	8.814	100.000	5.957	100.000	13.981	100.000	16.762	100.000	18.822	100.000
Volatalized Nitrate	0.519	5.885	0.243	4.082	0.270	1.933	0.559	3.332	0.482	2.560
Chloride	0.022	0.254	0.016	0.275	0.050	0.360	0.065	0.387	0.111	0.591
Nitrite	0.007	0.076	0.000	0.000	0.000	0.000	0.000	0.000	0.000	0.000
Nitrate	0.313	3.556	0.131	2.205	0.182	1.304	0.329	1.963	0.346	1.838
Phosphate	0.004	0.041	0.000	0.000	0.004	0.027	0.000	0.000	0.000	0.000
Sulfate	0.644	7.301	0.425	7.142	0.458	3.274	0.486	2.897	0.467	2.479
Ammonium	0.282	3.197	0.157	2.636	0.182	1.300	0.272	1.621	0.261	1.388
Soluble Sodium	0.066	0.747	0.067	1.126	0.095	0.679	0.097	0.582	0.135	0.718
Soluble Magnesium	0.010	0.117	0.006	0.107	0.010	0.070	0.012	0.070	0.011	0.057
Soluble Potassium	0.038	0.431	0.025	0.412	0.032	0.231	0.055	0.329	0.046	0.244
Soluble Calcium	0.074	0.842	0.054	0.906	0.093	0.668	0.117	0.700	0.146	0.778
O1TC	0.352	3.998	0.255	4.284	0.267	1.910	0.673	4.013	0.388	2.062
O2TC	0.296	3.362	0.194	3.259	0.281	2.010	0.844	5.034	0.604	3.211
O3TC	1.067	12.104	0.723	12.137	1.167	8.346	2.869	17.114	2.414	12.826
O4TC	0.484	5.490	0.310	5.202	0.470	3.359	1.037	6.186	0.905	4.807
OPTC	0.225	2.552	0.172	2.895	0.221	1.583	0.216	1.290	0.194	1.030
OCTC	2.424	27.506	1.655	27.777	2.406	17.209	5.638	33.636	4.505	23.936
E1TC	0.298	3.386	0.237	3.974	0.381	2.725	1.009	6.017	1.018	5.408
E2TC	0.178	2.018	0.152	2.557	0.267	1.907	0.357	2.128	0.382	2.028
E3TC	0.015	0.168	0.016	0.269	0.016	0.111	0.032	0.190	0.021	0.112
ECTC	0.266	3.020	0.233	3.906	0.442	3.161	1.181	7.046	1.227	6.518
TCTC	2.691	30.527	1.887	31.682	2.848	20.369	6.819	40.682	5.732	30.454
Sodium	0.045	0.506	0.017	0.287	0.052	0.371	0.032	0.190	0.038	0.201
Magnesium	0.018	0.206	0.017	0.280	0.019	0.135	0.010	0.061	0.023	0.123
Aluminum	0.371	4.206	0.208	3.496	0.928	6.636	0.590	3.519	0.799	4.244
Silicon	0.881	9.992	0.623	10.456	2.955	21.137	1.837	10.962	2.594	13.781
Phosphorus	0.000	0.002	0.001	0.017	0.001	0.007	0.000	0.002	0.001	0.005
Sulfur	0.287	3.251	0.206	3.451	0.233	1.666	0.217	1.294	0.220	1.169
Chlorine	0.002	0.025	0.006	0.096	0.130	0.928	0.080	0.480	0.123	0.656
Potassium	0.112	1.276	0.075	1.258	0.236	1.691	0.198	1.179	0.232	1.235
Calcium	0.137	1.551	0.098	1.649	0.402	2.876	0.237	1.413	0.340	1.805
Titanium	0.015	0.175	0.008	0.142	0.045	0.325	0.028	0.165	0.038	0.201
Vanadium	0.001	0.008	0.000	0.006	0.001	0.005	0.001	0.005	0.001	0.006
Chromium	0.000	0.005	0.001	0.019	0.001	0.005	0.001	0.003	0.001	0.003
Manganese	0.005	0.061	0.003	0.046	0.009	0.062	0.006	0.038	0.008	0.041
Iron	0.218	2.476	0.108	1.808	0.462	3.303	0.324	1.934	0.443	2.354
Cobalt	0.002	0.019	0.001	0.014	0.004	0.028	0.003	0.016	0.003	0.019
Nickel	0.000	0.004	0.000	0.007	0.000	0.002	0.000	0.002	0.000	0.002
Cupper	0.002	0.022	0.001	0.021	0.003	0.024	0.007	0.041	0.004	0.023
Zinc	0.003	0.033	0.002	0.032	0.009	0.065	0.013	0.076	0.014	0.072
Gallium	0.000	0.001	0.000	0.001	0.000	0.001	0.000	0.001	0.000	0.000
Arsenic	0.000	0.001	0.000	0.003	0.000	0.002	0.000	0.001	0.000	0.001
Selenium	0.000	0.001	0.000	0.002	0.000	0.001	0.000	0.001	0.000	0.000
Bromine	0.002	0.018	0.001	0.022	0.002	0.011	0.002	0.009	0.002	0.008
Rubidium	0.000	0.003	0.000	0.004	0.001	0.006	0.001	0.004	0.001	0.004
Strontium	0.001	0.010	0.001	0.013	0.006	0.045	0.003	0.016	0.004	0.023
Yttrium	0.000	0.002	0.000	0.004	0.000	0.003	0.000	0.001	0.000	0.002
Zirconium	0.000	0.005	0.000	0.004	0.002	0.012	0.001	0.005	0.001	0.007
Molybdenum	0.000	0.001	0.000	0.003	0.000	0.003	0.000	0.002	0.000	0.001
Palladium	0.000	0.001	0.000	0.002	0.000	0.001	0.000	0.001	0.000	0.001
Silver	0.000	0.003	0.000	0.004	0.000	0.002	0.000	0.001	0.000	0.001
Cadmium	0.000	0.003	0.000	0.004	0.000	0.001	0.000	0.002	0.000	0.002
Indium	0.001	0.007	0.000	0.006	0.001	0.004	0.000	0.003	0.000	0.002
Tin	0.002	0.025	0.001	0.016	0.001	0.010	0.002	0.011	0.002	0.011
Antimony	0.001	0.008	0.001	0.011	0.001	0.008	0.001	0.007	0.001	0.006
Barium	0.004	0.045	0.006	0.105	0.015	0.110	0.011	0.064	0.013	0.067
Lanthanum	0.007	0.082	0.006	0.103	0.006	0.046	0.004	0.024	0.006	0.032
Gold	0.000	0.000	0.000	0.003	0.000	0.002	0.000	0.000	0.000	0.001
Mercury	0.000	0.002	0.000	0.001	0.000	0.001	0.000	0.001	0.000	0.001
Thallium	0.000	0.000	0.000	0.000	0.000	0.000	0.000	0.000	0.000	0.000
Lead	0.001	0.014	0.001	0.017	0.002	0.013	0.002	0.011	0.002	0.008
Uranium	0.000	0.002	0.000	0.001	0.000	0.002	0.000	0.001	0.000	0.001

Table 3-5c. Annual average PM2.5 mass and chemical fractions for Two Week

	Big Hill		Thunderbird		Lake Forest		Sandy Way		SOLA	
	Average Concentration (ug/m3)	% Mass	Average Concentration (ug/m3)	% Mass	Average Concentration (ug/m3)	% Mass	Average Concentration (ug/m3)	% Mass	Average Concentration (ug/m3)	% Mass
Number in Average	19		28		28		29		25	
Mass	4.950	100.000	3.629	100.000	4.307	100.000	8.952	100.000	6.530	100.000
Volatalized Nitrate	0.470	9.505	0.231	6.375	0.253	5.868	0.527	5.883	0.471	7.214
Chloride	0.015	0.299	0.009	0.252	0.015	0.348	0.036	0.404	0.031	0.469
Nitrite	0.004	0.090	0.000	0.000	0.000	0.000	0.000	0.000	0.005	0.080
Nitrate	0.167	3.381	0.059	1.630	0.099	2.288	0.218	2.438	0.222	3.405
Phosphate	0.004	0.082	0.000	0.000	0.000	0.000	0.000	0.000	0.004	0.055
Sulfate	0.579	11.696	0.360	9.926	0.428	9.944	0.436	4.872	0.433	6.625
Ammonium	0.285	5.762	0.172	4.743	0.204	4.732	0.277	3.093	0.288	4.405
Soluble Sodium	0.031	0.632	0.016	0.440	0.011	0.265	0.018	0.204	0.026	0.391
Soluble Magnesium	0.002	0.035	0.001	0.038	0.001	0.033	0.001	0.015	0.001	0.020
Soluble Potassium	0.024	0.478	0.018	0.506	0.022	0.508	0.040	0.446	0.031	0.477
Soluble Calcium	0.006	0.126	0.005	0.150	0.009	0.200	0.009	0.101	0.012	0.191
O1TC	0.589	11.893	0.386	10.644	0.384	8.906	0.603	6.741	0.455	6.968
O2TC	0.330	6.669	0.186	5.124	0.236	5.478	0.746	8.338	0.462	7.073
O3TC	0.873	17.638	0.574	15.814	0.755	17.529	2.171	24.254	1.486	22.760
O4TC	0.334	6.745	0.231	6.378	0.299	6.938	0.788	8.803	0.568	8.697
OPTC	0.179	3.625	0.163	4.495	0.174	4.036	0.265	2.957	0.232	3.559
OCTC	2.305	46.570	1.541	42.454	1.847	42.887	4.574	51.092	3.203	49.058
E1TC	0.260	5.250	0.195	5.367	0.271	6.289	0.976	10.905	0.819	12.550
E2TC	0.151	3.060	0.156	4.298	0.247	5.739	0.379	4.237	0.444	6.804
E3TC	0.008	0.170	0.017	0.469	0.026	0.605	0.039	0.441	0.042	0.639
ECTC	0.240	4.855	0.205	5.639	0.370	8.596	1.130	12.626	1.073	16.433
TCTC	2.545	51.425	1.746	48.093	2.217	51.483	5.704	63.718	4.276	65.491
Sodium	0.009	0.188	0.034	0.937	0.015	0.339	0.025	0.281	0.034	0.516
Magnesium	0.007	0.147	0.007	0.194	0.010	0.222	0.007	0.081	0.008	0.121
Aluminum	0.024	0.489	0.017	0.456	0.030	0.705	0.032	0.356	0.035	0.529
Silicon	0.066	1.333	0.060	1.650	0.113	2.619	0.117	1.305	0.121	1.853
Phosphorus	0.000	0.004	0.000	0.005	0.000	0.001	0.000	0.000	0.000	0.000
Sulfur	0.273	5.517	0.208	5.732	0.197	4.572	0.194	2.172	0.190	2.916
Chlorine	0.000	0.004	0.000	0.004	0.001	0.034	0.005	0.060	0.004	0.058
Potassium	0.033	0.670	0.025	0.696	0.031	0.724	0.054	0.605	0.045	0.691
Calcium	0.016	0.326	0.015	0.402	0.026	0.613	0.025	0.282	0.028	0.431
Titanium	0.002	0.032	0.001	0.041	0.002	0.054	0.001	0.014	0.003	0.053
Vanadium	0.000	0.006	0.000	0.008	0.000	0.006	0.000	0.002	0.000	0.006
Chromium	0.000	0.004	0.000	0.003	0.000	0.003	0.000	0.001	0.000	0.002
Manganese	0.001	0.013	0.001	0.015	0.001	0.020	0.001	0.009	0.001	0.014
Iron	0.024	0.491	0.023	0.629	0.043	1.005	0.043	0.477	0.054	0.831
Cobalt	0.000	0.008	0.000	0.008	0.001	0.012	0.001	0.006	0.000	0.007
Nickel	0.000	0.004	0.000	0.002	0.000	0.002	0.000	0.001	0.000	0.002
Cupper	0.001	0.011	0.002	0.041	0.001	0.029	0.007	0.079	0.002	0.036
Zinc	0.002	0.033	0.002	0.059	0.003	0.062	0.009	0.097	0.005	0.080
Gallium	0.000	0.001	0.000	0.001	0.000	0.002	0.000	0.000	0.000	0.002
Arsenic	0.000	0.002	0.000	0.004	0.000	0.001	0.000	0.003	0.000	0.002
Selenium	0.000	0.003	0.000	0.002	0.000	0.003	0.000	0.001	0.000	0.001
Bromine	0.001	0.029	0.002	0.043	0.001	0.028	0.001	0.015	0.001	0.021
Rubidium	0.000	0.003	0.000	0.003	0.000	0.002	0.000	0.003	0.000	0.003
Strontium	0.000	0.003	0.000	0.005	0.000	0.010	0.000	0.004	0.000	0.007
Yttrium	0.000	0.005	0.000	0.005	0.000	0.003	0.000	0.002	0.000	0.004
Zirconium	0.000	0.002	0.000	0.003	0.000	0.003	0.000	0.001	0.000	0.001
Molybdenum	0.000	0.003	0.000	0.006	0.000	0.007	0.000	0.002	0.000	0.002
Palladium	0.000	0.002	0.000	0.001	0.000	0.003	0.000	0.002	0.000	0.002
Silver	0.000	0.003	0.000	0.007	0.000	0.005	0.000	0.002	0.000	0.004
Cadmium	0.000	0.009	0.000	0.004	0.000	0.007	0.000	0.004	0.000	0.004
Indium	0.000	0.006	0.000	0.009	0.001	0.014	0.000	0.003	0.000	0.003
Tin	0.001	0.025	0.001	0.022	0.001	0.034	0.001	0.013	0.001	0.018
Antimony	0.001	0.025	0.001	0.022	0.001	0.022	0.001	0.009	0.001	0.012
Barium	0.008	0.161	0.005	0.125	0.006	0.131	0.007	0.083	0.006	0.087
Lanthanum	0.005	0.111	0.005	0.146	0.006	0.139	0.008	0.088	0.005	0.074
Gold	0.000	0.002	0.000	0.003	0.000	0.003	0.000	0.001	0.000	0.003
Mercury	0.000	0.002	0.000	0.002	0.000	0.003	0.000	0.001	0.000	0.002
Thallium	0.000	0.001	0.000	0.000	0.000	0.001	0.000	0.000	0.000	0.001
Lead	0.001	0.012	0.001	0.022	0.001	0.021	0.002	0.018	0.001	0.013
Uranium	0.000	0.001	0.000	0.004	0.000	0.003	0.000	0.002	0.000	0.003

12/17/03. Geological material and unidentified mass contributed more than 60% of TSP mass from 05/21/03 to 10/22/03 and less than 50% from 02/26/03 to 04/23/03 and from 12/03/03 to 12/17/03 (**Figure 3-16a**).

TSP mass concentrations at the TB site (**Figure 3-16e**), considered to be the local background site, were generally less than 5 $\mu g/m^3$ during winter and spring (11/20/02 to 04/10/03 and 11/05/03 to 12/17/03) but increased during the period from 05/07/03 to 10/22/03. The temporal variation of TSP mass concentrations observed at the TB site was similar to that observed at the BH site; however, a temporal pattern of geological and unidentified material contributions to TSP did not emerge at the TB location. **Figures 3-16c and d** confirm the expectation of higher PM concentrations in South Lake Tahoe. These figures show that similar temporal trends and comparable TSP mass concentrations were observed at the SOLA and SW sites. **Figure 3-16b** shows that, if the sample collected on 12/04/02 (sampling period 2, 82 $\mu g/m^3$) is excluded, PM concentrations at Lake Forest were generally lower than South Lake Tahoe. TSP mass concentration decreases from > 25 $\mu g/m^3$ in January to 10 $\mu g/m^3$ in March and April, with a slight increase to 15 $\mu g/m^3$ in summer and fall (05/07/03 to 11/19/03). In general, TSP mass concentrations observed at the LF, SOLA, and SW sites were approximately two to three times greater than those observed at the BH and LF sites.

For TSP, in addition to geological and unidentified material, organic matter (OC) and soot (EC) were the second and the third largest chemical species that contributed to the temporal variation observed at the sites. (Note: OC concentrations were multiplied by 1.2 to correct for pyrolysis of organic carbon compounds to elemental carbon. Without this correction, the organic carbon fraction of the sample would be underestimated and the elemental carbon fraction would be overestimated by including some pyrolyzed organic carbon. (DRI, 2000)) Contributions of organic matter and soot to TSP mass concentration increased at the SOLA and SW sites during the period from 11/20/02 to 03/12/03, which was likely the result of wood smoke and increased traffic volume for winter sport activities in the vicinity of the SOLA and SW sites. PM10 composed > 80% of TSP at the five sites in LTADS. **Figures 3-16 and 3-17** show that the temporal and spatial variations of PM10 mass concentrations, geological material, organic matter, and soot are similar to those of TSP.

Figure 3-18 shows the very large OC contribution to PM2.5 at all sites. No clear temporal variation of PM2.5 mass concentration (**Figure 3-18a**) was observed at the BH site. The PM2.5 mass concentrations at the TB site were generally < 3 $\mu g/m^3$ for measurements prior to 04/10/03, and increased by 50% or more from 05/07/03 to 10/08/03. Significant increases in PM2.5 mass concentrations (8-15 $\mu g/m^3$) were observed at the SOLA and SW sites from 11/20/02 to 02/26/03. This increase was due to the increased organic matter and EC concentrations, which were twice as high as those measured at the TB site. Concentrations of geological material in PM2.5 were similar at all five sites and temporal variation was not observed. Organic matter and EC contributed approximately 80% of PM2.5 mass at the SOLA and SW sites from 11/20/02 to 02/26/03.

Figure 3-13a. PM Size Contributions to Total Mass Observed with the TWS at Big Hill.

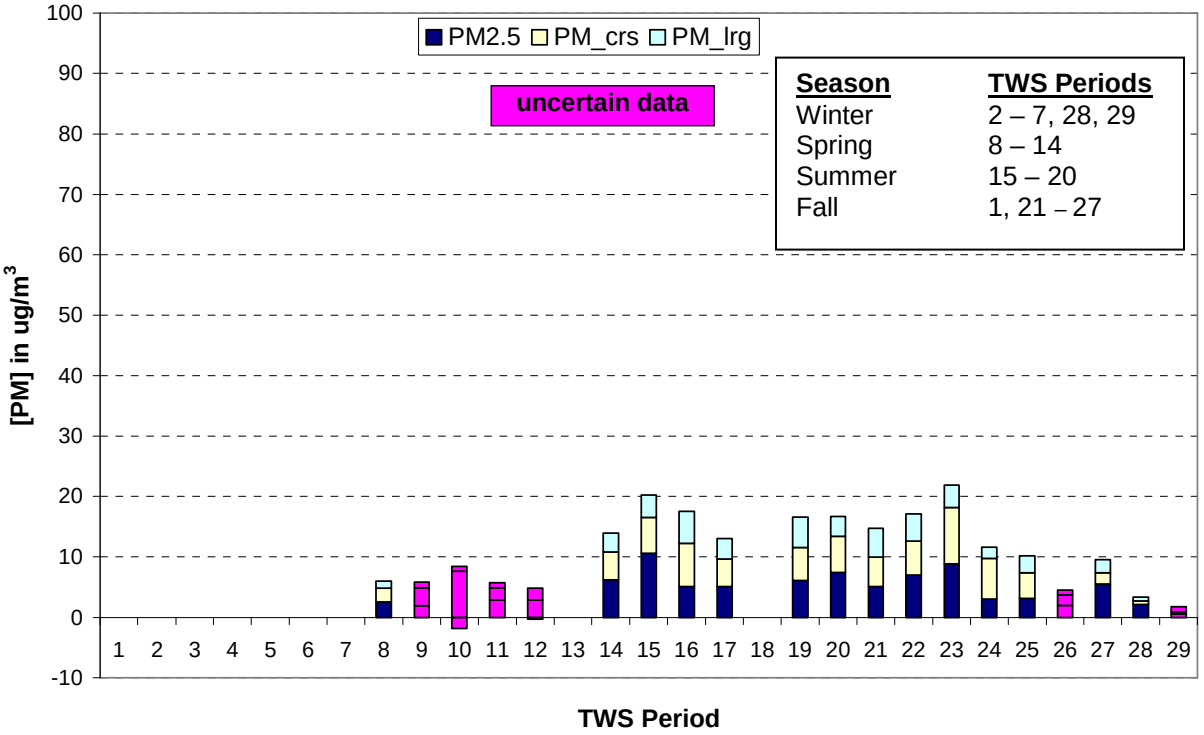

Figure 3-13b. PM Size Contributions to Total Mass Observed with the TWS at SLT-Sandy Way**.**

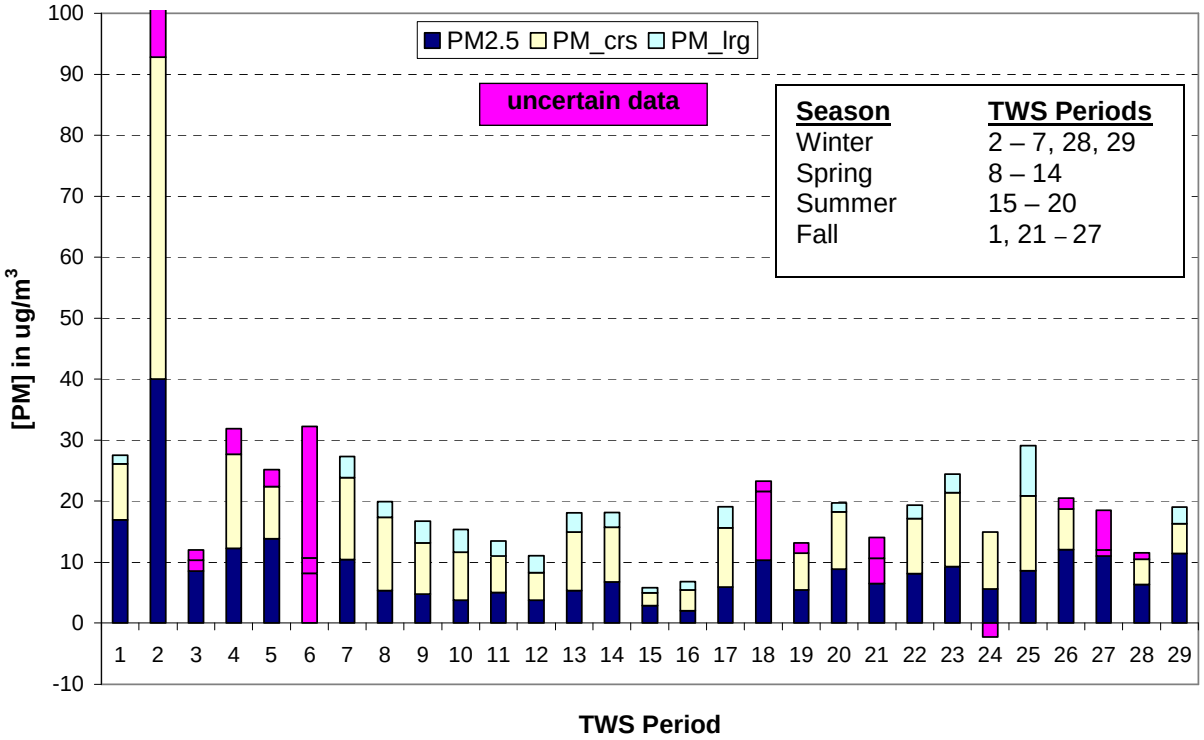

Figure 3-13c. PM Size Contributions to Total Mass Observed with the TWS at SLT-SOLA.

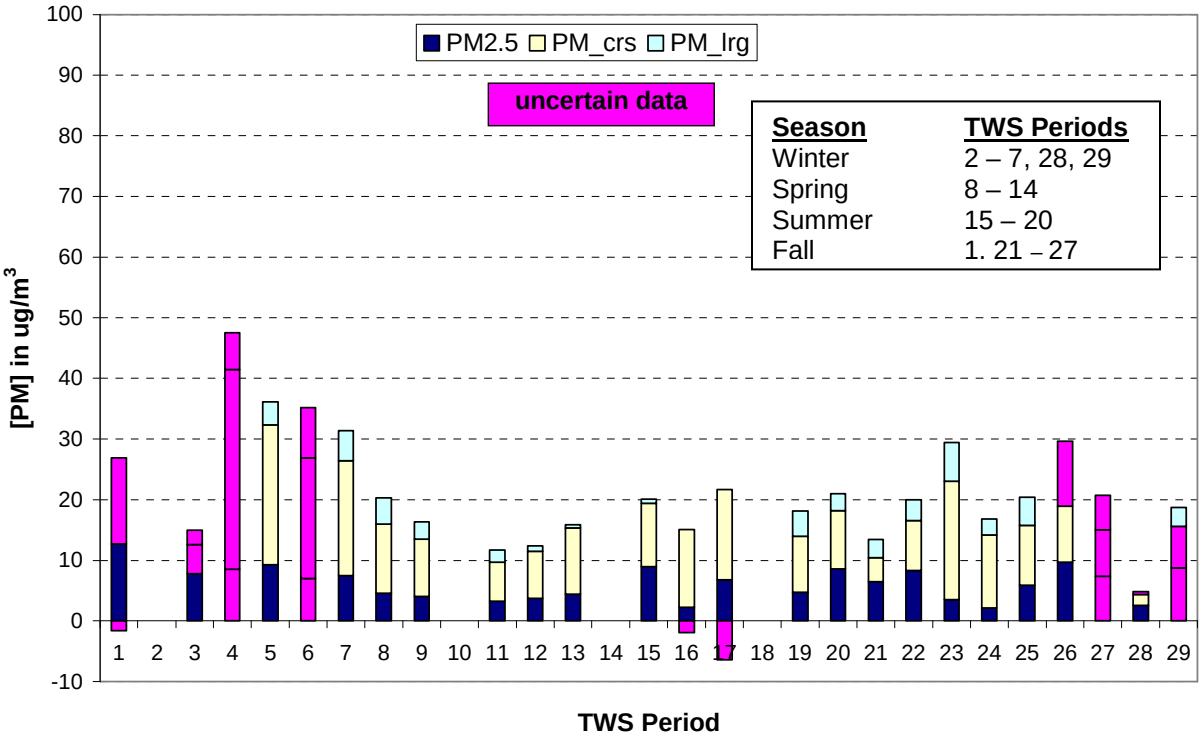

Figure 3-13d. PM Size Contributions to Total Mass Observed with the TWS at Thunderbird Lodge.

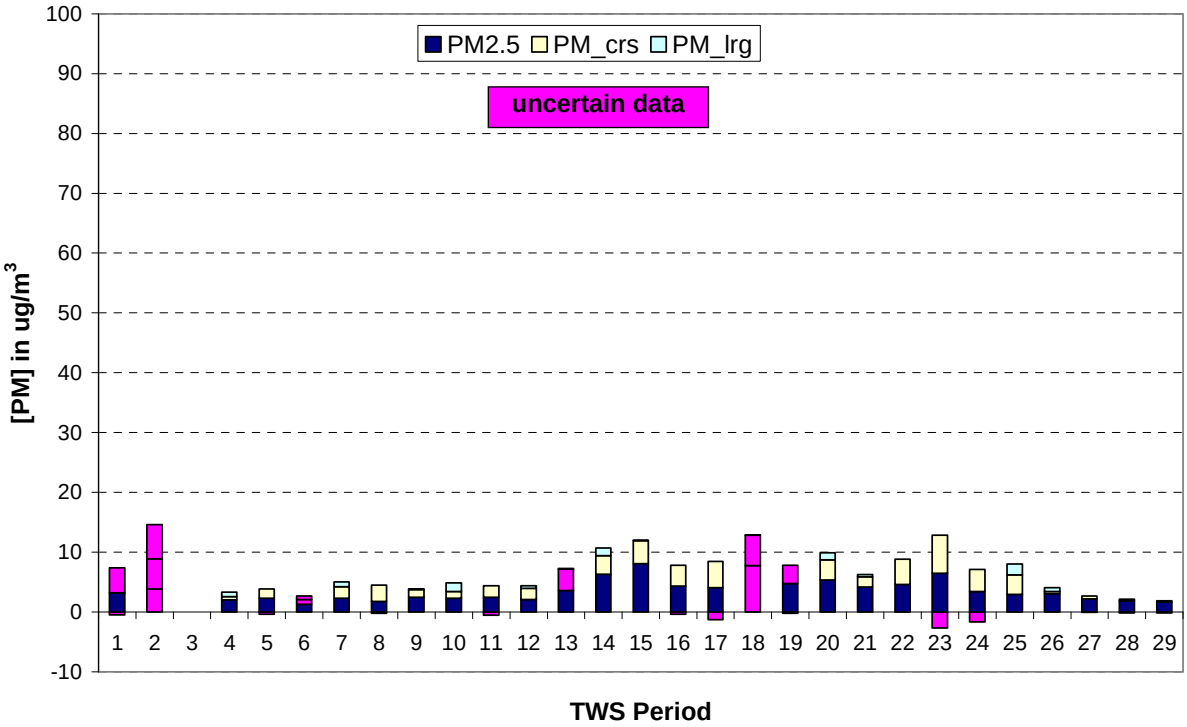

Figure 3-13e. PM Size Contributions to Total Mass Observed with the TWS at Lake Forest.

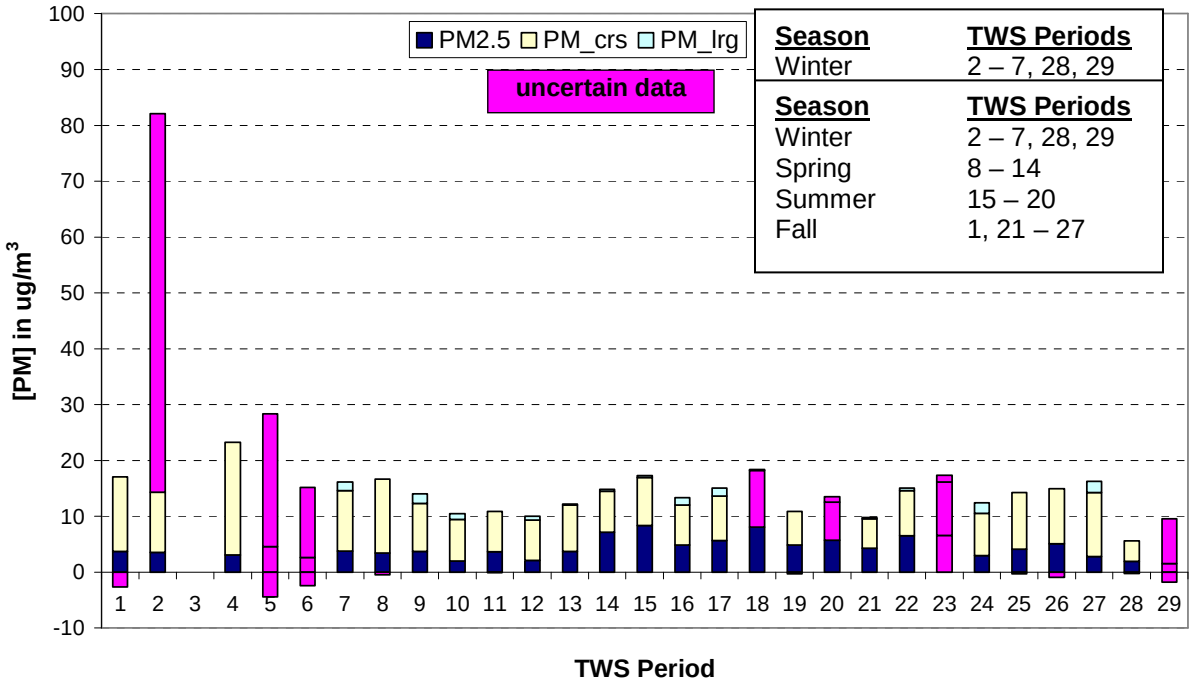

Figure 3-14a. PM Size Contributions to Nitrate Observed with the TWS at Big Hill.

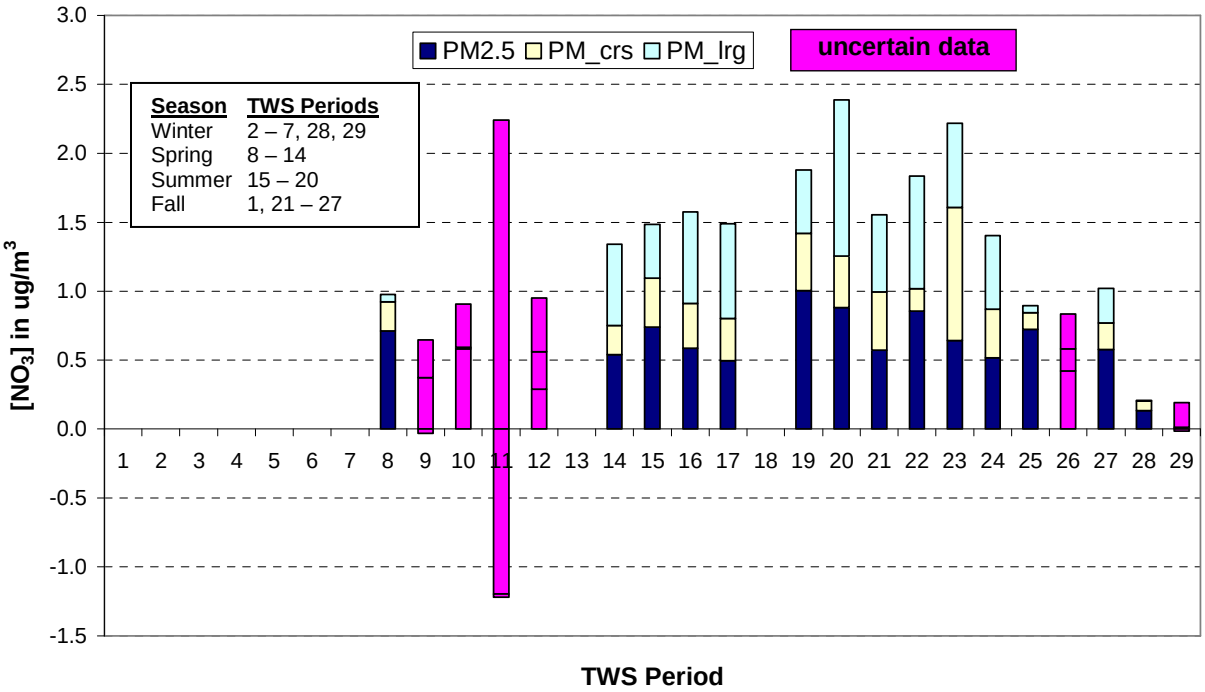

Figure 3-14b. PM Size Contributions to Nitrate Concentrations Observed with the TWS at SLT-Sandy Way.

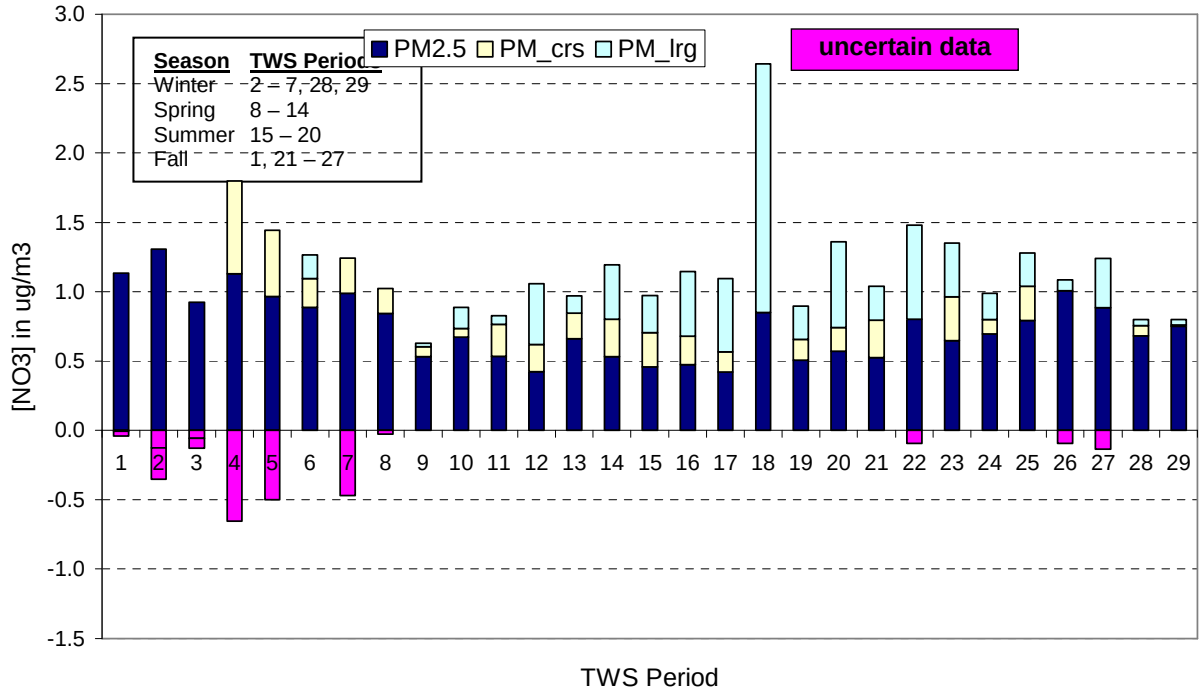

Figure 3-14c. PM Size Contributions to Nitrate Concentrations Observed with the TWS at SLT-SOLA.

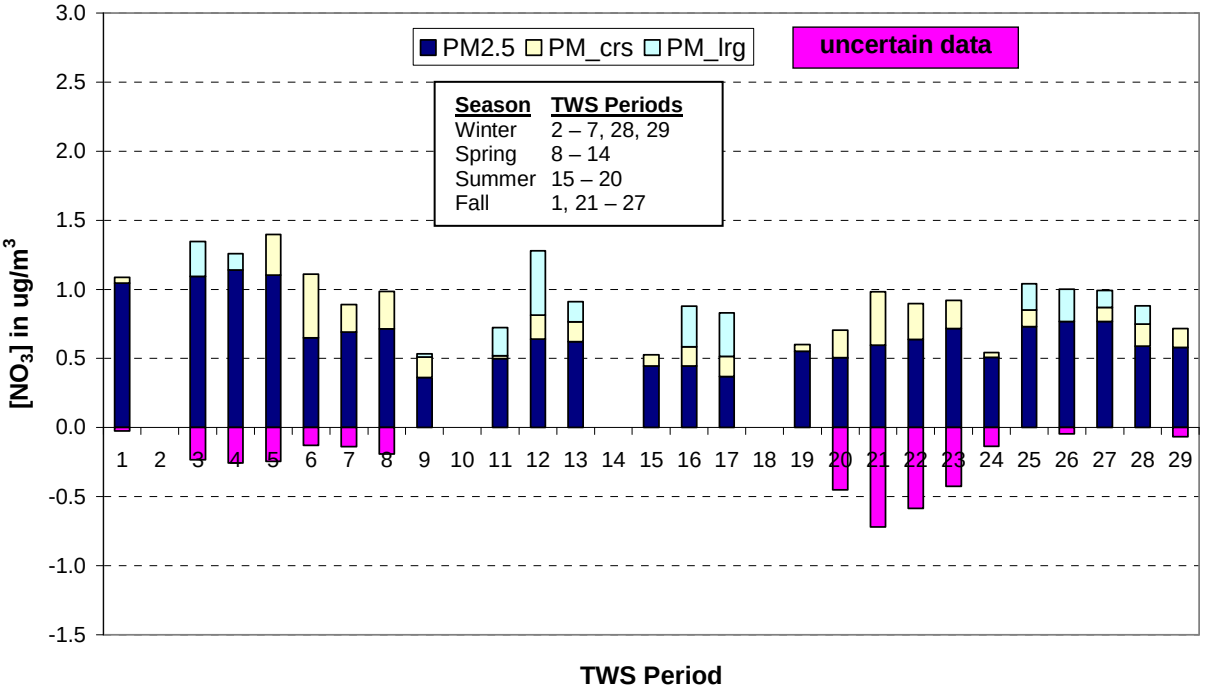

Figure 3-14d. PM Size Contributions to Nitrate Concentrations Observed with the TWS at Thunderbird Lodge.

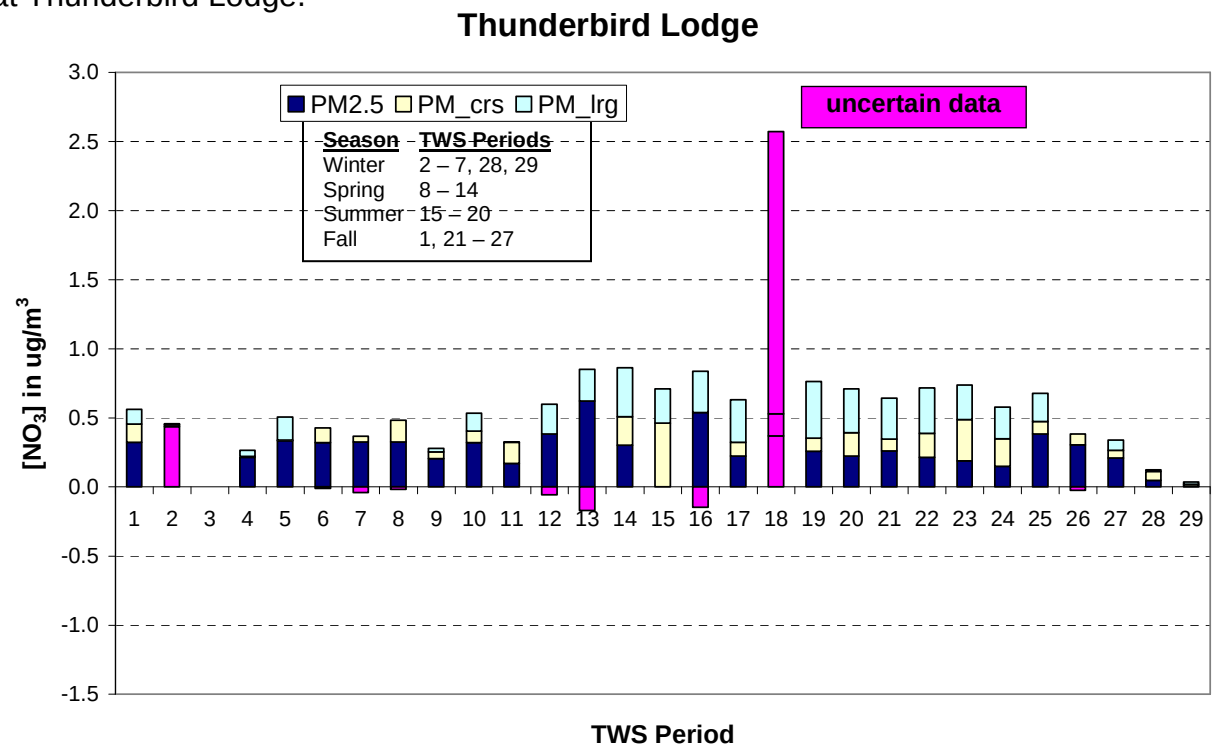

Figure 3-14e. PM Size Contributions to Nitrate Concentrations Observed with the TWS at Lake Forest.

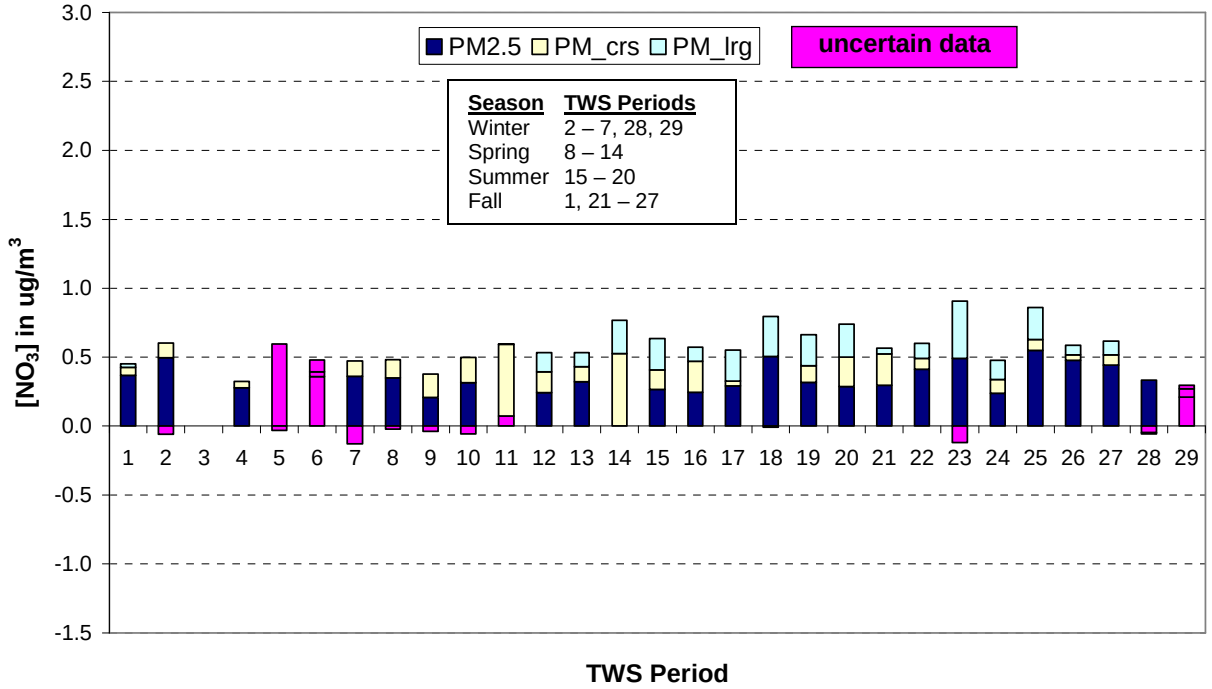

Figure 3-15a. PM Size Contributions to Ammonium Concentrations Observed with the TWS at Big Hill.

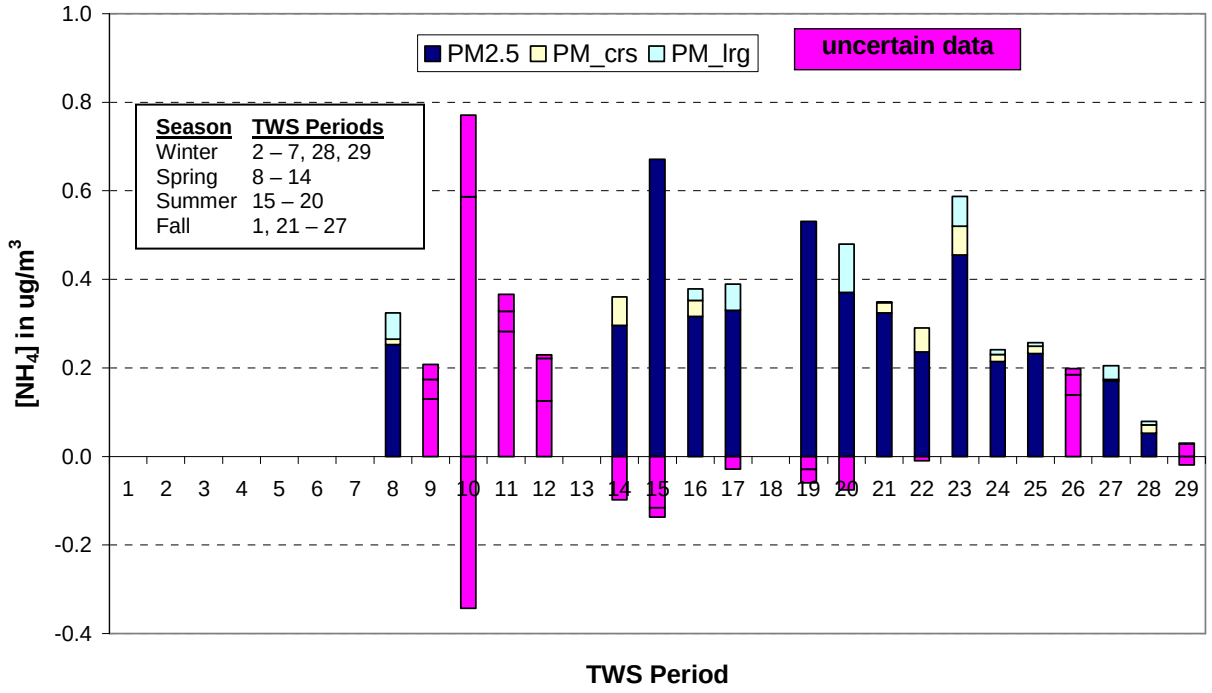

Figure 3-15b. PM Size Contributions to Ammonium Concentrations Observed with the TWS at SLT-Sandy Way.

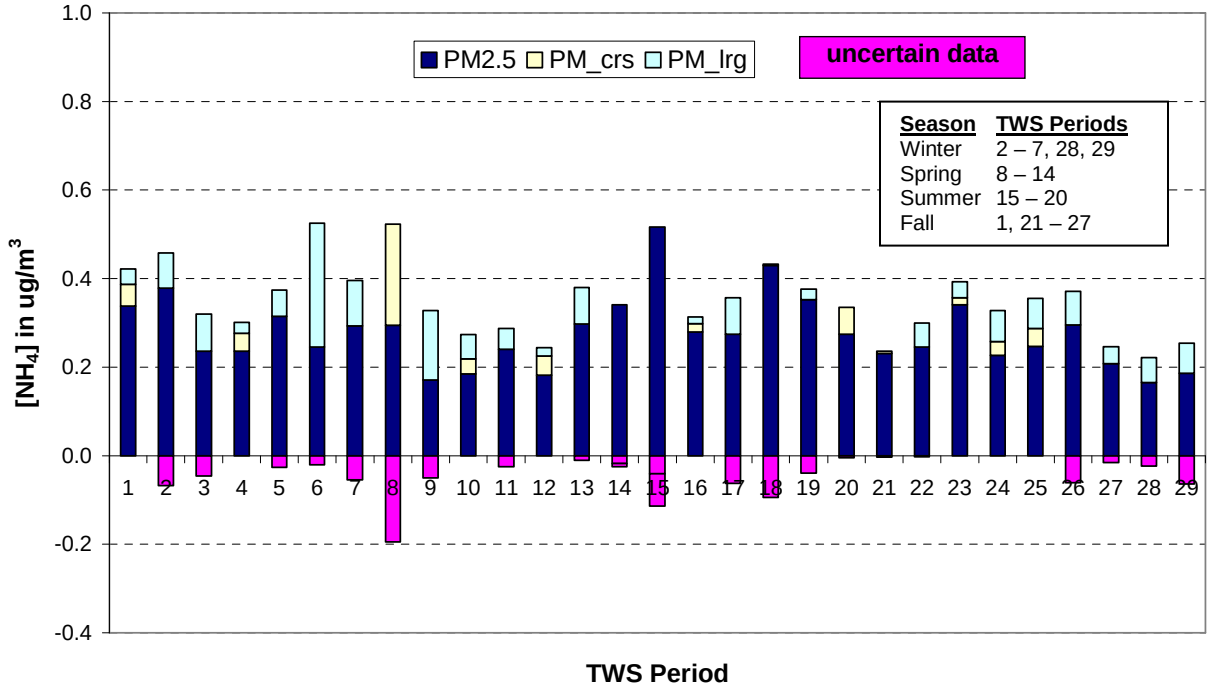

Figure 3-15c. PM Size Contributions to Ammonium Concentrations Observed with the TWS at SLT-SOLA.

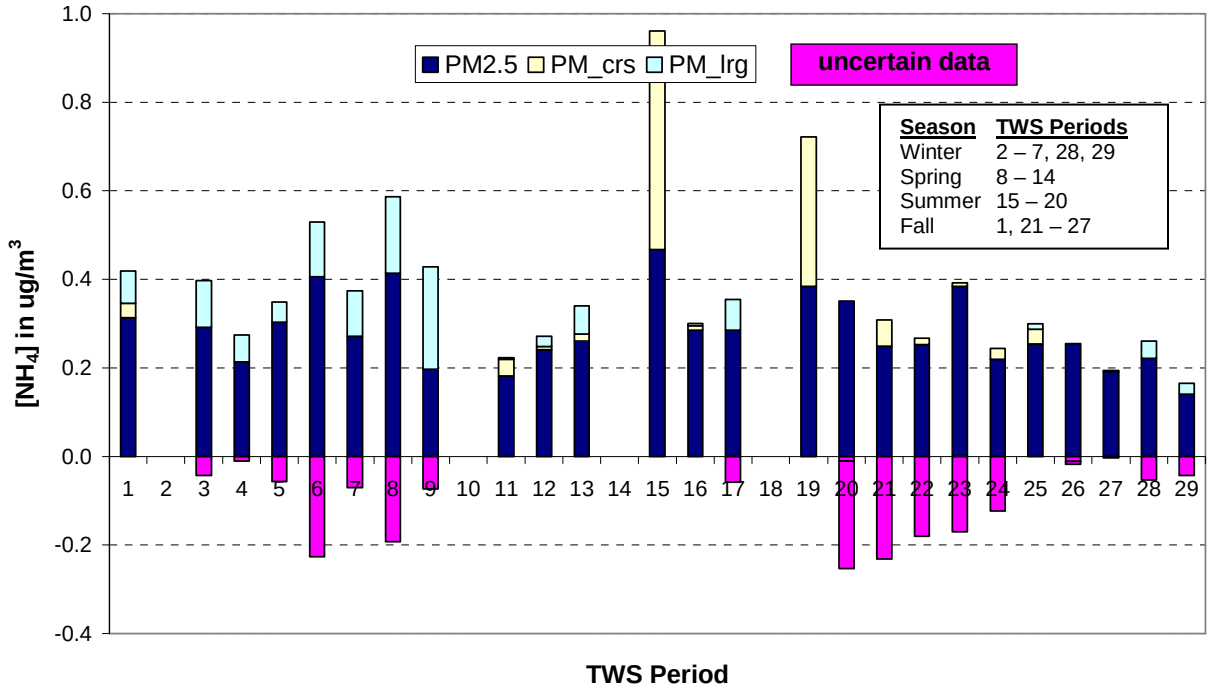

Figure 3-15d. PM Size Contributions to Ammonium Concentrations Observed with the TWS at Thunderbird Lodge.

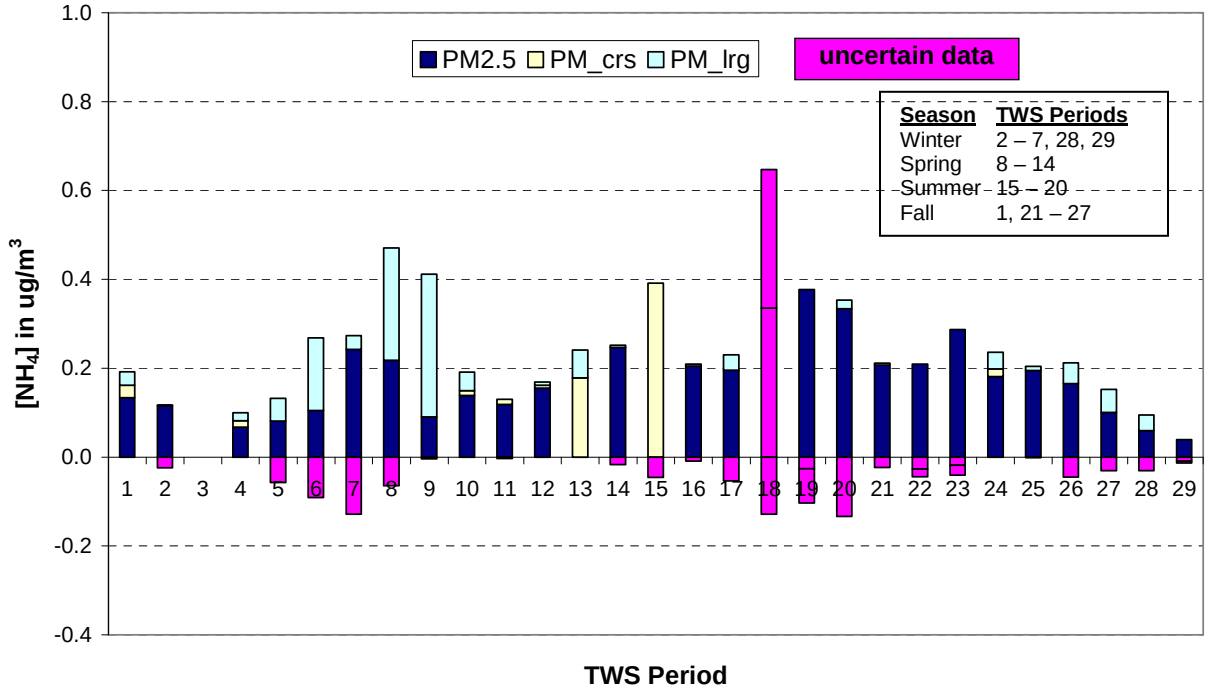

Figure 3-15e. PM Size Contributions to Ammonium Concentrations Observed with the TWS at Lake Forest.

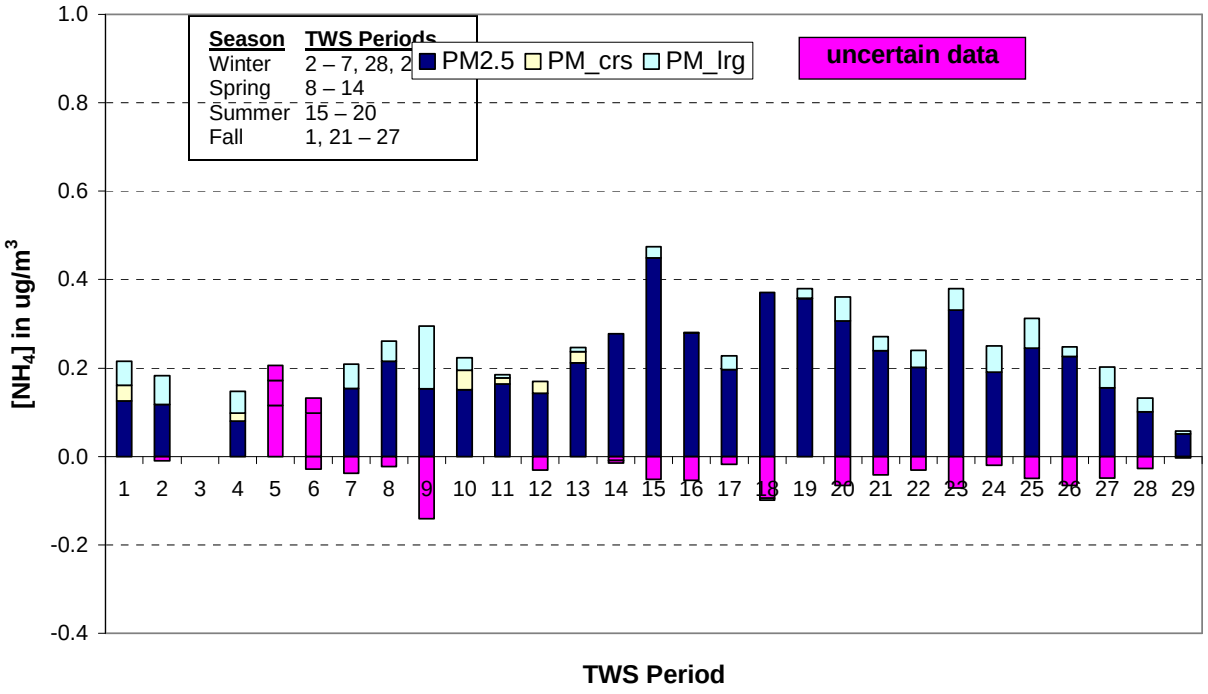

Figure 3-16. Time Series Plots of Contribution of Each Major Chemical Component to Fractional TSP Mass at a) Big HIll, b) Lake Forest, c) Sandy Way, d) SOLA, and e) Thunderbird.

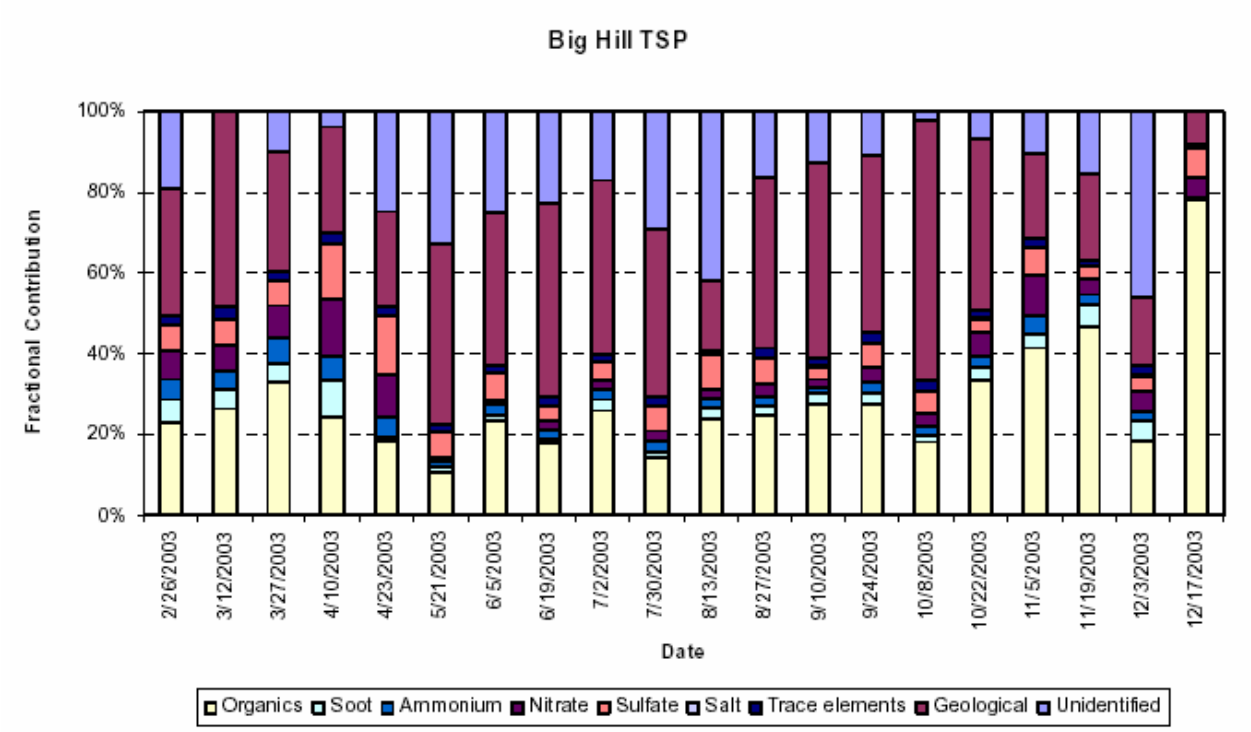

(a)

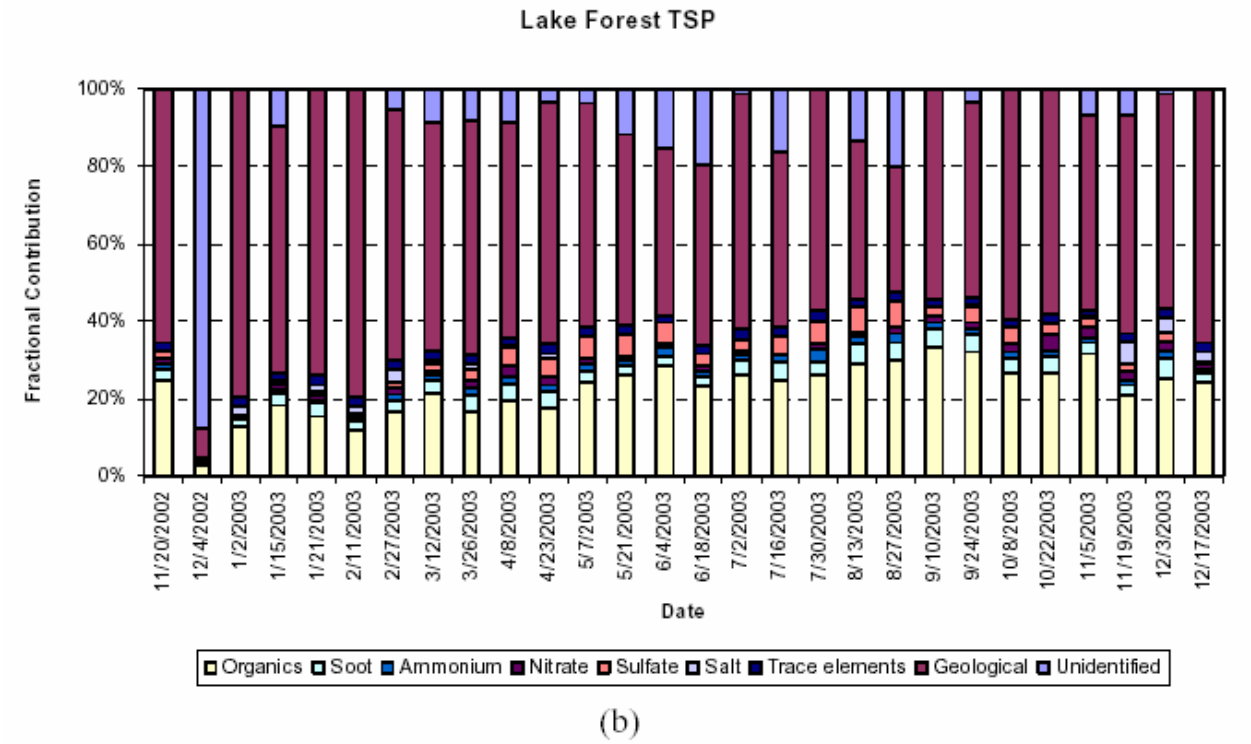

(b)

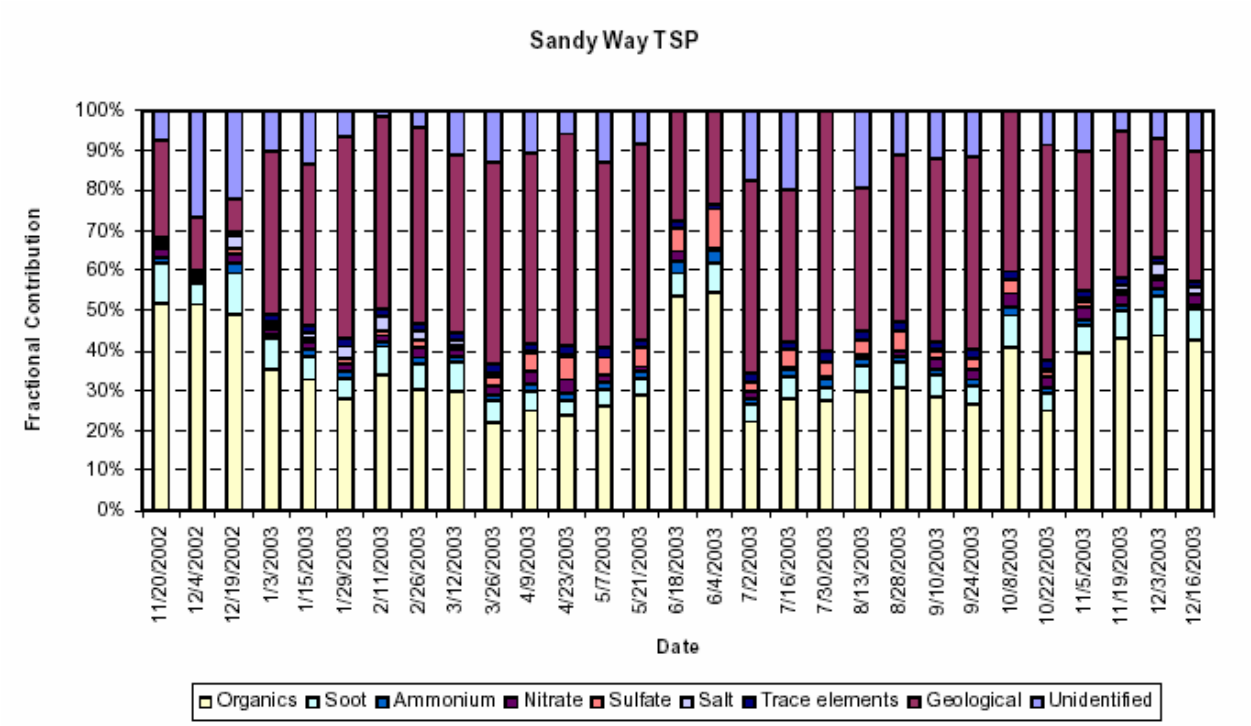
Sandy Way TSP
Fractional Contribution
100%
90%
80%
70%
60%
50%
40%
30%
20%
10%
0%
11/20/2002
12/4/2002
12/19/2002
1/3/2003
1/15/2003
1/29/2003
2/11/2003
2/26/2003
3/12/2003
3/26/2003
4/9/2003
4/23/2003
5/7/2003
5/21/2003
6/18/2003
6/4/2003
7/2/2003
7/16/2003
7/30/2003
8/13/2003
8/28/2003
9/10/2003
9/24/2003
10/8/2003
10/22/2003
11/5/2003
11/19/2003
12/3/2003
12/16/2003
Date
Organics
Soot
Ammonium
Nitrate
Sulfate
Salt
Trace elements
Geological
Unidentified

(c)

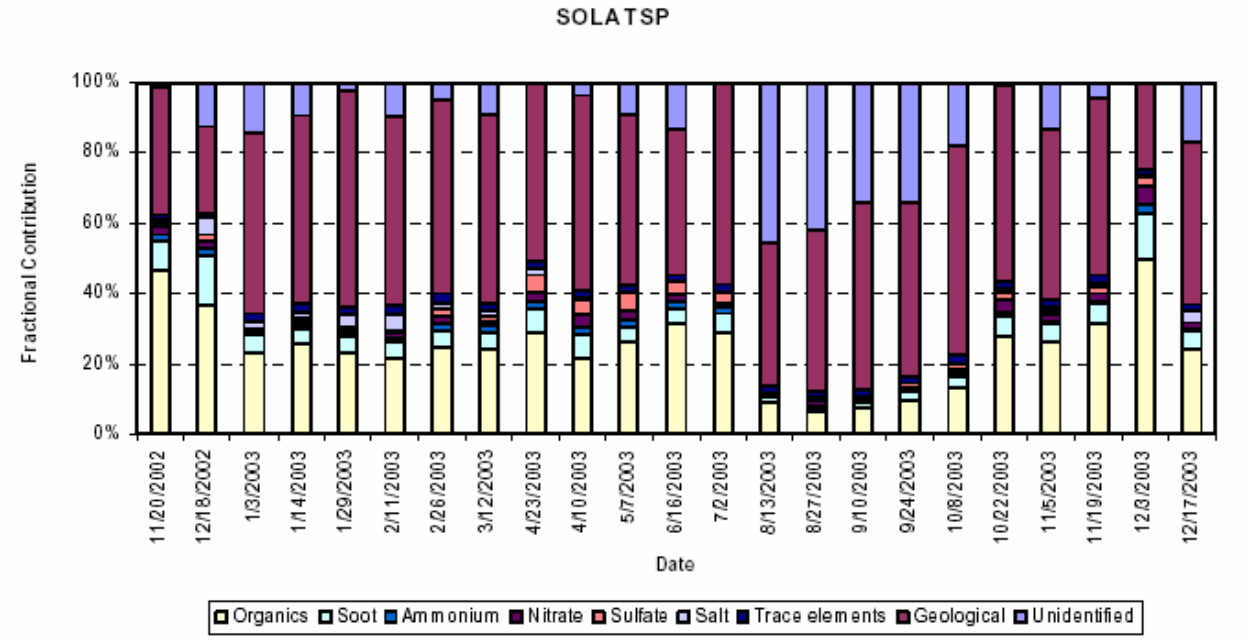
SOLA TSP
Fractional Contribution
100%
80%
60%
40%
20%
0%
11/20/2002
12/18/2002
1/3/2003
1/14/2003
1/29/2003
2/11/2003
2/26/2003
3/12/2003
4/23/2003
4/10/2003
5/7/2003
6/16/2003
7/2/2003
8/13/2003
8/27/2003
9/10/2003
9/24/2003
10/8/2003
10/22/2003
11/5/2003
11/19/2003
12/3/2003
12/17/2003
Date
Organics
Soot
Ammonium
Nitrate
Sulfate
Salt
Trace elements
Geological
Unidentified

(d)

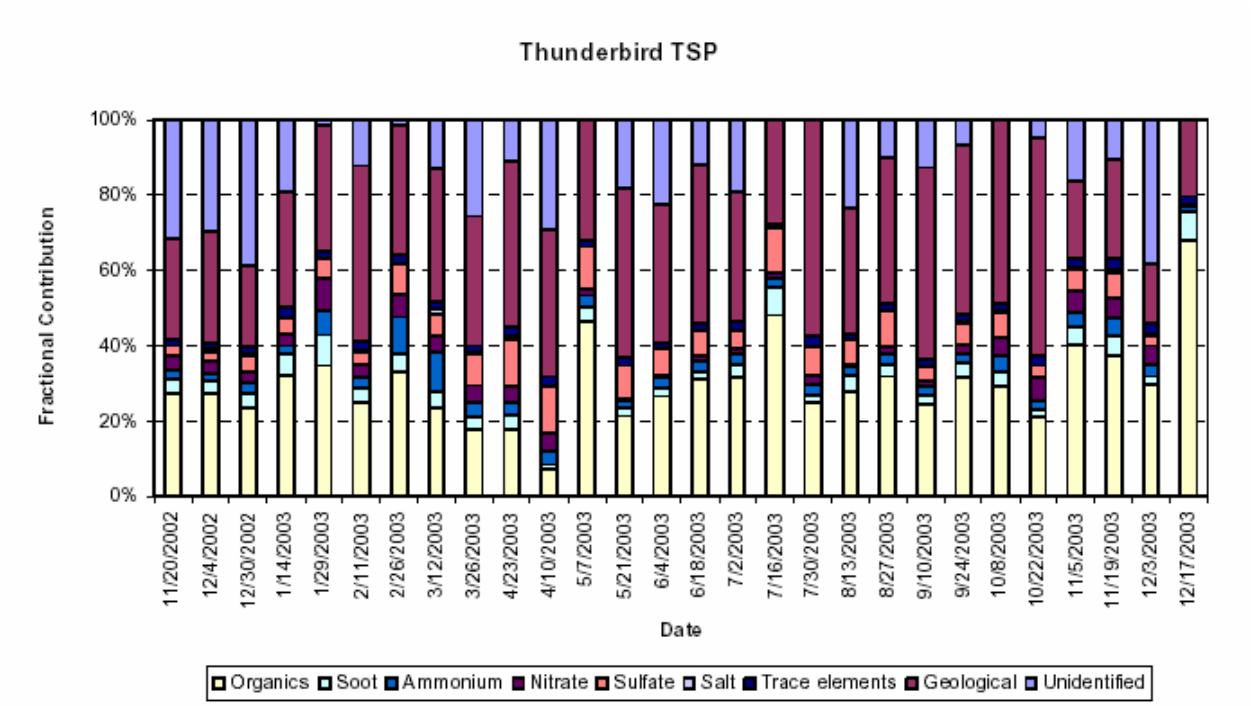
Thunderbird TSP
Fractional Contribution
100%
80%
60%
40%
20%
0%
11/20/2002
12/4/2002
12/30/2002
1/14/2003
1/29/2003
2/11/2003
2/26/2003
3/12/2003
3/26/2003
4/23/2003
4/10/2003
5/7/2003
5/21/2003
6/4/2003
6/18/2003
7/2/2003
7/16/2003
7/30/2003
8/13/2003
8/27/2003
9/10/2003
9/24/2003
10/8/2003
10/22/2003
11/5/2003
11/19/2003
12/3/2003
12/17/2003
Date
Organics
Soot
Ammonium
Nitrate
Sulfate
Salt
Trace elements
Geological
Unidentified

(e)

Figure 3-17. Time Series Plots of Contribution of Each Major Chemical Component to Fractional PM10 Mass at a) Big Hill, b) Lake Forest, c) Sandy Way, d) SOLA, and e) Thunderbird.

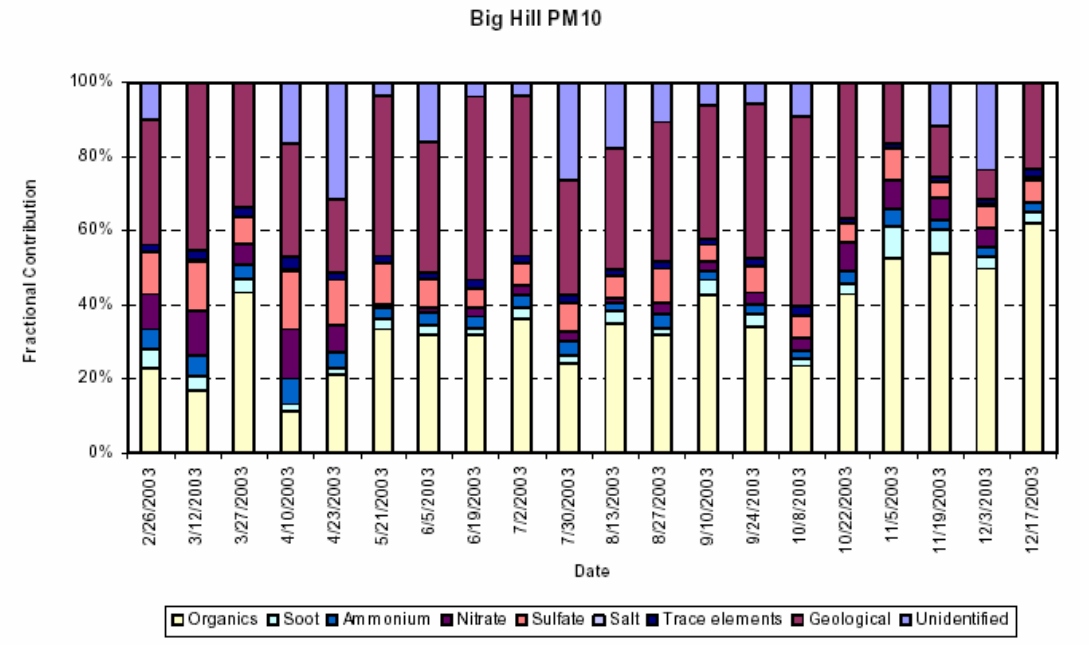

(a)

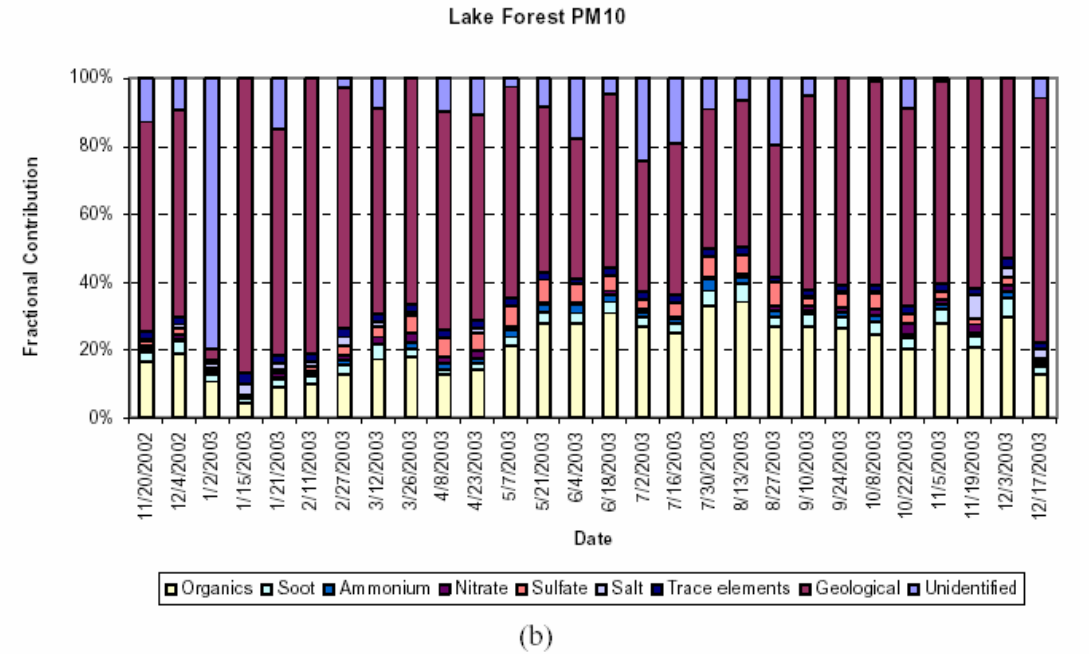

(b)

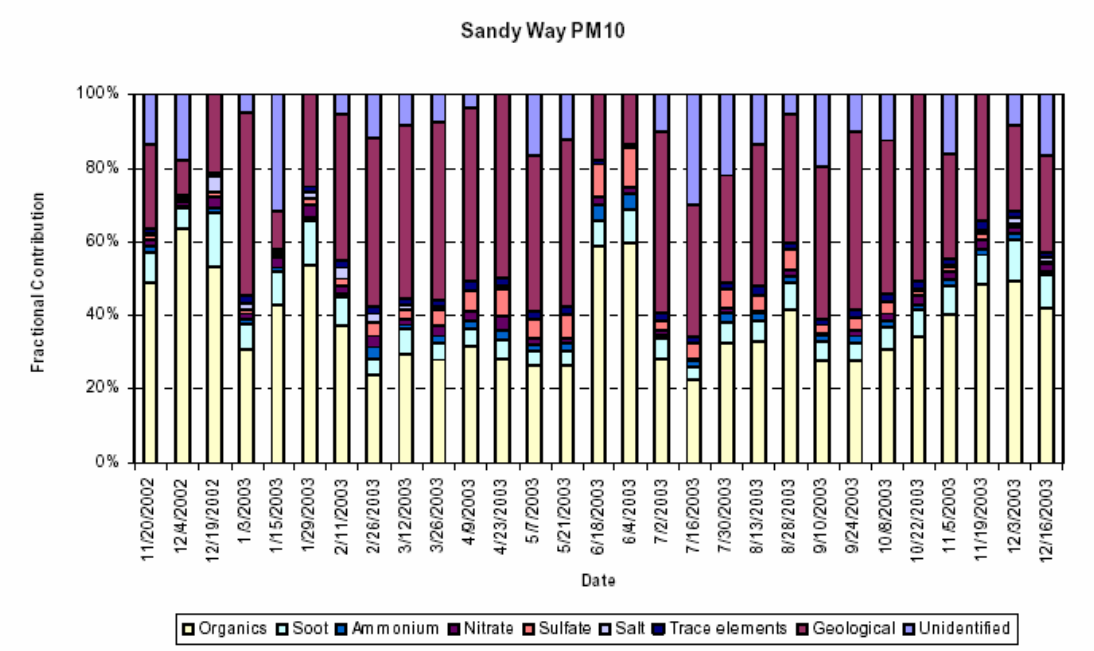
Sandy Way PM10
Fractional Contribution
100%
80%
60%
40%
20%
0%
11/20/2002
12/4/2002
12/19/2002
1/3/2003
1/15/2003
1/29/2003
2/11/2003
2/26/2003
3/12/2003
3/26/2003
4/9/2003
4/23/2003
5/7/2003
5/21/2003
6/18/2003
6/4/2003
7/2/2003
7/16/2003
7/30/2003
8/13/2003
8/28/2003
9/10/2003
9/24/2003
10/8/2003
10/22/2003
11/5/2003
11/19/2003
12/3/2003
12/16/2003
Date
Organics
Soot
Ammonium
Nitrate
Sulfate
Salt
Trace elements
Geological
Unidentified

(c)

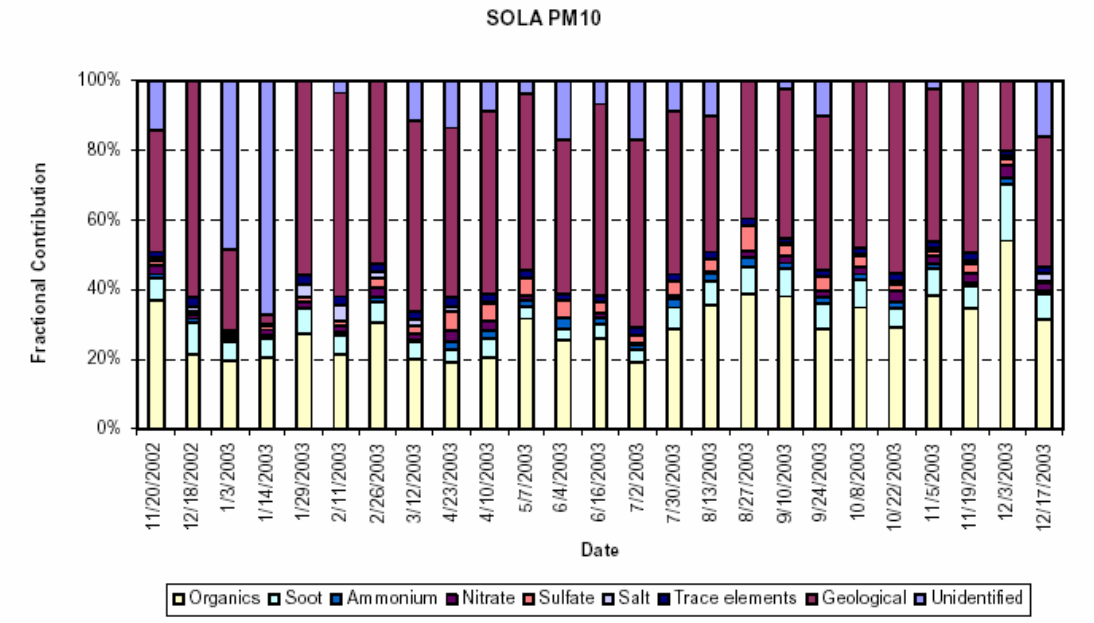
SOLA PM10
Fractional Contribution
100%
80%
60%
40%
20%
0%
11/20/2002
12/18/2002
1/3/2003
1/14/2003
1/29/2003
2/11/2003
2/26/2003
3/12/2003
4/23/2003
4/10/2003
5/7/2003
6/4/2003
6/16/2003
7/2/2003
7/30/2003
8/13/2003
8/27/2003
9/10/2003
9/24/2003
10/8/2003
10/22/2003
11/5/2003
11/19/2003
12/3/2003
12/17/2003
Date
Organics
Soot
Ammonium
Nitrate
Sulfate
Salt
Trace elements
Geological
Unidentified

(d)

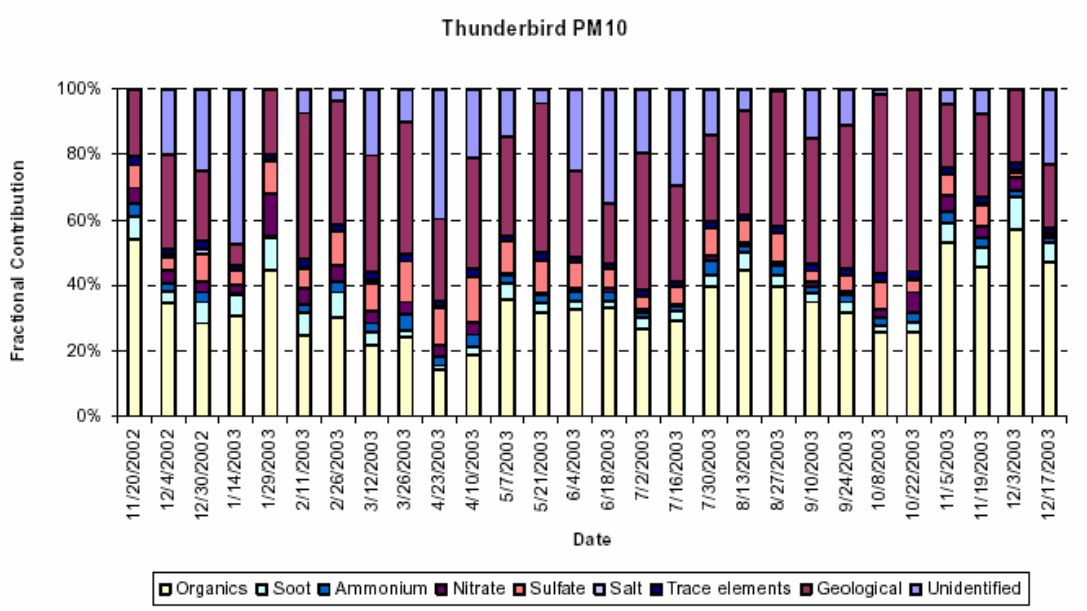
Thunderbird PM10
Fractional Contribution
100%
80%
60%
40%
20%
0%
11/20/2002
12/4/2002
12/30/2002
1/14/2003
1/29/2003
2/11/2003
2/26/2003
3/12/2003
3/26/2003
4/23/2003
4/10/2003
5/7/2003
5/21/2003
6/4/2003
6/18/2003
7/2/2003
7/16/2003
7/30/2003
8/13/2003
8/27/2003
9/10/2003
9/24/2003
10/8/2003
10/22/2003
11/5/2003
11/19/2003
12/3/2003
12/17/2003
Date
Organics
Soot
Ammonium
Nitrate
Sulfate
Salt
Trace elements
Geological
Unidentified

(e)

Figure 3-18. Time Series Plots of Contribution of Each Major Chemical Component to Fractional PM2.5 Mass at a) Big Hill, b) Lake Forest, c) Sandy Way, d) SOLA, and e) Thunderbird.

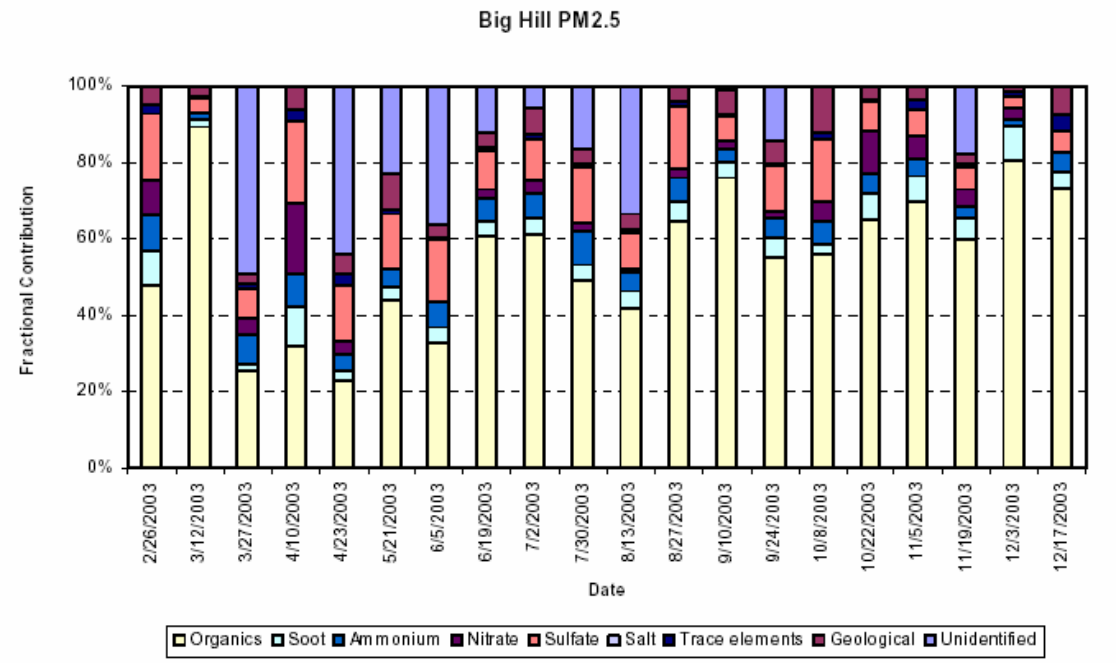

(a)

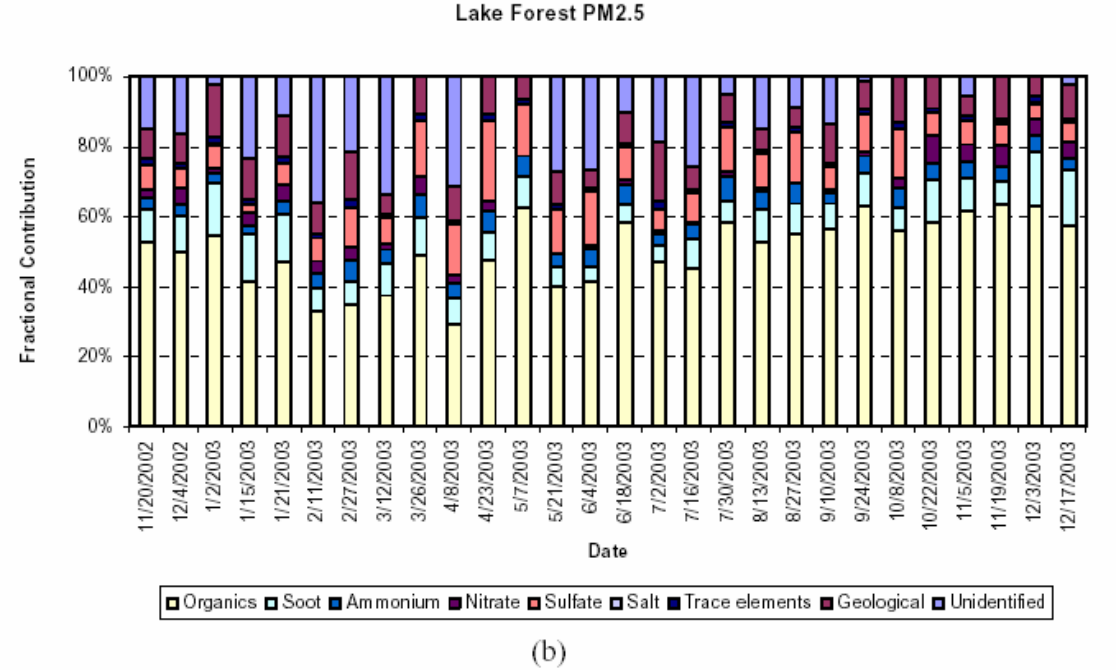

(b)

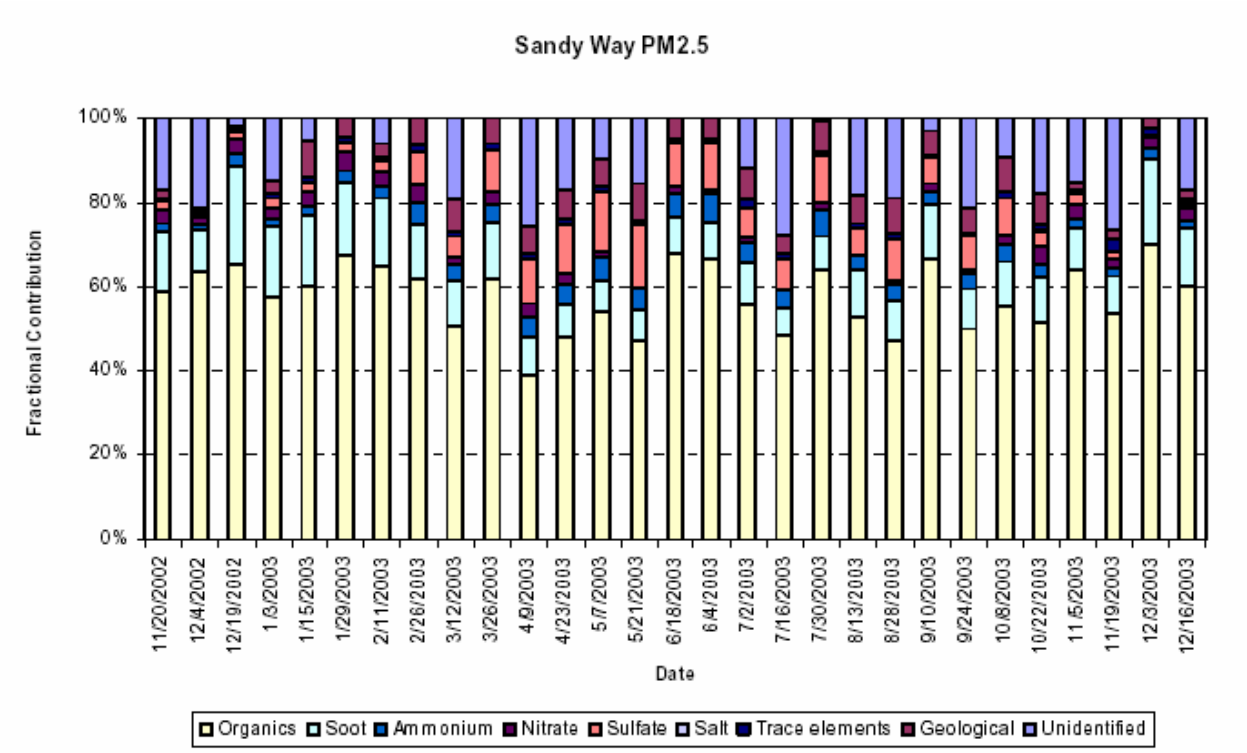
Sandy Way PM2.5
Fractional Contribution
100%
80%
60%
40%
20%
0%
11/20/2002
12/4/2002
12/19/2002
1/3/2003
1/15/2003
1/29/2003
2/11/2003
2/26/2003
3/12/2003
3/26/2003
4/9/2003
4/23/2003
5/7/2003
5/21/2003
6/18/2003
6/4/2003
7/2/2003
7/16/2003
7/30/2003
8/13/2003
8/28/2003
9/10/2003
9/24/2003
10/8/2003
10/22/2003
11/5/2003
11/19/2003
12/3/2003
12/16/2003
Date
Organics
Soot
Ammonium
Nitrate
Sulfate
Salt
Trace elements
Geological
Unidentified

(c)

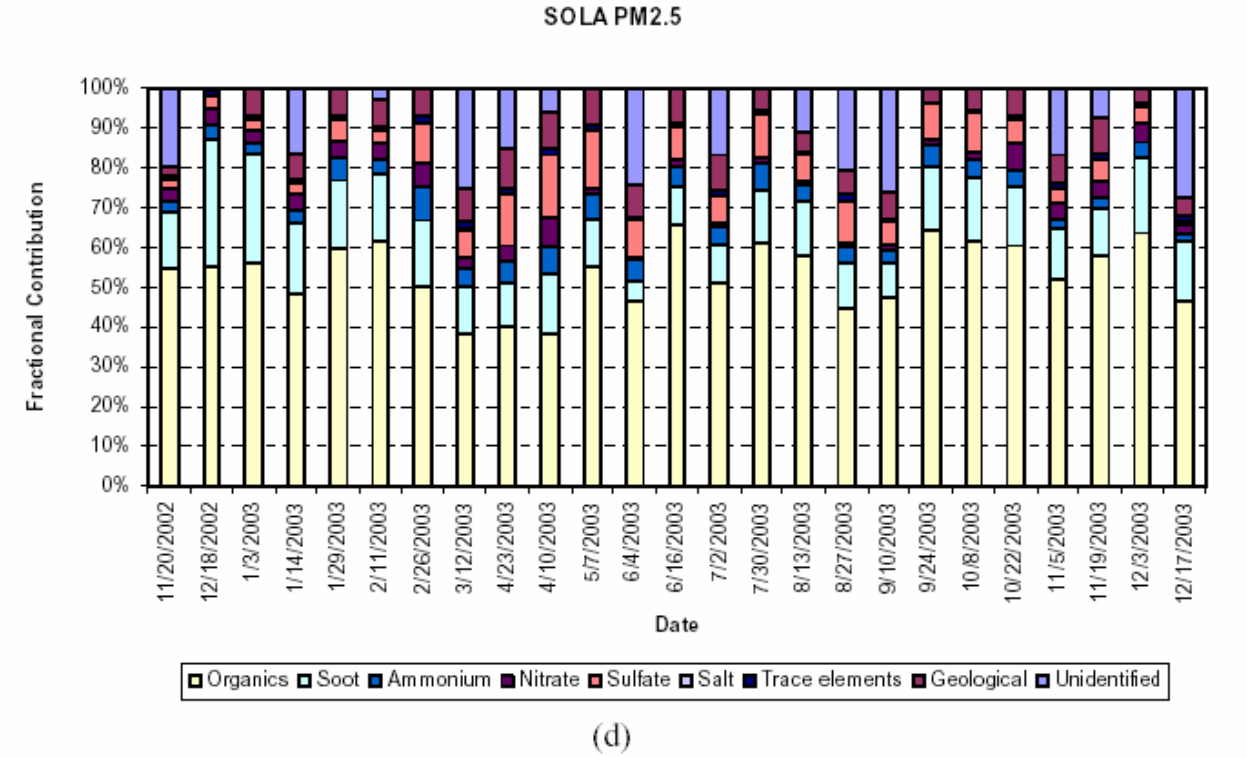
SOLA PM2.5
Fractional Contribution
100%
90%
80%
70%
60%
50%
40%
30%
20%
10%
0%
11/20/2002
12/18/2002
1/3/2003
1/14/2003
1/29/2003
2/11/2003
2/26/2003
3/12/2003
4/23/2003
4/10/2003
5/7/2003
6/4/2003
6/16/2003
7/2/2003
7/30/2003
8/13/2003
8/27/2003
9/10/2003
9/24/2003
10/8/2003
10/22/2003
11/5/2003
11/19/2003
12/3/2003
12/17/2003
Date
Organics
Soot
Ammonium
Nitrate
Sulfate
Salt
Trace elements
Geological
Unidentified

(d)

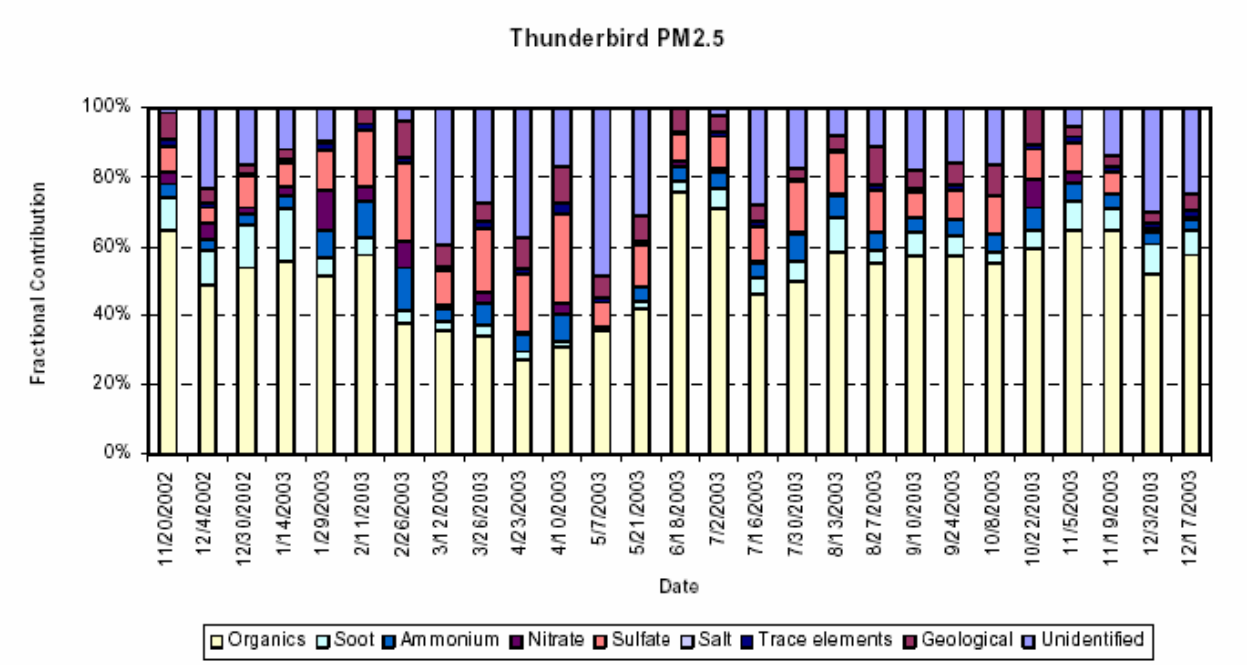

(e)

3.2.1.4 MVS Data

As noted earlier in **Table 3-4**, the MVS sampling network collected data for sampling periods as short as 24 hours and as long as two weeks for chemical composition data. Multi-site summaries of TSP and component concentrations collected with the mini-volume sampler (MVS) are provided in **Figure 3-19**. It should be noted that MVS samples were very infrequently made at the SOLA site during the first half of the field study. Although the MVS samples do not always have similar start or duration times, some seasonal and spatial variations can be inferred. For example, higher TSP concentrations were generally observed at the pier and shoreline sites than at the buoy sites but comparable concentrations of secondary pollutants (e.g., $SO_4^{=}$, NH_4^{+}, and NO_3^{-}) were observed on the buoys and piers. The measurements at the two buoy sites tended to be very similar. Interestingly, the highest sulfur concentrations tended to occur during the summer months. Almost all of the TSP concentrations greater than 20 µg/m^3 were associated with the SOLA and Zephyr Cove sites in the urbanized southeast quadrant of the basin. Lastly, non-zero measurements of phosphorus and phosphates were infrequent.

Although the sampling durations associated with the MVS and TWS networks varied, the seasonal results when combined generate a coherent summary of the seasonal and spatial pattern of TSP concentrations within the Tahoe Basin. The important concept to take from **Figure 3-20** is that PM concentrations are highest (15-25 µg/m^3) at the sites closest to emission sources (e.g., South Lake Tahoe and Lake Forest which are near busy roads), drop off (10-15 µg/m^3) at the sites that are near less busy roads or farther from the road (e.g., Wallis Tower or Zephyr Cove), and decline further (5-10 µg/m^3) at sites distant from local emission sources (e.g., buoys and Thunderbird Lodge).

Figure 3-19a. Total Suspended Particulate Matter (TSP) Concentrations Observed with the MVS Network.

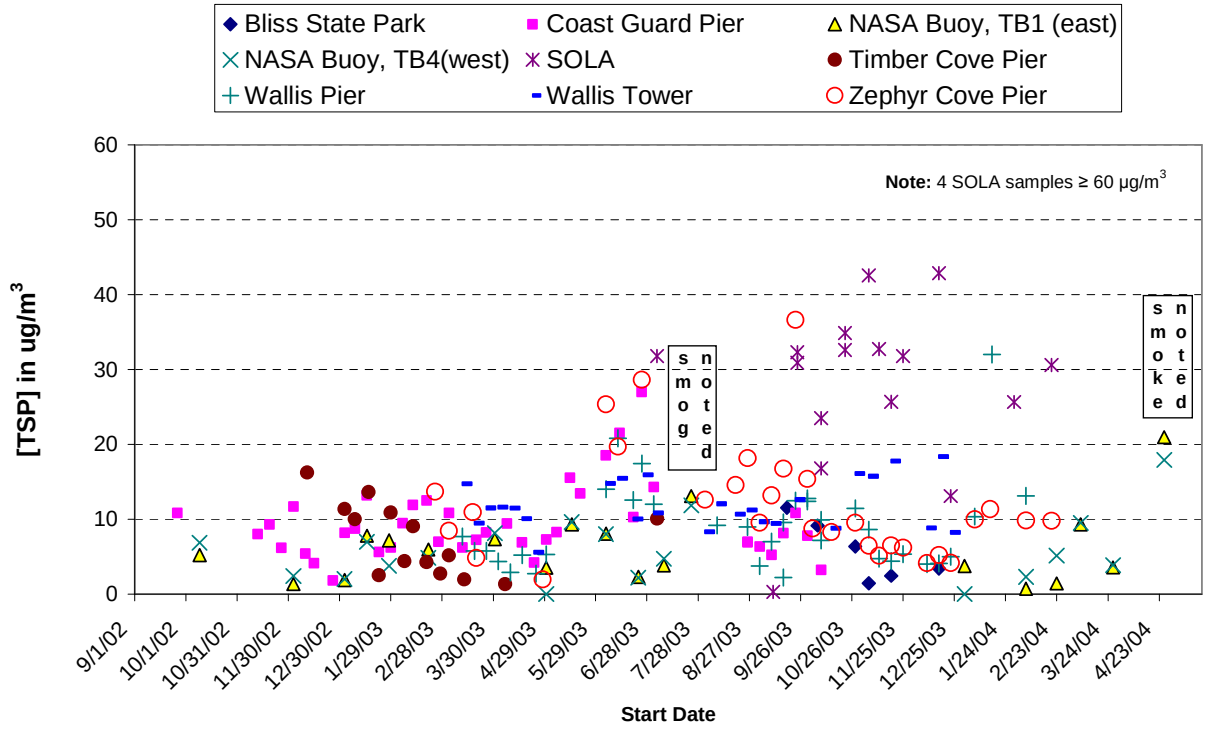

Figure 3-19b. TSP Sulfur (S) Concentrations Observed with the MVS Network.

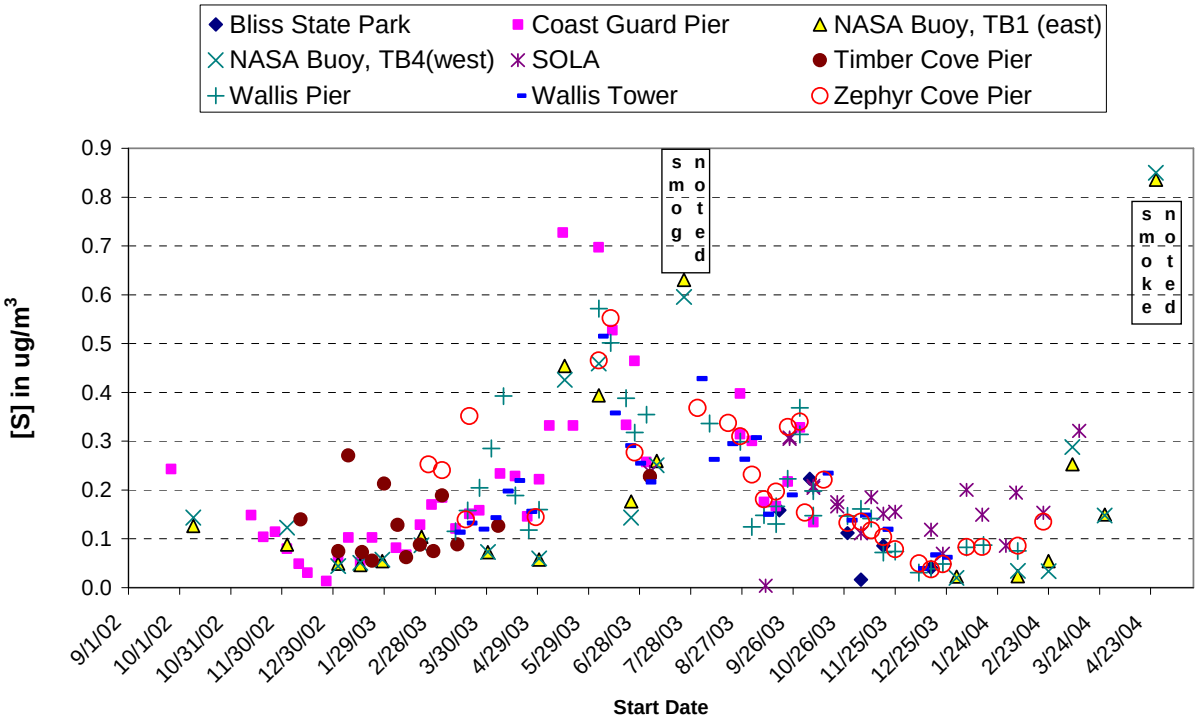

Figure 3-19c. TSP Sulfate (SO_4) Concentrations Observed with the MVS Network.

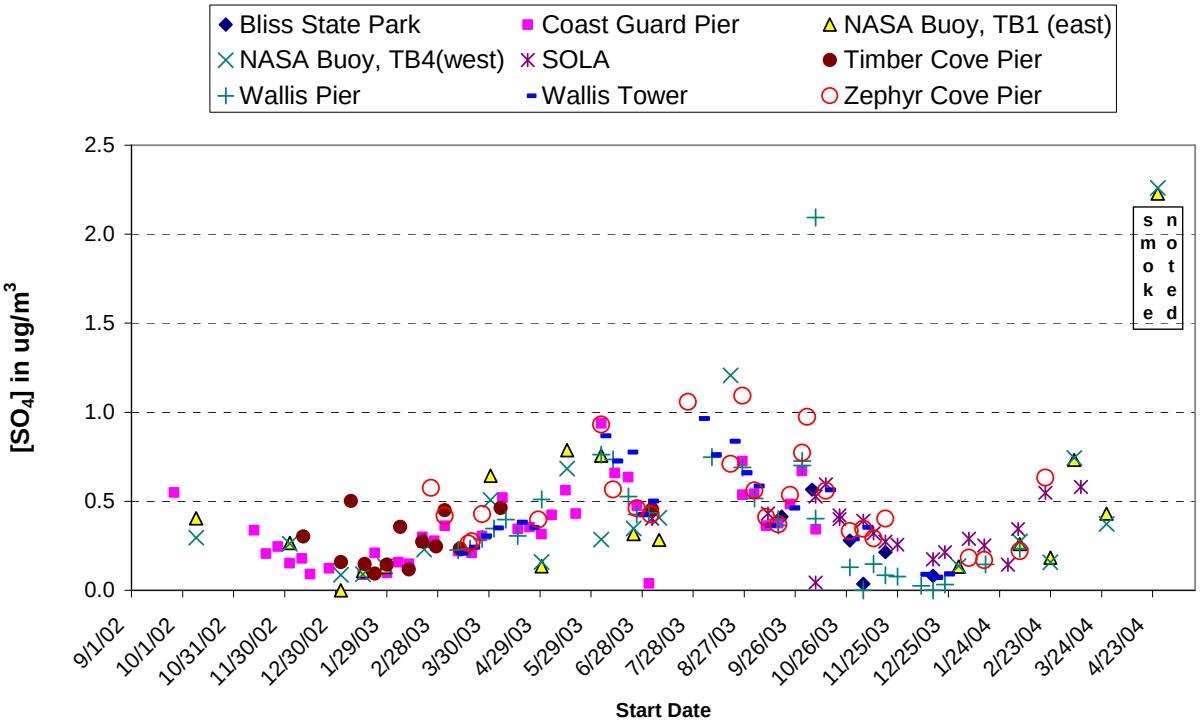

Figure 3-19d. TSP Phosphorus (P) Concentrations Observed with the MVS Network.

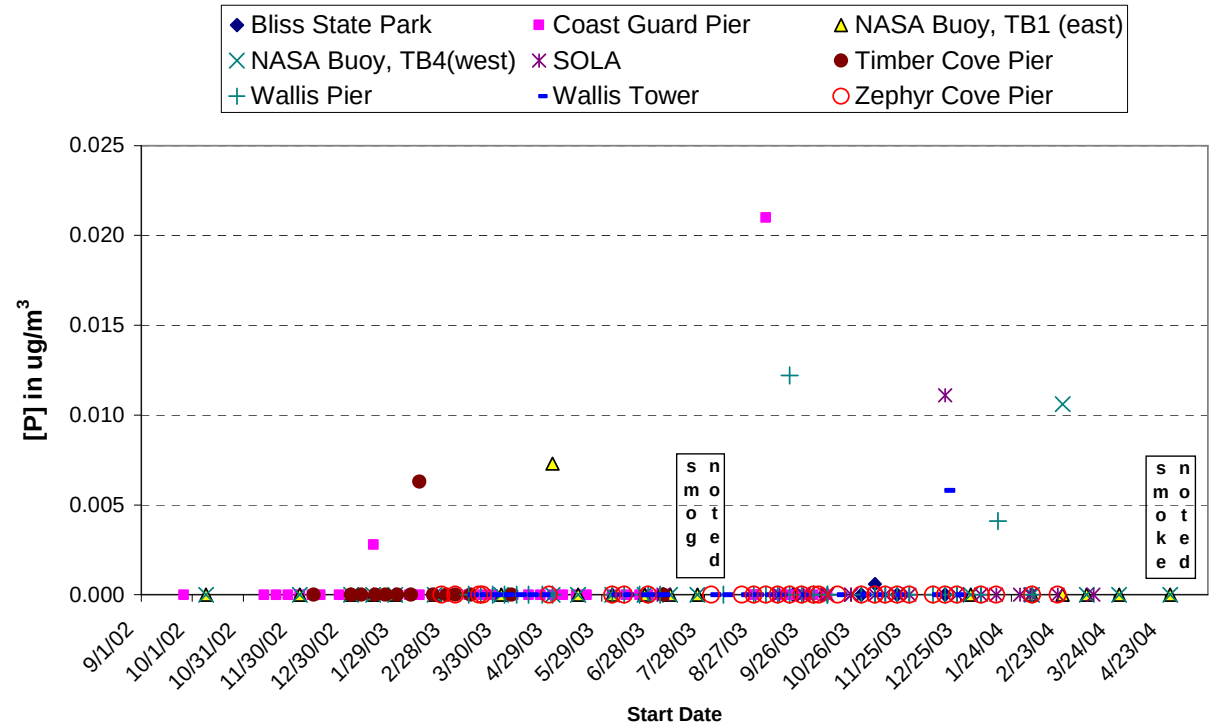

Figure 3-19e. TSP Phosphate (PO_4) Concentrations Observed with the MVS Network.

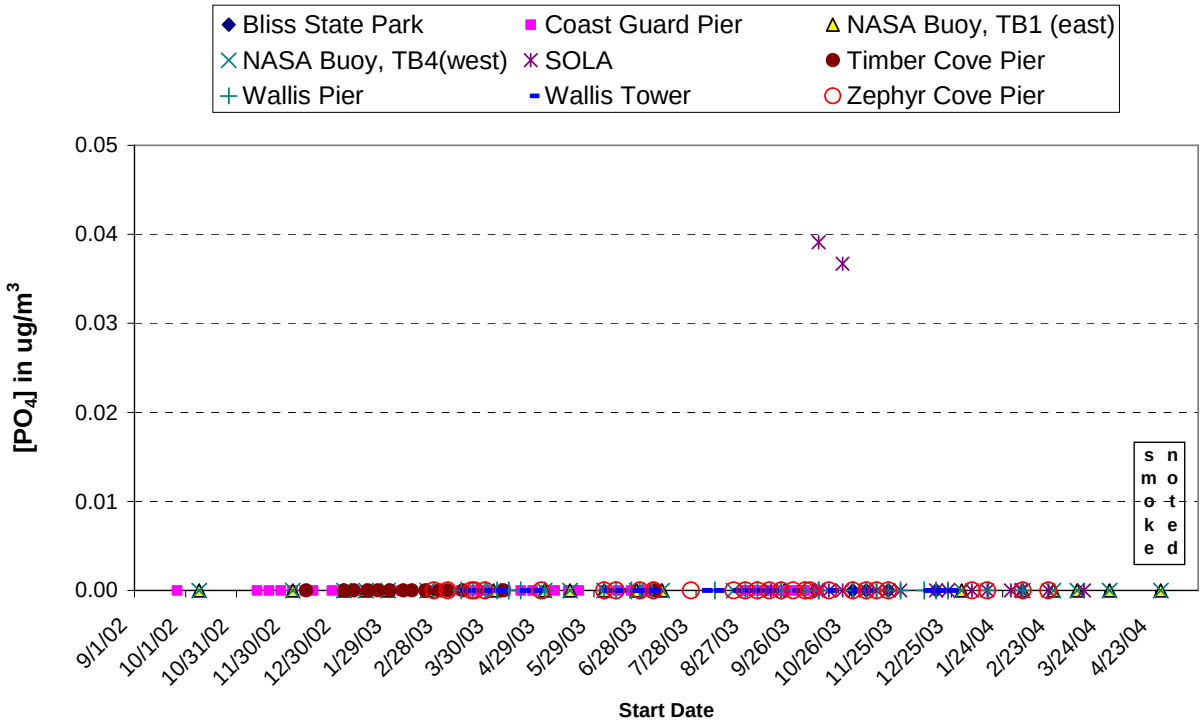

Figure 3-19f. TSP Nitrate (NO_3) Concentrations Observed with the MVS Network.

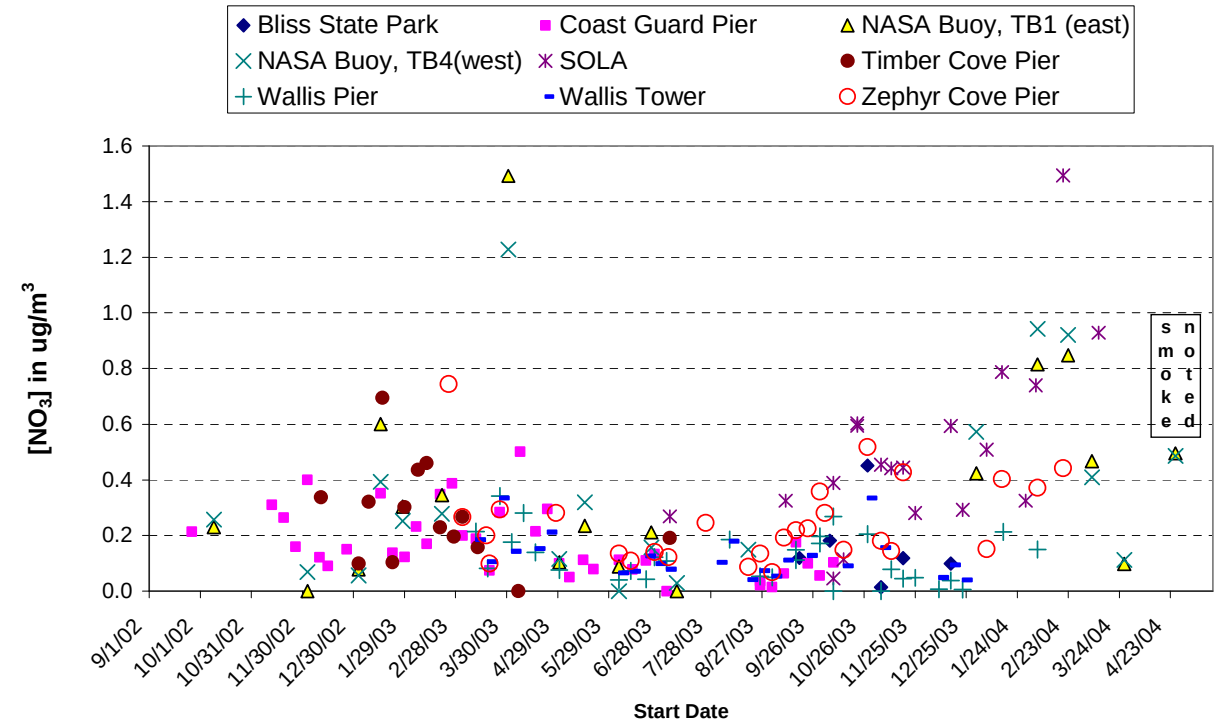

Figure 3-19g. TSP Ammonium (NH_4) Concentrations Observed with the MVS Network.

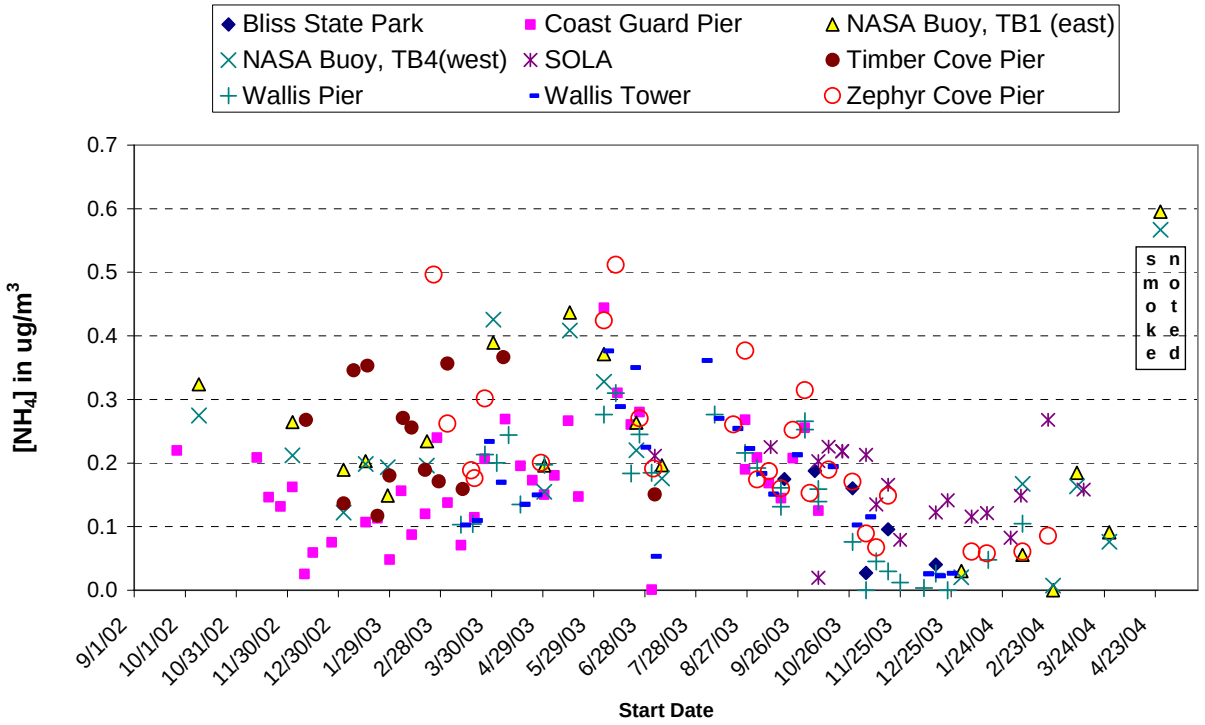

Figure 3-20. Seasonal TSP concentrations observed during LTADS with the TWS and MVS sampling networks.

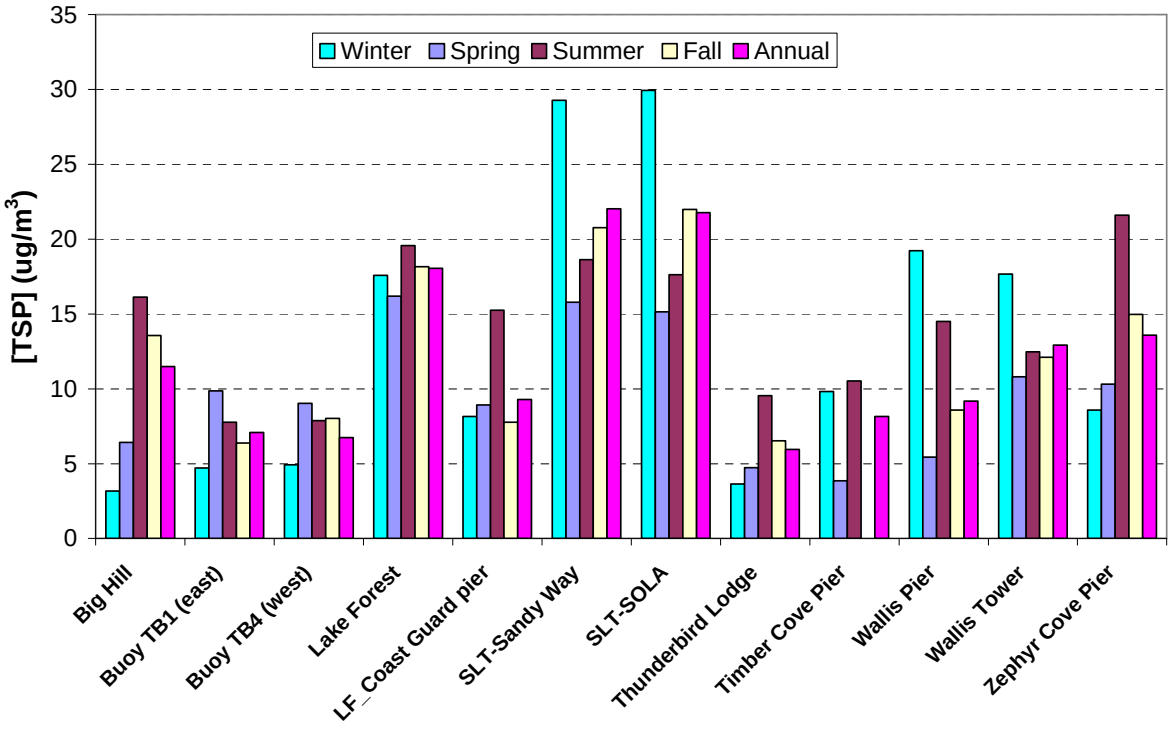

3.2.1.5 BAM Data

Deposition estimates require air pollutant concentration and deposition velocity data for the same time and general location. To develop deposition estimates that account for the dynamics of the meteorology in the Tahoe Basin, hourly deposition velocities are required. Consequently, hourly pollutant concentration profiles are needed to match with the temporal resolution of the meteorological data. The TWS provided ammonia, nitric acid, and detailed compositional information but on a two-week average. The BAMs provided not only some size information about aerosols but also the crucial hourly temporal information about aerosols. The hourly and sized aerosol data from the BAMs were used to construct hourly sized compositional estimates of the aerosols by season (see Chapter 4 for more detail). In a similar manner, the 2-week averages of nitric acid from the TWS network were scaled to seasonal hourly estimates based on the diurnal seasonal differences between NOy and NOx concentrations at SLT-Sandy Way. A limited number of day/night samples that were collected with a second TWS at the SOLA site but the results were inconclusive. Thus, a crude confirmation of the nitric acid by the difference method was not possible and the ammonia concentrations were assumed invariant during each season.

The BAM network collected hourly concentration data in TSP, PM10, and PM2.5 size fractions at several, though not all, stations. The BAM diurnal PM concentration profiles were used to parse seasonal TWS data into seasonal hourly concentration data for TSP, PM10, and PM2.5 and their compositional species. **Figure 3-21** provides a synopsis of BAM diurnal profiles for each of the four seasons at Big Hill (3-21a), Sandy Way (3-21b), SOLA (3-21c), Cave Rock (3-21d), Thunderbird Lodge (3-21e), and Lake Forest (3-21f). Because the BAM instruments collect all particles below a specified cut-point or size, the concentrations include overlapping measurements. For sites with all three size measurements the data can be segregated into three non-overlapping size fractions by subtracting the PM10 measurement from the TSP measurement to give the concentration of particles larger than PM10 (referred to as “PM_large”. In a similar manner, the PM2.5 concentration can be subtracted from the PM10 concentration to give the concentration of particles of size greater than 2.5 μm and smaller than 10 μm (referred to as “PM_coarse”).

The BAM data indicate that PM_coarse and PM_large both varied markedly with hour of day, being highest around sunrise and sunset when the air is more stable and traffic activities tend to be greatest. Ambient concentrations of PM_large and PM_coarse tend to decline from the early evening peaks at night when winds are lighter and anthropogenic activities are reduced. PM concentrations are often lower during mid-day when atmospheric mixing is greatest and winds tend to be onshore. This diurnal pattern is particularly pronounced during winter at monitoring sites located near roadways. In general, PM2.5 shows relatively small diurnal variation. The exception to this statement is a large nighttime increase in PM2.5 at the Sandy Way site in winter and fall. The evening peak in the diurnal pattern of fine PM (i.e., PM2.5) at the Sandy Way site is suggestive of wood smoke as the sample inlet is on the roof of a 1-story building that is located downwind of residential areas at that time of day. The magnitude and variation

in PM concentrations at Thunderbird Lodge are of interest because it is an in-basin site with limited local emissions (particularly during winter).

Because hourly chemical analysis would be prohibitively expensive, the PM chemical constituents were assumed to have diurnal variations similar to the variations in total mass.

3.2.1.6 Aerosol Nitrogen

Several nitrogen species contribute to the nutrient loading of Lake Tahoe and can deposit from the atmosphere in both aerosol and gaseous forms. This section discusses aerosol nitrogen species and the gaseous nitrogen components will be discussed in Section 3.2.2.1.

The most common nitrogen-containing aerosol species are ammonium nitrate (NH_4NO_3) and ammonium sulfate ($(NH_4)_2SO_4$). Both are water soluble and readily deposit to water. Ammonium (NH_4^+), nitrate (NO_3^-), and sulfate ($SO_4^=$) ionic concentrations in LTADS samples were measured by extracting a portion of an aerosol filter (quartz) in water, then analyzing the liquid by ion chromatography (IC).

Aerosol nitrate (NH_4NO_3) is not chemically stable; rather, it exists in equilibrium with the gas-phase concentrations of its precursors, ammonia (NH_3) and nitric acid (HNO_3) and water vapor. Collecting nitrate particles on a filter can produce a negative bias if the air flow through the filter causes some of the nitrate on the filter to return to the gas phase. On the other hand, if gas-phase precursors in the air stream condense on the filter, the measured nitrate on the filter will have a positive bias. In the TWS, it is assumed that any ammonium nitrate that volatilized as nitric acid vapor was captured by the nylon backup filter. Volatilized ammonia was estimated as the equal molar concentration of the volatilized nitrate captured on the backup. This assumption provides an upper estimate of ammonium because some of the particulate nitrates may be associated with other cations (i.e., calcium, magnesium, sodium).

Total nitrate was computed for the TWS network as the sum of nitrates on the primary and backup filters. Total ammonium was computed as the sum of primary filter ammonium and the estimated volatilized ammonium from the backup filter. NH_4^+ and NO_3^- data from the IMPROVE program are based on the same type of collection and lab analyses. Neither denuders nor backup filters can be used with the standard design of MVSs as they would decrease the airflow and change the particle size cutpoints when used for PM2.5 or PM10 sampling. Although the MVSs used during LTADS were for TSP sampling, which is less sensitive to airflow variations, the short study timeline precluded the design, construction, and testing of a more sophisticated MVS sampling system.

Figure 3-21a. Seasonal diurnal profiles of PM concentrations based on BAM data collected at Big Hill.

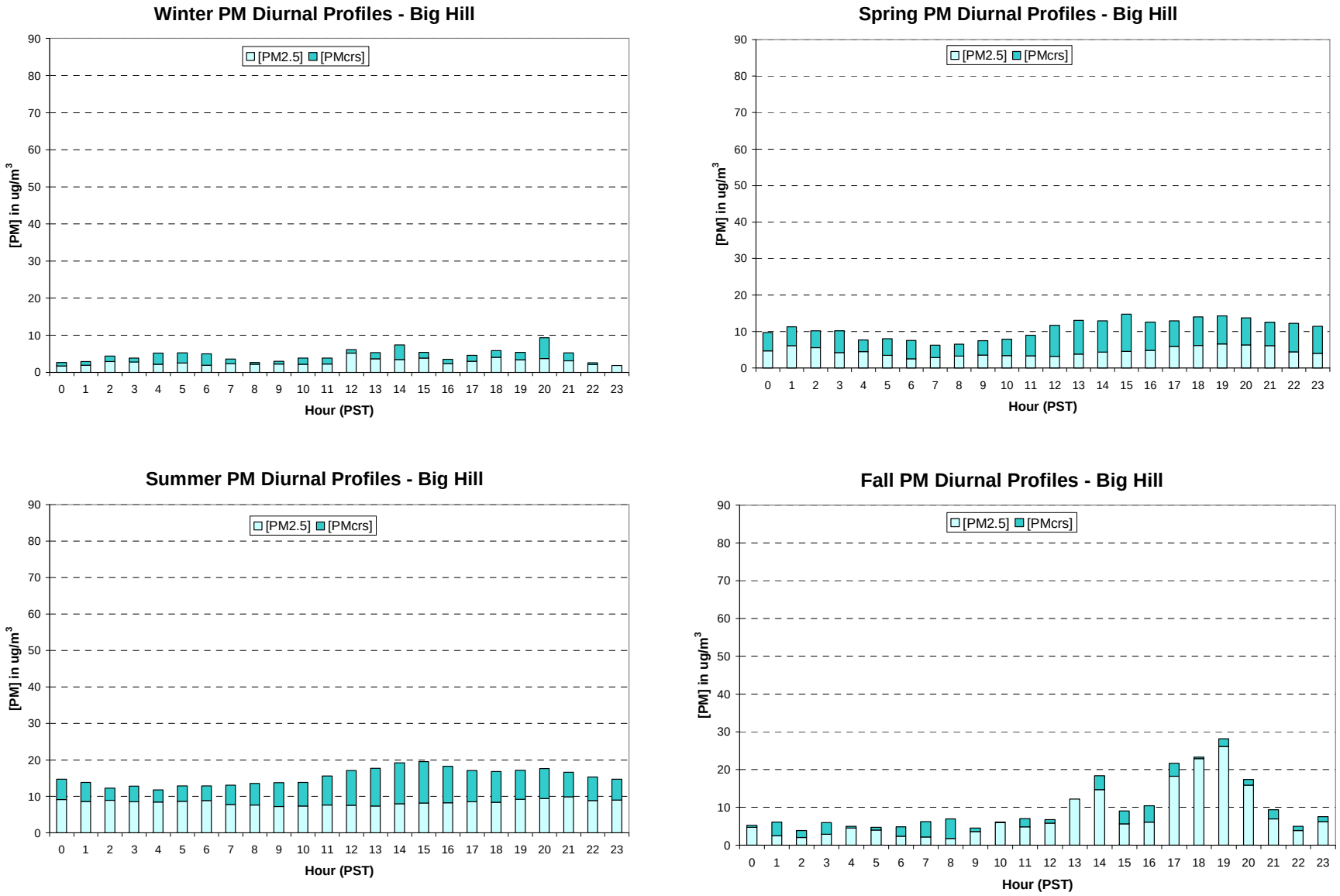

Figure 3-21b. Seasonal diurnal profiles of PM concentrations based on BAM data collected at SLT -Sandy Way.

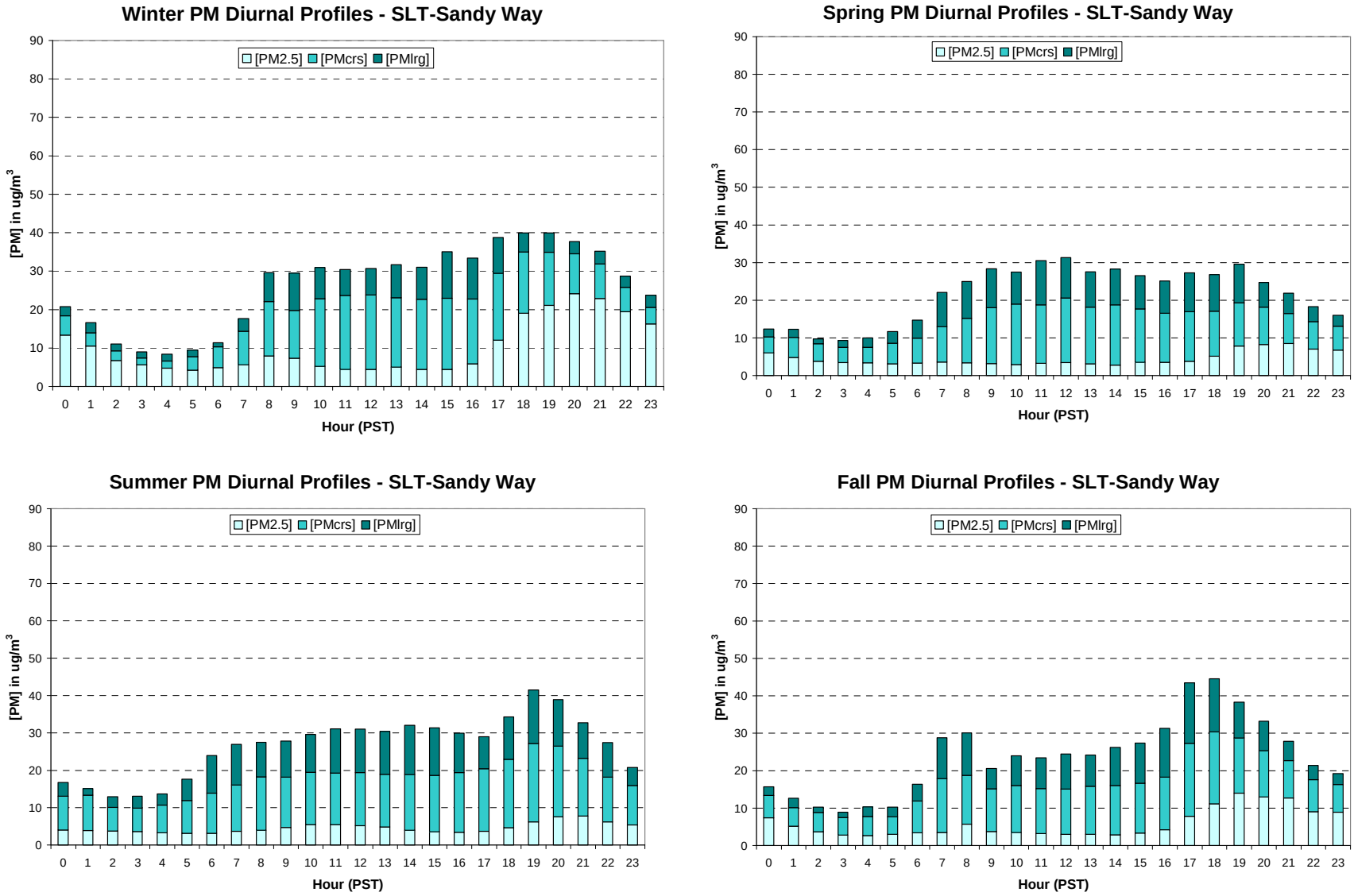

Figure 3-21c. Seasonal diurnal profiles of TSP concentration based on BAM data collected at SLT-SOLA.

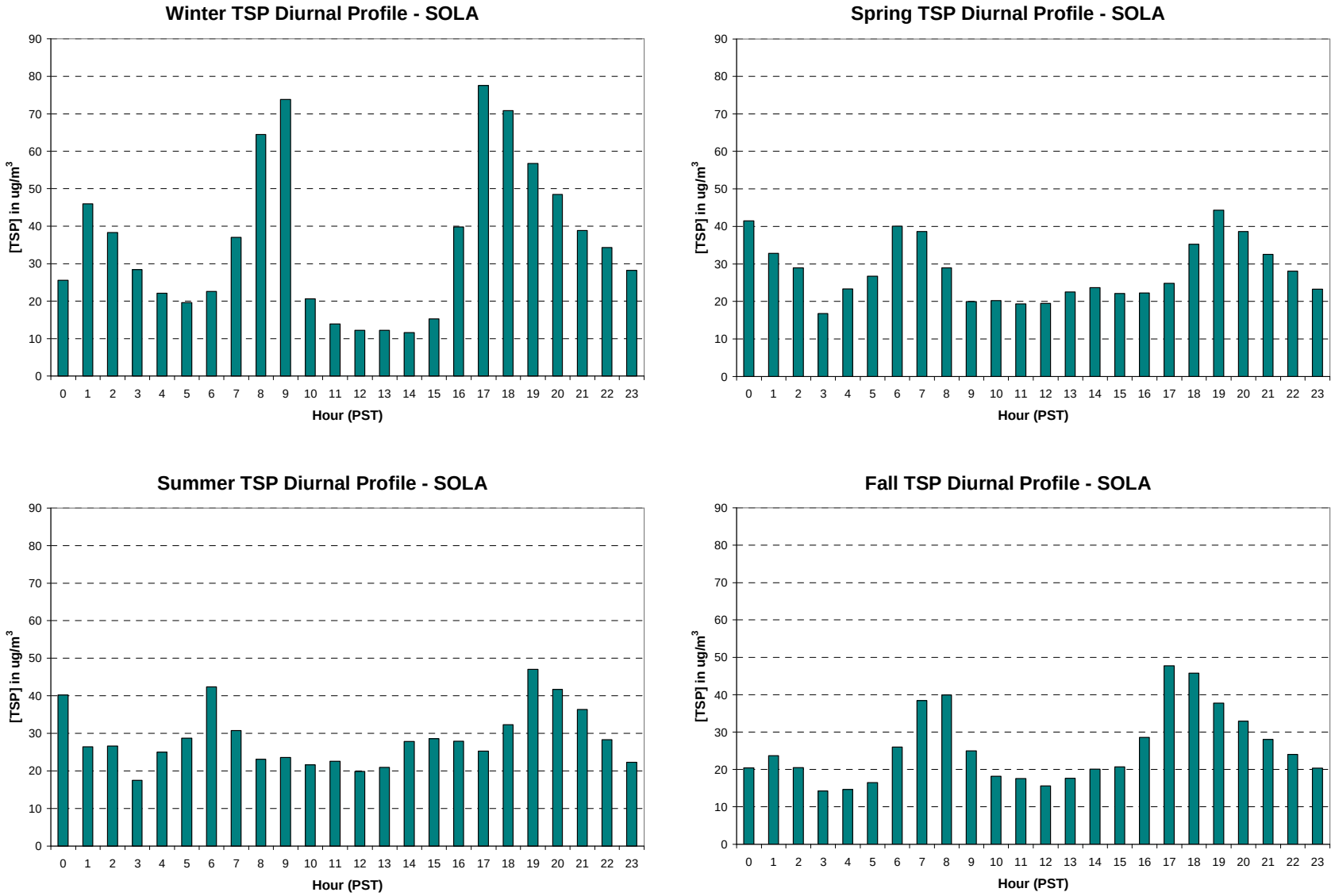

Figure 3-21d. Seasonal diurnal profiles of TSP concentration based on BAM data collected at Cave Rock.

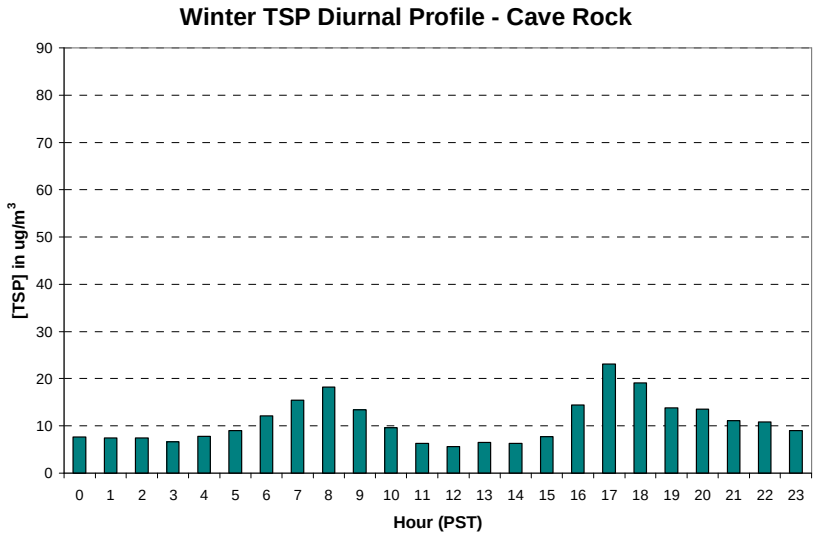

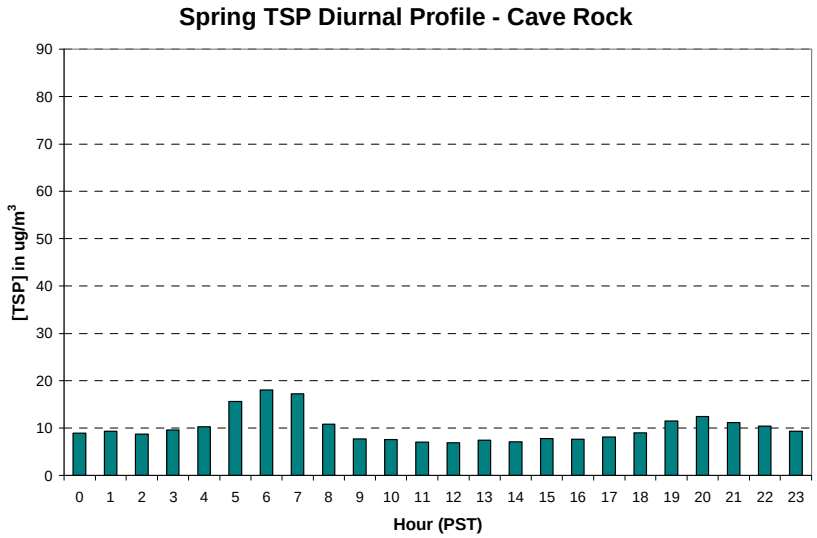

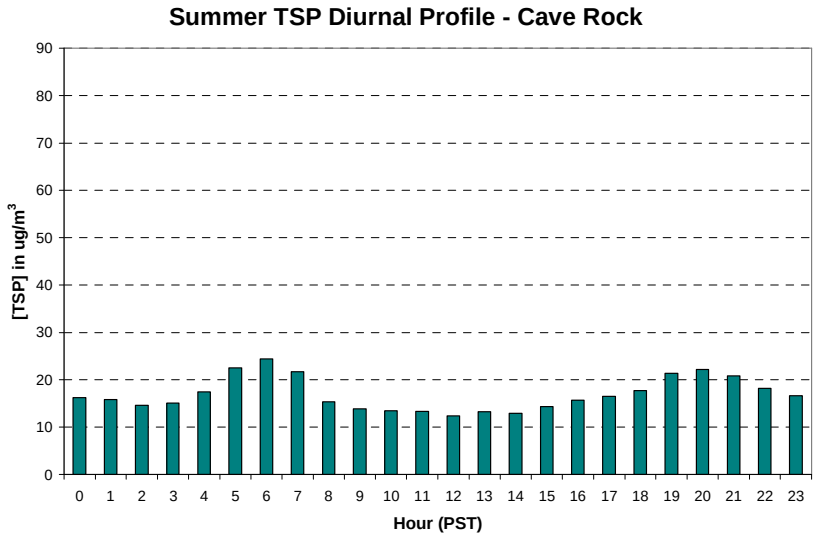

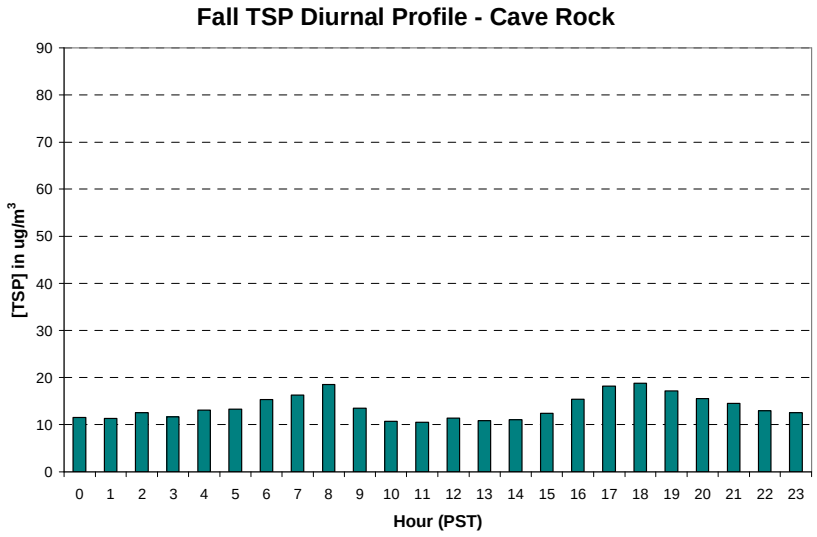

Figure 3-21e. Seasonal diurnal profiles of PM concentrations based on BAM data collected at Thunderbird Lodge.

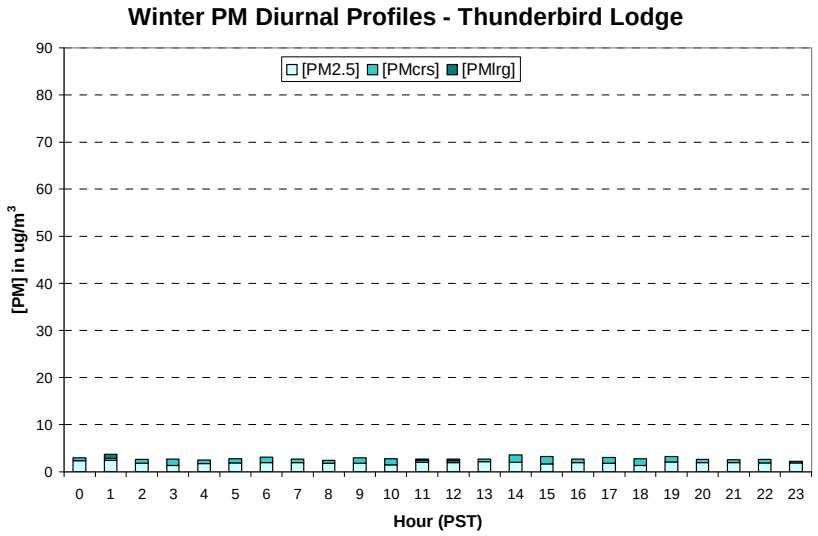

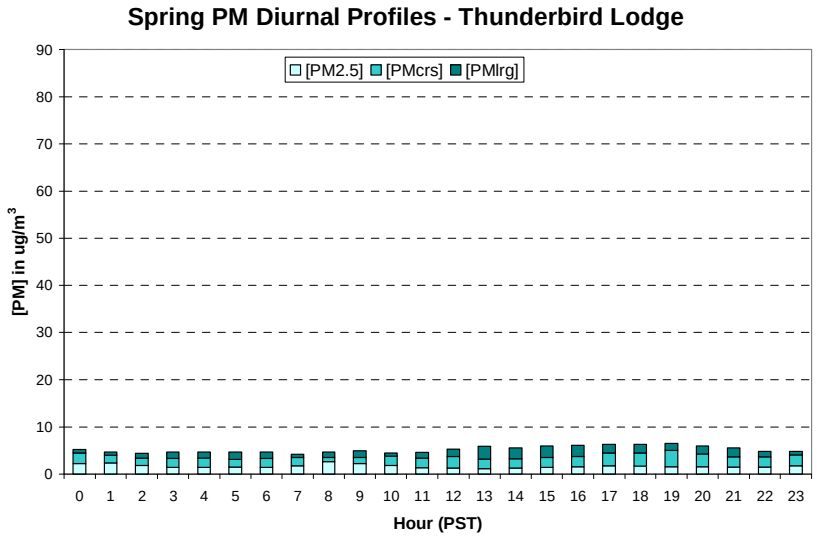

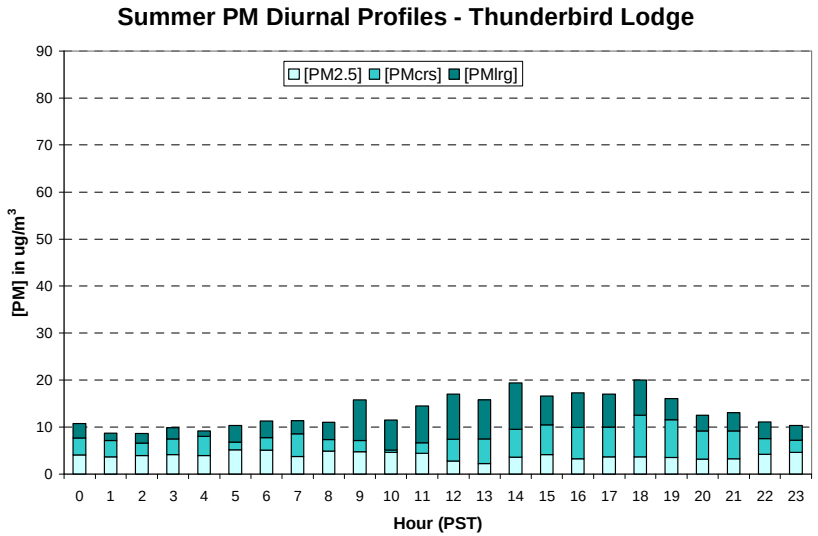

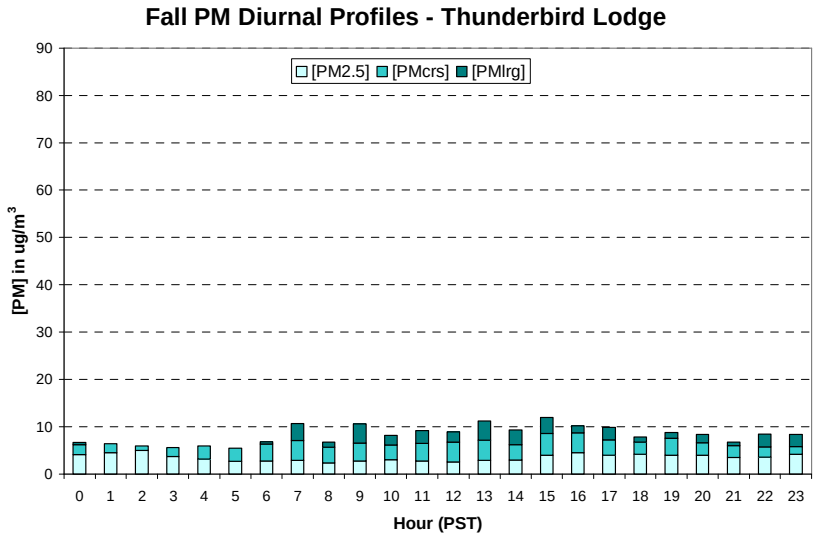

Figure 3-21f. Seasonal diurnal profiles of PM concentrations based on BAM data collected at Lake Forest.

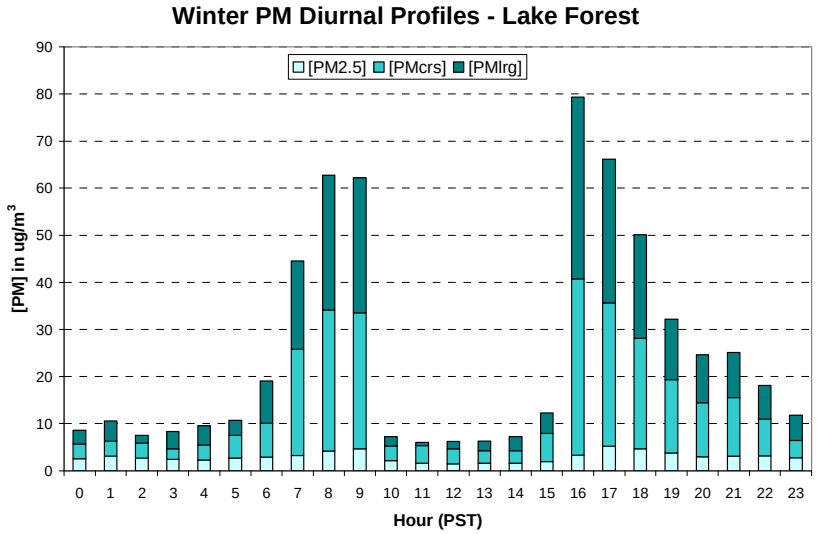

Lake Forest BAM had no matched size data during spring due to power and instrument failures.

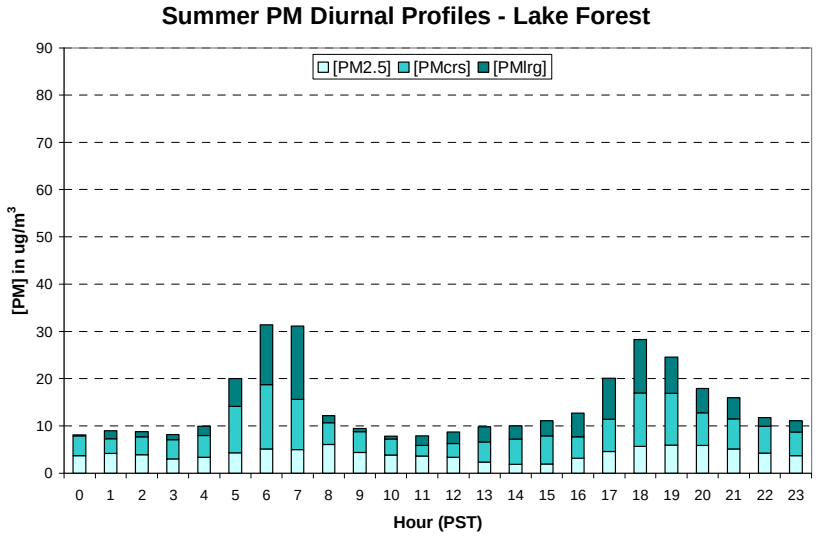

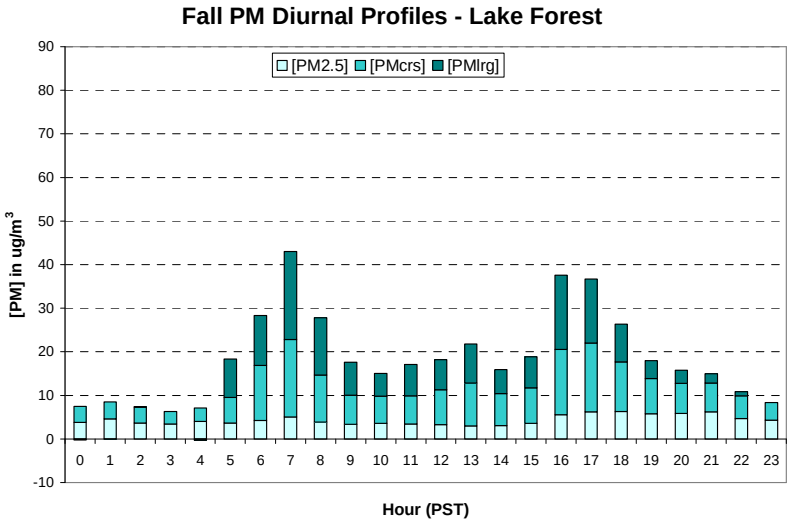

The nitrate/ammonium sampling and analytical procedures lead to six nitrogen measurement numbers, which are as follows:

1) Nitrate M: nitrate measured from the quartz filter on the TWS or MVS,
2) Nitrate V: volatilized nitrate measured from the backup nylon filter on the TWS,
3) Ammonium M: ammonium measured from the quartz filter on the TWS or MVS,
4) Ammonium V: volatilized ammonium estimated from Nitrate V,
5) Nitrate T: total nitrates (Nitrate M + Nitrate V), and
6) Ammonium T: total ammonium (Ammonium M + Ammonium V).

As stated earlier, it is unlikely that all volatilized nitrates are ammonium nitrate and therefore Ammonium V which assumes a mole of ammonium ion for every mole of volatilized nitrate ion overestimate Ammonium V and Ammonium T ambient concentrations.

An additional assumption is that ammonium nitrate does not dissociate to ammonia and nitric acid but remains at equilibrium. Because these are two-week average measurements, ammonium nitrate equilibrium is not maintained. Relative humidities above 62% (and cool temperatures) tend to promote aqueous instead of gas phase chemistry for ammonium nitrate. Further, within the proper relative humidity regimes, the gas/particulate phase partition coefficient (dissociation constant) is temperature dependent. Because substantial temperature swings occur daily and within a two-week sampling period, the ammonium-nitrate equilibrium varies throughout the sample collection period.

Ammonium T for the MVS was estimated from the ammonium measured by the MVS (Ammonium M) based on the Ammonium M to Ammonium T relationship observed with the TWS network. The difference between the estimated Ammonium T and Ammonium M for the MVS was then designated as Ammonium V. The Nitrate V was then estimated for the MVS by assuming it to be molar equal to the estimated Ammonium V. The Nitrate T estimate from the MVS was then the sum of the Nitrate M and the estimated Nitrate V. This approach allows the potential use of particulate nitrogen data from both of the TWS and MVS networks in estimating seasonal and annual deposition. However, the MVS flow rate was 5.0 liters per minute (lpm) compared to TWS flow rate of 1.3 lpm. In addition, the MVS samplers ran about 30 hours at mid-lake and 170 hours at piers while the TWS samplers ran for about 300 hours. Because of the potential difference in compound volatilization between the MVS and TWS systems, caution is recommended when comparing individually imputed Ammonium V and Nitrate V values between MVS and TWS. In the seasonal summary of particulate nitrogen measurements during LTADS shown in **Table 3-6**, the MVS Ammonium T, Nitrate T, and Total Particulate Nitrogen were calculated based on this treatment.

Table 3-6. Seasonal and Study Average NO_3^-, NH_4^+, and total particulate nitrogen concentrations from LTADS filter sampling.

LTADS Summary of Total Nitrogen Particulate, Nitrates, Ammonium							
	Nitrogen Particulate (as ug of N/m^3)					Nitrates	Ammonium
Site	Winter	Spring	Summer	Fall	Study Average	(ug/m^3)	(ug/m^3)
Big Hill PM2.5	*0.06*	0.49	0.62	0.42	0.47	0.64	0.42
Big Hill PM10	*0.07*	0.44	0.72	0.55	0.53	0.85	0.44
Big Hill TSP	*0.08*	0.54	1.00	0.74	0.71	1.25	0.55
Bliss State Park TSP	*0.07*	-	-	0.16	0.14	0.19	0.13
Coast Guard TSP	0.14	0.19	0.23	0.19	0.19	0.17	0.20
Lake Forest PM2.5	0.22	*0.21*	*0.35*	0.32	0.28	0.33	0.27
Lake Forest PM10	0.22	0.27	0.39	0.30	0.27	0.42	0.22
Lake Forest TSP	0.25	0.31	0.43	0.37	0.31	0.48	0.26
NASA Raft, TB1 (east) TSP	0.33	0.44	0.32	0.42	0.36	0.52	0.32
NASA Raft, TB1 (west) TSP	0.31	0.42	0.29	0.38	0.34	0.48	0.30
Sandy Way PM2.5	0.53	0.42	1.50	0.51	0.50	0.75	0.42
Sandy Way PM10	0.58	0.47	1.76	0.53	0.53	0.88	0.42
Sandy Way TSP	0.57	0.54	0.66	0.65	0.63	1.05	0.50
SOLA PM2.5	0.50	0.36	0.44	0.46	0.45	0.67	0.38
SOLA PM10	0.46	0.38	0.49	0.48	0.46	0.80	0.36
SOLA TWS TSP	0.59	0.54	0.43	0.38	0.48	0.81	0.39
SOLA MVS TSP*	0.53	*1.01*	*0.27*	0.21	0.41	0.58	0.17
Thunderbird PM2.5	0.13	0.18	0.16	0.13	0.15	0.30	0.10
Thunderbird PM10	0.15	0.25	0.36	0.27	0.26	0.38	0.22
Thunderbird TSP	0.20	0.37	0.48	0.35	0.35	0.53	0.29
Timber Cove TSP	0.31	0.34	*0.21*	-	0.32	0.39	0.30
Wallis Pier TSP	0.07	0.20	0.23	0.19	0.17	0.17	0.18
Wallis Tower TSP	0.10	0.18	0.25	0.18	0.19	0.16	0.19
Zephyr Cove TSP	0.14	0.35	0.35	0.23	0.26	0.28	0.25
Maximum Basinwide (excludes Big Hill)					2.57	2.57	1.04
2nd Maximum Lakewide (excludes Big Hill)					1.21	2.24	0.91
Average Lakewide (excludes Big Hill)					0.34	0.49	0.28
Median Basinwide (excludes Big Hill)					0.32	0.48	0.27
Minimum Basinwide (excludes Big Hill)					0.04	0.04	0.04

Underlined site names represent MVS measurements

Underlined data are estimates or rely on few data points; shaded cells indicate physically non-representative result

** SOLA MVS had higher flow & lower NH_4^+ than TWS (DRI ARB QA Review)*

Particulate nitrate and ammonium concentrations from the TWS network (i.e., Big Hill, SLT-Sandy Way, SLT-SOLA, Thunderbird Lodge, and Lake Forest) were summarized in **Figures 3-14 and 3-15**. During summer and fall (the seasons of greatest data capture at Big Hill), the nitrate concentrations at Big Hill are consistently higher than at sites within the Tahoe Basin. Comparing to the IMPROVE network, the Big Hill PM2.5 nitrate loadings are halfway between the averages for two transport-influenced sites in the southern Sierra Nevada - Yosemite (0.36 $\mu g/m^3$) and Sequoia (1.3 $\mu g/m^3$), suggesting that transport is an important component at Big Hill. The annual mean at Big Hill is somewhat uncertain. Most of the samples collected there are from the warm seasons when upslope transport from the Sacramento Valley is strongest (sampling began February 26, 2003), so much of the low nitrate winter period was likely missed. The Big Hill average is thus better viewed as an upper bound on the true annual average.

PM2.5 nitrate data from the TWS compare well with data from the IMPROVE network. At Bliss, IMPROVE nitrate averaged 0.22 $\mu g/m^3$, essentially the same as LTADS' limited MVS sampling of nitrate at Bliss, 0.19 $\mu g/m^3$. The Coast Guard, Wallis Tower, Wallis Pier, Thunderbird, and Lake Forest sites all show average nitrates concentrations of 0.2 to 0.9 $\mu g/m^3$, much lower than the 1.25 $\mu g/m^3$ observed at Big Hill. The SOLA and Sandy Way sites in South Lake Tahoe, with strong local motor vehicle and urban emissions, averaged about 1 $\mu g/m^3$ of nitrate. Although divorced from a more substantive meteorological assessment, aerosol nitrogen concentrations within the basin appear to be largely influenced by in-basin emissions, which is consistent with conclusions of Tarnay *et al*. (2002).

3.2.1.7 "Inert" Particles

Particles depositing from the atmosphere can dissolve in the lake water (the rate can vary) providing $SO_4^{=}$, PO_4^{-}, and NO_3^{-} that act as nutrients, stimulating biological growth, which can adversely impact water clarity and aesthetics. Insoluble particles depositing to the water will scatter and absorb light, thus also reducing visibility into the water. Little is quantitatively known at this time about the relative fates of atmospheric particles once they enter the water. As a crude estimate, the analysis of atmospheric particles by ion chromatography (water-soluble analysis of particulate matter) would provide an indication of the soluble fraction of particulate matter. An upper estimate of the inert particles would then be the difference between the total atmospheric PM and the soluble portion identified by ion chromatography. Furthermore, summation of the concentrations of $SO_4^{=}$, PO_4^{-}, NO_3^{-}, NH_4^{+}, Cl^{-}, Ca_2^{+}, K^{+}, Na^{+}, and a few other potentially soluble species permits an estimate of the total soluble fraction on a mass basis. An average of the LTADS data indicates that the soluble fraction is about 25% of the TSP mass at the transport site (i.e., Big Hill) and ranges from about 10 to over 20% of the TSP mass at the sites within the Tahoe Basin. As might be expected, the soluble fraction of PM2.5 is larger, being almost 30% at Big Hill and over 25% at all the TWS sites within the Tahoe Basin. Because large particles would deposit closer to their sources than small particles and some of the large particles would not be transported to the Lake, the direct atmospheric PM deposition estimates presented in later in Chapters

4 and 5 should be reduced by about 20% to better approximate the deposition of inert particles that truly affect the water clarity.

However, to begin a comprehensive assessment of inert particle light scattering and absorption for various water columns at Lake Tahoe, the LTADS information on the soluble fraction of PM is only a starting point. Very small particles produce Rayleigh scattering while larger particles undergo geometric scattering (Finlayson-Pitts and Pitts 1986) and particles in the middle of the size spectrum (comparable to the wavelength of visible light) may undergo Mie scattering. Rayleigh scattering occurs equally in the forward and backward directions, geometric scattering is about light refraction through large particles and is handled by classic optics, Mie scattering is non-uniform forward scattering and has a refraction index of 1.333 in water. In essence, to properly judge inert particle light scattering in the water column, very specific particle size (as many size cuts as possible), particle counts in each size, and particle concentration information in each size would be required. Particle composition and particle shape would also be extremely useful. The variable sunlight angle, the variable rates of particle accumulation (including disaggregation, conglomeration, chemical reaction), and the resultant particle settling within the water column would be additionally required information. Collecting these types of information was beyond the scope of LTADS.

3.2.1.8 Dust Experiments

A limited number of "dust experiments" were conducted to aid in understanding the mechanisms of emission, dispersion, deposition, and loss into and out of the air parcels as they traveled from sources on to the lake. Complete analyses of these experiments and publication of the results in a peer-reviewed journal is planned for the future. Nevertheless, preliminary analyses of three dust experiments are particularly noteworthy in describing these mechanisms. Additional discussion of these experiments can be found in Section 4.4.

3.2.1.8.1 July 2003, On-Lake, Northwest Shore Zone

During this experiment, the Tahoe Research Group's boat (R/V Frantz) was equipped with ozone, and NO_Y gaseous instruments, as well as CLIMET particle counters and a 2-stage particle counter limited to roughly 3 and 0.3-micrometer aerosol aerodynamic diameter bins. Information provided to the data logger included relative humidity and temperature, as well as boat's position. **Figure 3-22** provides a synopsis of the experiment.

In this instance, strong down-slope drainage airflow carried pollutants from the backshore areas onto the lake during the evening; as activities and pollutant emissions declined, the drainage air became cleaner during late night hours. On the next morning, pollutant flux over the lake increased as human activity began - NO_Y associated with vehicle exhaust was observed starting about 5 am. Particle counts, probably associated with chimney smoke and motor vehicle exhaust, increased after 6 am. The key finding from this experiment was that the night-time down-slope flow of air carried pollutants over the lake and was important in the dispersion and deposition of those

pollutants. The strong connection of shoreline activity, in particular motor vehicle traffic, with near-shore concentrations was also confirmed in this experiment. The most significant observation, however, was that concentrations over the lake declined rapidly (within a short distance of the shoreline and within a few hours), and implying that the effect of emission sources is largely confined to the near-shore environment.

3.2.1.8.2 August 2003, On-Lake, West and South Shore Zone

An evening sampling cruise aboard the R/V Frantz from Tahoe City to Zephyr Cove encountered an interesting combination of air pollutants transported into the Tahoe basin from the west and an accumulation of local "in-basin" emissions. This event may represent an archetype for "typical" summer meteorology and pollutant movement in the Tahoe region, and warrants a fuller discussion that the previous dust experiment. **Figure 3-23** presents the observations during this dust experiment.

3.2.1.8.2.1 On-Lake Conditions

Winds at Tahoe City at the start of this boat trip were light and from the west. Proceeding south along the west side of the lake toward Tahoma, in the area exposed to the Rubicon Gap (Loon Lake area of Sierra crest), the wind built to about 20 knots as estimated by the steep chop and whitecaps. Looking up at the crest there was a visible light haze associated with the air flowing over the crest. Farther south the course entered the wind shadow of the Rubicon Peak – Mount Tallac – Desolation Wilderness highlands and winds were lighter, but gusty, and from the west. Near the south end of the lake the winds turned southerly as the regional SW flow was turned by the terrain to follow the upper Truckee drainage. By late evening, approaching Zephyr Cove, down-slope flow brought air from the east shore onto the lake. This pattern of winds permitted the sampling of both the regional flow and local influences around the western and southern sides of the lake.

3.2.1.8.2.2 Gas Data

Figure 3-23 shows gas and aerosol data at 1-minute intervals. The ozone data indicate a depleted "urban" air mass, with steady concentration at 8-9 parts per hundred million per volume (pphm) coming through the Rubicon Gap. As the boat moved out of the direct exposure to the regional flow and into the wind shadow of the mountain peaks, ozone concentrations dropped to about 6 pphm; then, near Zephyr Cove, concentrations dropped again to about 3 pphm. Nitric oxide (NO) titration of ozone from motor vehicles along the south shore is suspected as the reason for this drop. NO_Y concentrations are low in the regional flow but increase in the sheltered areas of the south end of the lake. This suggests that much of reactive nitrogen in the regional flow is exhausted before the air parcel reaches the Tahoe Basin. Note the peaks in NO_Y when the Frantz' course ran near shore in the vicinity of Cascade Creek where Highway 89 runs along the shore, and approaching Zephyr Cove, where down-slope movement exposed the Frantz to fresh emissions along Highway 50. Occasional extreme NO_Y peaks are due to crossing wakes of motorboats – only spikes seen in successive

minutes should be considered due to terrestrial sources. Titration of regional ozone by local NO_X is the apparent cause of the drops in ozone concentrations.

3.2.1.8.2.3 Aerosol Data

The aerosol data are plotted here as "optical mass". This is estimated from particle counts by applying a correction factor of 2 for detection efficiency for sub-micron particles and using a sliding density scale of 1 for fines (assuming OC and water dominate the mass) to 2.5 (quartz) for coarse particles (assuming soil dominates the mass). This optical mass characterization provides a convenient scale for looking at these data, is internally consistent so that masses in different size bins can be compared, and is probably within a factor of 2 or so of real concentrations.

Fine aerosol data show regional material (PM2.5) accompanying the ozone in the regional flow below Rubicon Gap, then a modest enhancement from local sources around the southern end of the lake. Note that peaks near Cascade Creek and Zephyr Cove mimic the NO_Y data. The large (>2.5 μm) aerosol sizes show spotty effects along the west shore and stronger enhancement in the southern end of the lake, consistent with strong, localized sources. Some of the very large particles detected below the Rubicon gap may be spray.

These data track the regional/local split seen in the long term IMPROVE data. Although further work is needed to identify the source(s) of the regional ozone/fine PM, describe the synoptic and micro-scale meteorology, and quantify the local pollutant contributions, several key observations were made. Coarse particles (aerodynamic size>2.5 μm or larger than PM2.5) are significantly affected by local sources and their largest immediate impact is from sources in the southern end of the lake. NO_Y from local sources is sufficiently strong to reduce regional ozone concentrations. A large in-basin source region of reactive nitrogen is around South Lake Tahoe. Although meteorological processes indicate that summer is the primary season for potential transport of ozone and fine particles to the Tahoe Basin, these regional airflows are not likely to be the source of reactive nitrogen in the Tahoe Basin. A complete understanding of this event and the relevant local and regional contributions will require gathering all observational data for this time period, including synoptic and local meteorology and air quality data from upwind urban areas, western Sierra slope monitoring sites (Big Hill, Echo Summit, etc.), and in-basin sites.

Figure 3-22. On-Lake Dust Experiment, July 2003.

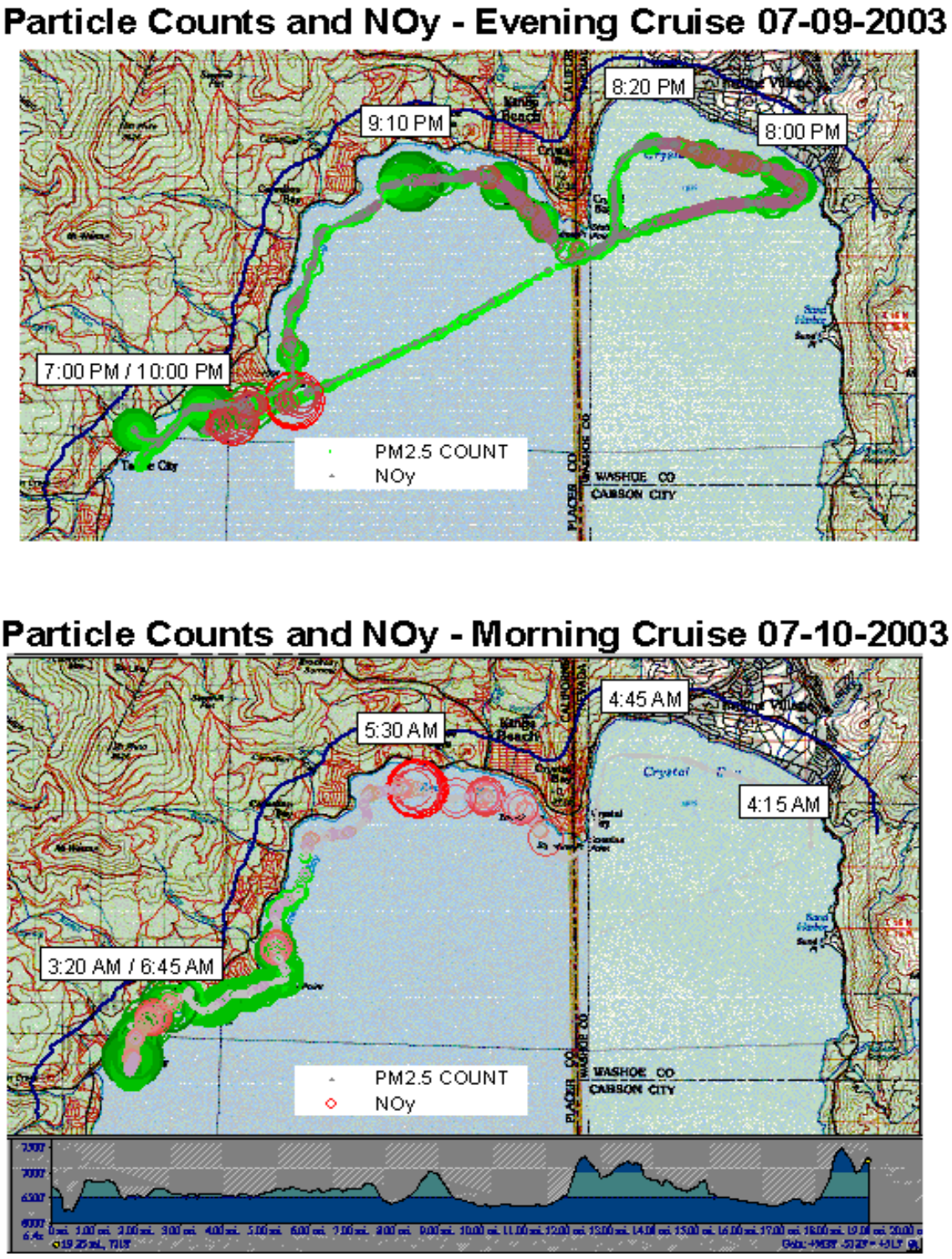

Note: Green circles denote PM2.5 and red circles denote total reactive nitrogen (NO_Y) concentrations with the size of any circle proportional to the amount of concentrations present.

Figure 3-23. On-Lake Dust Experiment, August 18, 2003 (6-9 pm).

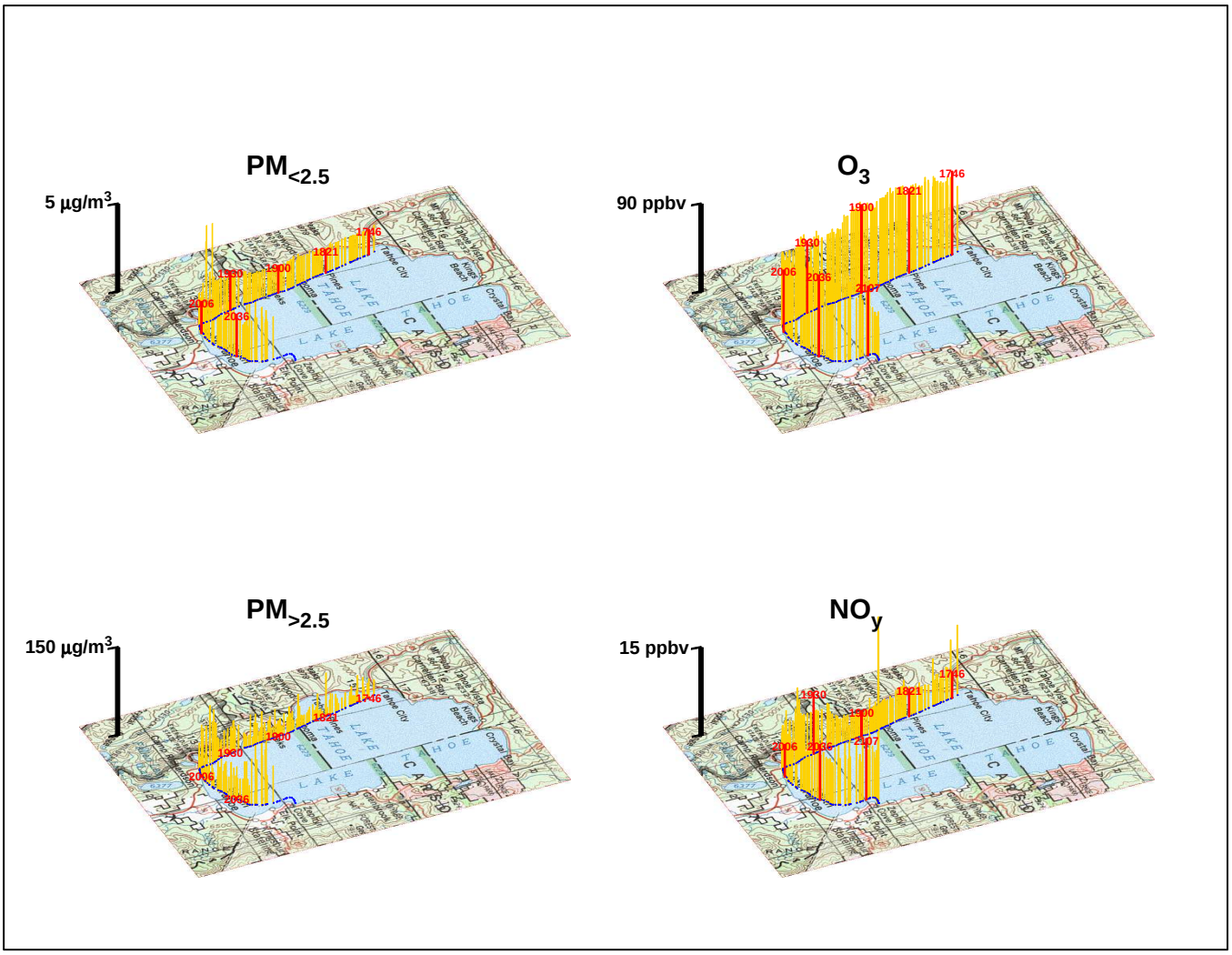

3.2.1.8.3 March 2004, SOLA Dust Experiments

To understand dispersion and loss as a function of distance from a likely source such as motor vehicle traffic, we designed and executed the SOLA Dust Experiments. SOLA site was situated roughly 50 feet away from the very busy Highway 50, also known as Lake Tahoe Boulevard in that stretch of the highway in South Lake Tahoe, and 100 feet away from the beach on the south shore. During Dust Experiments in March 2004, we placed CLIMET instruments at increasing distances from the road - a few feet away, 18 feet away, at SOLA, and one instrument roughly at the beach. **Figure 3-24** provides a synopsis of the experiment with S1 to S6 denoting 0.5 to 1, 1 to 2.5, 2.5 to 5, 5 to 10, 10 to 25, and >25 micrometer size fractions.

Even for particles in the smallest size fraction (0.5 to 1 micrometers in aerodynamic diameter), between the roadway, the emission sources, and the beach, there was nearly a 40% loss in number of particles due to dispersion, deposition, and interactions

with tree canopies. For the heavier particles (10 to 25 and >25 micrometers in diameter), there was a nearly 90% loss. The key lesson was that concentrations measured at our shoreline sites would almost always, and by a significant margin, overestimate concentrations near the middle of the lake. The monthly 24-hour TSP samples collected with MVS on two buoys were essentially identical with each other and remarkably similar to TSP concentrations at Thunderbird Lodge. The comments of peer reviewers and these insights led staff to account for depletion of particles over the Lake. Staff depleted PM_coarse and PM_large in the northern and southern quadrants of the Lake (primary source regions) by 25% of the difference between the PM concentrations at Lake Forest (north) and at SLT (south) and the PM concentrations at Thunderbird Lodge (east; basin background). Even with this depletion correction factor in the deposition estimates, the true (actual) deposition could be lower. Much more analysis is required to understand the full implications of dust experiments for mechanisms of air parcel transport within Tahoe Basin.

3.2.1.9 Phosphorus

Phosphorus (P) in either gaseous or aerosol form is not commonly a focus of air quality monitoring. We are not aware of any gaseous P measurements in California. California has a limited set of aerosol P data collected as part of the Toxic Air Contaminant (TAC) monitoring program. These TSP samples are collected on a 1-in-12 day schedule at urban sites throughout the state and are analyzed using X-ray fluorescence (XRF) by ARB staff. Phosphorus data were also reported by ARB's Dichot (PM10) network for PM2.5 and PM_coarse size fractions. The IMPROVE network also reports P concentrations in the PM2.5 size fraction. LTADS attempted to measure aerosol P, but had only limited success (see below). This section summarizes the P data available from the IMPROVE and LTADS sampling in the Tahoe Basin and, utilizing P data collected in other areas of California during other sampling programs, constructs a rough estimate of P concentrations in the basin.

3.2.1.9.1 Constraints on Aerosol Phosphorus Measurement

All of the sampling programs summarized here rely on XRF analysis of Teflon filters to measure aerosol P. In ambient aerosols, P detection is hampered by chronically low P concentrations and by strong interference from two common elements, sulfur (S) and silicon (Si).

The S interference is driven by three factors: 1) the strongest spectral fluorescence lines for P and S are separated by only a little more than the minimum energy resolution of typical fluorescence detectors (about 1.5 times the minimum resolution); allowing for some electronic "noise," the two peaks nearly overlie one another; 2) S fluoresces more strongly than P does; and finally, 3) S is usually present at several times the concentration of P. Together these factors often cause the S signal to overwhelm the P signal.

The Si interference is not as intrinsically strong, because the peak energies are more separated (nearly 3 times typical detector energy resolution). However, Si is generally

Figure 3-24. Normalized Particle Counts in Six Size Bins as Observed at SOLA during Early Morning Offshore Winds on March 12, 2004.

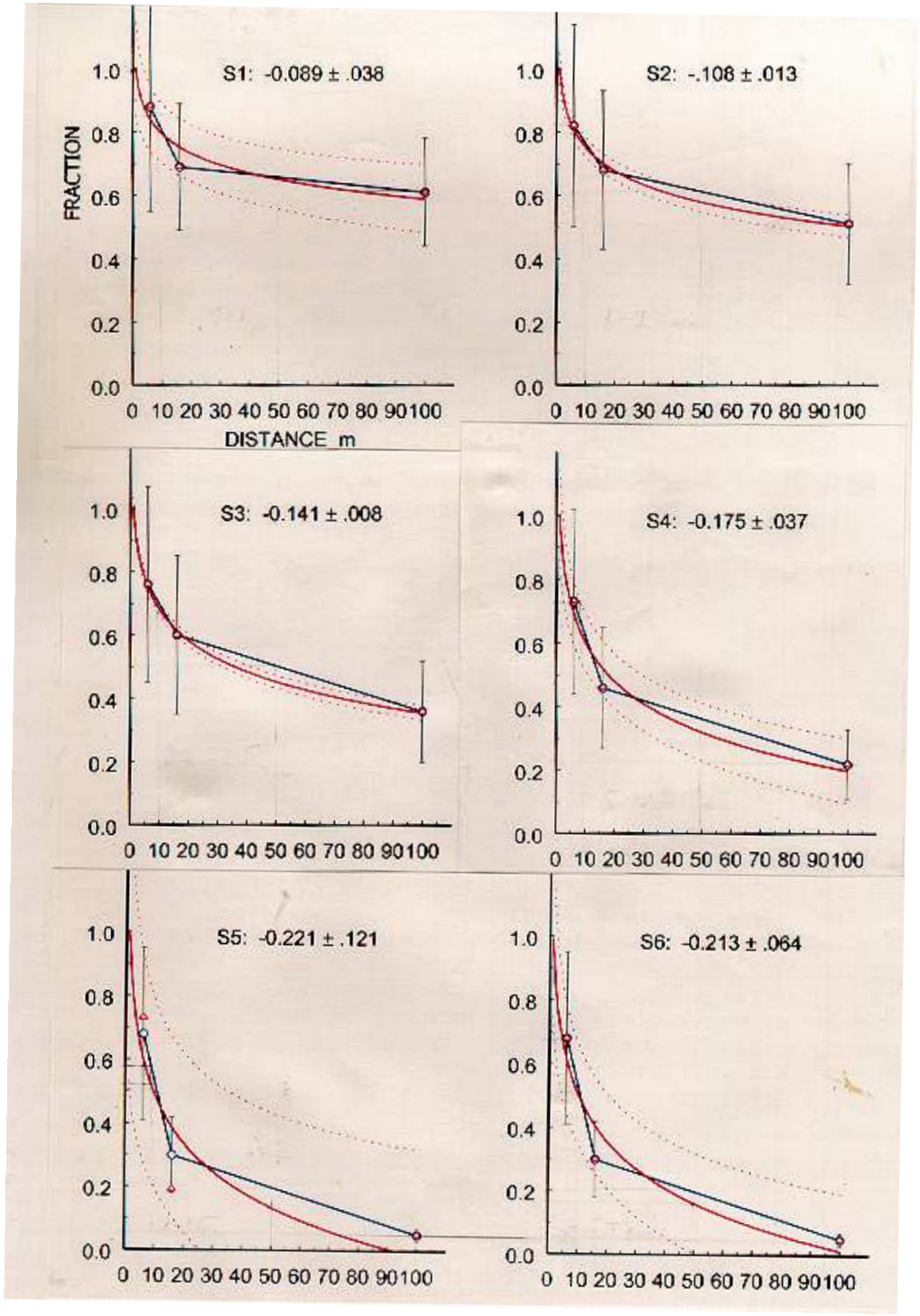

present in much higher concentrations than P, and the large concentration peaks have wider electronic “noise” footprints, so the net effect on the P peak is similar to that of S.

The relatively clean air in the Tahoe Basin accentuates the P detection problem. Although P can accurately be measured in pure standards, low P concentrations and interferences in ambient samples makes detecting P concentrations above measurement uncertainties in most XRF systems difficult to achieve in the best of circumstances. During the LTADS sampling program, 606 filters were analyzed by XRF. Of those filters, only 49 had P values greater than zero (i.e., there was a distinguishable P signal), and only ten of those were above measurement uncertainty limits (three other samples with [P] above uncertainty were compromised by other sampling problems and were invalidated). These measurements are presented in **Figure 3-25**. Most of the high [P]s were observed during winter with the other two cases occurring during late summer. The mean P concentration for the ten measurements was 11.1 ng/m^3 and the maximum observed was 21 ng/m^3. None of the phosphorus detections greater than measurement uncertainty were in the PM2.5 size fraction.

Figure 3-25. All 10 Occurrences When [P] Greater than Measurement Uncertainty.

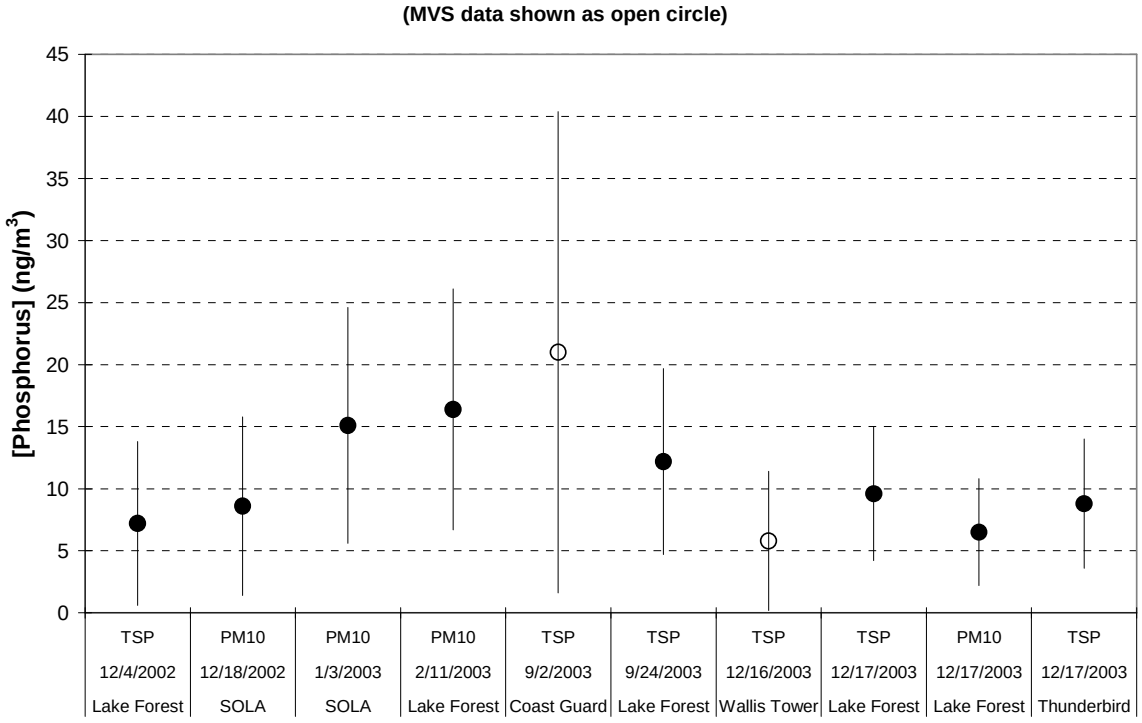

The average of the measurement uncertainties (i.e., the analytical uncertainties propagated from the counting statistics associated with each sample and background spectra) for the P non-detects indicates that the typical LTADS XRF limit of detection

(LOD) for P was about 10 ng/m^3. LOD denotes a statistical likelihood of detection. To increase confidence that the P was actually present, the operational limit of detection (O-LOD) is estimated by multiplying the standard deviation of the non-detect uncertainties by a factor of 3 (i.e., 97.5% confidence). For LTADS, the standard deviation of the P non-detect uncertainties, was 9.9 ng/m^3, providing an O-LOD of 30 ng/m^3. Note that although LODs in the range of 1 to 5 ng/m^3 have been reported by other studies, the analytical difficulties noted above result in an O-LOD of at least 20 ng/m^3. After careful review of data, staff believed that the O-LOD for detecting during LTADS was about 30 ng/m^3. However, as discussed later, peer review of the draft final report indicated other inherent P measurement problems with XRF in ambient settings that may make the O-LOD higher than 30 ng/m^3.

As noted before, P non-detects likely occur due to S and Si interference. The aerosol sample matrix may be the governing factor on whether or not XRF measurements successfully detect P. The fact that LTADS detected no P in the PM2.5 size fraction indicates that such concentrations were below the LOD. Furthermore, the phosphorus measurements of the source samples that were reanalyzed were variable and inconsistent. Therefore, conclusions regarding phosphorus concentrations in wood smoke and other combustion sources thought to dominate fine PM emissions are premature.

The LTADS P detection efficiency was about one-third that reported by the IMPROVE sampling. From 1989 to 2000, the IMPROVE sampling network collected 571 PM2.5 filters at Bliss State Park, reporting 30 P detects above uncertainty. Among 751 PM2.5 filters that were collected at SOLA over the same period, IMPROVE reported 31 P detects above uncertainty. The minimum detected P for IMPROVE appears to be around 1 ng/m^3. However, the IMPROVE LOD is likely much higher than 1 ng/m^3 because interferences from S and Si are expected. These data are summarized in **Table 3-7**.

In urban South Lake Tahoe, the IMPROVE data (PM2.5) reported a maximum P concentration of 21.5 ng/m^3 at SOLA. Similarly, the maximum P concentration observed during the 1-year LTADS was 21 ng/m^3 in a TSP sample (mini-vol sampler) at the US Coast Guard site in Lake Forest. In a more remote area in the basin (Bliss State Park, a site well above lake level and on western side of the Lake), the IMPROVE PM2.5 sampling recorded a maximum P concentration of 9.6 ng/m^3. LTADS only had six measurements (TSP by MVS) at Bliss and reported no P detects.

3.2.1.9.2 Phosphorus Measurement Difficulties in LTADS

In addition to the well-known overlap of the P x-ray emission spectrum with the tails of the emission spectra of the much more abundant sulfur (~20x) and silicon (~200x) atoms, the phosphorus x-rays can be self-absorbed within the particle. This self absorption effect is known to be relatively small (<10%) for fine (PM2.5) particles. Self absorption is potentially much greater in larger particles but depends on the amount and distribution of the P within the particle. The P data originally reported for LTADS included a 1.72 correction factor for the P measurements in PM10 and TSP samples.

One of the external peer reviewers of the draft version of this report, Professor Emeritus Tom Cahill of the University of California (Davis), whose expertise is in particulate matter measurements, pointed out that phosphorus x-rays in soil (an alumino-silica matrix) are strongly absorbed by Al and Si, which are abundant components of soil. A theoretical 3-layer particle model analysis indicated that large P correction factors may be necessary for particles larger than 2.5 µm. Assuming that PM_coarse particles (size between 2.5 and 10 µm) have an average diameter of 6.7 µm, their self absorption correction factor would be a factor of about 3.4; assuming that PM_large particles (size larger than 10 µm) have an average diameter of 12 µm, their self absorption correction factor would be a factor of about 6.8 (both estimates include a 1.42 factor for signal absorption within a silicon detector system that, in theory, should be accounted for during calibration of the analyzer response). Discounting the factor for absorption within a Si detector system, the self absorption correction factors for PM_coarse and PM_large would be about 2.4 and 4.8, respectively. Because the P data reported for PM10 and TSP samples in LTADS already included a 1.72 correction factor for self absorption within the particles, the P data in PM_coarse and PM_large sizes in the LTADS database would only require multiplicative factors of 1.4 and 2.8, respectively.

Table 3-7. Phosphorus concentration (ng/m^3) and S/P & Si/P ratio statistics based on 1989-2000 IMPROVE PM2.5 measurements in South Lake Tahoe (SOLA) and Bliss State Park (BLIS).

Statistic | Site \ Parameter:	[P]	S/P	Si/P
SOLA			
Minimum	5.39	2.48	2.63
Mean	11.84	12.38	16.25
Maximum	21.52	33.35	42.81
Median	10.99	9.91	16.25
Standard Deviation	4.06	7.85	10.76
Standard Error of Mean	0.73	1.43	1.96
# Samples detecting phosphorus	31	30	30
# Samples	751	751	751
BLISS			
Minimum	1.03	2.92	0.31
Mean	4.56	18.43	11.97
Maximum	9.61	57.62	72.09
Median	4.75	16.88	9.63
Standard Deviation	2.11	11.90	13.64
Standard Error of Mean	0.38	2.17	2.49
# Samples detecting phosphorus	30	30	30
# Samples	571	571	571

Nearly all XRF P data reported to date (not just LTADS) suffer from these particle size and soil matrix difficulties. However, additional research and peer review is necessary before the historical measurements could possibly be corrected for these measurement complexities. To understand these difficulties and to correct for their effects, a substantive knowledge of the particle sizes associated with the P measurements will be required. Knowledge of the chemical composition of the particles would also be necessary to account for absorption of P x-rays by other components. However, because detailed knowledge of particle size and composition is generally limited, it is clear that correcting the existing P data would be very challenging. The crude P corrections presented below assume that P atoms are uniformly distributed throughout the particle. In theory, the biologically available forms of P would more likely be near the surface of the particle. Thus, this approach of including large corrections for signal absorption deep within particles would significantly overestimate the P that is biologically available.

Because the number of P detections with the TWS (TSP, PM10, and PM2.5) and MVS (TSP only) PM networks was very limited with the standard XRF analysis, CARB contracted for a more sensitive analysis (synchrotron XRF) of 70 ambient samples at the Advanced Light Source (ALS) laboratory. The synchrotron XRF detected phosphorus in 49 of the samples while standard XRF detected phosphorus in only 15 of the samples. For the 11 matched "non-zero" measurements, the ALS results averaged over two times the standard XRF results (12 ng/m^3 vs. 5 ng/m^3).

The new theoretical absorption corrections were applied to the P data. Because the routine PM sampling during LTADS had limited PM size information, these corrections were necessarily constrained to estimates of the fraction of total PM mass (TSP) in the PM_fine (PM2.5), PM_coarse (PM10 minus PM2.5), and PM_large (TSP minus PM10) sizes with an assumed mean particle size in each size fraction. TSP measurements with the MVS were allocated among the three particle size bins based on the PM measurements from the Two Week Sampler network. These allocations were based on the general nature of the mini-vol sampling site as shown in **Table 3-8**. The SOLA, Sandy Way, Lake Forest, and Wallis Tower sites were classified as urban and the Thunderbird, Bliss, and buoy sites were classified as remote (i.e., limited influence from local emission sources). The sites on piers were assigned an intermediate classification.

Table 3-8. PM size fraction allocations to TSP samples from the mini-volume sampler program.

Sampling Sites	Exposure Type	PM_fine fraction	PM_coarse fraction	PM_large fraction
Thunderbird, Bliss, buoys	Remote	60%	35%	5%
Piers (US Coast Guard, Wallis, Timber Cove, Zephyr Cove)	Intermediate	50%	40%	10%
SOLA, Sandy Way, Lake Forest, Wallis Tower	Urban	40%	45%	15%

Because of the uncertainties in measuring P concentrations, a variety of information is relevant and necessary for estimating the range of central tendencies in P concentrations. Because P was not detected in many of the samples, an estimation is needed of the P concentration is needed for samples below the analytical detection limits (LOD). LTADS estimated an operational LOD for P measurements by the DRI and ALS systems by multiplying 3 times Standard Deviation of the P non-detect measurement uncertainties. For the ALS measurements, the O-LOD was 3 x 3 ng/m^3 or 9 ng/m^3. For the DRI measurements, the O-LOD was 3 x 9.9 ng/m^3 or ~30 ng/m^3. Typically, one-half of the O-LOD is used to estimate concentrations of substances below the analytical technique's detection limit.

The average P concentration of the 49 P detects with the ALS analysis was 61 ng/m^3 (after accounting for field blank values, the new self absorption correction factors, and the 1.42 silicon detector bias needed for the ALS data). Because 21 of the 70 ALS samples resulted in no detection of P, an estimate of the unknown P concentration in those samples is needed. Usually, one-half of the O-LOD is used for this estimate. However, the original P measurements do not account for the size-dependent self absorption and so the O-LOD also needs to be increased to account for the self absorption of the signal. Comparing average P concentrations originally reported by ALS for TWS TSP samples with the average P concentrations associated with the matched sized P corrections for self absorption (P_coarse * 2.4; P_large * 4.8) and the ALS correction factor for measuring P with a silicon detector (1.42) indicates a rather large P_TSP correction factor of 4.4 when accounting for the net impact of self absorption and calibration on the ALS P concentrations. Assuming the O-LOD is impacted in a similar proportion, the corrected O_LOD is 9 ng/m^3 * 4.4 or ~40 ng/m^3. Assuming one-half of the corrected O-LOD (½ x 40 ng/m^3) for the 21 samples without detection of P yields an average P concentration for the 70 ambient samples analyzed at the ALS of 49 ng/m^3. Assuming the 70 ALS samples were spatially and temporally representative of the 600+ total ambient samples collected during LTADS, an average P concentration of 49 ng/m^3 would be estimated for LTADS.

Although the ALS samples were selected on the basis of the highest P concentrations initially reported by DRI, the samples actually submitted to ALS for analysis included all of the available samples from other sites during the same sampling period (some filters were not available because they had been digested during a supplemental analysis by ICPMS). Consideration in the sample selection was also given to balance seasonal representation. Because the selection process for filters to be reanalyzed at ALS focused on the higher P concentrations reported by DRI, the possibility of a positive bias exists. However, the original DRI measurements of detectable phosphorus concentrations were infrequent and often unrelated in space and time. Thus, the ALS analysis of all associated samples (mostly P non-detect samples by DRI) and the consideration of seasonal balance in the sample selection process, the ALS phosphorus results are likely to be representative of the actual annual and seasonal concentrations.

However, if the ALS analytical set were assumed not to be temporally representative, the average LTADS phosphorus concentration could be estimated by assuming P concentrations equal to ½ of the DRI O-LOD for the ~540 samples with non-detects (assuming all the DRI P detects were analyzed by ALS) and averaging with the mean P concentration of the ALS samples (i.e., 49 ng/m^3). As noted above, staff conservatively estimated the O-LOD of the original DRI P measurements by using three times the standard deviation of the uncertainty associated with the reported "zero" P concentrations (9.9 ng/m^3) or ~ 30 ng/m^3. Based on the annual mean size fractions from the TWS data (10% in PM_large, 40% in PM_coarse, and 50% in PM_fine), the 30 ng/m^3 O-LOD for the original DRI data were adjusted upward to account for the larger self absorption correction factors in PM_coarse (x1.4) and PM_large (x2.8) particles. Thus, staff estimated a corrected O-LOD of 40 ng/m^3 for the DRI P measurements. Using the average P concentration of 49 ng/m^3 for the 70 ALS samples and ½ of the DRI self-absorption-corrected O-LOD (i.e., 20 ng/m^3) for the ~540 DRI samples with non-detects, this approach estimates an average P concentration of ~25 ng/m^3 during the LTADS sampling. This analysis is summarized in tabular form in **Table 3-9**. Based on the estimation approaches described above, the staff can confidently assume that the "true" annual average P concentration in the Tahoe Basin is not likely to be less than 25 ng/m^3 nor greater than 50 ng/m^3, including the large new theoretical correction factors.

Table 3-9. Estimation of LTADS average phosphorus concentration if assuming the mean P concentration from ALS subset of LTADS samples is not temporally representative. LTADS [P]avg = (sum of (# of samples x measurement or ½ x MDL))/total # of samples.

Analysis method	O-LOD (ng/m^3)	Number	x	Mean Measurement Or ½ x O-LOD (ng/m^3)	=	Product (ng/m^3)
ALS detects	---	49	x	61	=	2,989
ALS non-detects	40	21	x	20	=	420
DRI detects*	---	0	x	0	=	0
DRI non-detects	40**	536	x	20	=	10,720
Sum	---	606	x	---	=	14,129
LTADS [P] $_{avg}$	---	---	-	**23.3**	-	---

* Note: DRI detects were reanalyzed at ALS and so # of DRI detects is zero even though 10 were actually observed.

** estimated as 3 x StdDev of measurement uncertainty associated with DRI [P]s reported as 0 ng/m^3 (for TSP samples) and adjusted for updated size-specific self absorption correction factors (size distribution of P assumed to be the same as annual mean observed with TWS network: 10% in PM_large fraction (x 2.8), 40% in PM_coarse fraction (x 1.4), and 50% in PM_fine fraction (x 1.0)).

3.2.1.9.3 LTADS vs. Other Phosphorus Measurements

In addition to the LTADS and IMPROVE measurements within the Tahoe Basin, additional P measurements are available from the ARB'S Dichotomous (PM2.5 and PM_coarse) program for measuring PM10 and from ARB's Toxic Air Pollutants (TAC) monitoring network. Annual mean P concentrations for dichot sampling sites in the mountains are shown in **Table 3-10**. Note that no P was detected in the PM2.5 samples. Similarly, P was not detected in any LTADS PM2.5 samples. The IMPROVE sampling program has reported some P detects in the fine fraction (~4% of samples), however.

The mean annual P concentrations in the PM_coarse samples from the dichot network were roughly comparable (approximately 25 ng/m^3) among the four sampling locations in the mountains. Assuming that the PM_fine, PM_coarse, and PM_large fractions of TSP are 50%, 40%, and 10% respectively (based on average LTADS TWS results) and that P is uniformly distributed among PM sizes yields a 62 ng/m^3 annual mean concentration estimate of total P. However, no P was detected in any of the PM2.5 samples. Thus, 25 ng/m^3 serves as a lower bound and 60 ng/m^3 serves as an upper bound of annual average P concentrations. Assuming the updated size-dependent P self absorption correction factors (P_coarse * 1.4 and P_large * 2.8) creates a skewed corrected estimate of annual P concentrations of 35-85 ng/m^3.

The Toxic Air Contaminant (TAC) network samples in urban areas on a 1-in-12 day schedule. Median P concentrations from the TAC network seldom exceeded 60 ng/m^3. Stations not impacted by obvious agricultural or dairy impacts (e.g., Riverside-Rubidoux) have reported a P concentration exceeding 200 ng/m^3 only once, in Azusa in 2002 (ARB, 2002). The group median value of the eight site-specific annual median P concentrations is shown for each year (1996 through 2002) in **Table 3-11**. The annual median P concentrations ranged from 44 to 54 ng/m^3, based on standard XRF analysis. The minimum annual median P concentration at any site in the TAC (urban) network, a number more likely to be representative of less populated areas such as Lake Tahoe, ranged from 32 to 43 ng/m^3, with a multi-year mean of 36 ng/m^3. Based on a typical 10:40:50 split in PM_large:PM_coarse:PM_fine and accounting for the new, size-specific, theoretical self absorption correction factors (i.e., x 1.0 for P in PM2.5, x 1.4 for P in PM_coarse, and x 2.8 for P in PM_large), yields an absorption-corrected annual mean P concentration estimate of 1.34 x P_original or 43-58 ng/m^3 for the range of minimum concentrations in the TAC network and ambient concentrations in the Tahoe Basin. Based on the TAC data, annual mean P concentrations in the Tahoe Basin could be as low as 30 ng/m^3 and as high as 60 ng/m^3.

3.2.1.9.4 Phosphorus Estimated from PM Emission Inventory

As an alternative approach to estimating the phosphorus concentrations in the Tahoe Basin, staff also estimated seasonal average P concentrations from seasonal average PM concentrations by developing a P emission factor based on source profiles of P as a function of PM, weighted to the mix of PM sources in the Tahoe Basin. The PM

emissions were also divided into 3 sizes (PM_fine, PM_coarse, and PM_large) to apply the theoretical self absorption correction factors, which are not in the current P source profiles, to the PM_coarse and PM_large fractions. This analytical approach resulted in an average P concentration estimate of 22 ng/m^3 in the Tahoe Basin and is described in detail in **Table 3-12**.

Table 3-10. Annual mean P coarse concentrations (ng/m^3) from ARB's dichot PM10 (PM_fine & PM_coarse) monitoring network. All P measurements in the PM_fine fraction were non-detects. The dichot measurements are collected on a 1-in-6 day schedule.

Site \ Year:	1991	1992	1993	…	1998	1999	2000	Mean
Mammoth Lake	28.1	22.2						25.2
Truckee		24.6	31.2					27.9
Quincy		22.3	21.4					21.8
Portola					26.6	25.3	27.5	26.5

Table 3-11. Median annual P concentrations (ng/m^3) from ARB's toxic air contaminant monitoring network. The toxic network samples on a 1-in-12 day schedule.

Site \ Year:	1996	1997	1998	1999	2000	2001	2002	Mean
Azusa	---	---	---	---	59	68	54	60.3
Burbank-W Palm	57	65	62	64	54	55	63	60.0
Los Angeles-NM	53	---	56	56	47	---	51	52.6
N. Long Beach	32	44	43	51	36	35	37	39.7
Riverside-Rubidoux	210	---	---	250	220	240	230	230.0
Roseville-Sunrise	37	37	40	43	32	35	33	36.7
San Jose – 4th St	34	40	42	44	44	44	---	41.3
Stockton-Hazelton	46	53	56	52	51	50	54	51.7
MEDIAN	46	44	48	52	49	50	54	**49.0**
MINIMUM	32	37	40	43	32	35	33	**36.0**

Table 3-12. Estimation of LTADS average phosphorus concentration based on emission inventory P source profiles and ambient PM concentrations. LTADS [P]avg = (emissions-weighted source-specific P emission factor x PM emission estimate from that source measurement (or ½ x O-LOD))/total # of samples.

a) Phosphorus emission factors (i.e., P=f(PM)) based on ARB emission profiles.

Source	%TSP	%PM10	%PM2.5	Notes
Construct/demolition	0.1499	0.0979	0.2273	
Unpaved road dust	0.1225	0.1225	0.1225	
paved road dust	0.1372	0.1372	0.1372	
fireplaces & stoves	0.0288	0.0288	0.0196	based on orchard prunings as official inventory assumes 0.0000 for firewood
Waste burning	0.0295	0.0295	0.0205	
other (estimated)	0.0795	0.0795	0.0750	estimated as mean of P profiles for above 5 major PM sources

b) Estimated PM emissions (tons/day) based on ARB emission inventory.

(**Note:** The PM emission inventory does not include secondarily generated PM (e.g., NH_4NO_3) that can contribute significantly to ambient PM concentrations.)

Source	TSP	PM10	PM2.5	Notes
construct/demolition	0.85	0.42	0.09	
unpaved road dust	2.31	1.37	0.29	
paved road dust	2.16	0.99	0.17	
fireplaces & stoves	1.91	1.79	1.72	
waste burning	0.31	0.31	0.29	
other (estimated)	0.53	0.40	0.29	
TOTAL	8.07	5.28	2.85	

c) Development of PM source-weighted phosphorus emission factor based on ARB's PM emission inventory. Source-weighting multiplies equivalent cells in sub-tables a) and b) and divides by TOTAL PM emissions in sub-table b). The integrated source-weighted P emission factor by size is then the sum of the factors for each PM source.

	P fraction			
Source	**of TSP**	**of PM10**	**of PM2.5**	**Notes**
construct/demolition	0.000158	0.000078	0.000072	
unpaved road dust	0.000351	0.000318	0.000125	
paved road dust	0.000367	0.000257	0.000082	
fireplaces & stoves	0.000068	0.000098	0.000118	
waste burning	0.000011	0.000017	0.000021	
other (estimated)	0.000052	0.000060	0.000076	
Source-weighted P emission factor	**0.001007**	**0.000828**	**0.000494**	

d) Assuming that the ambient PM concentrations reflect the relative impact of PM emission sources and that the emission sources have the same average mix throughout the air basin, multiplying the integrated source-weighted average phosphorus emission factor in sub-table c) times the respective annual average PM concentrations observed during 2003 at each site in the Tahoe Basin yields the estimated annual [P]s. This analysis could also be done on a seasonal basis (provides more temporal detail but yields essentially the same annual results).

	$[PM]_{annual\ mean}$ in ng/m^3			$[P]_{annual\ mean}$* in ng/m^3		
PM Monitoring Site	**TSP**	**PM10**	**PM2.5**	**TSP**	**PM10**	**PM2.5**
SLT-Sandy Way	22,032	16,762	9,177	22.2	15.2	4.5
SLT_SOLA	21,773	18,551	7,270	21.3	16.5	3.6
Lake Forest	18,059	13,981	4,914	18.2	12.7	2.4
Thunderbird Lodge	5,958	5,957	3,629	6.2	5.3	1.8
Buoy-West (TB4)+	6,066	5,713	3,548	6.1	5.2	1.8
Buoy-East (TB1) +	6,251	5,887	3,656	6.3	5.3	1.8

* based on average P fraction: of TSP=0.001007, of PM10=0.000908, and of PM2.5=0.000494

+ because only TSP is sampled on buoys, PM10 and PM2.5 values are based on size relationships observed at Thunderbird.

e) Subtracting the P_PM10 estimate from the P_TSP estimate yields the [P] in PM_large; subtracting the P_PM2.5 estimate from the P_PM10 estimate yields the [P] in PM_coarse. P_fine equals P_PM2.5 and P_TSP equals the sum of P_fine plus P_coarse, and P_large.

	$[P]_{annual\ mean}$ in ng/m^3			
PM Monitoring Site	**P_large**	**P_coarse**	**P_fine**	**P_TSP**
SLT-Sandy Way	7.0	10.7	4.5	22.2
SLT_SOLA	4.9	12.9	3.6	21.3
Lake Forest	5.5	10.3	2.4	18.2
Thunderbird Lodge	0.9	3.5	1.8	6.2
Buoy-West (TB4)	0.9	3.4	1.8	6.1
Buoy-East (TB1)	1.0	3.5	1.8	6.3

f) Applying the updated self absorption correction factors for the DRI data, which already includes a 1.72 self absorption correction factor (x 2.8 for P_large, x 1.4 for P_coarse, and x 1.0 for P_fine), to the estimated annual average ambient P concentrations by particle size results in an enhanced estimate of ambient P concentrations (an annual mean 4-quadrant shoreline [P] estimate of 22 ng/m^3, all-site LTADS annual mean [P] of 20 ng/m^3, and, as shown in the table below, a mid-lake-weighted 4-quadrant annual mean [P] of 16 ng/m^3 (i.e., each quadrant's shoreline concentration averaged with the mid-lake concentration).

	Corrected $[P]_{annual\ mean}$ in ng/m^3			
PM Monitoring Site	**P_large**	**P_coarse**	**P_fine**	**P_TSP**
SLT-Sandy Way	19.4	14.9	4.5	38.8
SLT_SOLA	13.5	17.9	3.6	35.0
Lake Forest	15.3	14.3	2.4	32.0
Thunderbird Lodge	2.5	4.8	1.8	9.1
Buoy-West (TB4)	2.6	4.8	1.8	9.1
Buoy-East (TB1)	2.7	4.9	1.8	9.4
4-quad mean*	**9.2**	**10.1**	**2.5**	**21.8**
Mid-lake weighted 4-quad mean**	**5.9**	**7.5**	**2.2**	**15.5**

* 4-quadrant mean = ((SW+SOLA)/2 + LF + 2*TBL)/4

** mid-lake weighted 4-quadrant mean = {((SW+SOLA)/2 + LF + 2*TBL + 4*((TB4+TB1)/2)}/8

3.2.1.9.5 Selection of a phosphorus concentration for LTADS deposition estimates

Because ambient phosphorus concentrations were typically below the detection limits of the sampling and analysis protocols used in LTADS, staff was forced to estimate P concentrations for input into the analyses to estimate the direct dry and wet atmospheric deposition of P to Lake Tahoe. Because of all the uncertainties noted above, staff used a temporally and spatially constant P concentration of 40 ng/m^3 in both the dry and wet deposition modeling approaches to arrive at seasonal and annual estimates of phosphorus loading to Lake Tahoe. [Note: assuming that P is a consistent function of PM, one could generate seasonal and site-specific variations in P based on PM measurements.] The various measurements and insights that led to the selection of this concentration of phosphorus in the deposition analyses are summarized below.

a) DRI XRF measurements of P during LTADS. P detections during LTADS were limited (49 samples with [P] > 0 ng/m^3; only 10 samples with [P] > the measurement uncertainty and none of those were in the PM2.5 size). The average of the 49 detections of P was 5 ng/m^3 and the average of the 10 samples with concentrations greater than the measurement uncertainty was 11 ng/m^3, with a maximum of 21 ng/m^3. Assuming that the P O-LOD equals the 3 times the standard deviation of the "zero" P measurement uncertainties, the P O-LOD for MVS samples was ~30 ng/m^3 (3 x 9.9 ng/m^3). The estimated range of [P] was about 5 - 30 ng/m^3 given that the means are less than the O-LOD. Accounting for new self absorption correction factors, the range of the estimated annual [P] is approximately 10 – 45 ng/m^3. The best estimate of [P] from the DRI measurements is ½ of the O-LOD or ~20 ng/m^3.

b) Supplemental reanalysis of selected LTADS filters by synchrotron-XRF. Reanalysis of 70 ambient filter samples collected during LTADS by synchrotron_XRF analysis at the Advanced Light Source (ALS) laboratory detected P more frequently than the standard XRF method (ALS reported 54 detects out of 70 ambient samples). After correction for relatively high field blank values, the number of P detects dropped to 49 and the mean P concentration was 10 ng/m^3, with a maximum observed concentration of 38 ng/m^3. The mean P concentration of the samples where the [P] was greater than the measurement uncertainty was ~15 ng/m^3. Assuming that the P O-LOD equals the 3 times the standard deviation of the "zero" P measurement uncertainties, the P O-LOD for UCD samples was ~10 ng/m^3 (3 x 3 ng/m^3). Considering a recommended silicon detector calibration factor (x 1.42) for these data and also the self absorption correction factors, the mean P concentration would be on the order of 20-40 ng/m^3 with a maximum of ~95 ng/m^3. The corrected O_LOD would also be about 20 ng/m^3. Thus, the estimated range of [P]s is about 10 – 40 ng/m^3. The best estimate of [P] from the ALS measurements is ~30 ng/m^3 because of the improved measurement sensitivity and relatively high proportion of P detects.

c) Historical measurements of P from ARB's dichotomous sampler network. Although phosphorus has not been the focus of sampling programs, P measurements are available from various programs that have used XRF

analysis. Thus, these PM_coarse measurements would also be subject to the uncertainty associated with potentially large self absorption correction factors. In those that analyzed PM2.5 samples (e.g., dichot, IMPROVE), detection of P in PM_fine has been quite rare without special practices for higher sensitivity. In those programs that measure PM_coarse (i.e., dichot), the annual means of P concentrations in mountain settings (i.e., Truckee, Quincy, Portola, and Mammoth Lakes) were quite consistent at about 25 ng/m^3. The reported MDL for this XRF analytical technique was 15 ng/m^3. Based on the TWS results during LTADS, the following TSP size fractions were assumed: 50% in PM_fine, 40% in PM-coarse, and 10% in PM_large. Assuming the P is uniformly distributed, irrespective of the size of the PM particle, the P_coarse results from the dichot suggest that the total annual P concentration could be about 62 ng/m^3 (i.e., 25 ng/m^3/0.40). However, because no P detects were reported in the PM_fine samples and PM_large was not sampled, the estimated range of total P concentrations is 25 – 60 ng/m^3. Allowing for self absorption correction factors, the estimated range of total P concentrations expands to 35 to 85 ng/m^3.

d) Historical measurements of P from ARB's toxic air contaminant (TAC) sampler program. The TAC network collects TSP samples on a 1-in-12 day schedule in primarily urban areas. TAC data accessed by staff featured annual median P concentrations for 8 urban sites operating between 1996 and 2002. The TAC network average of the annual median P concentrations at the 8 sites was 49 ng/m^3. The minimum annual median P concentration among the 8 sites during each year ranged from 32 to 43 ng/m^3 and averaged 36 ng/m^3. Given the lower population and activity levels in the Tahoe Basin compared to an urban area, the minimum annual median P concentration is more likely than the average urban median P concentration to be representative of conditions in mountain communities such as South Lake Tahoe. Based on the minimum annual median TAC data, P concentrations in the Tahoe Basin are estimated to be 45 – 60 ng/m^3. Including adjustment for the theoretical self absorption correction factors, the estimated range of annual P concentrations in the Tahoe Basin becomes 60 – 80 ng/m^3.

e) Estimation of P as a function of PM concentrations. A limited number of PM samples for various emission sources result in emission source profiles for the PM constituents. Using the P fractions from these TSP, PM10, and PM2.5 source samples and assuming the mixture of P in ambient air is proportional to the mixture of P in source samples, an average P source profile, weighted to reflect the mixture of PM emission sources in the Tahoe Basin, can be applied to ambient PM concentrations measured during LTADS to estimate the concentration of P at the PM measurement sites within the Tahoe Basin. Thus, the spatial and temporal distribution of the P closely matches to PM distributions.

The P emission profiles for TSP, PM10, and PM2.5 were applied to the PM measurements to estimate P concentrations in those sizes. The sized P concentrations were differenced to yield P concentrations in PM_coarse and

PM_large sizes. The new theoretical self absorption correction factors were then applied to these sized P concentrations to yield the final estimate P concentrations at the measurement sites. The result of this analysis yielded a 4-quadrant (SLT + LF + BL + TB) average P concentration of 22 ng/m^3. The estimated annual [P] at the various monitoring sites ranged from 10 – 40 ng/m^3 with a best annual basin estimate of ~20 ng/m^3.

The variety of P estimation results highlight the uncertainty associated with phosphorus measurements and ultimately with estimates of its deposition to Lake Tahoe. From a strictly emission inventory perspective (P profiles and PM emissions), the P emissions within the Tahoe Basin are estimated to be 8 metric tons per year. The fraction of this emission total being deposited directly to the Lake would be appreciably less (less than half based on wind directions alone). Assuming a lake surface area of 500 km^2 and an average dry deposition velocity of 0.5 - 1 cm/sec, a 4 metric ton per year dry deposition estimate would require an average ambient P concentration of 25 - 50 ng/m^3 (assuming total deposition is equally comprised of wet deposition and dry deposition). This concentration analysis based on the emissions inventory yields an estimated annual P concentration range of 25 – 50 ng/m^3, which is comparable to the ambient concentration data analyses. Considering the range in estimates and the uncertainties in detection and self absorption correction factors (likely overestimating available P in larger particles), staff selected an intermediate phosphorus concentration value of 40 ng/m^3 for the LTADS depositional analyses.

3.2.2 Gases

3.2.2.1 Temporal and Spatial Variation of Ammonia and Nitric Acid

The TWS measurements also included denuder measurements of two important nitrogenous gases from a nutrient perspective, ammonia (NH_3) and nitric acid (HNO_3). **Figure 3-26** presents plots showing the variations in these gases. Nitric acid was measured via nitrate extraction from carbonate denuders while ammonia was measured via extraction of ammonium from citric acid denuders. Due to the long integration time of the TWS during variable conditions, stoichiometric balance among the gases and aerosols was not expected, and statistics only indicate weak relationships among the species. This lack of systematic relationships eliminates any basis for estimating nitric acid or ammonia for the MVS network. Gas-phase nitrogen calculations are therefore based entirely on data from the TWS network. Ammonia concentrations were highest at the SOLA site, which had concentrations noticeably higher than the nearby Sandy Way site. The concentrations of ammonia and nitric acid were lowest at the Thunderbird Lodge site. In general, concentrations were lowest during the spring. However, seasonal patterns were relatively weak with the exception of concentrations of both gases being higher in summer and fall at Big Hill and ammonia concentrations being higher during winter at the SOLA site.

Figure 3-26a. Ammonia and Nitric Acid Concentrations Observed with the TWS at Big Hill.

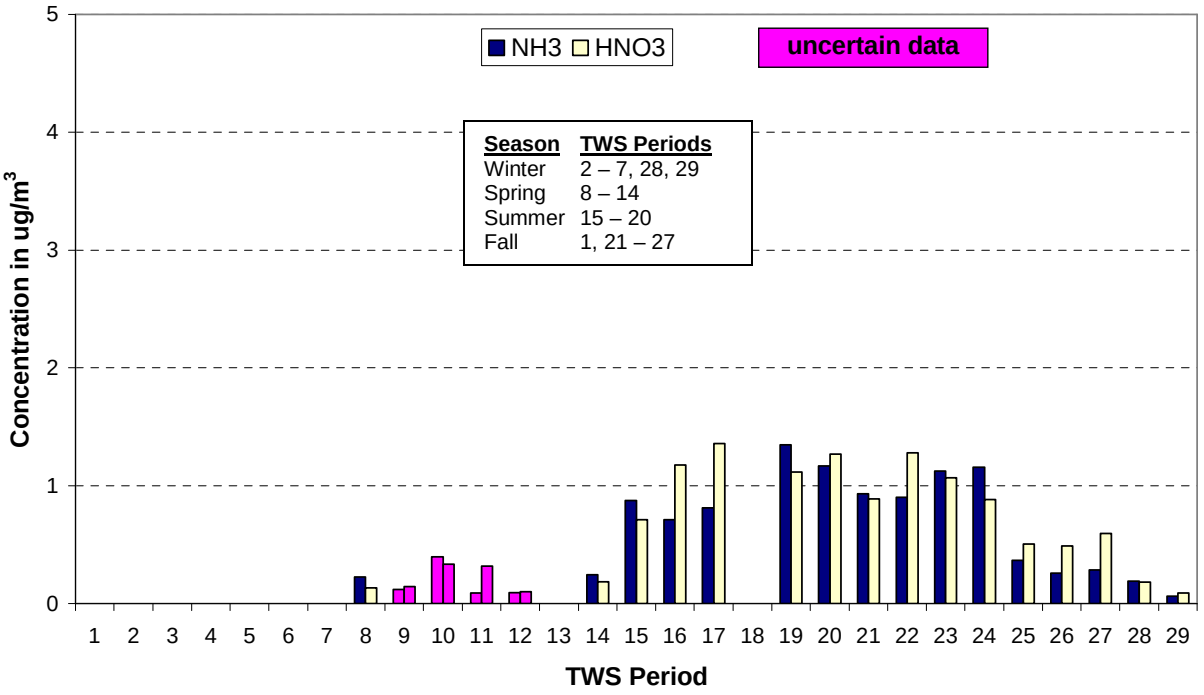

Figure 3-26b. Ammonia and Nitric Acid Concentrations Observed with the TWS at SLT-Sandy Way.

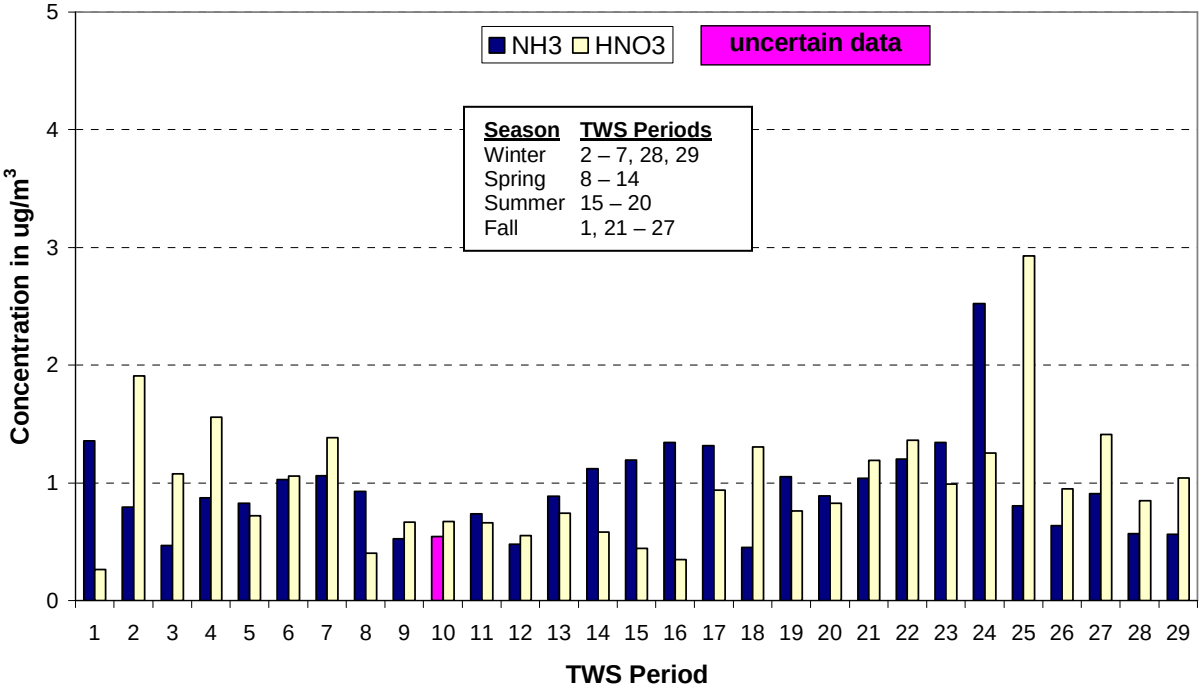

Figure 3-26c. Ammonia and Nitric Acid Concentrations Observed with the TWS at SLT-SOLA**.**

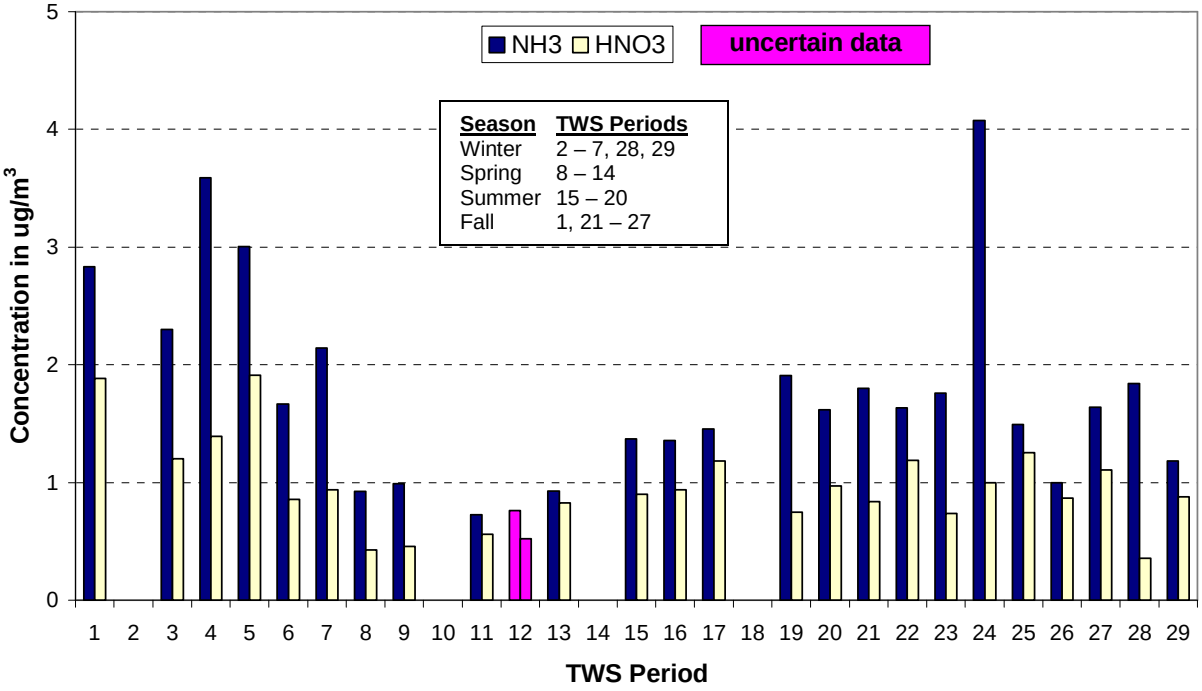

Figure 3-26d. Ammonia and Nitric Acid Concentrations Observed with the TWS at Thunderbird Lodge.

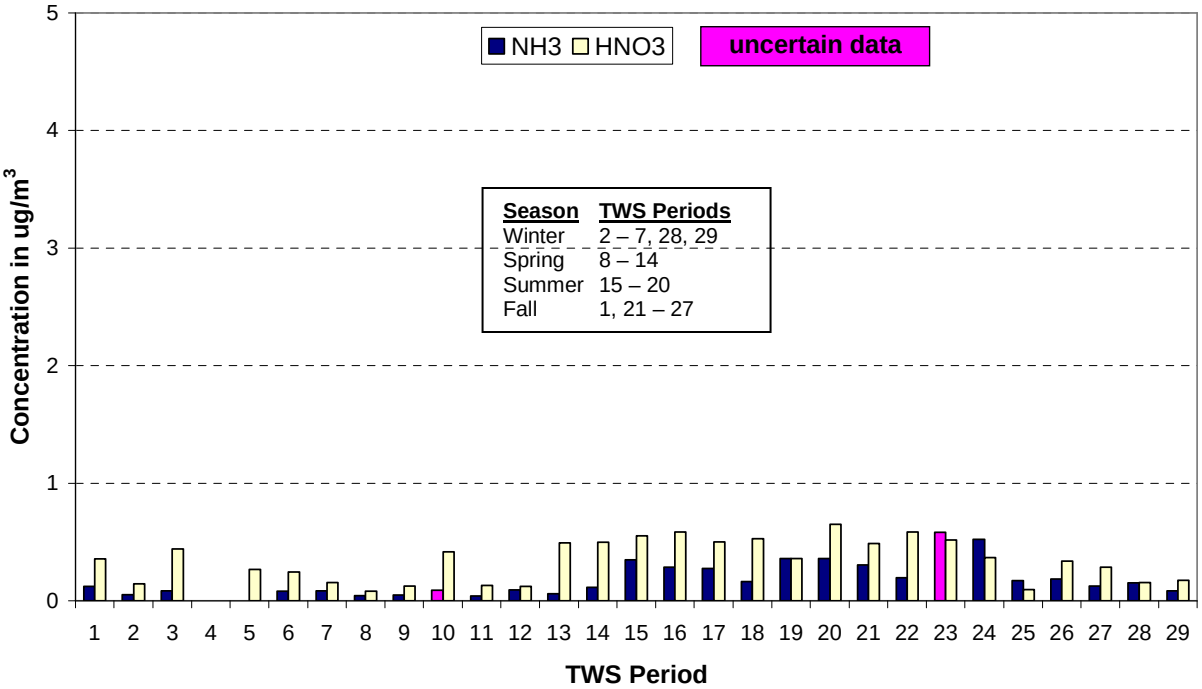

Figure 3-26e. Ammonia and Nitric Acid Concentrations Observed with the TWS at Lake Forest.

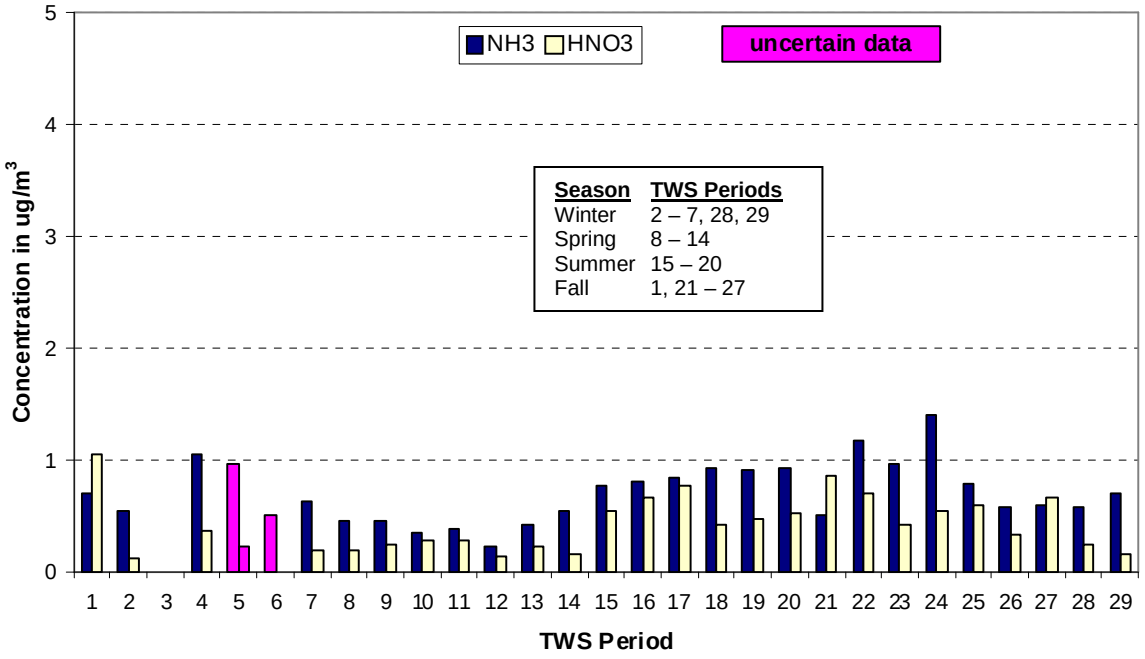

Difficulties in accurately measuring nitric acid were significantly enhanced due to positive artifacts for denuder samplers, and large uncertainties in the denuder method for the low ambient nitric acid concentrations present at all the LTADS sites. Denuder measurements can be biased upwards by conversion of nitrous acid into nitric acid within the denuder, and they also have significant uncertainties in nitric acid collection efficiency at low concentrations, in laboratory extraction efficiency, and the whole analytical process suffers from occasional high blank values. These uncertainties are usually small compared to ambient nitric acid levels in the urban areas where this technology was developed, but at very low concentrations, such as those in the Lake Tahoe Basin, they presented substantial challenges to achieving high data quality.

Review and analysis of the TWS data identified several occasions when nitric acid data were atypically low and deemed suspect. DRI reviewed the laboratory calculations, identified errors, and corrected the suspect values.

Gaseous nitrogen species were also measured using laser-induced fluorescence (LIF) at the Big Hill site by a research group from UC Berkeley. These measurements included alkyl nitrates, peroxy-acetyl nitrates, nitrogen dioxide, and nitric acid. Thus, measurements of nitrates and nitric acid by the LIF and TWS could be compared.

Thermal stability is of critical importance to LIF operations and generating high quality data. For a substantial amount of time at Big Hill, the power failed and the LIF unit was off line leading to difficulties in maintaining thermal stability. DRI has completed their QC work on the denuder database, while UC Berkeley believes that further work is

required to compare the two sets of data. Nevertheless, **Figure 3-27**, which compares data from the LIF and the TWS denuder (uncertainty bars represent the range of hourly concentrations), provides some confidence in the methods once operations stabilized by summer.

A review of the TWS ammonia data indicated fewer problems than was seen with nitric acid. Thus, the TWS-based seasonal and annual ammonia estimates are thought to be more reliable. Gaseous nitrogen measurements with the TWS are summarized in **Table 3-13**.

Using the ammonium nitrate equilibrium, ammonia concentrations, ambient temperature, and relative humidity, it is possible to estimate the dissociation constant K and consequently one could estimate nitric acid concentrations from the following equations (Stelson and Seinfeld, 1982):

$K = P_{HNO3} \times P_{NH3}$

$\text{Ln } K = 84.6 - (24{,}220/T) - 6.1\text{Ln } (T/298)$,

where T = Temperature in degrees Kelvin and RH is lower than 62%. The dissociation constant, K, is in units of $(\text{ppbV})^2$.

Table 3-13. Gaseous nitrogen from the LTADS TWS network.

Lake Tahoe Atmospheric Deposition Study Nitrogen Total Gas, Nitric Acid, Ammonia (ug/m^3)							
	Nitrogen Gas (N)					Nitric Acid	Ammonia
Site	Winter	Spring	Summer	Fall	Study Average	(Mass)	(Mass)
Big Hill	0.22	0.76	1.95	1.52	1.33	0.65	0.57
Lake Forest	0.93	0.67	1.17	1.20	0.97	0.47	0.67
Sandy Way	1.47	1.24	2.83	1.94	1.63	1.00	0.95
SOLA	2.73	1.38	1.88	2.30	2.13	0.96	1.73
Thunderbird	0.32	0.47	0.82	0.67	0.57	0.34	0.18
Maximum Basinwide (excludes Big Hill)					3.58	2.93	4.08
2nd Maximum Basinwide (excludes Big Hill)					3.26	1.91	3.59
Average Basinwide (excludes Big Hill)					1.32	0.69	0.88
Median Basinwide (excludes Big Hill)					1.30	0.71	0.81
Minimum Basinwide (excludes Big Hill)					0.04	0.08	0.00

However, a two-week sampling period invalidates the ammonium nitrate equilibrium assumption. Average two-week temperature and relative humidity data do not adequately describe second-to-second temperature and relative humidity profiles that likely govern nitric acid and ammonia concentrations, even if the ammonium nitrate equilibrium held. The 1997 Southern California Ozone Study data suggested that theoretical K values ought to consider dilution and the aerosol matrix of surfaces where ammonium nitrate reactions might take place. LTADS data do not include sufficient

time resolution and sufficient aerosol matrix and plume dilution information necessary for proper assessment of K.

As noted earlier, hourly concentration profiles are needed for integration with hourly meteorological data to estimate atmospheric deposition. Hourly BAM data were used to apportion the PM data. For nitric acid, the diurnal profile was estimated using gaseous NO_Y-NO_X concentration differences from South Lake Tahoe station at Sandy Way. Total reactive nitrogen (i.e., NO_Y) includes total oxides of nitrogen (i.e., NO_X) plus such species as peroxy acetyl and other organic nitrates, as well as, nitric and nitrous acids. Formulation of diurnal profiles presumes that nitric acid (plus nitrous acid, the positive artifact of nitric acid measurements) well exceeds other constituents of NO_Y. The seasonal mean diurnal HNO_3 concentrations are shown in **Figure 3-28**. Based on limited data from the day/night TWS denuder samples and no method during LTADS to estimate hourly concentrations of ammonia, no diurnal variation was assumed for ammonia concentrations.

3.2.2.2 LTADS vs. Other Tahoe Basin N-species Reports

Tarnay collected denuder gaseous nitric acid and ammonia data at remote forested locations in Bliss State Park and a high alpine forest near Incline Village (**Table 3-14**). Ammonium nitrate data reported in Tarnay *et al.* (2001) is from the IMPROVE network's Bliss site and is thus most relevant to rural, elevated, undeveloped regions of Tahoe Basin. In 2002, Tarnay expanded the network to several other stations but still only covered the summer months (July-September).

Please note that the different sampling years indicated opposite day/night relationships for ammonia. This is most likely the product of the difficulties we have noted in gaseous N species measurements using denuders. Nitric acid concentrations observed during LTADS are in the range of those reported by Tarnay *et al.* (2001 and 2003). However, despite similar sampling protocols, LTADS observed substantially higher ammonia concentrations than were reported by Tarnay *et al.* (2003). LTADS also reported substantially higher ammonium nitrate concentrations than those reported from IMPROVE network for Bliss State Park and at SOLA, for summer and fall seasons of 1990-96. LTADS data from the remote site at Bliss however do agree with ammonium nitrate concentrations reported by Tarnay *et al.* (2001).

Zhang *et al.* (2002) reported limited aircraft sampling in and near the Tahoe Basin. These show a wide range, but are within the range of LTADS reported concentrations. Note that ammonium plus ammonia concentrations reported in aircraft measurements are between LTADS reported median and maximum values (**Table 3-15**).

Figure 3-27. Comparison of nitric acid at Big Hill between LIF & Denuder Methods.
Note: Lighter colors represent the LIF measurements.

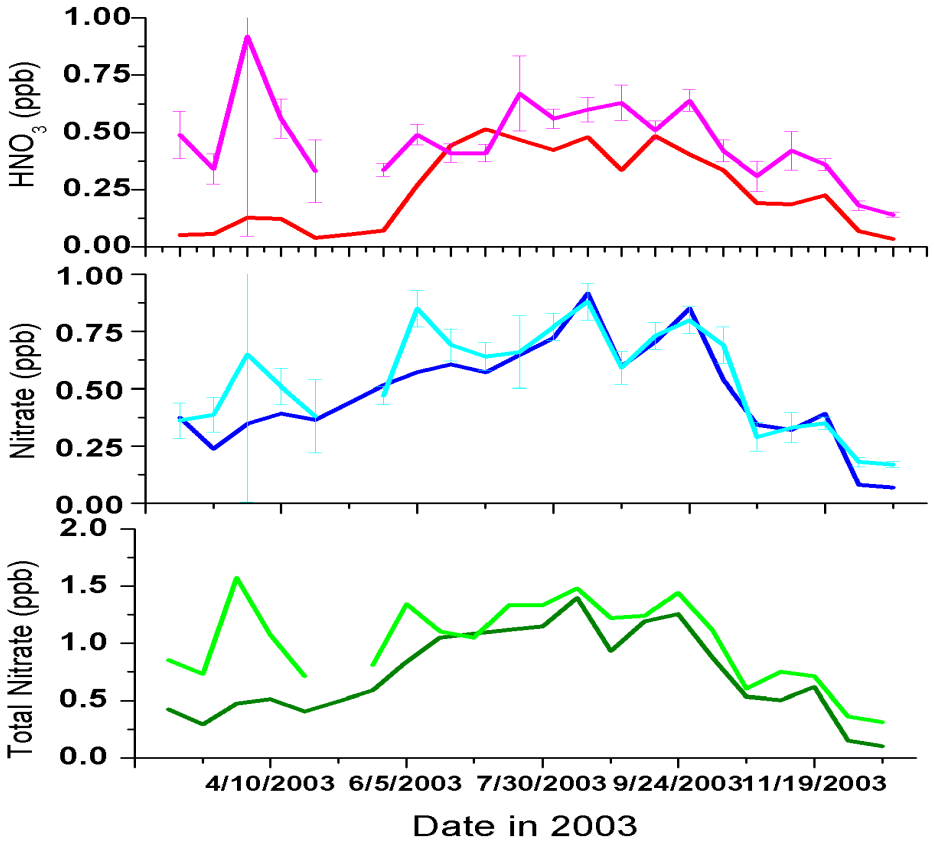

Figure 3-28. Estimated seasonal diurnal profiles of nitric acid (HNO_3) developed from NO_Y and NO_X measurements at SLT – Sandy Way monitoring station. The estimate method may include small amounts of nitrous acid (HONO) and nitrates (NO_3^-).

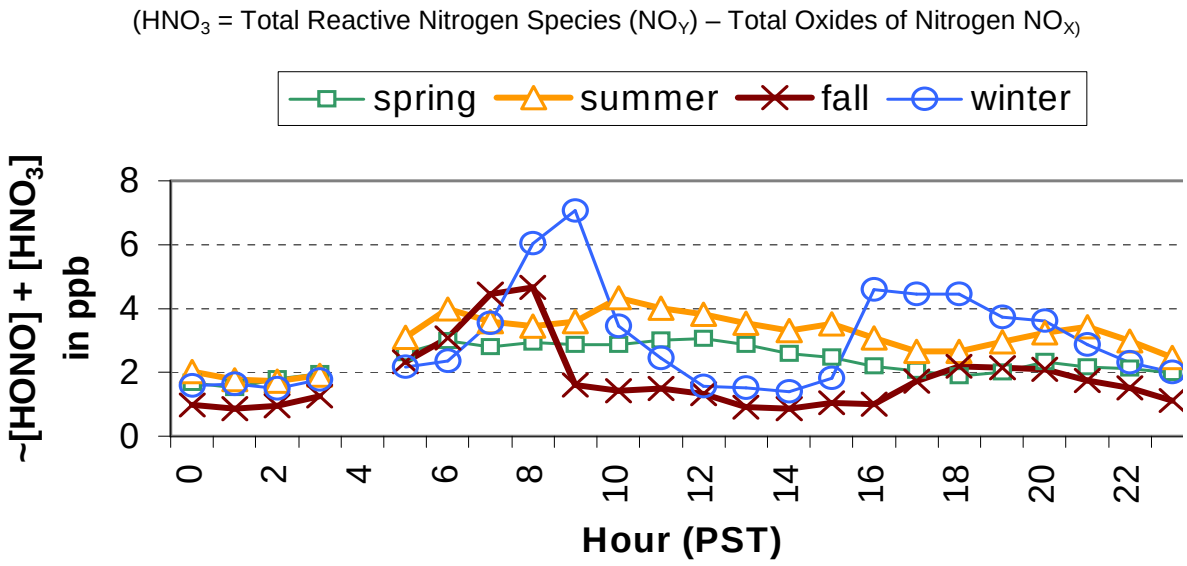

Table 3-14. Nitrogen-specie measurements as reported by Tarnay and LTADS.

Nitrogen Specie	Concentrations (ng N/m^3) observed by:				
	Tarnay during summers (2001 / 2002) in alpine forests near Bliss State Park & Incline Village			LTADS annual (2003)	
	Day	Night	Mean	Median	Maximun
HNO_3	364 / 238	154 / 182	234	127	651
NH_3	280 / 294	686 / 140	350	634	3,360
NH_4NO_3 @ Bliss	101*	101*	101*	49**	107**

* from IMPROVE PM2.5 during summer and fall of 1990-1996

** based on only 6 samples (collected between 9/18/03 – 12/16/03)

Carroll *et al*. (2003) performed detailed air and boat sampling over and on Lake Tahoe in coordination with LTADS. They noted high blank values and other analytical difficulties that the TWS also encountered. Nevertheless, using averages of the ensemble of denuder filter pack samples, it appears that ammonia increased slightly with height above the lake while nitric acid gas decreased slightly with height. The ammonium nitrate and gaseous nitrogen concentration range from Carroll *et al*. (2003) are between TWS reported median and maximum values. Please also note that ammonia fraction of nitrogen species from Carroll et al. (2003) and the TWS agree quite well.

Table 3-15. Aircraft measurements of nitrogen-species over Lake Tahoe during summer/fall seasons.

Nitrogen Specie	Concentrations (ng N/m^3) observed by:				
	Zhang (2001)[1]	Carroll (2002)[2]		LTADS (2003)	
	Mean	Minimum	Maximum	Median	Maximun
HNO_3 (g) + NO_3^- (p)	420	---	---	290	939
NH_3 (g) + NH_4^+ (p)	1330	---	---	1,015	3,492
ON (g) + ON (p)	210	---	---	---	---
TN (g)+(p)	1,960	---	---	1,278	3,843
NH_4NO_3	---	84	714	270	1,010
TN (g)	---	364	4,310	775	3,579
NH_3 fraction of TN	---	55%		51%	

[1] based on three samples from *Zhang et al.* (2002)

[2] based on *Carroll et al.* (2003)

3.2.2.3 Seasonal Concentration Profiles by Specie

Both the dry and wet LTADS deposition estimates were generated from ambient concentrations. The ambient concentrations used as the basis of the deposition estimates are presented in **Table 3-16**. Concentrations tend to be higher in the more urbanized locations with season of peak concentrations depending on the pollutant specie. Concentrations at Big Hill tend to be highest in summer and fall when upslope air flow transports pollutants into the Sierra Nevada. The northern portion of the Tahoe Basin also tends to have the highest concentrations during summer and fall when soils are drier and activities are greater. In the southern portion of the basin, concentrations tend to be higher in winter and fall when the air is more stable and the down slope flows that collect the urban emissions persist longer.

Table 3-16. Seasonal average concentrations (ng/m^3) of particulate matter, nitrogenous species, and phosphorus as observed during LTADS.

Site	Network	Parameter	Winter	Spring	Summer	Fall	Annual*
Big Hill	TWS	HNO_3	135	196	1009	816	*646*
Lake Forest	TWS	HNO_3	214	229	470	647	390
SLT-Sandy Way	TWS	HNO_3	1201	617	1075	1294	1047
SLT-SOLA	TWS	HNO_3	1136	548	940	1111	934
Thunderbird Lodge	TWS	HNO_3	227	228	525	379	340
Big Hill	TWS	NH_3	127	182	892	719	*574*
Lake Forest	TWS	NH_3	708	373	767	835	671
SLT-Sandy Way	TWS	NH_3	773	684	1060	1227	936
SLT-SOLA	TWS	NH_3	2286	868	1506	2029	1672
Thunderbird Lodge	TWS	NH_3	77	62	290	277	177
Big Hill	TWS	NH_4	50	428	789	552	*548*
Bliss SP	MVS	NH_4	56			144	*129*
Buoy TB1 (east)	MVS	NH_4	254	383	349	421	*329*
Buoy TB4 (west)	MVS	NH_4	233	367	313	364	*304*
Lake Forest	TWS	NH_4	210	260	377	297	286
LF_Coast Guard	MVS	NH_4	112	192	264	195	191
SLT-Sandy Way	TWS	NH_4	456	438	520	496	478
SLT-SOLA	TWS	NH_4	400	411	443	382	409
Thunderbird Lodge	TWS	NH_4	160	336	412	287	299
Timber Cove	MVS	NH_4	278	344	192		*298*
Wallis Pier	MVS	NH_4	57	190	259	184	173
Wallis Tower	MVS	NH_4	44	163	289	182	170
Zephyr Cove	MVS	NH_4	97	324	400	213	259
Big Hill	TWS	NO_3	192	936	1691	1394	*1254*
Bliss SP	MVS	NO_3	129			206	*193*
Buoy TB1 (east)	MVS	NO_3	607	617	286	427	*503*
Buoy TB4 (west)	MVS	NO_3	571	582	197	438	*450*
Lake Forest	TWS	NO_3	404	475	656	617	538
LF_Coast Guard	MVS	NO_3	253	192	96	173	179
SLT-Sandy Way	TWS	NO_3	934	894	1137	1155	1030
SLT-SOLA	TWS	NO_3	949	862	855	1012	920
Thunderbird Lodge	TWS	NO_3	342	471	729	577	530
Timber Cove	MVS	NO_3	418	317	275		*368*
Wallis Pier	MVS	NO_3	128	221	122	196	167
Wallis Tower	MVS	NO_3	112	215	129	161	154
Zephyr Cove	MVS	NO_3	286	437	185	277	296
Big Hill	TWS	P	40	40	40	40	40
Bliss SP	MVS	P	40	40	40	40	40
Buoy TB1 (east)	MVS	P	40	40	40	40	40
Buoy TB4 (west)	MVS	P	40	40	40	40	40
Lake Forest	TWS	P	40	40	40	40	40

Site	Network	Parameter	Winter	Spring	Summer	Fall	Annual
LF Coast Guard	MVS	P	40	40	40	40	40
SLT-Sandy Way	TWS	P	40	40	40	40	40
SLT-SOLA	TWS	P	40	40	40	40	40
Thunderbird Lodge	TWS	P	40	40	40	40	40
Timber Cove	MVS	P	40	40	40	40	40
Wallis Pier	MVS	P	40	40	40	40	40
Wallis Tower	MVS	P	40	40	40	40	40
Zephyr Cove	MVS	P	40	40	40	40	40
Big Hill	TWS	PM10	1810	5526	12142	9859	*8672*
Lake Forest	TWS	PM10	15835	11708	13852	13907	13826
SLT-Sandy Way	TWS	PM10	21829	12719	13324	17734	16402
SLT-SOLA	TWS	PM10	24424	13080	17460	17582	18137
Thunderbird Lodge	TWS	PM10	3311	4523	9120	6198	5788
Big Hill	TWS	PM2.5	1357	3735	6602	4962	*4821*
Lake Forest	TWS	PM2.5	5032	2981	6142	4789	4736
SLT-Sandy Way	TWS	PM2.5	10154	4889	7111	9772	7982
SLT-SOLA	TWS	PM2.5	8963	3982	7049	8238	7058
Thunderbird Lodge	TWS	PM2.5	2341	2446	5800	3745	3583
Big Hill	TWS	TSP	3163	6429	16120	13559	*11484*
Bliss SP	MVS	TSP	3600			6414	*5945*
Buoy TB1 (east)	MVS	TSP	4725	9866	7757	6389	7184
Buoy TB4 (west)	MVS	TSP	4909	9029	7871	8028	*7270*
Lake Forest	TWS	TSP	17574	16183	19562	18155	17869
LF_Coast Guard	MVS	TSP	8170	8914	15263	7760	10027
SLT-Sandy Way	TWS	TSP	29279	15779	18628	20770	21114
SLT-SOLA	TWS	TSP	29929	15148	17635	21971	21171
Thunderbird Lodge	TWS	TSP	3640	4738	9120	6528	6007
Timber Cove	MVS	TSP	9826	3840	10535		*8167*
Wallis Pier	MVS	TSP	19230	5422	14513	8579	11936
Wallis Tower	MVS	TSP	17666	10810	12469	12110	13264
Zephyr Cove	MVS	TSP	8575	10318	21602	14971	13867

* The annual mean is the average of the seasonal means. In cases when the seasonal mean is based on incomplete data (potentially non-representative mean), the cell has been highlighted in yellow. The annual mean for the pollutants with incomplete data is based on the median result of the 4-season mean, the mean of the representative seasons, and the average of all individual samples. The annual means not represented by the 4-season mean are presented in italicized blue font.

3.2.2.4 Temporal and Spatial Variations in Ozone

Ozone was not a primary pollutant of interest in LTADS. However, ozone is a pollutant of concern in many areas of California. Although the Tahoe Basin is currently in attainment of the national 1-hour and 8-hour and the California 1-hour ambient air quality standards, its air quality does exceed the TRPA threshold for forest health (1-hr

average, 0.070 ppm). In addition, ozone concentrations in the Tahoe Basin have historically exceeded the concentration level associated with the recently adopted California 8-hour health-based standard. During LTADS, ozone was monitored at two new locations (Big Hill and Lake Forest) and at four long term monitoring sites (Echo Summit and SLT – Sandy Way in California; Cave Rock and Incline Village in Nevada). The various ozone ambient air quality standards applicable in the Tahoe Basin and a summary of the ozone concentrations observed during 2003 are presented in this section.

Various governmental authorities have established ozone air quality standards/thresholds to protect health and welfare in the Lake Tahoe Air Basin. The averaging periods and concentration levels are illustrated in **Figure 3-29**. Note that the State of California recently adopted an 8-hour standard in addition to its current 1-hour standard. Both of the California standards are more stringent than the National standards. These standards are established to protect public health. The Tahoe Regional Planning Agency has adopted an environmental threshold to protect forest health. As shown in **Figure 3-29**, the TRPA ozone threshold (1-hour not to exceed 0.08 ppm) is the most restrictive standard applicable to the Tahoe Basin. Because 1-hour concentrations infrequently exceed the TRPA threshold (equivalent to 80 ppb), a 70 ppb cutpoint was used in several analyses to assess the frequency, timing, and spatial distribution of high ozone concentrations.

To provide a regional context of the ozone concentrations downwind of the Sacramento metropolitan area, the maximum 1-hour and 8-hour average ozone concentrations observed in the central Sierra Nevada are shown in **Figure 3-30**. The ozone plume downwind of Sacramento typically achieves its maximum concentrations in the foothills of the Sierra Nevada (e.g., Folsom, Placerville, Auburn). As illustrated in **Figure 3-30**, peak 1-hr ozone concentrations drop off significantly by the time the plume reaches the Sierra (Big Hill at 6155' elevation) and more by the crest of the Sierra (Echo Summit at 7382' elevation). The peak 1-hour concentrations in the Tahoe Basin were comparable to that observed at the crest (i.e., Echo Summit). The peak 8-hour concentrations decline most between Big Hill and Echo Summit. The maximum 8-hr ozone concentrations observed within the Basin were comparable and slightly lower than at Echo Summit, perhaps due in part to local emissions of nitric oxide (NO), which suppresses (initially) ozone concentrations.

The number of days when ozone concentrations at different sites exceeded the 1-hr California Ambient Air Quality Standard (CAAQS) (95 ppb) and the 8-hr National Ambient Air Quality Standard (NAAQS) for ozone during 2003 decreased even more dramatically than peak concentrations (**Figure 3-31**). Neither of the standards was exceeded at Echo Summit or within the Tahoe Basin. **Figure 3-31** illustrates that the Sacramento ozone plume does not transport intact high into the Sierra. In fact, the light winds associated with high ozone episodes in the Sacramento Valley seldom transport the polluted air in the surface layer far into the Sierra before the slopes cool in the evening and downslope airflow develops. The more likely scenario is that warm air

rising above the western slopes of the Sierra mixes the ozone into a deeper volume of air and increasing the regional background concentration of ozone.

Because the frequency of ozone concentrations exceeding the NAAQS or the CAAQS is so low in the LTADS study area, the counts of hours when 1-hr ozone concentrations exceeded 70 ppb, the TRPA threshold (80 ppb), and California standard (95 ppb) during 2003 are shown in **Figure 3-32** for the monitoring sites in the Sierra. The 1-hour CAAQS was not exceeded within the Tahoe Basin during 2003. In fact, the Lake Tahoe Air Basin is classified as attaining the CAAQS. However, the 1-hr CAAQS was exceeded on occasion at the Big Hill site, which is located ~20 miles upwind of the Tahoe Basin on the western slope of the Sierra Nevada. More significantly, the 70 ppb cutpoint and the TRPA threshold were exceeded during more than 400 and 125 hours, respectively, at the Big Hill site, which is primarily impacted by pollutants from the Central Valley. The 70 ppb cutpoint and the TRPA threshold were exceeded much less frequently (less than 100 and 10 hours, respectively) at the Echo Summit site located further east on the Sierra crest at the southwestern edge of the Tahoe Basin. Exceedances of the 70 ppb cutpoint on the floor of the Tahoe Basin declined another 70% from that at the Echo Summit site (i.e., to < 30 hours). Although South Lake Tahoe is the largest urbanized area, and presumably most polluted, in the Basin, the number of exceedances there is least because the fresh emissions of nitric oxide (NO) suppress the ozone levels.

The pattern of exceedances of the National and the new California 8-hour ozone standards (**Figure 3-33**) is similar to that of the 1-hour exceedances. The NAAQS is only exceeded at the Big Hill site upwind of the Tahoe Basin. Although the Lake Tahoe Air Basin currently attains the 1-hour CAAQS, the Basin will be designated as a non-attainment area because ozone concentrations within the Basin exceeded the new California 8-hour standard of 0.070 ppm on 7 days alone in 2003 at the Echo Summit site. As with the 1-hour exceedances, the 8-hour standard is exceeded about 10 times more often at Big Hill than at Echo Summit (62 vs. 7 days).

The number of hours when the 70 ppb cutpoint was exceeded is shown by hour of the day in **Figure 3-34** for the Big Hill and Echo Summit sites. Although ozone concentrations exceeding 70 ppb can occur essentially any hour of the day, the most prevalent period, at both sites, is in the late afternoon and early evening – past the time of peak local formation but consistent with potential transport up the Sierra slopes from the Central Valley. The much higher frequency of exceedances during these hours at Big Hill than at Echo Summit indicate that the polluted air mass once it passes Big Hill often does not arrive at Echo Summit or that the ozone concentrations are reduced below 70 ppb by the time the air arrives at Echo Summit. Both sites have minor local sources of NO, so any decrease in concentrations is due to some combination of dispersion, deposition, or advection out of the area. The high number of exceedances in the early morning hours at Big Hill is consistent with upslope air flow reversing to downslope flow and remaining on the western slope of the Sierra throughout the night. The only period of the day when the number of exceedances is comparable at the two

sites is during the late morning when both sites would experience increased vertical mixing of the atmosphere and downmixing of potentially polluted air aloft. The hourly distribution of exceedances of the 70 ppb cutpoint within the Tahoe Basin is shown in **Figure 3-35**. Most of the high ozone hours in the northern portion of the basin occur around midday when local formation would be greatest but also when vertical mixing of the air is greatest and could tap potentially high ozone concentrations transported aloft. Interestingly, the exceedances of the 70 ppb cutpoint are most frequent in the late afternoon at the Cave Rock site (east side of Lake), not unlike at the Echo Summit site in the late afternoon. High ozone concentrations during daylight hours, when photosynthesis is active and stomata are open, would have the most adverse impact on plants and trees.

The monthly distribution of ozone concentrations exceeding the 70 ppb cutpoint is shown in **Figure 3-36** for the two upwind sites and in **Figure 3-37** for the in-basin sites. Ozone concentrations can exceed the 70 ppb cutpoint during any month around summer (May – October) but are most likely during July and August at the Big Hill site. Concentrations exceeding 70 ppb at the Echo Summit site were most frequent in May and July (June to a lesser extent). In-basin exceedances of the 70 ppb cutpoint occurred between May and August with a greater tendency in May and June. It is interesting to note that the periods with the greatest frequency of exceedances of the 70 ppb cutpoint are in the late spring/early summer at the Tahoe sites; this is before the season of peak exceedances at the Big Hill site.

The diurnal variation in ozone concentrations at a trio of sites representing upwind (Big Hill), basin boundary/Sierra crest (Echo Summit), and in-basin lake level (Cave Rock) is shown by month in **Figures 3-38 through 3-41**. Unlike the two upwind sites, which are minimally impacted by local emissions, the ozone pattern at Cave Rock exhibits a dip around 7 am when fresh NO emissions associated with the morning commute drain from the highway toward the Lake and the monitor. A corresponding dip in ozone concentrations is typically not observed in the afternoon commute when winds are typically upslope (from the west) and thus the monitor “sees” the ozone before the air mass reaches the NO emissions along the highway and are depressed. Focusing on the Echo Summit data, which represent regional background ozone concentrations approaching the Tahoe Basin, the diurnal variation is very small. The ozone concentrations hover around 40 ppb during the winter and shift up to over 50 ppb during spring. The concentrations exhibit the greatest diurnal variation during summer when minimums are in the 40s and maximums approach 60 ppb. During July and August, the broad peak in concentrations reaches its maximum in the late afternoon. The ~4 ppb bump-up during these months, when the length of days and the duration of upslope air flow are longest, is consistent with the movement of polluted air into the Sierra Nevada. During fall, the diurnal range decreases and becomes stable in the low 40s by November.

Figure 3-29. Applicable ozone standards in the Lake Tahoe Air Basin.

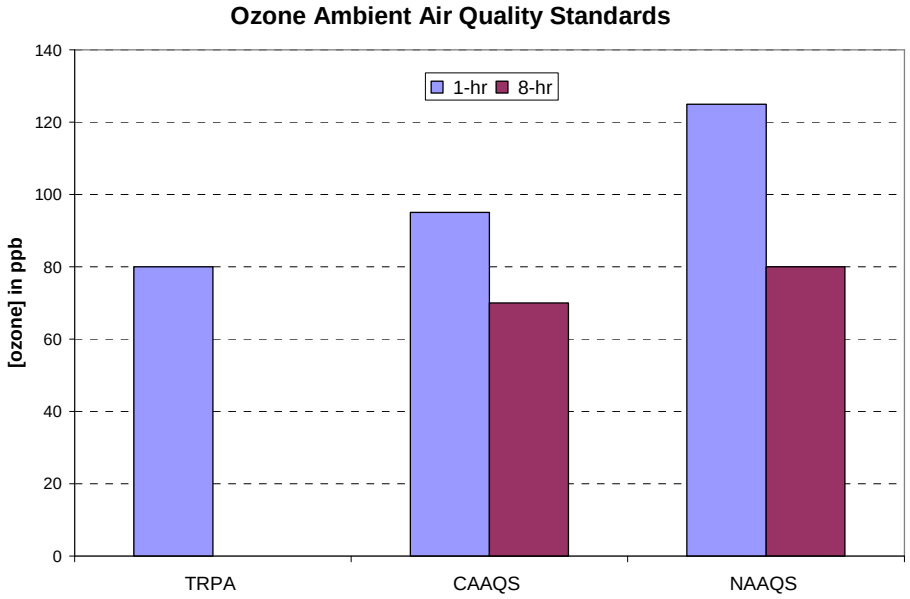

Notes:
TRPA – Tahoe Regional Planning Agency threshold to protect forest health (80 ppb for 1-hr mean)
CAAQS – California Ambient Air Quality Standards (≡95 ppb for 1-hr mean; 70 ppb for 8-hr mean)
NAAQS – National Ambient Air Quality Standard (≡125 ppb for 1-hr mean; 80 ppb for 8-hr mean)

Figure 3-30. Maximum 1-hour and 8-hour ozone concentrations observed in 2003 at locations west of and within the Lake Tahoe Air Basin.

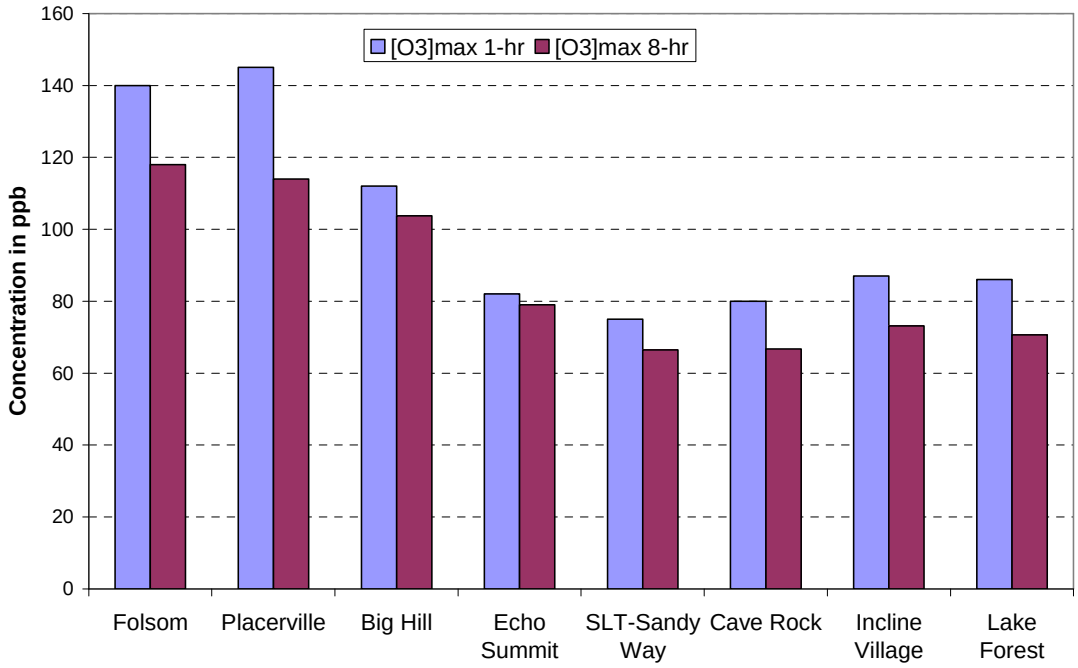

Figure 3-31. Number of days during 2003 when the California 1-hr and national 8-hr ambient air quality standards for ozone were exceeded at locations west of and within the Tahoe Air Basin.

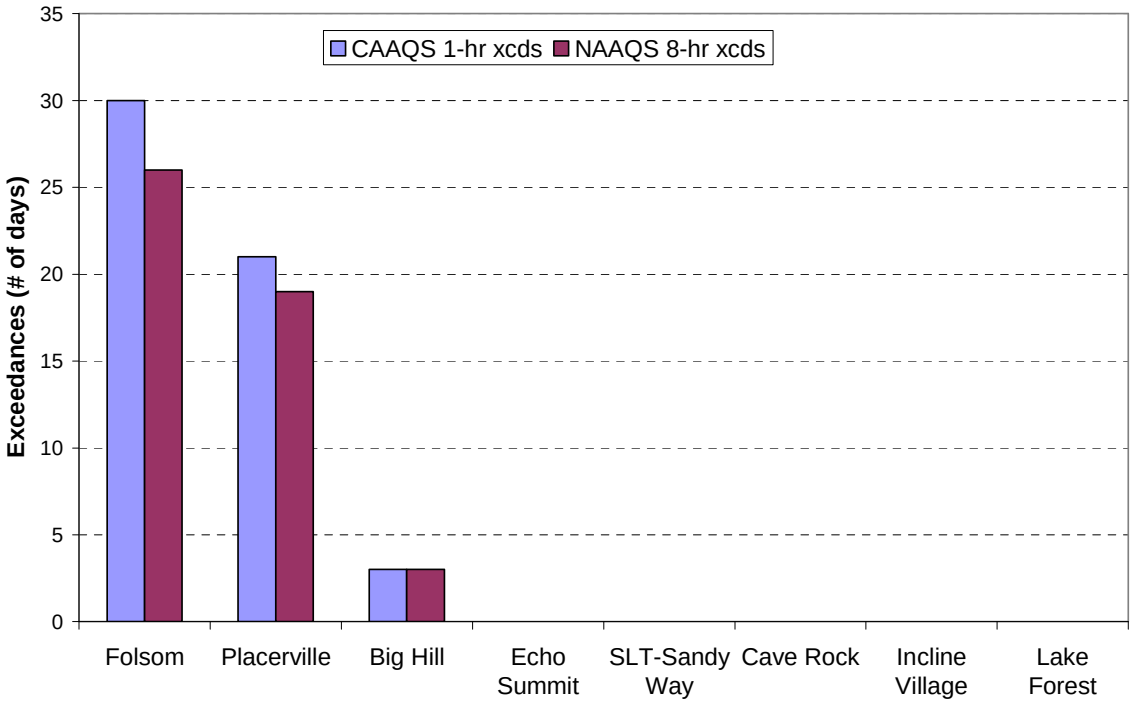

Figure 3-32. Annual total of hours during 2003 when 1-hour ozone concentrations exceeded selected cutpoints (70 ppb; TRPA threshold – 80 ppb; CAAQS – 95 ppb) at Big Hill and the five ozone monitoring sites located within the Tahoe Basin.

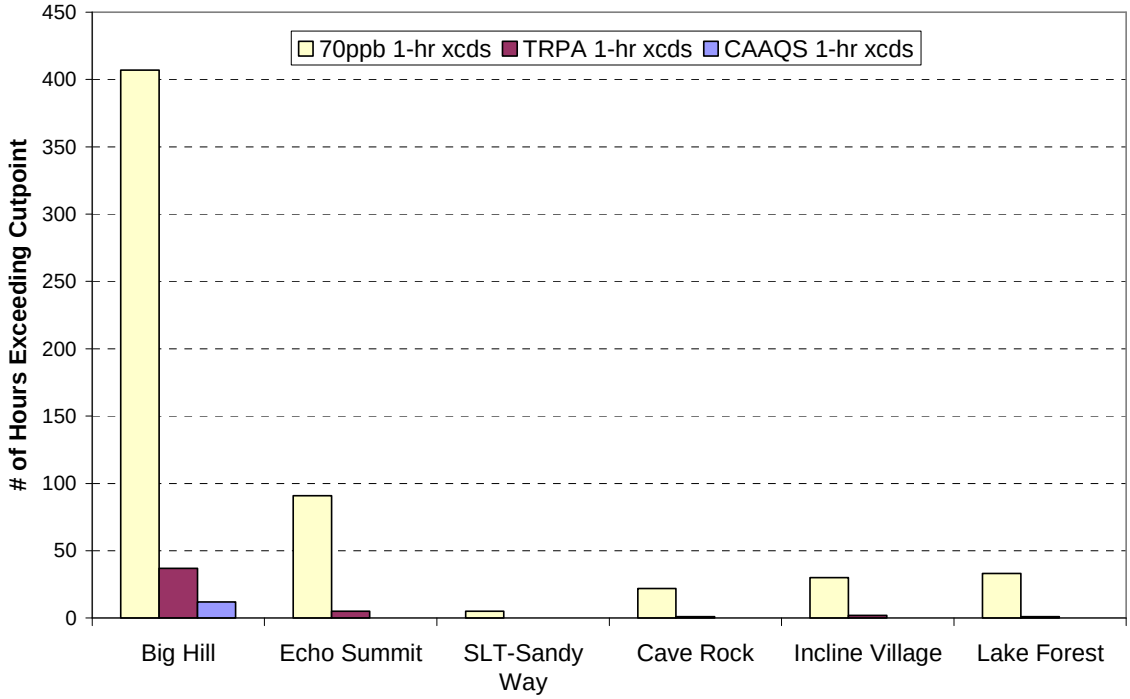

Figure 3-33. Annual number of days during 2003 when 8-hour ozone standards (CAAQS – 70 ppb; NAAQS – 85 ppb) were exceeded at Big Hill and the five ozone monitoring sites located within the Tahoe Basin.

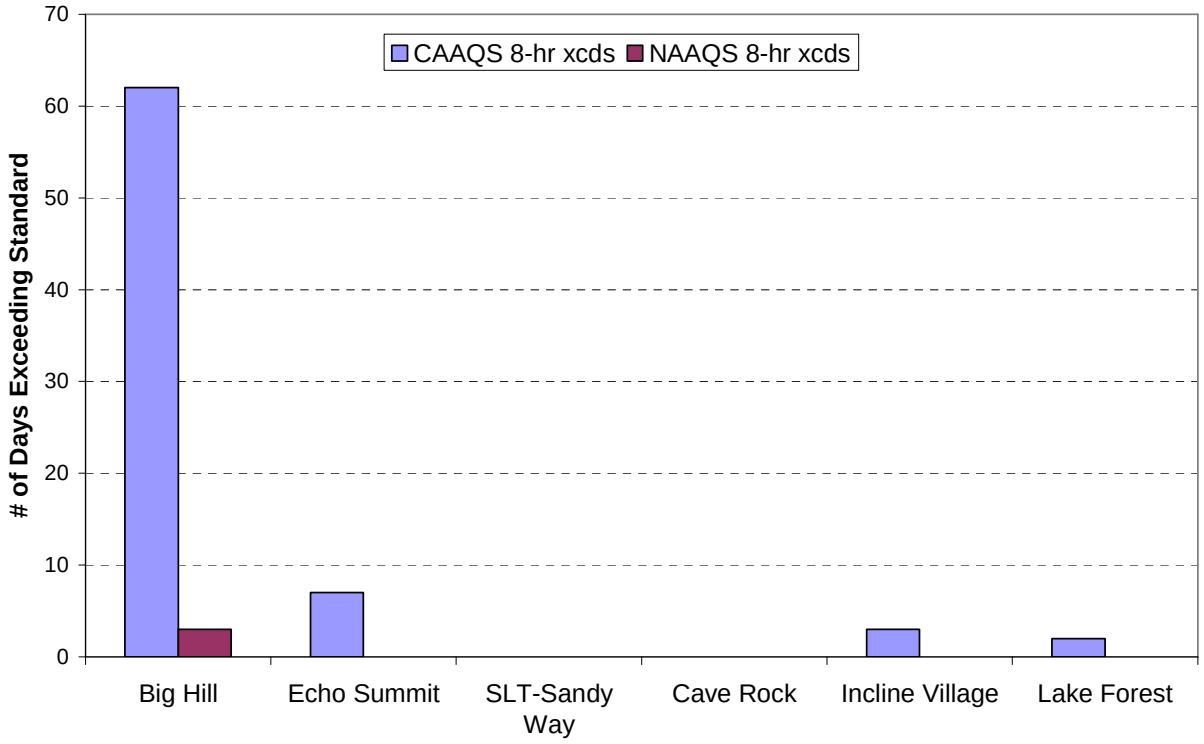

Figure 3-34. Frequency of hours during 2003 when 1-hour ozone concentrations exceeded 70 ppb at the Big Hill and Echo Summit sites.

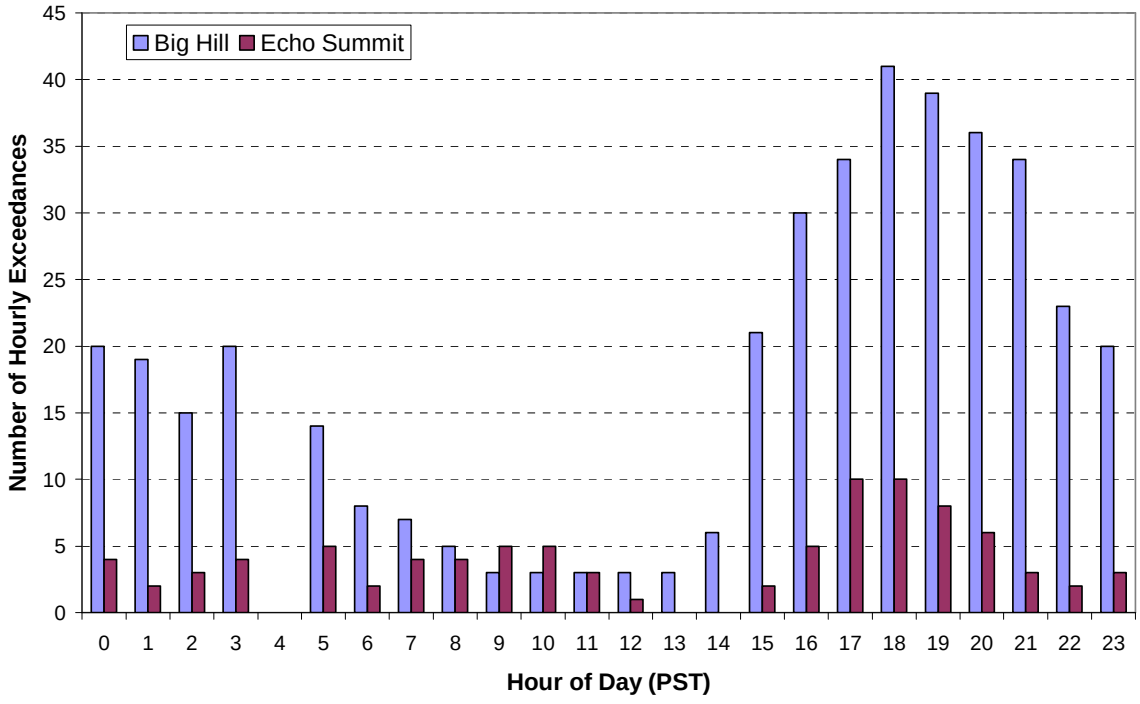

Figure 3-35. Frequency of hours during 2003 when 1-hour ozone concentrations exceeded 70 ppb at sites within the Lake Tahoe Air Basin.

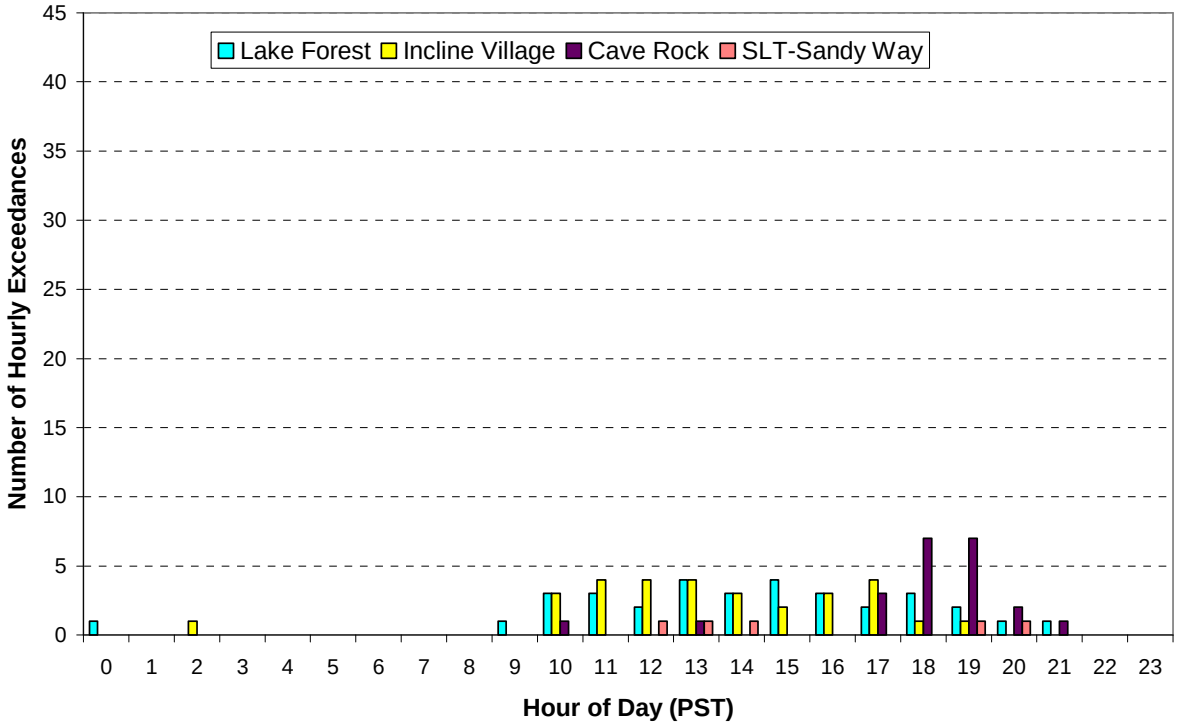

Figure 3-36. Frequency of hours by month during 2003 when 1-hour ozone concentrations exceeded 70 ppb the at Big Hill and Echo Summit sites.

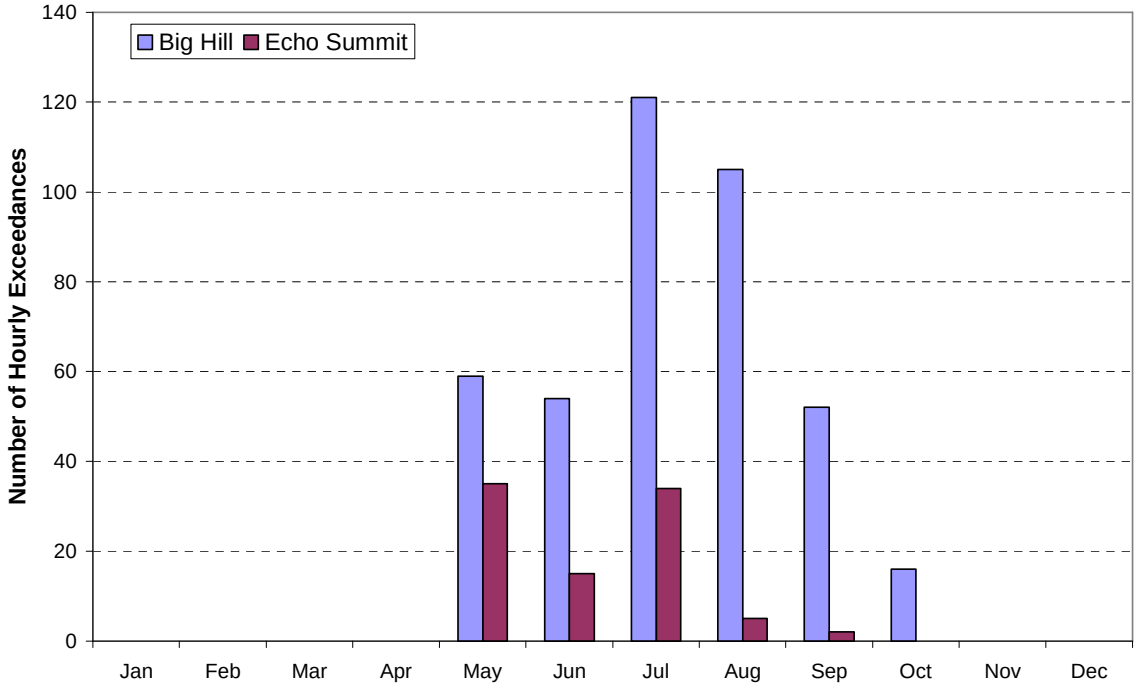

Figure 3-37. Frequency of hours by month during 2003 when 1-hour ozone concentrations exceeded 70 ppb at sites in the Tahoe Basin.

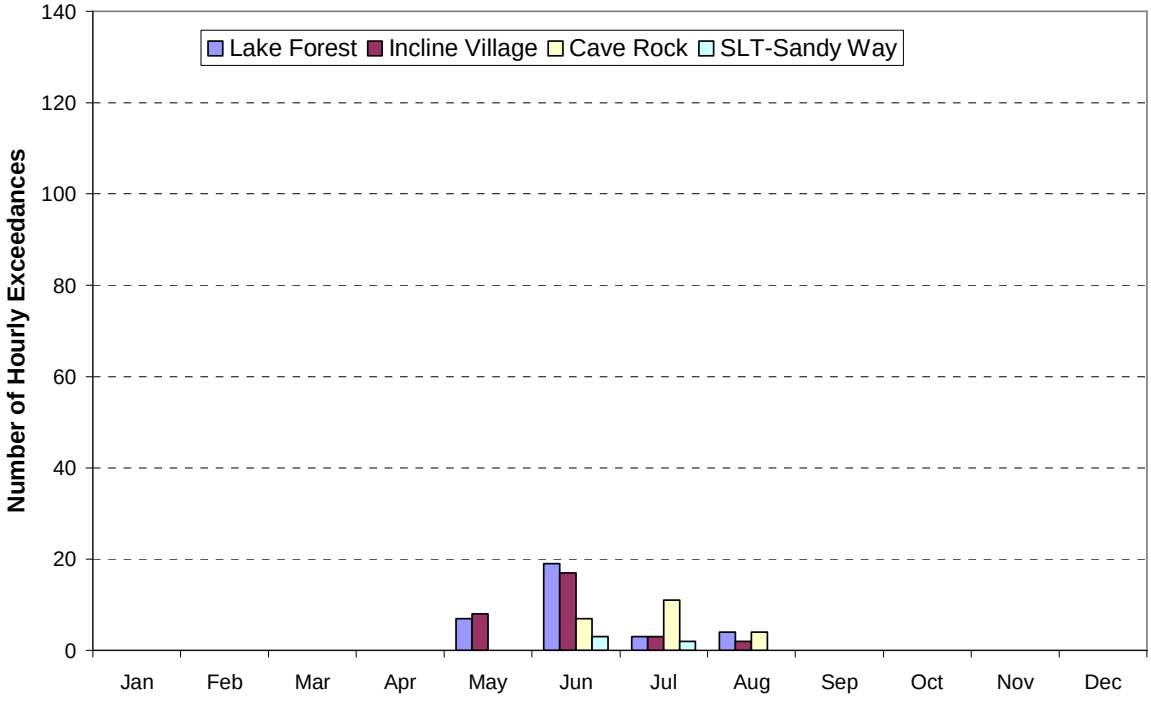

Figure 3-38. Diurnal variations in ozone concentrations during Dec, Jan, Feb (winter).

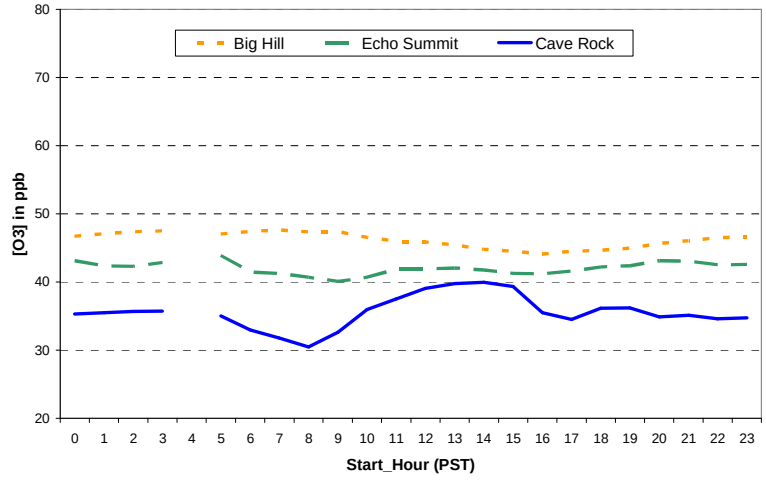

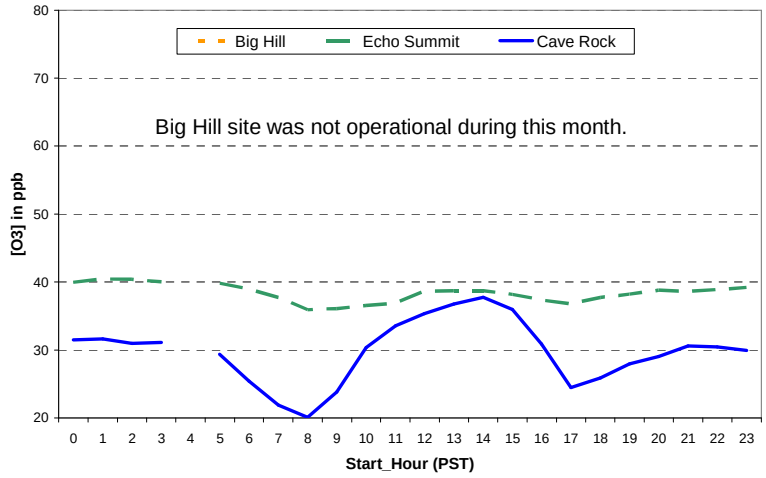

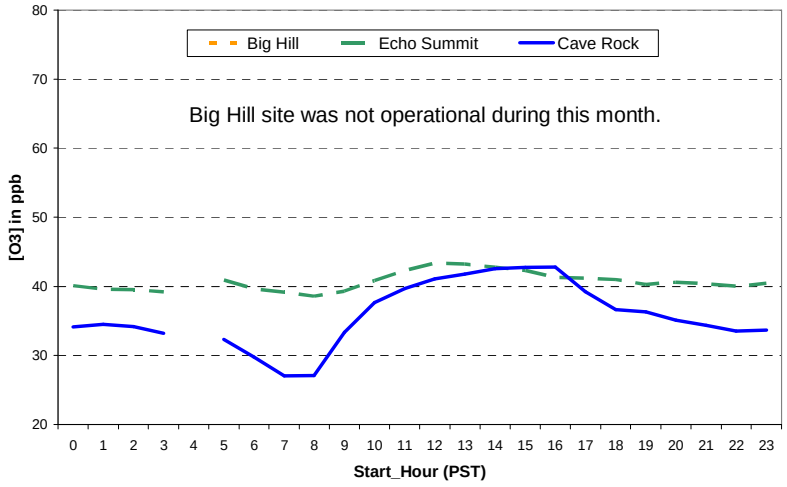

Figure 3-39. Diurnal variations in ozone concentrations during Mar, Apr, May (spring).

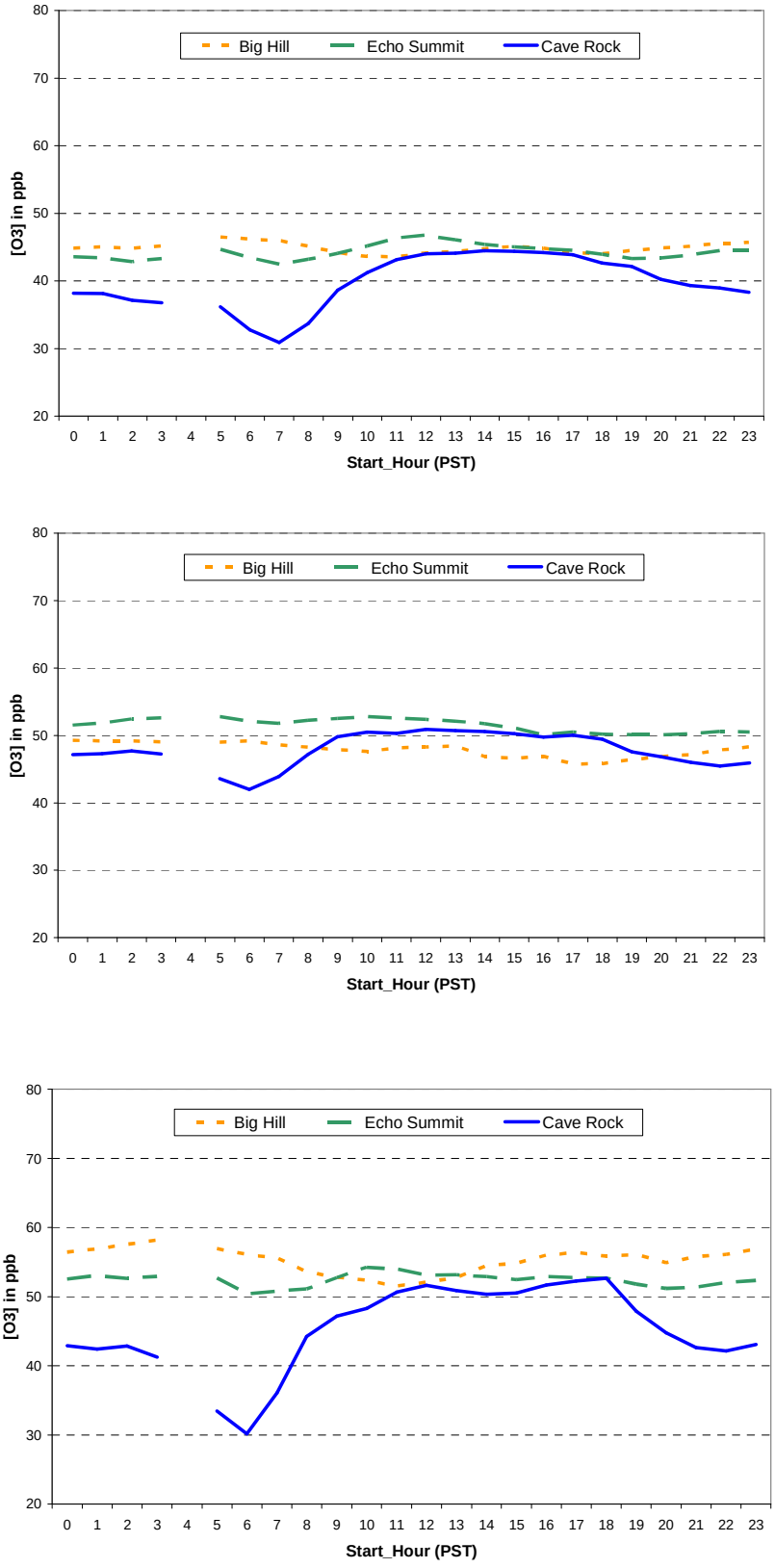

Figure 3-40. Diurnal variations in ozone concentrations during Jun, Jul, Aug (summer).

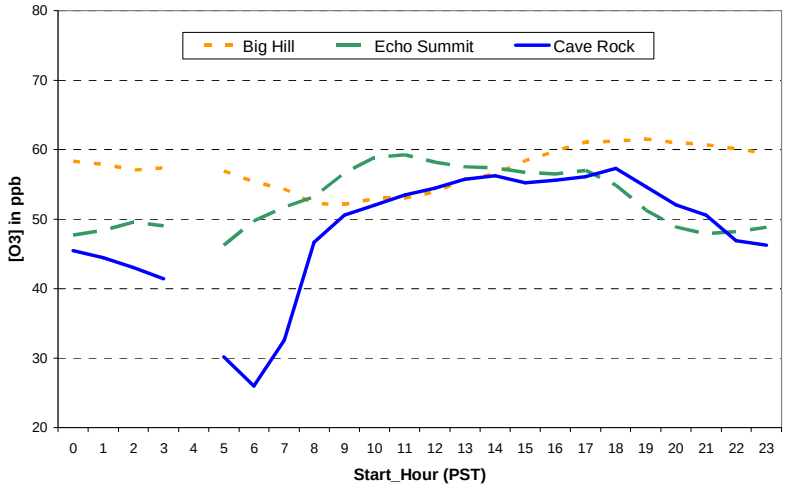

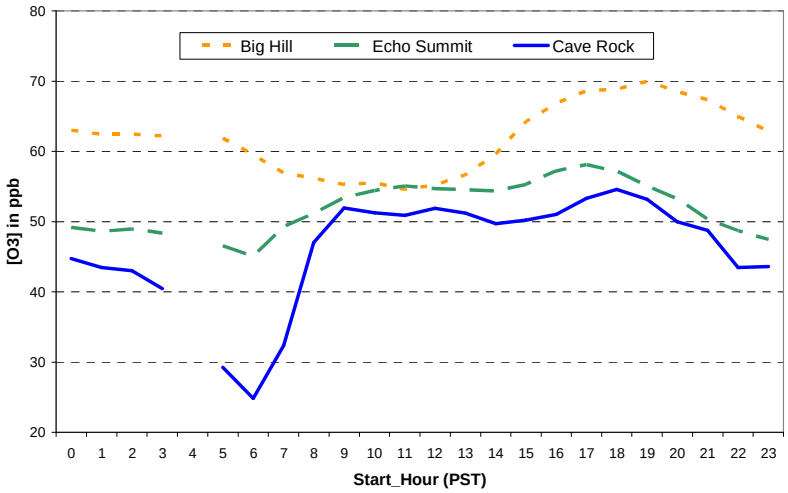

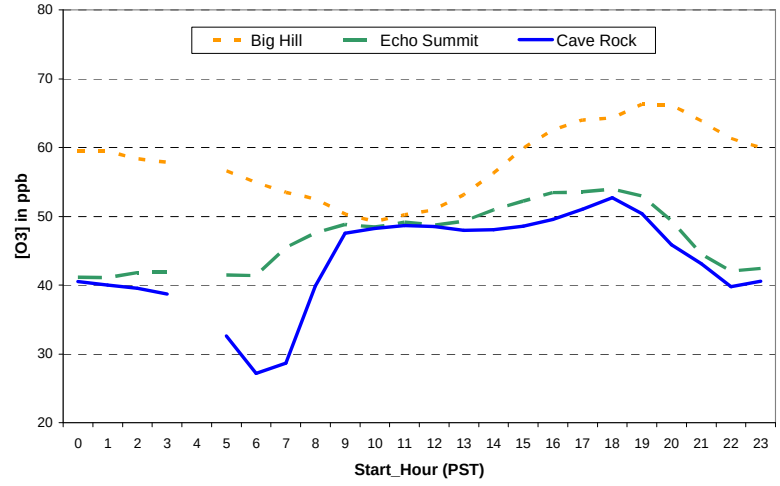

Figure 3-41. Diurnal variations in ozone concentrations during Sep, Oct, Nov (fall).

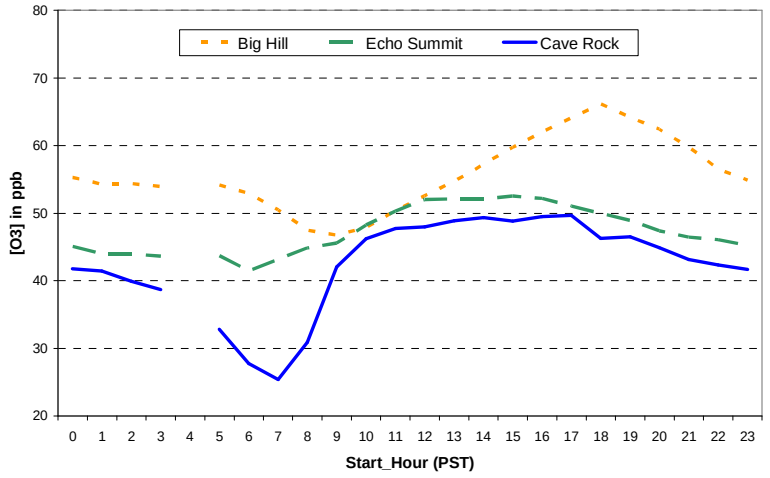

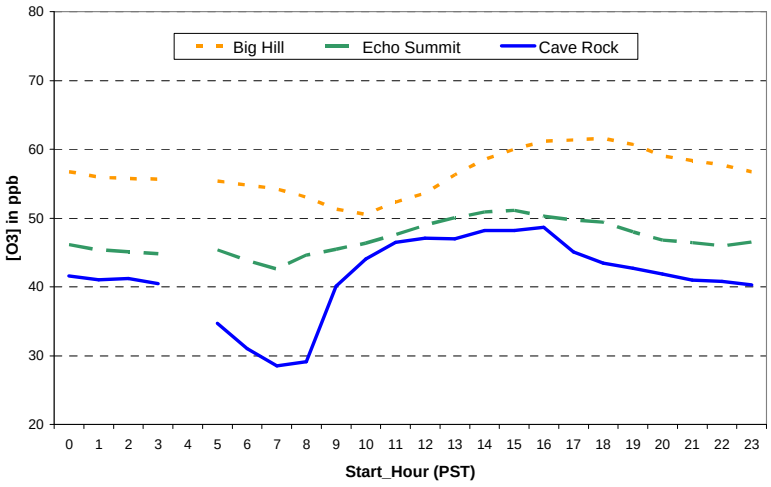

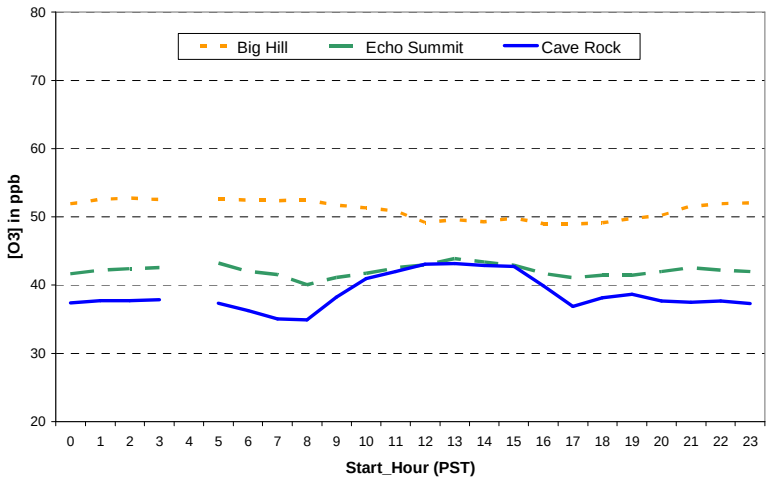

3.2.3 Total Nitrogen

Because a total nitrogen calculation is only possible for locations with both gas and particle phase concentrations, the data summaries of total nitrogen are confined to TWS sites (**Table 3-17**).

There is a wide seasonal variation across these sites. In winter, the populated sites in the basin are clearly highest, with the south shore sites (Sandy Way, SOLA) much higher than the other sites. In summer, the south shore still is high but the difference from winter is modest. At Big Hill total nitrogen is very low in the winter (the limited number of samples may have been a factor), rises in spring, and peaks in the summer to levels comparable to South Lake Tahoe. Lake Forest shows a pattern similar to south Lake Tahoe with the lowest levels in the spring and moderately high levels in the other seasons. The unpopulated east shore (Thunderbird) shows the least seasonal signal and is the lowest year-round.

The split among the gas and aerosol species is also highly variable across the network. Total nitrogen distributions (percent of N) are shown in **Table 3-18**. Approximately 70% of the dry N deposition comes from the deposition of NH_3 and NH_4^+, both being highly water soluble.

The aerosol fraction (nitrate + ammonium) is greatest at the less-populated sites (Thunderbird and Big Hill), while the ammonia gas fraction peaks in the populated areas (SOLA/Sandy Way and Lake Forest). Nitric acid, by contrast, is a relatively constant fraction at all sites. On average, 70% or more of total N is from ammonia plus ammonium, with over 50% of total N from ammonia alone. Thus, total atmospheric N is primarily determined by the supply of ammonia, regardless of its site-specific aerosol-gas partitioning.

Table 3-17. Total nitrogen from TWS aerosol and gas measurements.

Lake Tahoe Atmospheric Deposition Study Nitrogen Total, Nitrates, Ammonium Ion, Nitric Acid, Ammonia (ug/m3)									
	Nitrogen Particulate & Gas (N)					Nitrates	Ammonium	Nitric Acid	Ammonia
Site	Winter	Spring	Summer	Fall	Study Average	(Mass)	(Mass)	(Mass)	(Mass)
Big Hill	0.22	0.76	1.95	1.52	1.33	1.25	0.55	0.65	0.57
Lake Forest	0.93	0.67	1.17	1.20	0.97	0.48	0.26	0.47	0.67
Sandy Way	1.47	1.24	2.83	1.94	1.63	1.05	0.50	1.00	0.95
SOLA	2.73	1.38	1.88	2.30	2.13	0.81	0.39	0.96	1.73
Thunderbird	0.32	0.47	0.82	0.67	0.57	0.53	0.29	0.34	0.18
Maximum Basinwide (excludes Big Hill)					3.84	1.79	0.78	2.93	4.08
2nd Maximum Basinwide (excludes Big Hill)					3.84	1.73	0.71	1.91	3.59
Average Basinwide (excludes Big Hill)					1.35	0.47	0.27	0.69	0.85
Median Basinwide (excludes Big Hill)					1.28	0.38	0.25	0.57	0.77
Minimum Basinwide (excludes Big Hill)					0.15	0.02	0.01	0.08	0.04

Table 3-18. Contributions of nitrogen species from TWS measurements.

	Nitrates	Ammonium	Nitric Acid	Ammonia	$NH_4^+ + NH_3$	$HNO_3 + NO_3^-$	Total N (ng/m^3)
Site	**% of Total**	**% of Total**	**% of Total**	**% of Total**	**% of Total**	**% of Total**	**Study Average**
Big Hill	21	32	11	36	68	32	1,333
Lake Forest	11	21	11	57	78	22	973
Sandy Way	15	24	14	48	72	28	1,627
SOLA	9	14	10	67	81	19	2,125
Thunderbird	21	40	13	26	66	34	566

3.3 Summary

The CARB initiated the LTADS in 2002 to quantify the contribution of atmospheric deposition to the declining clarity of Lake Tahoe. The initial study design, which included routine monitoring supplemented by special studies to address pertinent atmospheric processes (e.g., emissions, chemistry, conditions aloft, particle deposition), was described in a June 10, 2002 draft work plan for LTADS. The monitoring network was designed to provide information on the spatial variations around the lake and upwind of the basin. A total of five sites were selected for a one-year monitoring program featuring the TWS. The fives sites selected were: South Lake Tahoe (SOLA and Sandy Way) representing the major urban environment in the basin; Lake Forest (near Tahoe City) representing a less urban environment; Thunderbird Lodge representing the background conditions in the basin; and Big Hill representing the environment upwind of the Tahoe basin. The TWS provided two-week integrated samples of ammonia, nitric acid, TPS, PM10, and PM2.5 and served as the backbone of the monitoring plan. The two week sampling duration avoided problems associated with episodic sampling and non-representative contributions from specific sources. Mini-Vol samplers were used to measure TSP at remotes sites and were deployed under two different monitoring schemes: buoy Mini-Vols for TSP (typically 24 hours) and non-buoy Mini-Vols for TSP (duration and frequency varied).

Field blanks were applied to subtract the background contribution from the sampling environment and field operation. TWS field blanks were collected only at a single site (SOLA) for 10% of the ambient sampling period. Three field blanks were collected for Mini-Vol TSP samples. The limited and site specific field blanks may affect the results of the ambient samples.

A total of 129 sets of TWS samples, including TSP, PM10, and PM2.5, 36 sets for buoy Mini-Vol TSP samples, and 129 sets for non-buoy Mini-Vol TSP samples were collected in LTADS. Replicate analyses were performed on 10% of the ambient samples. The chemical data were evaluated for internal consistency by examining the physical consistency and balance of reconstructed mass, based on chemical species versus measured mass. In general, the samples collected met the criteria of internal physical consistency. A few TWS samples were suspected to be outliers; however, no field flag was noted for these samples (with the exception of one laboratory flag).

The highest annual averages TSP (22 µg/m^3) and PM10 (19 µg/m^3) mass concentrations were observed at the SOLA site and the highest annual average PM2.5 mass concentration (9 µg/m^3) was observed at the SW site. The lowest TSP, PM10, and PM2.5 mass concentration were 6, 6, and 4 µg/m^3, respectively, and were observed at the TB site. PM10 mass comprised 80-90% of TSP mass and was approximately twice that of PM2.5 mass. The most abundant chemical species were OC (17-30%), silicon (11-16%), and aluminum (4-5%) for TSP; OC (16-28%), silicon (10-21%), and aluminum (4-7%) for PM10; and OC (42-52%), EC (5-16%), and ammonium (3-6%) for PM2.5. The lowest TWS TSP, PM10, and PM2.5 mass concentrations were observed from March to April 2003 at all five sites. TWS TSP, PM10, and PM2.5 mass concentrations observed at the BH, TB, and LF sites from May to October 2003 were twice as high as those observed from November 2002 to February 2003; however, TWS TSP, PM10, and PM2.5 mass concentrations were comparable during these two periods at the SOLA and SW sites. The elevated TWS TSP, PM10, and PM2.5 mass concentrations at the SOLA and SW sites from November 2002 to February 2003 were due to elevated OC and EC concentrations, which were likely the result of the increased traffic volumes and wood burning associated with winter activities.

The annual average mass concentrations and chemical species were the highest in TPS and the lowest in PM2.5 at the same site; however, such physical consistency was not necessarily observed for TWS samples at the same sampling period. For example, PM_{10} mass concentration higher than TSP mass concentration was occasionally observed. Such sampling bias can be attributed to the low TWS sampling flow rate of 1.67 liter per minute, low mass concentration of ambient particulate matters, long sampling duration, and sampling artifacts of semi-volatile species.

The annual average PM_{10} mass concentration comprised more than 80% of the TSP mass concentration. Bounces and penetration of particles larger than 10 µm through the impactor can increase the PM10 mass concentration. Particle bounce and penetration efficiency depends on the characteristics of 50% cutpoint curve and material of impaction substrate and particle bounce is more pronounced as the sampling time (i.e., particle loading on impaction substrate) increases (Chang, et al, 1999, Tsai, et al, 1995), as well as at low particle concentrations.

The sampling artifacts of semi-volatile species on sampling media can either introduce positive or negative sampling artifacts. The sampling artifacts of semi-volatile species depend on ambient sampling temperature, relative humidity, the species' disassociation constant, the ratio of species in particulate and gas phases, and the pressure drop through the sampling media (Chang et al 2000b, Stelson, and Seinfeld, 1982, Zhang and McMurry 1987, Zhang and McMurry 1992). Although negative sampling artifacts of nitrate losses can be quantified through the backup filter, it is not clear how absorption of OC onto the quartz filters might create positive sampling artifacts during analysis. As OC is the most abundant species in TWS TSP, PM10, and PM2.5, a denuder for volatile organic species and a backup filter should be used for better assessment of PM mass and chemical concentrations.

Except for a couple of sites in the winter period, staff has confidence in the LTADS seasonal particulate matter concentrations in TSP, PM10, and PM2.5. Staff believes the LTADS nitrogen specie concentrations (gas and particulate matter in all size fractions) are representative of Tahoe Basin atmospheric chemistry and processes. The LTADS phosphorus observations suffered from the difficulties all analyses of ambient P face. The dust experiments suggest that particulate concentrations at the shoreline are significantly higher than concentrations over the lake. The LTADS deposition estimates, because they are based on shoreline observations, are thus likely an overestimation as well. Staff did not study inert particles in detail. By using all PM data (i.e., all species), the staff's analysis presents a maximum bounding estimate for atmospheric deposition of PM to Lake Tahoe. A simple analysis of likely soluble materials (i.e., ion chromatography and automated colorimetry measurements) indicates that about 20-25% of the PM mass is soluble and would not remain as particles in the water. Other potentially soluble components would reduce the number and mass of inert particles further. Thus, a crude adjustment factor of 75% to the total PM deposition estimates presented in Chapters 4 and 5 may be needed to accurately represent the atmospheric PM that remains as PM once deposited to the Lake.

With respect to gaseous pollutants, concentrations are typically representative of clean conditions. Seasonal mean concentrations of nitric acid ranged from about 200 to 1300 ng/m^3 (0.1 to 0.5 ppb) and generally being lowest in the spring and highest in the fall. Seasonal mean concentrations of ammonia ranged from about 200 to 2300 ng/m^3 (0.3 to 3.3 ppb) and generally being lowest in the spring and highest in the summer and fall. The highest ammonia concentrations were observed at the SOLA site, which is strongly influenced by activity on Highway 50, during winter when the number of hours with downslope air flow across Highway 50 is greatest. The peak ozone concentration in the Tahoe Basin during 2003 was 87 ppb, below the California public health 1-hour standard but above the TRPA forest health 1-hour threshold. The number of hours during 2003 when ozone concentrations were greater than 70 ppb declined from 400+ hours at the Big Hill site (on the western slope of the Sierra Nevada) to 90+ hours at the Echo Summit site (on the Sierra crest and the southwestern boundary of the Tahoe Basin) to 30+ hours at Incline Village (near lake-level in the Tahoe Basin).

3.4 References

Bevington, P.R., (1969). Data Reduction and Error Analysis for the Physical Sciences. McGraw Hill, New York, NY.

Carroll, J.J., Anastasio, C., and Dixon, A.J., (2004). Keeping Tahoe Blue through Atmospheric Assessment: Aircraft and Boat Measurements of Air Quality and Meteorology near and on Lake Tahoe, report prepared for California Air Resources Board, Sacramento, CA, June.

Chang, M.C., Kim, S., and Sioutas, C., (1999). "Experimental studies on particle impaction and bounce; effects of substrate design and material." *Atmospheric Environment*, **15**: 2313-2323.

Chang, M.-C.; Sioutas, C.; Kim, S.; Gong, H. Jr.; and Linn, W.S., (2000a). Reduction of nitrate losses from filter and impactor samplers by means of concentration enrichment. *Atmos. Environ*. **34**, 85-98.

Chang, M.C**.**, Kim, S., Sioutas, C., Gong, H., Anderson, K., and Linn, W., (2000b) "The effect of concentration enrichment on losses of nitrate from filters and impactor samplers." *Atmospheric Environment*, **34** (1): 85-98.

Chow, J.C. and Watson, J.G., (1989). Summary of particulate data bases for receptor modeling in the United States. In Transactions, Receptor Models in Air Resources Management, Watson, J.G., editor. Air & Waste Management Association, Pittsburgh, PA, pp. 108-133.

Chow, J.C.; Watson, J.G.; Pritchett, L.C.; Pierson, W.R.; Frazier, C.A.; and Purcell, R.G., (1993). The DRI Thermal/Optical Reflectance carbon analysis system: Description, evaluation and applications in U.S. air quality studies. *Atmospheric Environment* **27A** (8), 1185-1201.

Chow, J.C. and Watson, J.G., (1994a). Guidelines for PM10 sampling and analysis applicable to receptor modeling. Report No. EPA-452/R-94-009. Prepared for U.S. EPA, Office of Air Quality Planning and Standards, Research Triangle Park, NC, by Desert Research Institute, Reno, NV.

Chow, J.C.; Watson, J.G.; Fujita, E.M.; Lu, Z.; Lawson, D.R.; and Ashbaugh, L.L., (1994b). Temporal and spatial variations of PM2.5 and PM10 aerosol in the Southern California Air Quality Study. *Atmospheric Environment* **28** (12), 2061-2080.

Chow, J.C. and Watson, J.G., (1999). Ion chromatography in elemental analysis of airborne particles. In Elemental Analysis of Airborne Particles, Vol. 1, Landsberger, S., Creatchman, M., editors. Gordon and Breach Science, Amsterdam, pp. 97-137.

Chow, J.C., Watson, J.G., and Wiener, R.W., (2005) Method No. 508: PM2.5 sampling and gravimetric analysis by Federal Reference Method. In Methods of Air Sampling

and Analysis, Lodge, J.P. Editor. Air and Waste Management Association, Pittsburgh, PA.

Cliff, S., (2005). Quality Assurance Analysis of Filter Samples Collected during the Lake Tahoe Atmospheric Deposition Study using Synchrotron X-Ray Fluorescence, report prepared for California Air Resources Board, Contract No. 03- 334. April 30, 2005.

DRI (2000). DRI Standard Operating Procedure #2-204.6 - Thermal/Optical Reflectance Carbon Analysis of Aerosol Filter Samples, Reno, NV, June.

Fitz, D. and Hering, S., (1996). Further Evaluation of a Two-Week Sampler for Acidic Gases and Fine Particulate, report prepared for California Air Resources Board, Contract No. 93-339, May.

Hidy, G.M., (1985). Jekyll Island meeting report: George Hidy reports on the acquisition of reliable atmospheric data. *Environmental Science & Technology* **19** (11), 1032-1033.

Lioy, P.J.; Mallon, R.P.; and Kneip, T.J., (1980). Long-term trends in total suspended particulates, vanadium, manganese, and lead at near street level and elevated sites in New York City. *Journal of the Air Pollution Control Association* **30** (2), 153-156.

Pathak, R.K.; Yao, Z.; and Chak, K.C., (2004). Sampling artifacts of acidity and ionic species in PM2.5, *Environ. Sci. Technol.* **38**, 254-259.

Stelson, A.W. and Seinfeld, J.H., (1982). Relative humidity and temperature dependence of the ammonium nitrate dissociation constant, *Atmos. Environ.* **16**:983-992.

Tarnay, L., Gertler, A.W., Blank, R.R., Taylor Jr., G.E., (2001). Preliminary measurements of summer nitric acid and ammonia concentrations in the Lake Tahoe Basin air-shed: implications for dry deposition of atmospheric nitrogen. *Environmental Pollution* **113**, 145-153.

Tarnay, L.W., Gertler, A.W., and Taylor Jr., G.E., (2002). An Inferential Model for HNO_3 Deposition to Semi-arid Coniferous Forests, *Atmos. Environ.*, **36**, 3277-3287.

Tsai, C.J. and Chen, Y.H., (1995). Solid particle collection characteristics on impaction surface of different design. *Aerosol Sci. Technol.* **23**: 96-106.

Watson, J.G.; Lioy, P.J.; and Mueller, P.K., (1989). The measurement process: Precision, accuracy, and validity. In Air Sampling Instruments for Evaluation of Atmospheric Contaminants, Seventh Edition, Hering, S.V., editor. American Conference of Governmental Industrial Hygienists, Cincinnati, OH, pp. 51-57.

Watson, J.G. and Chow, J.C., (1992). Data bases for PM10 and PM2.5 chemical compositions and source profiles. In Transactions, PM10 Standards and

Nontraditional Particulate Source Controls, Chow, J.C. and Ono, D.M., editors. Air & Waste Management Association, Pittsburgh, PA, pp. 61-91.

Watson, J.G.; Lioy, P.J.; and Mueller, P.K., (1995). The measurement process: Precision, accuracy, and validity. In Air Sampling Instruments for Evaluation of Atmospheric Contaminants, Cohen, B.S. and Hering, S.V., editors. American Conference of Governmental Industrial Hygienists, Cincinnati, OH, pp. 187-194.

Watson, J.G.; Chow, J.C.; and Frazier, C.A., (1999). X-ray fluorescence analysis of ambient air samples. In Elemental Analysis of Airborne Particles, Vol. 1, Landsberger, S. and Creatchman, M., editors. Gordon and Breach Science, Amsterdam, pp. 67-96.

Watson, J.G.; Turpin, B.J.; and Chow, J.C., (2001). The measurement process: Precision, accuracy, and validity. In Air Sampling Instruments for Evaluation of Atmospheric Contaminants, Ninth Edition, Cohen, B.S. and McCammon, C.S., Jr., editors. American Conference of Governmental Industrial Hygienists, Cincinnati, OH, pp. 201-216.

Zhang, X. and McMurry, P.H., (1987). Theoretical analysis of evaporative losses from impactor and filter deposits. *Atmos. Environ.* **21**: 1779-1789.

Zhang, X. and McMurry, P.H., (1992). Evaporation losses of fine particulate nitrates during sampling. *Atmos. Environ.* **26A**: 3305-3312.

Zhang, Q., Carroll, J.J., Dixon, A.J., and Anastasio, C. (2002). Aircraft Measurements of Nitrogen and Phosphorus in and around the Lake Tahoe Basin: Implications for Possible Sources of Atmospheric Pollutants to Lake Tahoe. *Environ. Sci. Technol.*, Vol. 36, 4981-4989.

This page blank intentionally.